# Emissions of volatile organic compounds from household plastics and their controls: An experimental and modelling approach

**Georgia Beel**

**Doctor of Philosophy**

**University of York**

**Environment and Geography**

**June 2023**

# Abstract

Increased consumption and consumer habits over recent decades have led to the accumulation of plastic products within our homes. Although assumed to be chemically inert, these materials can release a multitude of volatile organic compounds (VOCs). Currently, little is understood about VOC emissions from common household plastics, in terms of rates or composition. Consequently, the role that these play within the indoor atmosphere, in terms of secondary product formation, is also relatively unexplored. The aims of this thesis are to quantify emission rates of selected VOCs from common household plastics, determine how they are controlled by abiotic factors such as temperature, sunlight and natural ageing processes, as well as modelling their degradation pathways.

Experimental results showed that emission rates of aromatic VOCs, such as benzene, and styrene, increased linearly with temperature, from 0.009-0.03 and 0.02-0.05 ng cm$^{-2}$ h$^{-1}$, respectively, between 18 to 28 °C, averaged across all plastic types investigated. UVA light-driven emissions showed a S-shape relationship, with the greatest emission rates between 0.1-1.2 W m$^{-2}$ 0-0.13 and 0-0.025 ng cm$^{-2}$ h$^{-1}$, for propene and benzene, respectively. Natural ageing experiments showed high initial VOC emissions between months 1 and 4, which gradually decreased over time, with aromatic compounds showing a 50-90 % reduction in emissions from months 1 to 12.

Modelling results show that the diurnal profile of secondary chemical species is driven by the simulated sunlight. The highest impact on the simulated concentrations of ozone and the hydroxyl radical (OH), was produced by the plastic types with the highest overall VOC emissions; the polystyrene-tubing plastic caused an increase in ozone by 1.8 % and a decrease in OH by 15.6 % at 28 °C, in comparison to background simulations without plastics present. This thesis contributes to the understanding of VOC emissions from common household plastics. Evidence from these studies suggests that lowering the presence of plastics indoors can help reduce exposure to harmful VOCs, as well as potentially more harmful secondary pollutants.

# Table of Contents

# List of Figures

# List of Tables

# Acknowledgements

# Declaration

I declare that this thesis is a presentation of original work and that I am the sole author. This work has not been presented for an award at this or any other University. All sources are acknowledged as references.

Part of this work has been published in:

Beel, Georgia, Ben Langford, Nicola Carslaw, David Shaw, and Nicholas Cowan. 2023. "Temperature Driven Variations in VOC Emissions from Plastic Products and Their Fate Indoors: A Chamber Experiment and Modelling Study." Science of the Total Environment 881 (January): 163497. https://doi.org/10.1016/j.scitotenv.2023.163497.

# 1. Introduction

Within the last 40 years, atmospheric scientists have turned their attention to the chemistry of the indoor environment and the pollutants within. In developed countries, we spend 90% of our time in indoor environments, such as our homes and workspaces (Klepeis et al. 2001). Numerous pollutants are detectable in these environments, including biological (viruses, microbes, fungal spores) and chemical (e.g. Volatile Organic Compounds (VOCs), particulate matter - $PM_{10}$ and $PM_{2.5}$), often at higher concentrations compared to those detected outside (Carslaw 2007). With the lockdown restrictions imposed during the year of 2020 and beyond, good indoor air quality has become more important, as these extended periods of time spent indoors prolong the duration of exposure to the aforementioned indoor pollutants (D'Amico et al. 2021).

Much attention has focused on outdoor air pollution in the past, with the recognition that fossil fuel burning for energy consumption can release harmful pollutants, e.g., carbon dioxide ($CO_2$), carbon monoxide (CO) and particulate matter (PM), into the atmosphere (IPCC 2018). This global issue has been acknowledged in the recent COP26 goals, and many countries signed the Paris Agreement as a pledge to develop low-carbon economies and reduce their emissions (Wang et al. 2023). Despite the focus on outdoor air pollution, there has become a greater recognition of the amount of time spent indoors. The World Health Organisation (WHO) stated that, within developing nations, household air pollution was responsible for an estimated 3.2 million deaths per year in 2020 caused by exposure to solid fuel burning, which includes over 237,000 deaths of children under the age of 5 (WHO 2022). This is why it's important to look at indoor pollution in the home, as the indoor environment is where people receive most of their exposure to air pollutants (Wang 2022).

Indoor air pollutants can be generated by human activities such as cooking (nitrogen oxides ($NO_x$), PM and CO), cleaning (VOCs, molecular chlorine ($Cl_2$)), painting (VOCs and limonene) and smoking (VOCs and CO) (Nazaroff and Weschler 2004; Weschler 2009). Also, pollutants are emitted from materials indoors, such as building materials and furniture, and products such as air fresheners (Nazaroff & Weschler 2004; Xiong et al. 2019; Zhou et al. 2019). Air pollutants from outdoors can also infiltrate into the indoor environment via ventilation through windows and doors (Matysik et al. 2010). Therefore, a complex mixture of chemicals will occur indoors. As well as the ingress of pollutants indoors, chemical species can also undergo chemical reactions and transformations to form secondary products (Carslaw and Shaw 2019) particularly oxygenated species such as formaldehyde (HCHO) (Blocquet et al. 2017). Two key indoor oxidants are ozone ($O_3$) and the hydroxyl radical (OH). $O_3$ can infiltrate from outdoors but also be generated indoors by air cleaners, laser printers and photocopiers (Yu et al. 2011). The OH radical can be produced through photolysis of nitrous acid (HONO) or ozonolysis reactions (Weschler & Shields 1996). Therefore, while outdoor air is controlled by legislation aimed at reducing

exposure to pollutants, it is important to understand the controls for indoor air quality (IAQ) which is not regulated by law, only by WHO recommendations (WHO 2018).

## 1.1. Why is indoor air quality important?

Investigations into exposures in indoor environments, and the health effects that are associated with such exposures, vary between nations across the world. Studies conducted in developing countries have mainly focused on the association between unvented indoor burning of biomass (for cooking and heating), and the onset of health effects such as acute respiratory infections (ARI), chronic obstructive pulmonary disease (COPD) and lung cancer (Smith 2003). In developed regions, buildings have vented cooking appliances, but have comparatively more furnished-materials and a lower rate of ventilation (Sundell 2004; Nazaroff 2021). Studies on exposure in indoor environments and health effects in developed countries have been conducted mainly in northern Europe and North America, as public awareness of poor indoor air quality in working and living areas continues to grow (Sundell 2004).

The intake of any airborne substances present in indoor air mainly occurs via inhalation and dust ingestion pathways (Hazrati et al. 2016). Indoor air contaminants found in workspaces and homes have been found to contribute to Sick Building Syndrome (SBS); a medical condition where people inside a building can suffer from symptoms of illness for an unknown reason (Menghi et al. 2018). SBS is accompanied by coughing, sneezing, headaches, dizziness, nausea, swelling and itching of the skin, and irritated mucous membranes of the throat, nose, and eyes (Norbäck 2009).

Other commonly observed health effects from exposure to household air pollution, occurring from activities previously stated, include reduced lung function, respiratory illnesses, and weakening of the immune system (Ahmed et al. 2019). It has also been reported that the products of VOC degradation may cause some of the reported symptoms instead of primary emissions (Nazaroff and Weschler 2004).

Adverse health responses attributed to, but not proven to be caused by, VOCs in non-industrial indoor environments include irritant effects resulting from mucous membrane irritation (Bernstein et al 2008) and systemic effects such as fatigue and difficulty concentrating (Menghi et al. 2018). Aldehydes, mono-aromatic compounds and PM have been associated with the onset of asthma development in children (Zhang and Smith 2007; Choi et al. 2010; Nandasena 2013). A decades-long investigation in Xuanwei, China found a relationship between the development of lung cancer in non-smoking women working with coal in open fire pits (Zhang and Smith 2007). West et al. (2013) looked into the relationship between eye diseases and household air pollution (HAP) in developing countries, concluding that while the diseases themselves are caused by infectious agents, there is data to suggest that the manifestation of eye diseases, such as Trachoma, may be exacerbated by HAP.

1.1.1 Guideline values of acceptable indoor concentrations for VOCs

The importance of monitoring VOC concentrations and keeping them at a safe level in both our indoor and outdoor settings has been recognised by the World Health Organisation (WHO), which published the first edition of the Air quality guidelines for Europe in 1987 (WHO Europe 1987). This included an annex on indoor air pollutants with significant adverse public health effects. A variety of editions followed in 2000, 2005 (with a global update of the air quality guidelines which drew attention to the impact of indoor pollution on health within developing countries) and 2010. The WHO Air Quality guidelines published in 2010 recognised that the work assessing the health effects of indoor air pollution lagged behind that on outdoor pollution.

The guideline values set out in the WHO documentation are based on reviewing globally accumulated scientific evidence linking exposure to selected pollutants with health outcomes (WHO 2010). They represent concentrations of individual gaseous compounds that are thought to be safe for the human population. However, the WHO recognises that exposure to combinations of air pollutants is inevitable. Information detailing the effects of co-exposure to air pollutants is very limited and therefore it is not possible to recommend guidelines for such combinations.

Within the UK, Public Health England (PHE) published an indoor air quality guideline document in 2019, summarising guideline concentrations of selected VOCs after conducting a comprehensive literature review. The presented values in Table 1.1 originate from a variety of sources including the WHO, Health Canada, the Agency for Toxic Substances and Disease Registry, USA and the EU EPHECT (Emissions, Exposure Patterns and Health Effects of Consumer Products) project (Trantallidi et al. 2015).

*Table 1.1: Summary of Indoor air quality guidelines for the UK outlined in PHE 2019 document.*

| VOC | Concentration limit ($\mu g\ m^3$) | | Notes |
|---|---|---|---|
| | Short term | Long term | |
| Acetaldehyde | 1420 (1hr) | 280 (1day) | |
| α-Pinene | 45000 (30mins) | 4500 (1day) | |
| Benzene | (No safe level of exposure can be recommended) | | Conc. of benzene with an excess lifetime cancer risk of 1:10000, 1:100000 and 1:000000 are 17, 1.7 and 0.17 $\mu g\ m^3$, respectively |
| D-limonene | 90000 (30mins) | 9000 (1day) | |
| Formaldehyde | 100 (30mins) | 10 (1yr) | |
| Naphthalene | - | 3.0 (1yr) | |

| Styrene | - | 850 (1yr) | |
|---|---|---|---|
| Tetrachloroethylene | - | 40 (1day) | |
| Toluene | 15000 (8hr) | 2300 (1day) | |
| Trichloroethylene | (No safe level of exposure can be recommended) | | Conc. of trichloroethylene associated with excess lifetime cancer risk of 1:10000, 1:100000 and 1:1000000 is 230, 23 and 2.3 µg m$^3$, respectively. |
| Xylene mixture | - | 100 (1yr) | |

To compare international guidelines, the International Society of Indoor Air Quality and Climate (ISIAQ) Scientific and Technical Committee (STC34), launched in September 2020, orchestrated an open indoor environmental quality database. The purpose of this online database is to continuously collect and organise information about indoor environmental quality guidelines worldwide. More information, and the database itself, can be found: https://ieqguidelines.org/index.html.

## 1.2. Factors controlling Indoor Air Quality (IAQ)

Since IAQ was recognised as being a significant factor influencing human health, an array of studies have investigated different aspects that influence the air quality indoors, and the subsequent air chemistry. Physical elements, such as temperature, lighting and ventilation, indoor activities, such as cooking and cleaning, and materials commonly found indoors have all been investigated. The temperature indoors and thermal comfort has been rated as one of the most important components of IAQ for occupant satisfaction, with air temperature being the main factor (Frontczak and Wargocki 2011; Taleghani et al. 2013). Indoor air temperature can be influenced by external factors like outdoor climate and season, as well as the type of building. The amount of light infiltrating indoors can also be controlled by these external factors. Work conducted by Wang et al. (2022) investigated both the attenuated light from outdoors as well as artificial indoor lighting types. Their work showed that window glass type had the highest impact on controlling indoor photolysis reactions and resultant concentrations of species such as hydroxyl radicals (OH) and nitric oxide (NO), compared to other factors such as cloudiness, time of year, latitude and artificial indoor lighting (Wang et al. 2022). Due to advancements in construction practices and improved insulation of houses in recent decades, contemporary buildings exhibit relatively low air exchange rates with outdoor air. This consequently leads to the build-up of pollutants within indoor spaces (Holøs et al. 2019).

The understanding that household activities such as cooking and cleaning can cause an increase in indoor air pollutant emissions sparked a large-scale collaborative investigation into House Observations of Microbial and Environmental Chemistry (HOMEChem) in 2018 (Farmer et al. 2019). A manufactured test house was used to observe indoor activities, with an emphasis on cooking, cleaning and variations in occupancy, whilst monitoring the air chemistry with a variety of instrumentation.

Sequential and layered experiments were carried out during this study, to determine the full effect of cooking and cleaning events, and how they altered the atmospheric chemistry throughout the day. It was found that in particular, cooking was a large source of VOCs, carbon dioxide ($CO_2$), nitrogen oxides ($NO_X$) and particles (Farmer et al. 2019).

Continuous VOC emissions from static objects or room furnishings are generally lower when compared to emissions from an episodic event or activity such as cooking, cleaning, painting or smoking (Wolkoff and Nielsen 2001). However, a study conducted by Lunderberg et al. (2021) found that the accumulation of emissions from continuous indoor sources, such as building materials themselves and the "static content" within, contribute more to our indoor exposure of VOCs, than compared to the aforementioned episodic sources. New or renovated buildings can emit primary VOCs from their building products, (e.g. solvents, paint, sealant, glues, etc.), which can dominate in indoor air for a few months (Holøs et al. 2019). The ageing of building materials, through degradation processes such as photo-oxidation, can result in secondary VOC emissions, as mentioned previously. The presence of these secondary compounds can extend for much longer than primary VOC emissions, because the degradation process of indoor materials is continuous (Brown et al. 2013).

## 1.3. Material emissions

With increased consumerism and societal pressures to keep up with the latest trends and fashion, individuals accumulate and hoard vast amounts of materials in our homes that can release volatile compounds into the air, through both primary and secondary emissions. Many materials have been investigated previously and extensively evaluated for their chemical emissions and influence on IAQ (Kruza et al. 2017). These include materials such as different types of flooring (Cox et al. 2002; Afshari et al. 2004), construction materials like particleboard and fiberboard (Jiang et al. 2017; Zhou et al, 2019), soft furnishings (Oz et al. 2019) and wooden furniture (Xiong et al. 2019). A class of relatively understudied indoor components includes plastic consumer products such as decorative articles, tools, utensils, textiles and children's toys. A few studies have found these items also emit a range of different compounds and for them to potentially be an important source of VOCs indoors (Haug et al. 2022).

At present, we live in a globalised world, with an economy that facilitates the exchange of goods worldwide. The production and consumption of plastic polymers has surpassed almost all other man-made materials across all industrial sectors (Geyer et al. 2017). Figure 1.2 demonstrates how annual plastic production has increased globally since the 1950's from 1.5 to 359 million tonnes in 2018 (Shanmugan et al. 2020). There is no denying that the development of plastic products has significantly improved our way of life, and a world without synthetic polymers seems unimaginable today. Within

the building and construction industry, plastic has become one of the most used materials for insulating our homes, as well as for pipes, valves, panels and plumbing fixtures. Within the transportation industry, plastics can be found in the doors, wheels and interior of cars. The thermal insulating properties of plastic make it the most suitable material for electrical appliances. Manufacturers use plastics regularly for circuit boards, chips, microwaves, hair dryers and refrigerators. Plastic has become the chosen material for use because of its malleability, durability and versatility, dominating domestic and industrial applications (Wright & Kelly 2017; Henry et al. 2019). This has resulted in high levels of competition between manufacturers to produce more attractive and cheaper plastic products, sometimes at the expense of quality (Even et al. 2019).
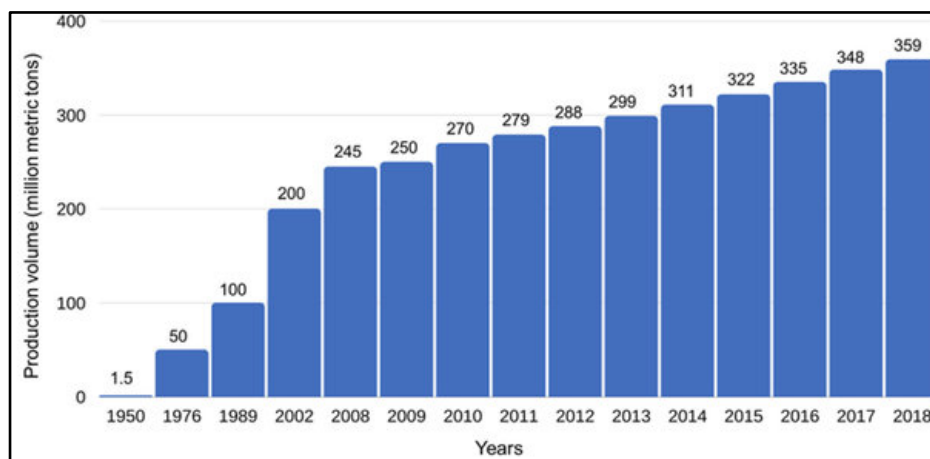


*Figure 1.1: Production of plastics worldwide from 1950, 1976, 1989, 2002 and from 2008 to 2018 in million metric tonnes (from Shanmugan et al. (2020)).*

Plastic consumer products can contain additives, which are incorporated within the polymer structure itself. These can include ultra-violet (UV) stabilisers and antioxidants, which minimise the products ability to degrade over time (via thermal- or photo-degradation) (Yousif & Haddad 2013). These additives, however, can be harmful substances that can migrate out of the plastic as the material deteriorates over time in the form of VOC emissions. These emissions then end up in the indoor air and can negatively affect occupants' health (Even et al. 2020), as well as also having a notable impact on indoor air chemistry. Therefore, it is important to consider and investigate the mechanisms behind plastic degradation in the home, where humans experience the greatest exposure to pollutants from plastic consumer products.

## 1.4. Aims of thesis

The aims of this thesis are to:

- Investigate how VOC emissions from different household plastics respond to changes in temperature, within the range of typical indoor values.
- Investigate how VOC emissions from different household plastics respond to different levels of light, particularly within the visible and ultraviolet (UV) range, as these are the wavelengths observed indoors.
- Investigate how household plastics are naturally aged indoors and how their VOC emissions change over time.
- Carry out a series of model simulations to investigate how the VOC emissions from household plastics affect the indoor atmospheric chemistry using a new model: INCHEM-Py.

## 1.5. Thesis outline

This thesis aims to improve the understanding of VOC emissions from a variety of plastic types found within the indoor environment and the influence of these emissions on indoor air chemistry. The thesis is structured as follows:

**Chapter 2:** This chapter presents a literature review of what is currently known about VOC emissions from household plastic materials, defining what VOCs are and how these compounds are modelled indoors.

**Chapter 3:** A methodology section outlines the instrumentation used throughout this thesis to investigate the plastic polymers and to quantify the emission rates of key volatile species emitted from the plastics. This chapter also describes the laboratory set up and the method used for calculation of VOC emission rates. Finally, the parameters used in model simulations are outlined and discussed.

**Chapter 4:** This chapter describes experiments that determine the impact of temperature on VOC emissions from plastic polymers. It then describes how the measured emission rates have been used in model scenarios to determine how an increase in temperature indoors influences the indoor air chemistry and particularly, secondary pollutant production.

**Chapter 5:** This chapter describes the experiments that determine VOC emissions from plastic polymers in response to changing levels of attenuated sunlight indoors. It then describes how the light-driven emission rates have been used in model scenarios to determine how photolysis affects the indoor air chemistry and secondary pollutant production.

**Chapter 6:** This chapter investigates experimentally how the VOC emissions from household plastics vary over the course of one year after being naturally aged in a typical home, and consequently, how these emissions affect the indoor chemistry and the secondary pollutant production.

**Chapter 7:** This chapter summarises the overall findings of this thesis and will also suggest pathways for further research.

# 2. Literature review

## 2.1. Plastic types and degradation processes

With an increase in demand for polymer materials, the production of plastic polymers has increased exponentially since the 1950's (Groh et al. 2019), with polyethylene (PE) being the most common polymer type (Royer et al. 2018). The structure of PE is shown in Figure 2.1 along with other common plastic polymer types, also known as thermoplastics. The word "plastic" comes from the Greek term plastikos, which means a material that can remain shaped in various systems (Rajmohan et al. 2019). Plastic polymers consist of repeating monomers (Figure 2.1), making up long hydrocarbon chains that can be connected via cross-linking bonds in the polymer chain, creating a lattice structure.

High density polyethylene (HDPE) is the most common type of PE material, which is used to create different types of light-weight carrier bags, food containers and other household items such as shampoo and detergent bottles (Modern Plastics Global 2020). The polymer is made up of straight molecular chains that have a linear structure, with very little branching, giving it a high tensile strength. Polypropylene (PP) consists of a straight chain of molecules with methyl groups on every other carbon. These methyl groups are all in the same position on the carbon backbone, giving the polymer a degree of crystallinity, between that of low-density polyethylene (LDPE) and high-density polyethylene (HDPE). This property produces a strong material, typically used for containers or tubing and pipe material (Modern Plastics Global 2020). Polyethylene terephthalate (PET or PETE) is used as the material for plastic water bottles. PET is produced by the polymerisation of ethylene glycol and terephthalic acid: the presence of the aromatic ring gives the polymer strength in its structure.
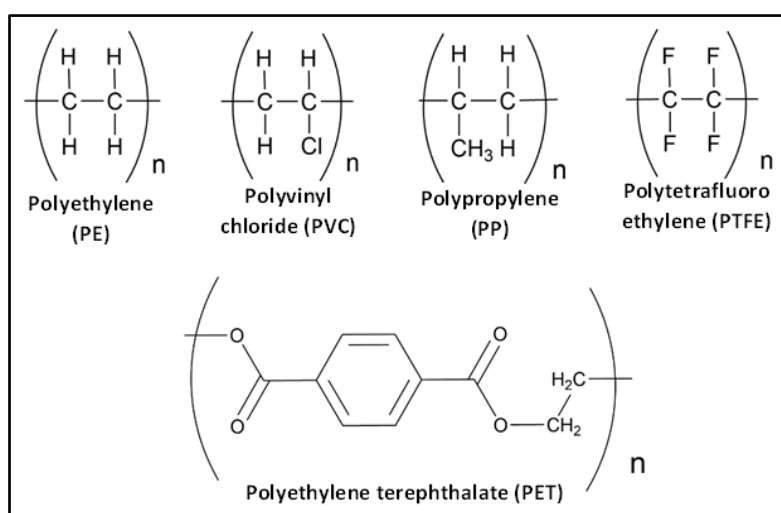


*Figure 2.1: Examples of major polymer types and their chemical structures.*

Polystyrene (PS) is a synthetic aromatic polymer made from the styrene monomer. General purpose PS is hard and brittle, but its uses include protective packaging, containers, lids, bottles, trays and tubing. Polyester rubber, or thermoplastic rubber (TPR), is a combination of rubber and other plasticisers, which gives it elastic properties as well as good heat, weather and age resistance (Sycor 2019).

Plastic polymers can experience different types of degradation throughout their entire life cycle, from production, during their use and after they have been discarded. In the following sections the different mechanisms of degradation that plastic polymers can undergo are addressed, with a focus on thermal and photo degradation. Both thermal and photo degradation are classified as oxidative degradation. The main difference between the two is the sequence of initiation steps that lead to the breakdown of the polymer through oxidation reactions (Singh & Sharma 2008).

2.1.1. Thermal degradation

Thermal degradation is the molecular deterioration of a polymer as a result of over-heating. This process affects the whole polymer, not just its surface. PS has been previously found to thermally degrade into compounds such as phenol, quinine and naphthalene at experimental temperatures of 350-450°C (Bortoluzzi et al. 2005; Ciliz et al. 2004). Thermo-oxidative degradation of polyesters results in a variety of products such as formaldehyde, acetaldehyde, formic acid, acetic acid, $CO_2$ and $H_2O$ (Boenig 1965). The mechanism for the thermal degradation of polymers consists of two distinct reactions, which can occur simultaneously; one is the random scission of bonds in the main polymer chain, causing change of polymer structure and consequently its properties, such as loss of tensile strength, reduced mobility, changes in colour, and cracking (Arkatkar et al. 2009). The other reaction is a chain-end scission of carbon to carbon (C-C) bonds, which generates volatile compounds (Singh & Sharma 2008). The chain-end degradation starts from the end of the chain and successively releases the monomer units, in a process also known as depolymerisation.

2.1.2. Photo-degradation

Photo-degradation is the process of decomposition of a material by the action of light, which is considered one of the leading sources of damage exerted upon plastic polymers in ambient conditions. Most plastic polymers are susceptible to degradation initiated by UV radiation (290 to 400 nm). This radiation has sufficient energy to split C-C bonds (Mark et al. 1985). Polymers will absorb this high energy radiation, which activates their electrons and causes cross-linking reactions and chain scissions (Shah et al. 2008). The most damaging UV wavelength for specific polymers depends on the bonds present. For PE, this is 300 nm, and for PP 370 nm (Singh & Sharma 2008).

Nagai et al. (1999) found that UV light absorbed by PS caused degradation to occur at the benzene ring, causing loss of mechanical properties and chain scission, and also found it to be a precursor to oxidative degradation. In photo-oxidative degradation, the mechanism involves an auto-oxidation cycle which includes numerous steps shown in Figure 2.2. This process involves the oxygen-induced formation of reactive oxygen species, also known as free radicals. In the initiation step, a hydrogen atom is extracted by an excited oxygen from the hydrocarbon chain, forming an organic radical ($ROO^\bullet$). Further reactions lead to the formation of polymer hydroperoxides (ROOH). Consequently, hydroperoxides and their decomposition products are responsible for the changes in molecular structure of the polymer, leading to the loss of mechanical properties e.g. flexibility and/or tensile strength (Marturano et al. 2016). Termination is promoted in oxygen deficient conditions, by combination of the various radical species.
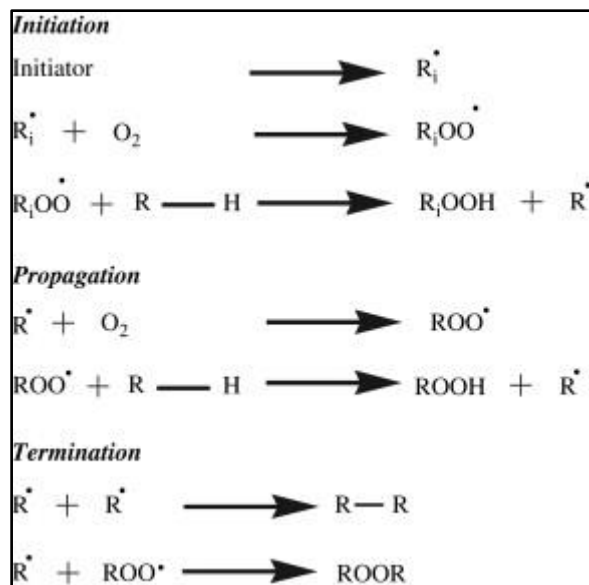


*Figure 2.2: General schematic for oxidation reactions occurring within polymer degradation (taken from Singh & Sharma (2008)).*

## 2.1.3. Other degradation types

Plastic polymers can be subjected to other forms of degradation. Mechanical disintegration is the breakdown of a material through the application of shear force. Polymers are exposed to several forms of mechanical degradation including ageing and breakage from atmospheric weathering, freeze-thaw cycles outdoors, pressure endured during use, or damage inflicted by animals or humans (Lambert 2013).

Hydrolytic degradation can occur within plastic polymers depending on the presence of hydrolysable covalent bonds, such as esters, ethers, and amide groups in the polymer (Lucas et al. 2008). Materials with these functionalities are able to absorb moisture, which then promotes hydrolytic cleavage of the polymer chain (Krzan et al. 2006). This type of degradation occurs when positively charged hydrogen ions in acidic media, or negatively charged hydrogen ions in alkaline media, attack the ester linkage, thus breaking the polymer chain. This reduces the polymer chain length, directly impacting the strength of the material (Lambert 2013).

These abiotic degradation processes can act as the first step in increasing the polymer surface area available for microbial colonisation (Lucas et al. 2008). Biological processes involving polymer disintegration start outside of the microbial cell with the secretion of enzymes. The enzymes can cleave the polymer chains on the surface of the material, as they are too large to penetrate deep into the polymer (Palmisano & Pettigrew 1992). Over time, abiotic and biotic factors work together to further the degradation process. Chain scission reduces the molecular weight of the polymer, which in turn provides greater accessibility for oxygen and moisture to further weaken the structure and make it more susceptible to microbial activity (Lambert 2013).

## 2.2. Plastic additives

Plastic polymers in their purest state are not typically used commercially; polymers are processed, through a series of polymerisation reactions with a variety of compounds, to adjust their characteristics, tailoring them for their intended purpose (Lambert 2013). Thus, plastic materials can contain many substances that are not chemically bound to the polymer matrix. These substances include unreacted monomers, additives and residual processing aids (Wiesinger et al. 2021), which can be released during the plastics life cycle, by migrating through the polymer to its surface before being released into the surrounding environment.

The definition of an additive, given by the European Community, is "a substance which is incorporated into plastics to achieve a technical effect in the finished product, and is intended to be an essential part of the finished article" (Marturano et al. 2016). Polymer formulations have been accurately designed by engineers to meet critical requirements within key industrial sectors, such as the automotive, healthcare and energy production. Therefore, polymer research and development evolves in parallel with additive technologies.

The first example of how additives dramatically improve polymer properties date back to 1839, when Charles Goodyear discovered vulcanisation; a method for adding sulphur to natural rubber, to increase the strength and resilience of the material (Calzonetti et al. 2010). Now, additives can be found in solid

(powders, flakes, beads, granulate, spheres, emulsions), or, more rarely, liquid states (Marturano et al. 2016). The incorporation of additives into the polymer matrix can be carried out at different stages of polymer processing; during the polymer production inside the reactor, during the processing stage of the finished polymer or even directly applied to the surface of the finished product (Zweifel et al. 2009). The top six categories of additives include plasticizers, flame retardants (FRs), impact modifiers, antioxidants, antimicrobials and UV stabilisers. The next sections summarise these and Table 2.1 gives examples and applications of each.

2.2.1. Plasticisers

Plasticisers, defined by the council of the International Union of Pure and Applied Chemistry (IUPAC), are a substance or material incorporated into a material (usually a plastic or elastomer), to increase its flexibility, workability or distensibility. The mechanism of plasticisation involves the formation of secondary bonds between the plasticiser compound and polymer chains, where they act like "spacers", increasing the distance of neighbour chains, hence increasing their mobility (Chanda & Roy 2007). The classification of plasticisers is most commonly based on their chemical composition in two classes: phthalates and non-phthalates. Phthalate plasticisers are not chemically bound to the polymer matrix, so they can leach, migrate or evaporate into indoor air and atmosphere, foodstuff and other materials. Consumer products containing phthalates can result in human exposure through direct contact and use, and indirectly through leaching into other products, or general environment contamination (Guo & Kannan 2012). Two of the most common plasticisers are diethylhexyl phthalate (DEHP) and diisononyl phthalate (DINP), with their structures reported in Table 2.1. DEHP, which remains the most frequently used plasticiser in medical applications, has been substituted by DINP in children's healthcare products. This is because DINP is formed by longer hydrocarbon chains, possesses a higher molecular weight, and therefore presents a lower solubility and slower migration rate (Marturano et al. 2016).

2.2.2. Flame retardants (FRs)

Combustion of polymers leads to the scission of the hydrocarbon chains within their matrix into smaller units, which eventually become small enough to become volatile and be released into the atmosphere. These small units, formed by elements such as nitrogen, oxygen, carbon and sulphur, are potentially harmful (Morgan & Gilman 2012). For this reason, FRs are added to polymer formulations. Over 175 different FRs can be grouped into three major chemical groups: halogenated, organo-phosphorous and inorganic.

- Halogenated FRs only contain chlorine and bromine in synthetic plastic formulations. Brominated flame retardants (BFRs) are by far the most widely used because they are more effective, cost less and have wider application (Marturano et al. 2016). From an environmental

point of view however, the contamination of terrestrial and marine environments with BFRs has been widely documented (De Wit 2002).

- BFRs and phosphorus-containing flame retardants (PFRs) operate in the same way. The mechanism of action occurs in the gas phase, induced by the high combustion temperatures. Hydrogen and hydroxyl radicals are replaced by less energetic radicals or combine to form non-toxic gaseous products. However, PFRs enhance char formation; where during the burning process they produce phosphoric acids, which react with the substrate and produce char that acts as a protection of the substrate itself. The main area of application of PFRs is in polyesters, thermoplastics and polystyrene (PS) formulations (Scharte 2010).

- Inorganic flame retardants (IFRs) typically include aluminium and magnesium hydroxide ($Al(OH)_3$ and $Mg(OH)_2$). The mechanism of action of these compounds differs from the organic FRs. IFRs cannot evaporate by application of combustion heat but decompose into non-flammable gases (mostly water) by endothermic reactions (Posner 2009). Currently, aluminium hydroxide is the most widely used IFR, due to its low cost and good compatibility with most plastic materials, especially PE. The endothermic decomposition of aluminium hydroxide primarily leads to the cooling of the polymer and the formation of a protective layer of aluminium oxide. Moreover, the formation of water vapour decreases the oxygen concentration near the surface, hindering the combustion reaction (Posner 2009).

2.2.3. Impact modifiers

Most plastic materials suffer from excessive brittleness when subjected to stress during their use. Unmodified polystyrene (PS) is brittle at room temperature, while thermoplastics become brittle at lower temperatures. The purpose of an impact modifier is to absorb the impact energy by inducing plastic deformation before cracks in the material can occur. In general, impact modifiers are elastomeric or rubbery in nature, and can be incorporated either in the polymerisation reaction, or as a solid particulate in the processing step as particles. Rubber toughening of polyvinyl chloride (PVC) was introduced in the 1930s and 1940s and involved the addition of small amounts of acrylonitrile-butadiene copolymer elastomer and other elastomeric materials (Seymour et al. 1987) during the polymerisation reactions.

2.2.4. Antioxidants

The resistance of polymeric materials to weathering is a key issue when taking into account the wide range of applications in which plastics are exposed. Weathering does not simply result in discoloration, but also changes in mechanical properties (Marturano et al. 2016). Weathering includes mainly thermal or UV light-induced oxidation, day/night or seasonal temperature variations, humidity or contact with highly corrosive elements in the atmosphere (Kockott 1989). Oxidative degradation, which is further

16

explained in the following sections, can be inhibited by the addition of stabilising additives called antioxidants. Antioxidants are generally classified into two groups, according to their protection mechanism (Rabek 1990):

- Primary antioxidants, also known as chain-breaking antioxidants, are able to scavenge free radicals via a process called chain-breaking electron donor mechanism. Lactones are a class of cyclic esters suitable as alkyl radical scavengers, in particular benzofuranone derivatives, and hindered phenols are very effective even at low concentrations (Meng et al. 2016).
- Secondary antioxidants are able to decompose hydroperoxides forming inert secondary products, and therefore are also known as hydroperoxide decomposers. Their use in combination with primary antioxidants often yields synergistic stabilisation effects. The most widely used classes of hydroperoxide decomposers are organic compounds containing phosphorus and sulphur.

One of the main downsides to these antioxidants is their derivation from oil-based products, together with their potentially harmful interaction within the human metabolism. Naturally occurring antioxidants include the likes of tocopherols, vitamin C and phenolic compounds (Lugasi 1997). Tocopherols are Vitamin E constituents, exclusively synthesised by plants, present in seed oil, leaves and other green parts (Kamal-Edin & Appelqvist 1996), and can act as a chain-breaking electron donor, much like the primary antioxidants described above. Up to this date, the antioxidant activity of several natural products has been reported in both commercial polymers, such as PE (Tátraaljai et al. 2014) and PP (Ambrogi et al. 2011) as well as bio-based polymers, such as PLA (Byun et al. 2010).

2.2.5. Antimicrobials

Bio-stability of plastics is a key factor to consider in polymer formulations, to prevent microbial growth on the surfaces of materials. Antimicrobials are added to polymers to hinder the reproduction of microorganisms. Antimicrobial additives are mostly used in medical and food packaging applications (Marturano et al. 2016). There are two general classes of antimicrobial agents: organic and inorganic. The most common organic antimicrobial agents are organometallic compounds, in particular arsenic-based materials, such as oxybisphenoxarsine (OBPA). Because arsenic is universally perceived as a hazardous compound, investigations for alternative organic antimicrobial agents are growing (Marturano et al. 2016). Inorganic antimicrobial agents use metal ions for their intrinsic biocidal properties. The difference between organic and inorganic antimicrobial agents is that the latter do not migrate through the polymer matrix. An example of an inorganic antimicrobial agent is the use of silver ions, which has long been recognised for its antimicrobial properties, dating back to Ancient Roman times. Their mechanism of action involves the binding of the metal ion to the microorganism's cell

membrane, causing an imbalance in the diffusion in and out of the cell, leading to loss of cell function and eventually cell death (Sharma 2012).

2.2.6. UV Stabilisers

For polymers used for outdoor applications, the absorption of photons of sunlight radiation (including ultraviolet, visible and infrared radiation) is inevitable, and can eventually lead to the oxidative degradation of photosensitive molecules (Yousif & Haddad 2013). Visible and infrared light are relatively benign; therefore photo-stabilisation of polymers involves protection against photo-oxidation reactions caused by high-energy UV radiation (Shalaby 1979). UV stabilisers can be classified into three main classes:
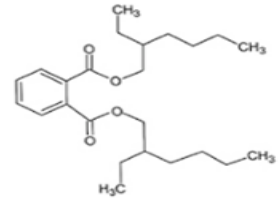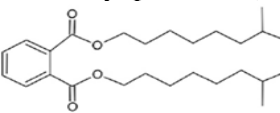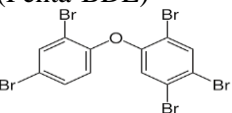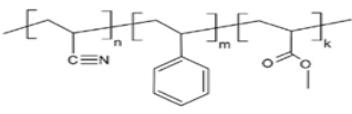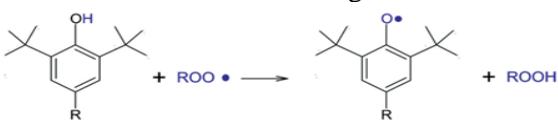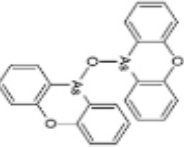
- UV absorbers interact with the first step of the photo-oxidation process by absorbing the harmful UV radiation (between 300 to 400 nm). Black carbon is one of the most effective and commonly used light absorbers, as well as titanium oxide. These compounds provide energy dissipation, a mechanism where UV radiation is converted to harmless infrared radiation or heat that dissipates through the polymer matrix (Yousif & Haddad 2013). These compounds are modified but not destroyed in the stabilisation process.

- Quenchers are a class of UV stabilisers that are able to deactivate photosensitive groups in their excited states before disruption of the molecular bonds can occur (Yousif & Haddad 2013). A quenching reaction is represented in equations 2.1 and 2.2. An excited chromophoric group (a chemical group that absorbs light at a specific frequency and imparts a colour to a molecule) in a polymer (donor, D*), responsible for the initiation step in the photo-degradation process of the polymer, is deactivated by an acceptor molecule (quencher, A) (Rabek 1990):

$$D * + A \rightarrow D + A * \qquad\qquad [2.1]$$

$$A * \rightarrow A + Energy \; (heat \; or \; light \; emission) \qquad\qquad [2.2]$$
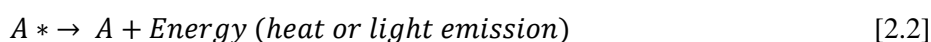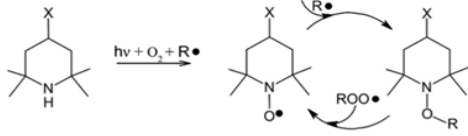
Nickel, for example, is a very effective quencher for carbonyl groups in many thermoplastics. This has been previously tested for photo-stabilisation of polybutadiene, as well as polystyrene (PS) (George 1974).

- Hindered amine light stabilisers (HALS) mechanism of action involves trapping free radicals formed during the photooxidation of the polymer material, hindering the propagation of the photodegradation process (Gijsman et al. 1993). This is also referred to as the Denisov Cycle (Hodgson et al. 2010). Currently, a wide range of HALS products are commercially available, however, they all share the same 2,2,6,6-tetramethylpiperidine ring structure (Bottino et al. 2004).

*Table 2.1: Examples of different polymer additives and their applications.*

| Type of Additive | Example(s) | Applications |
|---|---|---|
| Plasticisers | Diethylhexyl phthalate (DEHP)<br><br>Diisononyl phthalate (DINP)<br> | Both DEHP and DINP are used in PVC plastic types.<br><br>DEHP can be used in shoes, clothing, raincoats, medical devices, tubing and storage bags.<br><br>DINP can be used in teethers and rattles for children, spoons, toys and drinking straws. |
| Flame retardants | Poly-brominated diphenyl ether (Penta-BDE)<br> | PBDEs are predominantly used in electrical and electronic equipment. |
| Impact modifiers | Acrylonitrile-butadiene-styrene (ABS)<br> | ABS can be used to make light, rigid, moulded products such as pipes, automotive parts, wheel covers and even protective headgear. |
| Antioxidants | Phenolic stabiliser deactivating ROO* radicals<br> | These types of antioxidants can be used in plastic types such as PP, PE and synthetic rubbers. |
| Anti-microbials | Vinyzene<br> | An antimicrobial that can be used for bath and kitchen mats, floor/wall coverings and even footwear/shoe soles. |

| UV stabilisers | During UV irradiation, when oxygen (from the air) and radicals (R*) are made available, hindered piperidine, the model compound for HALS, is able to produce hindered peperidinoxy radicals which further trap other radicals in a cyclic reaction:  | Plastic types that are for outdoor use such as PP and PE. |
| --- | --- | --- |

The substances listed in Table 2.1 are intentionally incorporated into the polymer mixtures to give the resultant polymer its desired characteristics. In addition to these added chemicals, other non-intentionally added substances (NIAS) can also be present in plastics (Wiesinger et al. 2021). Volatile emissions can derive from NIAS, which include contaminants, by-products of the manufacturing process, or reaction products of additives that form over the lifetime of the product (Haug et al. 2022). However, NIASs are not yet comprehensively understood, and their identification can be challenging. There is a general lack of transparency regarding substances present in plastics and their concentrations. This is mainly due to limited public accessibility to production information because much of the information reported by manufacturers and distributors is claimed to be confidential business information. Currently, there are several initiatives targeting better communication of information on chemicals in products along supply chains, for example, the EU Sustainable Product Policy Initiative (European Commission 2020).

## 2.3. Volatile Organic Compounds (VOCs)

As explored in the previous section, many different compounds can be incorporated into polymer mixtures through the addition of polymer additives. Some of these compounds, which are not chemically bound to the hydrocarbon chains, can migrate through the polymer and be released from the material into the surrounding environment. Other compounds that are chemically bound to the polymer chains can still be released from the material, after having undergone various degradation processes discussed in previous sections. Many of these compounds can be described as volatile organic compounds (VOCs).

VOCs comprise a large group of chemical species that occur in the air, mainly in a gaseous form. They include alkanes, alkenes, aromatic hydrocarbons, aldehydes, ketones, esters and alcohols. They have high vapour pressures at room temperatures, which result in a low boiling point. The World Health

Organisation (WHO) have defined VOCs with respect to boiling point; Very Volatile Organic Compounds (VVOCs) have boiling points in the range of <0 to 50-100 °C, Volatile Organic Compounds (VOCs) have boiling points in the range of 50-100 °C to 240-260 °C and Semi-Volatile Organic Compounds (SVOCs) have boiling points in the range of 240-260 °C to 380-400 °C (Panagiotaras et al. 2013).

VOCs are not only emitted from polymer materials, in fact, they are ubiquitous in the environment and are also emitted from a wide variety of both natural and anthropogenic sources (Gouw and Warneke 2006). They can be released from different plants and animals in order to communicate or to compete with each other. Some plants release volatile compounds such as β-terpineol, linalool, eugenol and tetradecanoic acid to delay germination and reduce growth of surrounding plants in efforts to give themselves a competitive advantage (Effah et al. 2019). Other natural VOCs such as isoprene, and alpha- and beta-pinene are common compounds occurring from tree species, which have been extensively researched in tropical rainforests (Carvalho et al. 2005). The use of fossil fuels is a large anthropogenic source of VOCs, such as long and short chain hydrocarbons as well as aromatics. In urban areas, vehicle emissions are a large source of outdoor VOCs, which can infiltrate into the indoor environment (Panagiotaras et al. 2014).

Both indoor and outdoor sources contribute to the concentrations of VOCs present in the indoor environment (Bartzis et al. 2008). For some VOC pollutants, their concentrations are found to be higher indoors than out (Carslaw 2007). Indoor VOC pollutant sources can be categorised into primary and secondary. Primary VOCs are directly emitted from the source, whereas secondary species are produced through chemical reactions in the air (Farmer et al. 2019). Indoor primary sources of VOCs include interior furnishings and building materials (Zhou et al. 2019; Ruiz-Jimenez et al. 2022), activities such as cooking and cleaning (Nazaroff and Weschler 2004), microbial and human metabolic emissions (Roberts et al. 2020), consumer products such as self-care products (deodorants, body sprays, etc) (Bari et al. 2015) and candle burning (Bekö et al. 2013) and intentional, and unintentional, ventilation via opening windows and doors allowing outdoor air into the indoor space (Farmer et al. 2019).

Gas phase chemistry occurring inside is a secondary source of VOCs. Chemical processes such as gas phase oxidation, partitioning of semi-volatile species and multi-phase chemistry occurring on surfaces of materials or even airborne particles and dust (Weschler and Carslaw 2018). It should be noted, however, that some surfaces can act as both sources and sinks for VOCs (Carter et al. 2023). Products such as carpets (Hodgson et al. 1993) and polyurethane foam (PUF), which is widely used in offices and homes (Zhao et al. 2004), have been previously investigated for their sink effects due to the sorption of VOCs onto their surfaces. Therefore, the presence of different materials, and their surfaces, can have an impact on the concentration of VOCs indoors.

A variety of volatile compounds can be found within the indoor air, from the numerous sources described in the previous section. Table 2.2 summarises common compounds found throughout the literature.

*Table 2.2: Examples of volatile compounds occurring indoors and their potential sources.*

| Compound | Material emission source | Reference |
|---|---|---|
| Formaldehyde | Particleboard, Medium density fibreboard (MDF) | Jiang et al. (2017), Zhou et al. (2019) |
| | Tobacco smoke | Schaller et al. (1989) |
| Benzene, Toluene, Ethylbenzene, xylene (BTEX compounds) | Tobacco smoke | Hazrati et al. (2016), Wheeler et al. (2013) |
| | Infiltration from outdoor air | Matysik et al. (2010) |
| Phenol | Vinyl flooring | Cox et al. (2002) |
| | Personal care products | Levasseur et al. (2021) |
| Naphthalene | Toilet deodorant blocks | Wan-Kuen et al. (2008) |
| | Moth repellents and air fresheners | Jia and Batterman (2010) |
| Phthalates | PVC Flooring | Afshari et al. (2004) |
| | Released from plasticiser additives from products | Wolkoff (2013) |
| Terpenes | Cleaning products and air fresheners | Nazaroff and Weschler (2004) |
| Chlorinated compounds | Bleach and cleaning products | Arata et al. (2021) |
| | Degrading PVC | Noguchi and Yamasaki, (2020) |
| | Particleboard | Jiang et al. (2017) |
| Aldehydes | Cooking emissions | Arata et al. (2021) |

2.3.2. VOCs emitted from plastics.

Literature is lacking on emissions from degraded or aged plastic types in the indoor environment, but there has been a particular focus on the degradation rates of plastic waste outdoors. It is widely accepted that plastic waste pollution is a global issue, with 400 Mt of plastic waste being generated annually (Chamas et al. 2020). Over half of globally manufactured plastic ends up in landfill or the natural environment (Geyer et al. 2017). The amount of plastic waste entering the oceans has also emerged as a major concern, with large scale concentrated accumulations of plastic found in the South Pacific subtropical gyre and the Eastern Pacific Ocean gyre (Chamas et al. 2020). The general consensus by leading international governmental agencies is that many plastic types can persist in the environment for years, up to a millennia (Ward et al. 2019). Chamas et al. (2020) determined a standardised metric value for specific surface degradation rate (SSDR), in µm per year, to summarise the degradation rates of different plastic types according to their exposure to different environmental conditions throughout the literature, e.g., land (compost/soil), marine, biological and sunlight. From over 100 studies, the highest average degradation rates were found to be plastics exposed to photolytic degradation processes during their exposure to sunlight. However, large variabilities in SSDR values were determined for land, marine and biological environmental conditions, e.g., from 1.6 - 83 µm year$^{-1}$.

Some studies within the literature have investigated VOC emissions from plastic types as they undergo different accelerated ageing conditions. An artificial ageing study of plastic debris was conducted by Lomonaco et al. (2020). After 1 month of ageing plastic samples at 40 °C with a xenon lamp at 750 W/m$^2$, the total amount of emitted VOCs spanned over more than two orders of magnitude among the different polymer types, e.g., from 10 to over 1700 µg g$^{-1}$ for PET and PS, respectively. Royer et al. (2018) demonstrated that environmentally aged low-density polyethylene (LDPE), incubated for 14 days at ambient outdoor temperature (18.5 - 32.5 °C), produced $0.37 \pm 0.11$, $0.14 \pm 0.09$, $0.21 \pm 0.12$, and $0.06 \pm 0.03$ nmol g$^{-1}$ per day of methane ($CH_4$), ethene ($C_2H_4$), ethane ($C_2H_6$) and propene ($C_3H_6$), respectively. Noguchi and Yamasaki (2020) investigated VOC emissions from polymer sheets under thermal degradation over different lengths of time. They found highest emissions, of aromatic hydrocarbons such as phenol, from samples stored at higher temperatures, but the emissions still decreased over time. The authors attributed these VOC emissions to the polymer chains degrading and oxidation reactions occurring (Noguchi and Yamasaki 2020).

A few studies have explored human exposure to VOC emissions specifically from plastic consumer household products, focusing on how the plastics emit VOCs during their intended use indoors, rather than through degradation. Even et al. (2019) quantified aromatic VOC emissions, such as o-xylene, phenol and cyclohexanone, through chamber measurements from four children's toys: three were made from PVC and the other from PE. The softer, more porous, plastics emitted a broader range and higher concentrations of VOCs than harder plastics. The VOC emission rates decreased quickly in the first few

hours or days after unpacking toy samples. Phenol emissions from one of the PVC toys decreased from 594 ng hr$^{-1}$ to 48.5 ng hr$^{-1}$ per sample piece in 5 days and then slowly decreased further, below the detection limits, after 10 days. These VOC emission rates were then diluted into a 30 m$^3$ volume to assess human exposure to these compounds. Compared to indoor air concentration guidelines, no VOC concentrations determined exceeded guideline values.

Palmisani et al. (2020) measured VOC emissions through controlled chamber experiments, from three polymer personal care items (portable electric heating bags; typically used for general comfort and/or therapeutic uses) and scaled the emission rates to a 30 m$^3$ room. Naphthalene emissions were found to contribute to over 80 % of the total VOC emissions from one of the polymer items, over a 72-hour sampling period. In the room-scale simulations, these high naphthalene emissions were found to be 8 times higher than compared to the European Lowest Concentration of Interest (LCI) guideline value. With some of the most documented VOCs emitted from plastics being aromatic VOCs, including the likes of benzene, toluene, phenol and styrene, these will be among the of interest throughout this thesis.

## 2.4. How to measure VOC emissions from plastics

Emissions from materials can be defined as either primary emitents from the physical release of compounds from a product, or secondary emitents, which are compounds produced by a chemical reaction within the product or in the surrounding environment. The level of primary emissions tends to be highest after a material has been manufactured and then diminishes during the days and months that follow; whilst secondary emissions may increase with time and can be long lasting (Brown et al. 2013). Primary emissions from material surfaces can be estimated through experimentation, whereas some secondary emissions can be determined through chemical modelling. Obtaining primary measurements of VOC emissions from plastic consumer products can be determined by the following two steps; sampling and instrumental analysis. Due to the diverse sizes and shapes of such products, as well as their different uses, a one-size-fits-all approach for measuring VOC emissions is not possible (Haug et al. 2022), thus, sampling procedures amongst studies in the literature differ.

### 2.4.1. Sampling methods for VOCs emitted from consumer products.

Collection and determination of VOCs in air samples can be categorised into four main methods; headspace techniques, sampling bags, emission test chambers and alternative methods mainly applied in other fields (Haug et al. 2022). Sampling approaches can also be differentiated between active and passive sampling. In active sampling, a pump is used to draw a defined volume of sample gas, either in a sampling receptacle or over a sorbent material (Dodson et al. 2018). By comparison, passive sampling works without any external influence and relies solely on the diffusion of gaseous compounds from the

sample into the headspace gas and onto a sorbent material (Bartkow et al. 2005; Partyka et al. 2007). The following subsections describe each of the four sampling methods in turn.

2.4.1.1 Headspace methods

The premise of headspace sampling is that volatile compounds, being emitted from sample materials, partition between the surface of the sample and the surrounding gas (Haug et al. 2022). There are several approaches for headspace sampling and analysis, which include static sampling, static enrichment and dynamic enrichment (Kremser et al. 2016). Static headspace sampling is achieved by placing the sample of interest in a closed receptacle (e.g., a sealed glass vial), and allowing an equilibrium to occur between the sample VOC emissions and the headspace gas. An air sample is then extracted from the headspace and injected into an analytical instrument (Kolb et al. 1992).

Static enrichment sampling is a similar approach, however the VOCs in the headspace gas are captured onto a sorbent material. A common approach is solid phase micro-extraction (SPME), which involves putting a silica fibre coated with a thin sorbent film, into the headspace gas of a vial containing a sample, to allow the capture of VOCs via diffusion (Sajid et al. 2019). In dynamic headspace (DHS) sampling, compound extraction typically includes a process of enrichment, which is achieved through using sorbent-loaded thermal desorption (TD) tubes (Kremser et al. 2016). Using this approach, the vial containing the sample is purged with gas, thereby forcing headspace gas to pass through the TD tubes. The depletion of compounds in the vial headspace facilitates further transfer of VOCs from the sample into the gas phase. The amount of compounds sampled depends on the purge flow and sampling time (Wojnowski et al. 2019).

2.4.1.2 Sampling bags

Sampling bags are an alternative technique for sampling VOCs from materials, where the physical sample can be placed inside the bag in order to establish a headspace for subsequent extraction. Sampling can be conducted directly or onto sorbent materials. Before closing the bag, it can be filled with zero-air (i.e., purified air) to establish a clean background into which the VOCs from the sample can emit (Curran et al. 2016). As a passive method, bag sampling does not typically include air exchange. Although the sampling bag approach includes headspace enrichment, sampling cannot be as easily automated as for the headspace sampling methods.

2.4.1.3 Emission test chambers

Figure 2.3 summarises the different types of emission test chambers for VOC emissions testing. Emission test chambers are widely used to investigate VVOC, VOC or SVOC emissions from materials under controlled conditions. An emission test chamber is defined by ISO 16000-9 as an "enclosure with

controlled operational parameters for the determination of VOCs emitted from building products." (ISO 2006). Chambers are usually constructed from inert materials, such as glass or stainless steel. Such materials reduce or remove any influence of the chamber material on the outcome of the test, e.g., acting as a VOC sink, which is particularly relevant when measuring SVOC emissions (Haug et al. 2022). This "sink-effect" is where the volatile compounds that are emitted from a material are adsorbed onto the walls of the emission test chamber (Salthammer 2009). Samples, often cut to a suitable size with a defined surface area from which VOCs are emitted, are placed inside the chamber. Chamber air can be sampled either continuously (e.g., through the use of online analyzers, such as PTR-MS) or after specified periods using TD tubes (with subsequent analysis via TD-GC-MS) (Salthammer 2009).
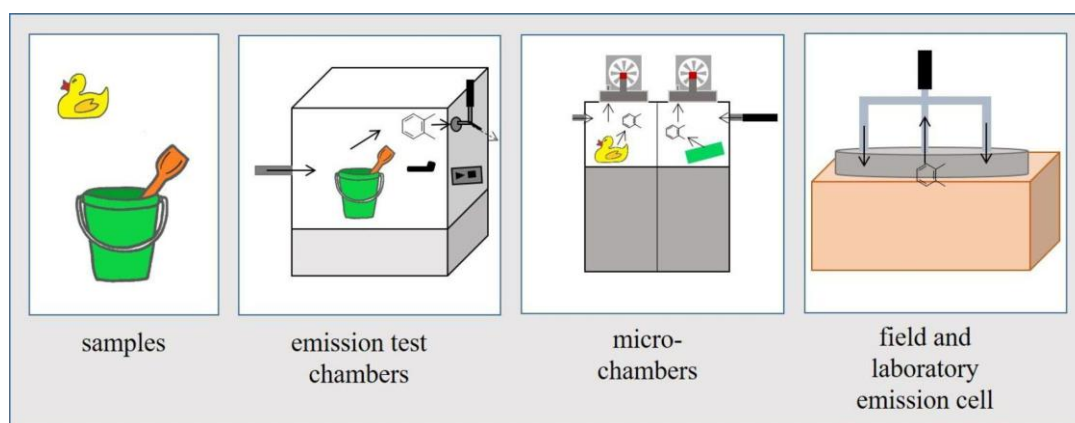


*Figure 2.3: Overview of the different types of emission test chambers that can be used for sampling VOC emissions (from Haug et al. (2022)).*

The most commonly used emission test chambers are small- and large-scale chambers, with sizes ranging from a few $dm^3$ to 100 $m^3$ (Salthammer 2009). Even et al. (2020) compared an emission test chamber (203 L), a desiccator (24 L) and a microchamber (44 mL) to explore the comparability of emissions derived from these different chambers. Similar VOC emission rates were obtained with the microchamber and the 203 L test system within a few hours after loading the chamber, although emission rates were higher in the first hours for the two smaller chambers, especially for the more volatile compounds (Even et al. 2020). The outcome of the study indicated that small emission test chambers were well suited to examine the emissions from small-sized consumer products (Haug et al. 2022).

Microchambers have been developed with the purpose of allowing quick screening of VOC emissions from materials. Schripp et al. (2007) compared six 44 $cm^3$ microchambers with a 1 $m^3$ chamber by assessing the emissions of three different sample materials. A good qualitative correlation between the results from both chamber types was established. Microchambers have been previously used to investigate a variety of materials and their emitents. Studies, such as Nohr et al. (2014) and Mull et al. (2017), have used microchambers to assess the reproducibility of emitting reference materials for VOCs

and SVOCs, whereas Marc et al. (2015) reports the use of microchambers to investigate the emissions of selected mono-aromatic hydrocarbons from children's toys. These particular children's toys were made of polyamide and ABS copolymer, placed in polyethylene packaging in chocolate snacks. The authors concluded from their experimental work that the emissions data obtained from the microchambers is suitable for use in the quality control of everyday objects made of polymer materials (Marc et al. 2015).

As seen in Figure 2.3, another type of emission test chambers are field and laboratory emission cells (FLEC), which were first developed in 1991 (Wolkoff et al. 1991). This type of chamber can be directly attached to the material of interest by mounting it on the surface of the test material to seal the emission cell. Due to its small size and transportability, the FLEC can be brought to the sample site (in situ sampling), which is an advantage over most other emission test chambers (Marc et al. 2012). The FLEC was developed to allow non-destructive, in situ emission testing of VOCs from construction materials (Uhde et al. 1998), such as walls and floor coverings made from PVC (Clausen et al. 2010), floor varnish or carpet (Wolkoff 1998) and painted surfaces (Afshari et al. 2003).

### 2.4.1.4 Alternative methods

Besides the investigations of VOC emissions from consumer products, the release of volatiles is studied in various other settings, such as in relation to building materials and furniture (Marć et al. 2015; Plaisance et al. 2014) or from biological samples and food (Bicchi et al. 2007). Although less commonly used, sorptive tape extraction (STE) is an alternative sampling approach that utilises a tape consisting of a thin polydimethylsiloxane (PDMS) film that is either exposed to the sample headspace or brought into direct contact with the sample matrix (Bicchi et al. 2007). Passive flux samplers (PFS) represent sampling systems for niche applications. The sampling device is similar to a petri dish equipped with an adsorbent material on the inner surface (Marc et al. 2012; Shinohara et al. 2007). The PFS is placed on a flat surface and VOCs emitted from this surface are sampled onto the adsorbent, after which they can be thermally desorbed prior to analysis. Marc et al. (2017) compared emissions of selected VOCs from building materials that were sampled either with a PFS or with a microchamber. Although the use of PFS was deemed advantageous for in situ sampling, stationary chamber approaches were noted as being beneficial when more detailed emissions data are required (Marc et al. 2017).

### 2.4.2. Analytical methods to determine VOC emission from consumer products.

Due to the complex mixture of VOCs emitted from plastic materials, precisely identifying compounds using analytical methods involves separation of compounds, predominantly by their molecular weight. The most widespread approach for the separation of volatiles is gas chromatography (GC) (Marć et al. 2015; Xu et al. 2016). The ability of a GC system to analyse individual compounds depends on the

transfer of these compounds into the system. Volatile compounds that are captured in canisters or absorption tubes must be subsequently liberated, which is usually achieved through thermal desorption (TD) (Jochmann et al. 2014), as the chemical compounds enter their vapour phase (Minaeian 2016). This gas mixture is passed through a column using a carrier gas and heated, with the time taken for the compounds to exit the column known as the retention time. Differences in retention times allow the VOCs to be distinguished from one another (Minaeian 2016). After GC separation, detection of the eluting volatile compounds is most routinely performed using either mass spectrometry (MS) or flame ionisation detection (FID). In GC-MS, analytes are typically ionised via electron ionisation (EI) or chemical ionisation (CI), whereby their characteristic mass spectra are compared to reference spectra to aid in specific compound identification (Bartsch et al. 2016; Even et al. 2021). By comparison, GC-FID relies solely on the retention times of individual compounds in the related GC column but offers the advantage of providing a compound-independent response (proportional to carbon content of the volatile molecule) (Mametov et al. 2021).

An alternative approach is a fast and direct analytical method for the detection of VOCs offered by direct injection mass spectrometry (DIMS). DIMS is based on chemical ionisation and includes proton transfer reaction-mass spectrometry (PTR-MS), selected ion flow tube-mass spectrometry (SIFT-MS) and atmospheric pressure chemical ionisation-mass spectrometry (APCI-MS) amongst others and allows for real-time detection of gas phase VOC concentrations (Beauchamp and Zardin 2017). These VOC detection techniques have high sensitivity, fast response times without the need for extensive sample preparation (Miller 2014). A disadvantage of these DIMS techniques is the inability to distinguish structural isomers, providing only a molecular formula level identification. However, these techniques provide real-time measurements of atmospheric VOCs and match the highly sensitive and chemically detailed snapshot obtained by GC-MS techniques.

Ion mobility spectrometry (IMS), either as a direct measurement, online detector, or as a tool for intermittent analysis when coupled to GC (e.g., GC-IMS), has also been applied to measurements of VOC concentrations. In IMS, analytes are separated based on the mobility of the VOCs within an electric field (Dodds and Baker 2019). IMS has been used in many applications, including on-site environmental monitoring (e.g., screening for contaminants in water and soil) (Armenta et al. 2011), human breath research (Westhoff et al. 2009) and food analysis (Hernández-Mesa et al. 2019).

Beyond chromatographic or mass spectrometric methods, sensors can also be used to detect volatile compounds. A variety of sensors have been developed over recent decades, utilising optical fibres to monitor VOCs in real time with high sensitivity (Pathak and Viphavakit 2022). However, the most significant limitations of these techniques are typically time-consuming, expensive, need of skilled technicians and the requirement of off-site analyses (Pathak and Viphavakit 2022). After considering all of the potential VOC detection techniques, a PTR-MS instrument will be employed throughout the

experimentation stages of this thesis. See methodology section for a detailed description of the instrument used.

## 2.5. Indoor modelling of VOC concentrations

The VOC emission rates from various indoor materials may be considerably different in real world scenarios compared to those obtained through chamber experiments under controlled conditions. Also, there will always be limitations with any experimental instrument used, such as limits of detection of certain gaseous compounds. This is where models can provide us with a better understanding of the chemical processes that take place in indoor air, such as how VOCs degrade through oxidation reactions and also, how the concentrations of secondary pollutants vary over time. Previous studies (Weschler 2004; Weschler and Nazaroff 2008) suggest that the products of VOC degradation following the reaction with hydroxyl radicals (OH), nitrate radicals ($NO_3$) or ozone ($O_3$), may potentially be responsible for some of the health symptoms reported in section 1.1, rather than the primary emissions themselves. Research until recently, has focused on species that are emitted indoors and less on the reactions between them (Carslaw 2007). Air quality models can be used to better understand the indoor air chemical reactions that take place in real environments in the absence of measurements. Such models have been used since the 1980s and have increased in complexity over time.

2.5.1 History and development of indoor air quality models

One of the first indoor air quality models was devised by Nazaroff and Cass (1986), as a general mathematical model for predicting the concentrations of chemically reactive compounds over time in a simulated museum. Concentrations of pollutants were calculated by summing the contributions from all sources such as direct indoor emissions, chemical reactions, entrance through the ventilation systems from outdoors and transport between rooms, and then subtracting losses such as removal through chemical reactions and surface deposition.

$$\frac{dC}{dt} = S - LC \qquad\qquad\qquad [2.3]$$

Where S is the sum of all sources, L is the sum of all sinks and C is the concentration of a pollutant (molecule $cm^{-3}$). These components are used to determine the time derived concentrations (dC/dt) of a compound. The model was used to compare measured concentrations of NO, $NO_2$ and $O_3$ and was in relatively good agreement for $NO_2$ and $O_3$, with 6 % and 3 % difference respectively on average (Nazaroff and Cass 1986). However, their work highlighted the need for incorporation of further detail in the model, such as in the rate of chemical reactions, surface interactions and deposition processes.

A more complex indoor air quality model is the Indoor Chemistry and Exposure Model (ICEM), which was developed to study indoor concentrations of OH radicals by Sarwar et al. (2002). Along with the representation of formation and removal of OH radicals, the ICEM model included indoor emissions and chemical reactions of 51 species, 46 of which were VOCs. It assumed a single well-mixed environment, with half of the indoor lighting originating from sunlight and the other half from artificial lights indoors, with a surface area of 610 $m^2$, a volume of 500 $m^3$, an indoor temperature of 297 K, relative humidity was 50 % and the air exchange rate was 0.5 $hr^{-1}$ (Sarwar et al. 2002). The model showed that the predicted indoor OH concentration under background conditions was 1.2 x $10^5$ molecule $cm^{-3}$, which was within 0.5 % of the predicted concentrations by Weschler and Shields (1996), who used a simple mathematical model to calculate OH concentrations indoors. Sarwar et al. (2002) also found a wide range of secondary chemicals produced through the reaction between $O_3$ and limonene, leading to the formation of compounds with multifunctional groups, e.g., pinonaldehyde and 3-isopropenyl-6-oxoheptanal (IPOH). This led to the recommendation for further research on the production of secondary pollutants through the reactions between VOCs and OH radicals.

A near explicit chemical model constructed by Carslaw (2007) called the INdoor air Detailed Chemical box Model (INDCM) is the most detailed chemical model to date, aiming to replicate the chemical reactions occurring within indoor environments. This model was developed on the basis of the Master Chemical Mechanism (MCM v3.3.1 found at http://mcm.york.ac.uk/), a mechanistic and kinetic dictionary of the degradation of 143 gas phase VOCs, containing over 20,000 reactions and approximately 5,000 species. The MCM was originally developed to describe outdoor interactions of gaseous compounds (Jenkin et al. 1997; Saunders et al. 1999). It was included in the INDCM, along with surface reactions, deposition, emissions and exchange with outdoors. There is no simplification or use of surrogate species or lumping of similar species together in the MCM, which allows detailed understanding of the indoor air chemistry.

The degradation of each VOC in the MCM, is initiated with a radical, ozone ($O_3$), or, where appropriate, direct photolysis, and the species generated following the initiation process can undergo a number of further reactions. These initial processes produce hydroperoxy ($HO_2$), organic peroxy ($RO_2$), alkoxy (RO) and Criegee (R'R''COO) radicals as intermediate species, which themselves react in a further series of reactions until just carbon dioxide and water are produced (Jenkin et al. 1997). A sensitivity test conducted by Carslaw (2007) indicated that indoor photolysis and air exchange rates were the most important factors determining the indoor concentration of OH radicals. Over time, the INDCM model was improved by including gas to particle formation for limonene (Carslaw et al. 2012). Further studies used the INDCM model to investigate the major reaction pathways during high concentration cleaning events (Carslaw 2013), how indoor $O_3$ and particulate matter ($PM_{2.5}$) concentrations vary over summertime, and in particular during intense heat waves in offices (Carslaw et al. 2015), as well as

being used to compare OH and $HO_2$ concentrations in computer classrooms with measured data and during the use of an air cleaner (Carslaw et al. 2017).

2.5.2. Development of INCHEM-Py

Over the past 15 years, the INDCM model has probed the chemistry of indoor air. However, this model relies on specific proprietary software. More recently, Shaw and Carslaw (2021) translated this model into an open source and accessible box-model, to enable its availability to other users. The recent translation into an open-source Python model, as well as including some of the most up to date available kinetic and mechanistic data to help develop degradation schemes for a further suite of VOCs not in the MCM, has led to a new model called the INdoor CHEMical model in Python (INCHEM-Py). The model includes gas-to-particle partitioning for three terpenes, considers outdoor concentrations of pollutants (such as ozone), improved representation of photolysis and surface deposition indoors, and new chemical mechanisms for species created during indoor events such as cooking and cleaning.

INCHEM-Py can be used either alongside experimentation, where it can be used to gain a deeper understanding of results through its ability to track a vast array of species concentrations, or it can be used as a stand-alone method of investigating chemical events that occur indoors (Shaw and Carslaw 2021). INCHEM-Py is continuously being developed and updated, so the most recent version of the model to date (March 2021) will be used in this thesis. An explanation of how the model works is described in section 3.8.

# 3. Methodology

## 3.1. Introduction

This thesis investigates the emission rates of volatile organic compounds (VOCs) from plastics as they are exposed to different abiotic factors. Through a series of laboratory chamber experiments that encapsulated a variety of different plastics, light and temperature response curves were developed and implemented into an indoor atmospheric chemical model. Test chambers of different size and composition were considered for use in experiments. Once the chosen test chambers were established, the plastics were then exposed to typical indoor temperatures and to natural and artificial light. The VOCs were measured using a proton transfer reaction time-of-flight mass spectrometer with quadrupole ion guide (PTR-TOF-MS), which is described in detail in the following sections. The indoor air quality model, INCHEM-Py (Shaw and Carslaw 2021), is used to explore the degradation of VOCs and how the formation of secondary compounds, such as aldehydes, nitrates and others, can have an impact on indoor air chemistry.

## 3.2. Plastic types investigated

Twelve household plastics were selected for experimentation because of their widespread occurrence indoors and are listed in Table 3.1. Six shampoo bottle plastics were selected, because they occur within the top 20 leading shampoo brands used in the UK. All were made with the same polymer type but are different in colour, indicating different polymer additives. The colours included black, white, red, green, orange and blue. The other plastics were a selection of two common food storage containers (one clear and the other white), one clear drinking bottle, a piece of black wiring common to all electrical appliances, a black bin bag liner and a small white tubing piece used for plumbing fixtures around a kitchen sink.

*Table 3.1: Household plastics used for investigation in Chapters 4, 5 and 6.*

| Abbreviation | Material | Intended Use | Colour |
|---|---|---|---|
| HDPE-storage-container-white | High density Polyethylene (HDPE) | food container | white |
| PET-bottle | Polyethylene Terephthalate (PET) | water bottle | clear |
| Rubber-wire | Polyester rubber | electrical wiring cover | black |

| | | | |
|---|---|---|---|
| PP-storage-container-clear | Polypropylene (PP) | food container | clear |
| HDPE-binbag | (HDPE) | bin bag | black |
| PS-tubing | Polystyrene (PS) | tubing | white |
| HDPE-black | (HDPE) | shampoo bottle | black |
| HDPE-white | (HDPE) | shampoo bottle | white |
| HDPE-red | (HDPE) | shampoo bottle | red |
| HDPE-blue | (HDPE) | shampoo bottle | blue |
| HDPE-green | (HDPE) | shampoo bottle | green |
| HDPE-orange | (HDPE) | shampoo bottle | orange |

All of these plastic polymer materials will have additional plasticizers, colourants and other additives, which are included during the polymerisation processes and will contribute to the blend of VOCs emitted from the plastic. All of the plastics listed in Table 3.1 were purchased from local UK retailers between the years of 2019 and 2021. The product content, if any, was discarded and the plastics were each rinsed once with acetone for a few seconds to remove any product residue and then rinsed three times with deionised water to prevent any degradation from the acetone. All plastics were stored separately in zip-lock bags, so as not to cross-contaminate, within a cold room at 4°C in the dark prior to any testing so as to prevent exposure to any thermal- or photo-degradation.

## 3.3. Confirmation of identity of plastic types using ATR-FTIR

To confirm the identity of the polymeric materials of the selected household plastics, the Attenuated Total reflectance-Fourier Transform Infrared (ATR-FTIR) technique was used as a rapid and non-invasive assessment of identification. This technique involves placing a diamond in contact with the polymer sample. An infrared wave of light is passed through the diamond and the surface of the sample.

This evanescent wave provides a very small and specific depth of penetration into the sample before reflecting back into the detector of the spectrometer, displayed in Figure 3.1.
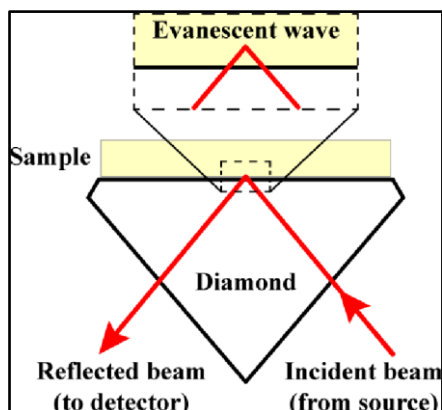


*Figure 3.1: Schematic diagram of how an infrared beam penetrates a sample after passing through the ATD diamond crystal (from Fahey (2017)).*

The diamond ATR accessory used with the FTIR instrument (Agilent Cary 630 FTIR, USA) was a type IIa diamond crystal. Advantages of a diamond crystal are its extreme hardness and chemical resistance. This means hard or abrasive samples can be safely analysed. The diamond in the Agilent ATR accessory is a single-reflection ATR, which is deemed most suitable for high light-absorbing samples such as polymers, rubber and fibres. This single-reflection diamond has a 1 mm diameter sampling surface with 200 μm active area and provides approximately 2 μm depth of penetration for infrared energy at 1,700 cm$^{-1}$.

Firstly, the protruding crystal within the ATR accessory arm and the metal plate below, called the diamond sampling window, are cleaned with isopropyl alcohol. A background spectrum is collected with no sample present. A single plastic sample was then mounted onto the metal plate, below a hanging arm with the ATR crystal. The crystal was then lowered to make contact with the sample, which is held in place by the surrounding metal disk, shown in Figure 3.2. The infrared scan range was set to 375–4000 cm$^{-1}$, with a spectral resolution of 4 cm$^{-1}$. Spectra were acquired in transmittance with 50 scans per sample. Three replicate measurements were obtained for each sample. Before a new sample was loaded onto the instrument, the device was cleaned again with isopropyl alcohol and another background spectrum was taken. Spectral analysis was performed using essential FTIR software, Agilent Microlab, where the background measurement was subtracted from the sample spectra. The sample spectra were then matched to a similar spectra with the Agilent Polymer ATR Library with a quality of fit of over 0.8 (with the highest possible HQ value being 1), a summary of which can be seen in Table 3.2. Figure 3.3 shows an example of a spectrum.

*Figure 3.2: Photograph taken of a plastic sample being analysed by ATR-FTIR.*
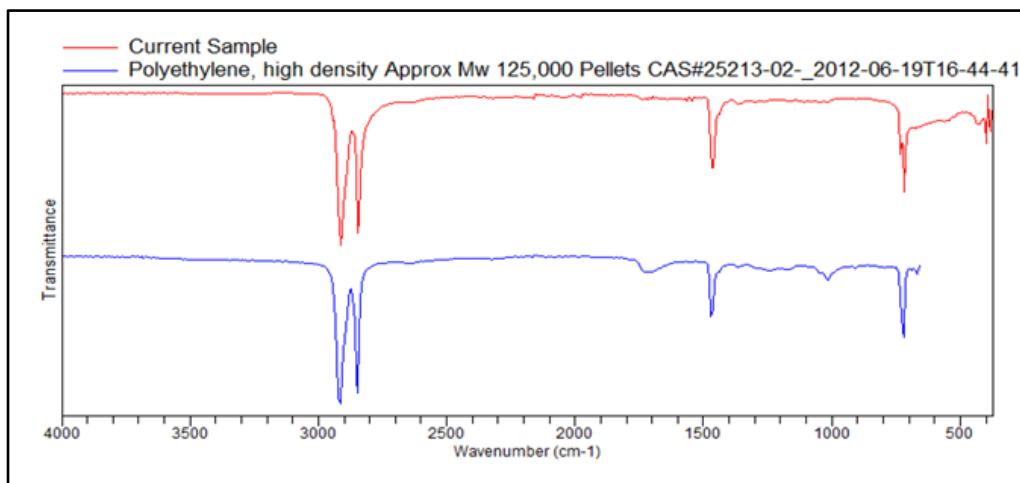


*Figure.3.3: An example spectra when sampling a white HDPE storage container using ATR-FTIR and its match with high density polyethylene library spectra, generated by Agilent Microlab software.*

*Table 3.2: Summary of the identification of the household plastics used throughout this thesis.*

| Plastic sample | Agilent Library Match | Average Reflectance HQ (<0.80) |
|---|---|---|
| HDPE-binbag | ETHYLENE PROPYLENE DIENE TERPOLYMER Ethylene 70% diene 4% Pellets CAS 25038-36-2 | 0.84 |
| HDPE-black | Polyethylene, high density Approx Mw 125,000 Pellets CAS 25213-02-9 | 0.89 |

| HDPE-blue | Polyethylene, high density Approx Mw 125,000 Pellets CAS 25213-02-9 | 0.88 |
|---|---|---|
| HDPE-green | Polyethylene, high density Approx Mw 125,000 Pellets CAS 25213-02-9 | 0.89 |
| HDPE-red | Polyethylene, high density Approx Mw 125,000 Pellets CAS 25213-02-9 | 0.90 |
| HDPE-white | Polyethylene, high density Approx Mw 125,000 Pellets CAS 25213-02-9 | 0.86 |
| HDPE-orange | Polyethylene, high density Approx Mw 125,000 Pellets CAS 25213-02-9 | 0.87 |
| PE-storage-container-white | Polyethylene, high density Approx Mw 125,000 Pellets CAS#25213-02-_2012-06-19T16-44-41 | 0.88 |
| PS-tubing | Styrene acrylononitrile copolymer, Acrylonitrile content 25% Pellets CAS 9003-54-7 | 0.82 |
| PP-storage-container-clear | Polypropylene, isotactic Pellets CAS 9003-07-0 | 0.87 |
| Rubber-wire | Polyester Rubber | 0.91 |
| PET | Polyethylene terephthalate Pellets CAS 29154-49-2 | 0.90 |

All plastic polymer samples were successfully identified with a quality of match fit of over 0.8, with the highest match fit to a library spectra being the polyester rubber wire, with a quality match fit of 0.91. Despite the HDPE shampoo bottles all being made of the same plastic types, their quality of fit varies from 0.86-0.90. This could be the result of additional plasticisers and colourant additives within the polymer structure, obscuring the accuracy of their identification.

## 3.4. Emission chambers

Several chambers of differing sizes and materials were trialled and tested in a series of preliminary studies to identify the most appropriate style of environmental chamber. The ISO (International Organisation for Standardisation) 16000 series provides guidelines for measuring emissions of VOCs within indoor air. The focus of the standard is on emissions from building materials, but also leaves interpretation open by including "furnishings" within its scope. However, consumer products, including household plastic consumer products, are not specified within the scope of this ISO standard (ISO

2006). The recommendation for a chamber size of up to 1000 L, is not suitable for investigations into small household consumer products, as the emissions would be too diluted in the air space and concentrations would be too low to detect.

The possible chamber materials and sizes available for the investigations carried out in this thesis are presented in Table 3.3, along with the considerations both for and against their use in this study.

*Table 3.3: Possible chamber types to use with their pros and cons.*

| Chamber type | Size of chamber | Pros | Cons |
|---|---|---|---|
| Low-grade Stainless-steel tins | 1.5 L | <ul><li>Blocks out all light</li><li>Conducts heat</li><li>Can withstand high temperatures.</li></ul> | <ul><li>VOCs may adsorb to or interact with the sides</li><li>Unable to visually observe the contents of the chamber.</li></ul> |
| PTFE Pots | 50 ml | <ul><li>Blocks out all light</li><li>Conducts heat</li><li>Cheaper material than steel</li><li>Inert material that doesn't interact with VOCs.</li></ul> | <ul><li>Unable to visually observe the contents of the chamber.</li><li>Semi-permeable material</li></ul> |
| Glass flask | 100 ml | <ul><li>Can visibly see contents of chamber</li><li>Low expense</li><li>Easy to cover outside to block out light.</li></ul> | <ul><li>Some wall interactions possible</li></ul> |

The three potential chambers were trialled in a series of preliminary studies, with borosilicate glass flasks (Schott-Duran, Cole-Palmer, UK) found to be the most suitable option. The flask lids contain two 1/8" sampling ports and are made of polyether ether ketone (PEEK), a chemically inert material commonly used for VOC sampling (Deming et al., 2019). The glass flasks come in a range of sizes but the 100 ml jars best minimised the ratio of sample to air volume and hence increased sensitivity.

## 3.5. Proton transfer reaction mass spectrometry

Proton transfer reaction mass spectrometer (PTR-MS) is an instrument used for measuring atmospheric pollutants (Lindinger et al., 2018) and was one of the first instruments to conduct online measurements

of trace gases at parts per billion (ppb) level (de Gouw et al. 2003). It has been continuously developed over the past two decades, with the first PTR-MS using a quadrupole analyser which was capable of unit mass resolution and a response time of 0.2 - 1 second. Now, PTR-MS technology has sensitivities of < 1 ppt levels with response times of < 100 milliseconds (Fischer et al. 2021). These characteristics make PTR-MS an ideal instrument for measuring real-time fluxes of VOCs. One disadvantage to PTR-MS is that it can only determine the nominal mass-to-charge ratio of the protonated product ions, therefore not always allowing for the identification of specific isomers of VOCs (Taiti et al. 2017). However, despite this, PTR-MS technology is ideal for fingerprinting and monitoring VOC emissions in the atmosphere.

### 3.5.1. Operating principles

A proton transfer time-of-flight mass spectrometer with a quadrupole ion guide (model: QiTOF-V104-1, Ionicon Analytik GmbH, Austria) was used to measure the concentrations of VOCs within each of the described chambers above. The PTR-TOF instrument consists of three internal regions: an ion source, a reaction chamber (or drift tube) and a detector, shown in Figure 3.4. A controlled water vapour flow, of 7.0 cc min$^{-1}$, continually passes through a high voltage hollow cathode, where electron ionisation produces positively charged hydronium ions ($H_3O^+$). These primary ions are then accelerated via a small aperture towards the drift tube reactor. Upon entering the drift tube reactor, these $H_3O^+$ ions are mixed with the flow of sample air where they collide and softly transfer protons to neutral VOC molecules (Equation 3.1):

$$H_3O^+ + R \rightarrow RH^+ + H_2O \qquad\qquad [3.1]$$

Here, $R$ represents a targeted compound in the drift tube of the instrument, the $H_3O^+$ is a primary hydronium ion, $RH^+$ is a product ion. The soft ionisation provided by the transfer of protons ensures that there is little fragmentation of the VOC molecules. This allows the majority of compounds to be sensitively detected at their protonated parent ion mass (Roberts et al. 2020). A small number of compounds that cannot be measured are those with a lower proton affinity (PA) than that of water (691 kJ mol$^{-1}$) such as CO, $CO_2$, $O_2$, $N_2$, NO, $CH_4$.
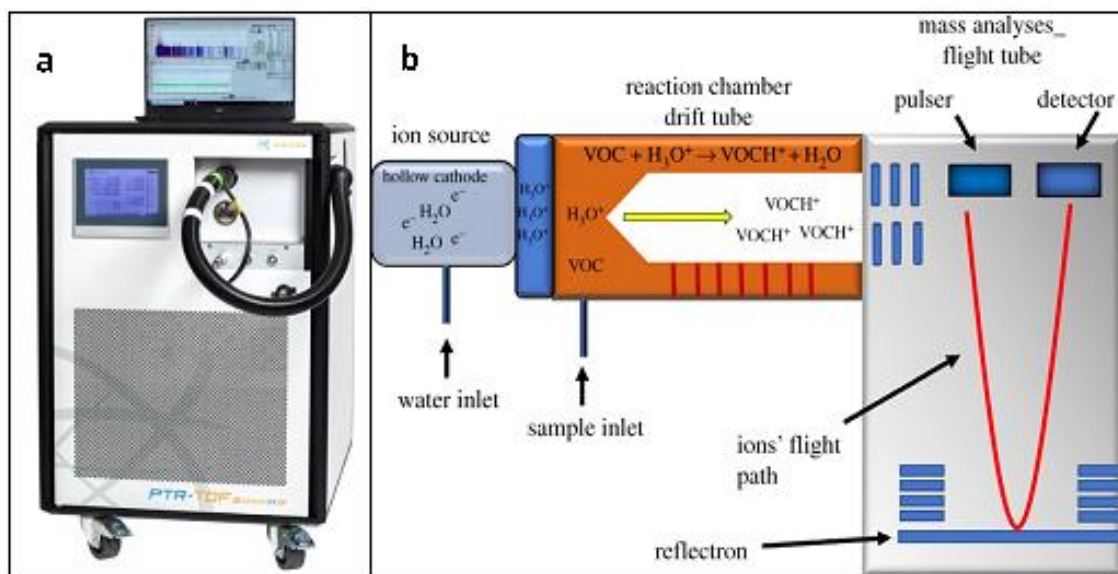
*Figure 3.4**Error! Use the Home tab to apply 0 to the text that you want to appear here.**: a) Image of a PTR-TOF-MS taken from https://www.ionicon.com/. b) Schematic of a PTR-TOF-MS with the ion source (left), drift tube (centre) and flight tube (right). The red line on the right-hand plot indicates the typical flight path of the ions from the pulser to the detector (from Roberts et al. (2020)).*

The mixture of protonated ions is pulsed into a low-pressure time-of-flight tube where they travel in a field-free region, arriving at the detector, a micro-channel plate (MCP) type electron multiplier. The ions are separated based on their molecular weight: small ions travel faster than larger and heavier compounds. The time in which these ions travel through the flight chamber is proportional to their mass-to-charge ($m/z$) ratio, where $m$ = mass and $z$ = charge. The charge always corresponds to $z = 1$ for this ionisation method. The resulting spectra for the PTR-TOF show counts per second (cps) plotted against $m/z$.

### 3.5.2. Operating conditions

Table 3.4 shows the operating conditions used throughout the duration of the studies presented in this thesis. The drift tube pressure, pressure controller and voltages (Udrift, Us, Uso and Udx) control the ionisation conditions within the reaction chamber. They are set to provide the optimal ionising conditions which is explained next.

*Table 3.4: Operating conditions for the PTR-TOF-MS.*

| Parameter | Condition |
|---|---|
| Drift tube Temp | 80°C |
| pressure controller | 325 mbar |
| Inlet flow | 50 sccm |
| *E/N* ratio | 120 Td |
| Drift tube pressure | 3.20 mbar |
| Ion source current | 4.3 mA |
| Voltage across the drift tube (Udrift) | 710 V |
| Voltage in second drift ring for extracting ions from the ion source (Us) | 150 V |
| Voltage in first drift ring for extracting ions from the ion source (Uso) | 80 V |
| Voltage across the ion transfer region (Udx) | 45 V |

The temperature of the PTR-TOF drift tube is kept at 80°C to keep the volatile compounds in their gaseous state, preventing them from cooling and potentially condensing onto the innermost material of the instrument. The Inlet flow determines the flow rate of the air being sampled.

Protonated water clusters, $(H_3O^+).(H_2O)_n$, can form in the PTR drift tube if the collision energies are too low. The water clusters can break up when they have higher kinetic energy, resulting from acceleration in the high electric field, E, or a free path due to reduced particle density, N, or both. This process is known as collision induced dissociation (CID). The ratio E/N is used to measure the collisional energy conditions. The E/N ratio has the SI units V $m^2$ but this is generally given in the unit Td, Townsend, where 1 Td = $10^{-21}$ V $m^2$. Previous work conducted by Miller (2014), found that the optimum E/N ratio was around 115 Td, as it enabled a good compromise between limiting water cluster formations (occurring at lower E/N ratios), and compound fragmentation (occurring at higher E/N ratios).

### 3.5.3. VOC concentration calculations (to ppbv)

### 3.5.3.1 Data processing

The PTR-TOF outputs values of detected ions in "number of ions" corresponding to their m/z ratio. To calculate the VOC concentrations within the chambers containing plastic samples, the flow chart in Figure 3.5 shows how initial data was processed.
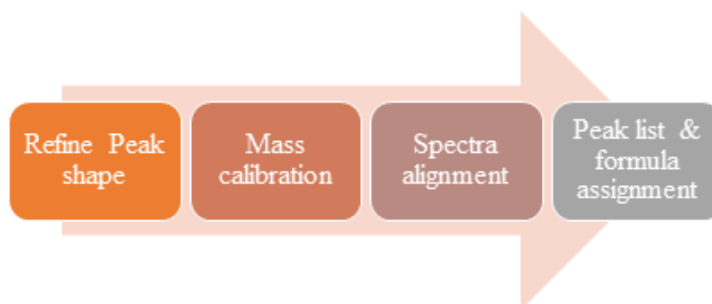


*Figure.3.5: Methodical flowchart of data processing steps.*

A Gaussian shape was the most common peak shape for the detected ions. When refining the peak shape in step one, peaks with obscure shapes and those not falling within the selected Gaussian peak shape were excluded. Mass calibration of the spectra was conducted in step two, where two known peaks, $NO^+$ at m/z 29.9 and $C_6H_5I^+$ at m/z 203.9, were averaged into two minute time periods. The mass spectra alignment was carried out in step three, where the minimum and maximum m/z values were selected as 20 and 450, as no ions found at masses on either side of these values were of interest. Peaks were then matched to a built-in peak list, with a given chemical formula. This, on average, would leave around 1000 filtered peaks. As previously mentioned, one disadvantage to PTR-MS is that it can only determine the nominal mass-to-charge ratio of the protonated product ions, therefore not always allowing for the identification of specific isomers of VOCs (Taiti et al. 2017). However, despite this, PTR-MS technology is ideal for fingerprinting and monitoring VOC emissions in the atmosphere.

The PTR-ToF-MS instrument monitors VOCs as ion count rates per second (cps), which are proportionally respective to the number of ions detected. Therefore, the volume mixing ratios of the target compounds in parts per billion (ppbv) can be calculated. The count rates of the protonated ions per second (cps) in the present work were normalised per one million hydronium ion ($H_3O^+$) count rates to compensate for the variations in the hydronium ions (De Gouw and Warneke 2007). These normalised product ion count rates (ncps) are directly proportional to the concentration of a target VOC (Han et al. 2010).

3.5.3.2 Calculation steps

There are numerous steps to calculating the volume mixing ratio (VMR) of compounds detected by PTR-MS. The first step uses the defined conditions of the drift tube and known kinetics of proton transfer reactions (Wright 2016). The VMR is calculated based on the fundamental physical conditions in the drift tube, such as the pressure, drift tube length, E/N ratio, per Hansel et al. (1995). The next step is the calibration which involves injecting VOC standards of known concentrations, ppb, into the instrument and measuring the signal of the calibrant. These steps are explained next.

Firstly, one must calculate the reduced primary ion mobility ($\mu 0$) within the drift tube of the PTR-ToF-MS, as suggested by (Wright 2016). The reduced primary ion mobility is the weighted average of the isotope $H_3O^{[18]+}$, detected at the peak m/z 21, and $H_3O(H_2O)^+$, detected at the peak m/z 37. This a representation of the fact that during its journey through the drift tube a hydronium ion may gain and lose a $H_2O$ ligand several times (de Gouw et al. 2007). The primary ion mobility is calculated as follows:

$$u_0 = \frac{I_{21} \times 488}{(I_{21} \times 488) + I_{37}} u_{0,19} + \frac{I_{37}}{(I_{21} \times 488) + I_{37}} u_{0,37} \qquad [3.2]$$

Here, $I_{21}$ and $I_{37}$ are the primary intensities in cps for the two peaks. $\mu_{0,19}$ and $\mu_{0,37}$ are the reduced ion mobilities of $H_3O^{[18]+}$ and $H_3O(H_2O)^+$, 2.7 cm$^2$/Vs and 2.3 cm$^2$/Vs respectively. The $H_3O^{[18]+}$ ion peak is an isotopologue, with a signal that is 488 times smaller than the parent ion signal $H_3O^{[16]+}$ detected at m/z 19, hence the multiplication of the $I_{21}$.

Again, this method uses a calibration standard containing a range of VOCs of known concentration. Briefly, the transmission efficiency $Tr_{RH^+}$, of each calibration species, listed in Table 3.5, is determined through the relationship of its $VMR_{RH^+}$ (in ppb) and a number of instrument parameters, as described in the following equation:

$$VMR_{RH^+} = \frac{I^+ \times 10^9 \times U \times \mu_0 \times 22400 \times 1013^2 \times (273.15 + T_d)^2 \times Tr_{H_3O^+}}{k_i \times 9.2^2 \times H_3O^+{}_0 \times P_d^2 \times 6.022 \times 10^{23} \times 273.15^2 \times Tr_{RH^+}} \qquad [3.3]$$

where, $I^+$ is the product ion signal (cps), $10^9$ is included for the conversion from the number density of molecules in the drift tube to ppbv, U is the drift voltage (V), $u_0$ is the reduced primary ion mobility calculation as seen in equation 3.2, 22400 is the molar volume at standard temperature and pressure (cm$^3$), 1013 is standard pressure (mbar), 273.15 is 0 °C in K, Td is the temperature in the drift tube (K) and $Tr_{H3O+}$ is the transmission efficiency of primary ions.

$k_i$ is the reaction rate constant of proton transfer from $H_3O^+$ (cm$^3$ s$^{-1}$), 9.2 is the drift tube length (cm), Pd is the drift pressure (mbar), and $6.022 \times 10^{23}$ is Avogadro's constant (mol$^{-1}$). This equation is

provided in the manual for the specific PTR instrument and is used throughout the experiments in this thesis.

Using the transmission efficiency values ($Tr_{RH^+}$) for each calibrant, a curve can be fitted through the data, see Figure 3.6 and the fit coefficients can then be used to extrapolated to other masses to find the $Tr_{RH^+}$ for other VOCs not in the calibration standard.

### 3.5.3.3 Calibration description

Prior to any recording of experimental data, the PTR-TOF was calibrated with a multi component gas standard (Apel–Riemer Environmental, Inc.) which was diluted using VOC free air (Swissgas Zero air generator). The gas standard contained nine VOCs, which are listed in Table 3.5 together with their concentrations. The zero air and gas standard flow were regulated and maintained throughout the calibration run through a series of mass flow controllers (EL Flow, Bronkhorst, NL), which allowed the gas standard air (10 ml min$^{-1}$) to be diluted into 100 ml min$^{-1}$ with a dilution factor of 0.1. PTFE tubing (1/8" O.D (1/16" I.D.)) was used to transfer the calibration gas mixture directly to the PTR-TOF-MS. The inlet lines were heated to 60°C, to minimise adsorption effects on tube walls. The calibration was run overnight to allow the gases to reach a steady state concentration, with zero air sampled first for seven hours and then the calibration standard for 20 hours.

*Table 3.5: Details of the Apel-Riemer Environmental gas standard used to calibrate the PTR-TOF-MS.*

| Compound Name | Chemical formula | Protonated Mass (amu) | CAS Number | Concentration (ppb) | Uncertainty |
|---|---|---|---|---|---|
| Methanol | $CH_4O$ | 33.033 | 67-56-1 | 939 | ±5 % |
| Acetonitrile | $C_2H_3N$ | 42.034 | 75-05-8 | 982 | ±5 % |
| Acetone | $C_3H_6O$ | 59.049 | 67-64-1 | 964 | ±5 % |
| Benzene | $C_6H_6$ | 79.054 | 71-43-2 | 975 | ±5 % |
| Toluene | $C_7H_8$ | 93.070 | 108-88-3 | 926 | ±5 % |
| o-Xylene | $C_8H_{10}$ | 107.086 | 95-47-6 | 957 | ±5 % |
| 1,2,4-Trimethylbenzene | $C_9H_{12}$ | 121.10 | 95-63-6 | 926 | ±5 % |

| | | | | | |
|---|---|---|---|---|---|
| 1,2-Dichlorobenzene | $C_6H_4Cl_2$ | 146.97 | 95-50-1 | 932 | ±5 % |
| 1,2,4-Trichlorobenzene | $C_6H_3Cl_3$ | 180.93 | 120-82-1 | 921 | ±5 % |

### 3.5.3.4 Calibration curve

Using Tofware software (v.3.2.2) in IGOR and the known concentrations of the nine compounds within the calibration standard, a sigmoid plot was created to form a calibration curve, from which other compound concentrations could be calculated. Similar to the data processing steps above, the peaks observed in the calibration mass spectra are matched with the most appropriate peak shape (Gaussian). A mass calibration was carried out, averaging over both the background and calibration gas spectrum, so that each mass spectrum was corrected to get the best possible calibration result. After these two steps have been carried out, a peak table can then be defined, including all VOC compounds in the calibration gas as well as the primary ion at m/z 21. Using the generated peak table, checks were performed so that each of the calibrated peaks that were found at their protonated masses matched the suggested chemical compound with a probability of over 90 %. Using this generated peak table, the compound formula, name, mass, concentration in ppb, any isotopes, the reaction rate constant between the VOC and hydronium ion (k-rate) (obtained from Zhao and Zhang 2004), and the dilution factor (0.1), the calibration curve can be calculated.

Figure 3.6 shows how a sigmoidal function fits well with the calibration compounds. The average transmission error between m/z 50 and m/z 180 was ± 16.8 %. This sigmoid curve also provided fit coefficients which can be used in the calculations of other VOC concentrations.
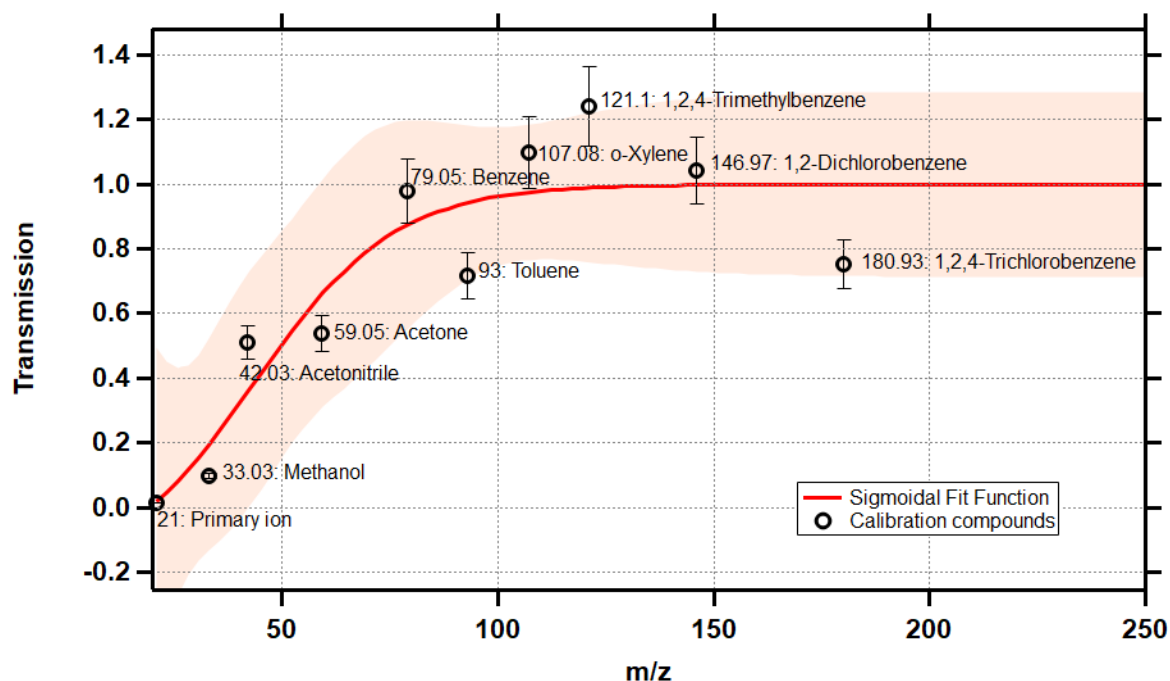
*Figure 3.6: Calibration curve with labelled calibration VOC compounds, plotted in Tofware software.*

3.5.4. Internal calibration

Before the start of each experimental run, a spectra alignment calibration of the PTR-TOF is carried out within the TOFDaqREC software which is based on aligning the mass spectrum to the known exact masses of two selected ions, in this case, $NO^+$ found at mass 29.9 and $C_6H_5I^+$ found at mass 203.9. Once these peaks are located along the mass spectrum, their exact masses are entered, and realignment of the spectra is complete.

## 3.6. Chamber measurements

3.6.1. Experimental set-up

Figure 3.7 shows the schematic diagram of the chamber and instrument set up for all of the experiments performed in this thesis.
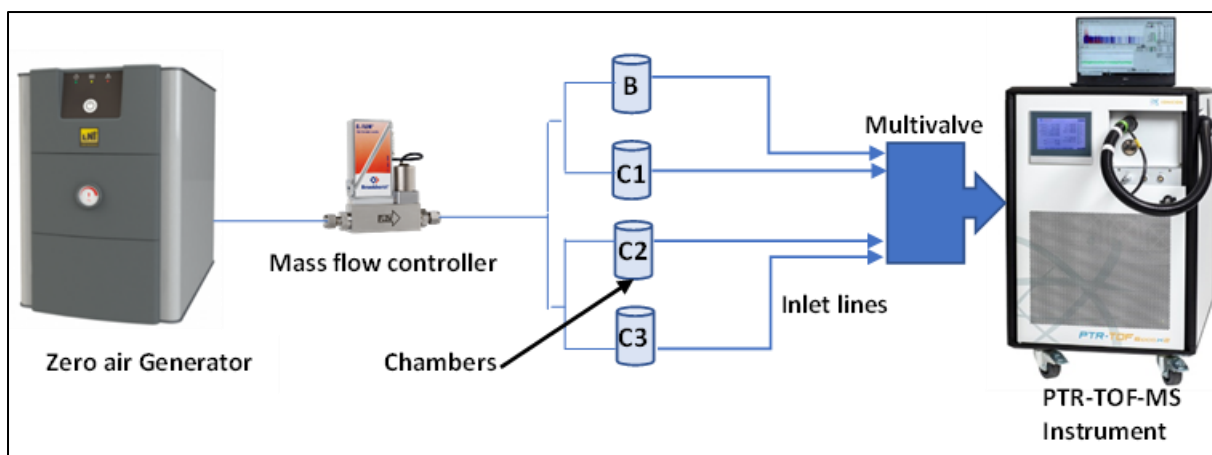
*Figure 3.7: The sampling set up with environmental chambers and PTR-TOF-MS.*

A zero air generator (ZA FID AIR C, Swissgas) was used to provide a source of VOC free air, which was circulated through the four glass chambers. The flow rate was controlled by a mass flow meter (EL Flow, Bronkhorst, NL) at 0.8 L min$^{-1}$, divided equally across each chamber (0.2 L min$^{-1}$), which was verified using a TSI flowmeter (4100 series, TSI, UK) before and after each set of measurements. This Zero Air Generator uses a palladium catalyst, so no water vapour was removed from the filtered air. In fact, due to the combustion of VOCs within the Zero Air Generator itself, water vapour concentration may slightly increase as the combustion of VOCs results in the formation of $H_2O$ and $CO_2$. However, both the temperature and humidity of the air exiting the chambers was monitored by an EI1050 digital temperature/humidity probe (Labjack, USA). The humidity remained consistent throughout all experiments at 50 % ($\pm 5$ %). The sample lines from each chamber were connected to an eight port multivalve (VICI Valco Instruments Ltd., Switzerland) within the instrument. Each port of the multivalve is continuously flushed, allowing the PTR-TOF to sample from any of the four chambers with zero dead volume and minimal carryover.

3.6.2. Sampling method

With four chambers used throughout all experiments, three contained plastic samples and one acted as a blank, containing no plastic. Plastic samples with known surface area were placed into the chambers. The test chambers were rinsed with deionised water three times and baked in an oven at 100°C, volatilising anything that could be detected by the PTR-TOF before the start of each experiment. Further details on the experimental information will be described in individual data chapters.

### 3.6.3. Calculation of VOC concentrations

To convert the calculated ppbv concentrations into an emission rate, the conversion in equation 3.4 was used, and normalised to the plastic sample surface area within the chamber ($cm^2$) in equation 3.5.

$$Conc. = \frac{VMR_{RH+} \times MW \times 273.15 \; x \; 1013}{22.414 \times (T+273.15K) \; x \; 1013} \qquad [3.4]$$

In equation 3.4, the calculation for concentrations (Conc.) in $\mu g \; m^{-3}$ uses $VMR_{RH^+}$ is the previously calculated VOC concentration in ppbv (in equation 3.3), MW is the molecular weight of the product ion, 22.414 mol/L is molar volume of an ideal gas, at standard temperature and pressure, used for calculating the volume of any gas at 1 mole, 1013 Pa is the relative pressure of 1 atmosphere in Pascals and T is the temperature, recorded by the temperature probe.

Emission rates, ER ($ng \; cm^{-2} \; h^{-1}$), of individual VOCs from the plastic samples on a per area basis, were calculated by

$$ER = ((\frac{(C_{average} - B_{average}) \times F}{SA_{sample}}) \times 60) \times 1000 \qquad [3.5]$$

where $B_{average}$ is the average background chamber concentration ($\mu g \; m^{-3}$), $C_{average}$ is the average plastic chamber concentration ($\mu g \; m^{-3}$), F is the flow rate ($cm^3 \; min^{-1}$) and $SA_{sample}$ is the surface area of the plastic sample ($cm^2$). The factor of 60 converts from per minute to per hour and the multiplication of 1000 converts from $\mu g$ to ng.

## 3.7. Targeted compounds of interest

In the interest of specificity, nine selected VOCs of interest were chosen to be the compounds of focus throughout this thesis as they satisfied the criteria laid out in Table 3.6.

*Table 3.6: Criteria for the selected measured VOCs.*

| |
|---|
| 1. The VOCs selected have either been associated with the cause or onset of one or more adverse human health effects, such as respiratory irritations. |

| | |
|---|---|
| 2. The selected compounds of interest have been previously identified as plastic emissions from studies in the literature. | |
| 3. Each compound is known to substantially contribute to its given m/z signal in PTR-TOF measurements. | |
| 4. Each compound's mass falls within the range of compounds used within the external and internal calibration of the PTR instrument ($NO^+$ with a mass of 29.9 and $C_6H_5I^+$ with a mass of 203.9). | |
| 5. The selected compound of interest has a degradation scheme implemented within INCHEM-Py, so that its chemical degradation indoors can be determined. | |

Specific masses, such as masses at m/z 71, m/z 107 and m/z 121, have been excluded from analysis, because these have been identified as m/z ratios where other isomeric compounds may potentially contribute (de Gouw & Warneke, 2007). The selected target compounds have been chosen because they are not confused with another chemical isomer with the same chemical formula. Table 3.7 lists the nine selected VOCs that will be the primary focus of this thesis as plastic emissions. There is, however, still a possibility that non-target compounds may contribute to the selected ion mass peaks during measurements. It should, therefore, be considered that emission rates determined throughout this thesis are upper limits for the plastic polymers measured under these conditions.

*Table 3.7: List of selected protonated VOCs under investigation in this thesis.*

| Protonated chemical formula | m/z measured | Compound ID |
|---|---|---|
| $(CH_2O)H^+$ | 31.018 | Formaldehyde |
| $(C_3H_6)H^+$ | 43.054 | Propene |
| $(C_2H_4O)H^+$ | 45.033 | Acetaldehyde |
| $(C_3H_4O)H^+$ | 57.033 | Acrolein |

| | | |
|---|---|---|
| $(C_6H_6)H^+$ | 79.054 | Benzene |
| $(C_7H_8)H^+$ | 93.07 | Toluene |
| $(C_6H_6O)H^+$ | 95.049 | Phenol |
| $(C_8H_8)H^+$ | 105.07 | Styrene |
| $(C_{10}H_8)H^+$ | 129.07 | Naphthalene |

Despite Naphthalene not meeting the final criteria, point 5, in Table 3.6, this compound was still included in the list of compounds of interest. Although this compound could not be modelled within INCHEM-Py, as it does not have a degradation scheme, this particular compound is very highly cited within the literature examining emissions from plastics and other consumer products as well as its general occurrence in the indoor environment (Halios et al. 2022; Jia and Batterman 2010; Palmsani et al. 2020). It was considered an additional species to report on, as it was believed it would still be a compound of interest to other researchers in the indoor air quality community to understand its emissions from different plastic types.

## 3.8. INCHEM-py model

The emission rates of VOCs obtained throughout the experimental chapters in this thesis will be used to initialise an indoor air quality model, to assess how much impact these VOCs from plastic have on the indoor air chemistry in typical indoor settings. The VOCs released from these plastics undergo further reactions in the atmosphere to produce a large range of complex chemical compounds. A new indoor atmospheric chemical model, devised by Shaw and Carslaw (2021) called the INdoor CHEMical model in python (INCHEM-py), has been reformed from a previous model: the INdoor Detailed Chemical Model (INDCM) (Carslaw 2007). This open source, 0-D box-model has been constructed based upon the Master Chemical Mechanism (MCM v3.3.3), a near explicit chemical mechanism describing the detailed gas phase degradation of VOCs and other intermittent compounds (Saunders et al. 1999, 2003; Jenkin et al. 2003). The full mechanism can be accessed and downloaded from the MCM v3.3 website at http://mcm.york.ac.uk/.

INCHEM-Py assumes a well mixed environment, and predicts indoor gas-phase species concentrations ($C_i$) over time by solving a series of ordinary differential equations in the form:

$$\frac{dC_i}{dt} = \sum R_{ij} + (\lambda_r C_{i,out} - \lambda_r C_i) - v_{d_i}(\frac{A}{V})C_i \qquad\qquad [3.6]$$

Where $R_{ij}$ represents the sum of the rates of reactions involving species $i$ with species $j$ in the gas or particle phase. The indoor-outdoor exchange of species is expressed using $\lambda_r$ as the air change rate (ACR) (s$^{-1}$), $C_{i,out}$ is the outdoor concentration of species $i$ (molecule cm$^{-3}$), and $C_i$ is the indoor concentration of species $i$ (molecule cm$^{-3}$). $v_{di}$ represents the deposition velocity of species $i$ (cm s$^{-1}$) onto indoor materials, $A$ represents the internal surface area (cm$^2$) and $V$ is the total volume of the indoor environment (cm$^3$).

### 3.8.1. MCM and how it works.

INCHEM-py is designed to solve a system of coupled Ordinary Differential Equations (ODEs) which calculate a species concentration at individual time steps, shown in equation 3.6, progressing the chemical compounds through their degradation mechanisms. As previously mentioned, INCHEM-py utilises the MCM v3.3 which includes degradation schemes for 143 VOCs, involving around 20,000 reactions and 5,000 species. Available kinetic and mechanistic data to help develop the degradation mechanisms of VOCs has increased significantly, with various aspects of the tropospheric chemistry of organic compounds being reviewed extensively (Saunders et al. 2003). The MCM uses the latest kinetic and product data where available, or structure activity relationships in their absence (Jenkin et al. 1997).

The first step (process of initiation) of any VOC degradation scheme is the oxidation reaction with either OH, NO$_3$ or O$_3$, and photolysis where relevant. Figure 3.8 shows the complexity which follows the initial oxidation step, as many products can be generated, including RO (oxy), RO$_2$ (peroxy), and RRCOO (Crigee) radicals. These can each undergo a number of further reactions until the final oxidation products of CO$_2$ and H$_2$O are formed – termination steps (Saunders et al. 2003).
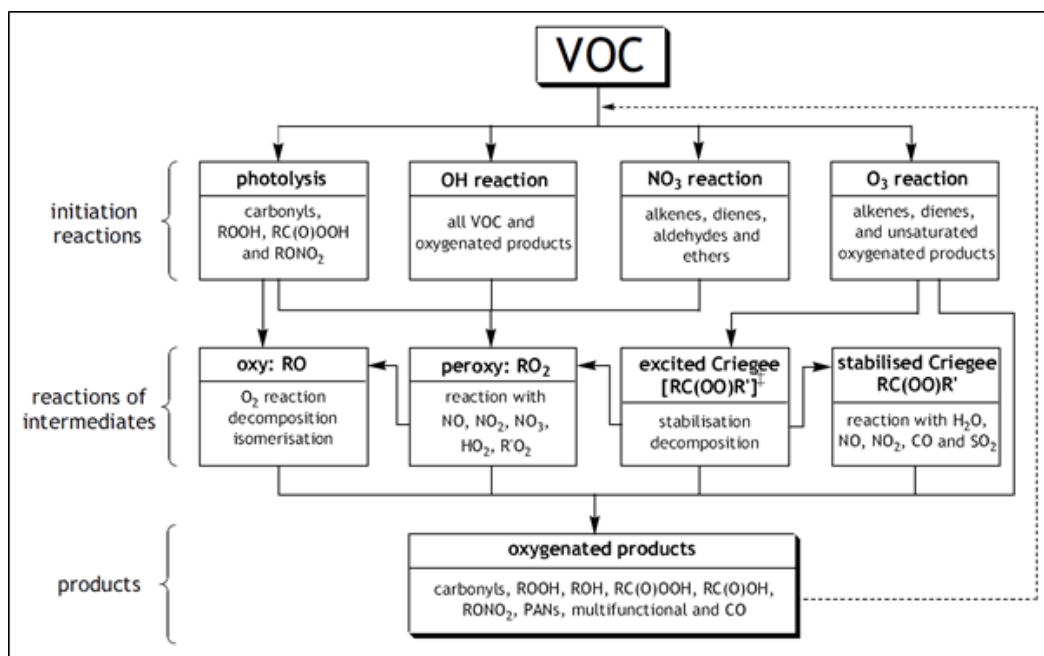
*Figure 3.8: Flow chart showing the degradation process of VOCs within the MCM (from Saunders et al. (2003)).*

To show an example, peroxy radicals ($RO_2$) can be formed through reactions of the hydroxyl radical (OH) with VOC species. All alkanes, alkenes, alkynes and aromatics can react with OH to produce $RO_2$, which themselves can undergo further reactions. The reactions in equation [3.7] show how the OH radical reacts with ethane (a simple alkane).

$$C_2H_6 + OH\ (+O_2)\ \rightarrow\ C_2H_5O_2 + H_2O \qquad\qquad [3.7]$$
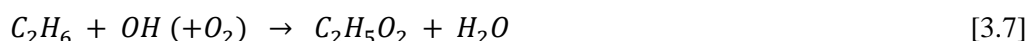
As shown in equation 3.7, ethane will lose an H atom when it reacts with OH. The $O_2$ then reacts with the $C_2H_5$ radical to form $C_2H_5O_2$. Alkenes, alkynes and aromatics also go through degradation reactions with OH. They will all undergo addition of OH to the double bond/triple bond/aromatic ring and then form a peroxy radical following the addition of $O_2$.

The degradation pathways for VOCs continue until the final oxidation products of $CO_2$ and $H_2O$ are produced. These pathways can become increasingly complex as the VOC compound increases in size. For example, methane ($CH_4$) degradation, from its preliminary oxidation step, can be represented by 23 reactions and 17 species. For the next simplest alkane, ethane ($C_2H_6$), a degradation pathway of 120 reactions including 46 species would be needed. Figure 3.9 shows a representation of the degradation pathway for benzene ($C_6H_6$), an alkene with six carbon atoms and three double bonds, involving 148 species and 409 reactions. The different colours represent different oxidation stages. Blues denote the preliminary oxidation steps, with subsequent reaction steps being shown in green, yellow, orange and red.

51
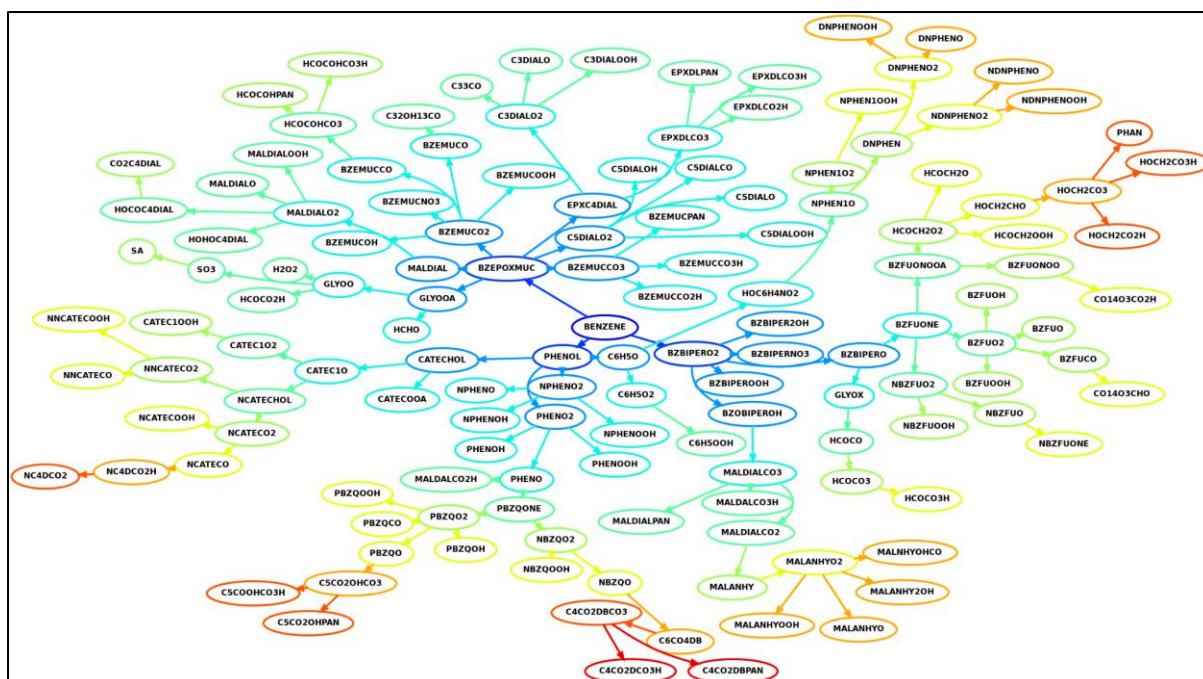
*Figure 3.9: A representation of the degradation scheme for benzene based on MCM chemistry. Note that several smaller molecules (NO₂, CO, HNO₃, OH, NO₃) have been ignored for simplicity.*

<u>3.8.2. Model parameters</u>

INCHEM-py uses additional chemistry mechanisms alongside the MCM input, developed specifically for indoor air. These include gas-particle partitioning, indoor photolysis for attenuated outdoor and artifical indoor lighting, indoor/outdoor exchange, surface deposition and other chemical mechanisms for species potentially created if one wanted to model indoor events such as cooking and cleaning.

Table 3.8 lists the settings that can be adjusted. The specific setting of parameters will be defined in each separate chapter.

*Table 3.8: List of settings available in the INCHEM-Py model.*

| Setting | Format option | Description |
|---------|---------------|-------------|
| Temp | Kelvin (K) | Temperature in degrees Kelvin |
| rel_humidity | Percentage (%) | Relative humidity as a percentage |
| M | Molecule cm$^{-3}$ | Number density of air in simulated environment |
| AER | 0.5/3600 | Air change rate per second |

| | | |
|---|---|---|
| city | "London_urban", "Bergen_urban" "London_suburban" or "Milan_urban_Aug2003" | Four pre-set outdoor measured concentrations for $O_3$, $NO_2$, $NO$ and $PM_{2.5}$. |
| date | "DD-MM-YYYY" | The day of simulation as a string, used in photolysis calculations to work out the angle of the sun. |
| lat | 45.4 | Latitude of simulated location in degrees |
| Light_type | "Incand", "Halogen", "LED", "CFL", "UFT", "CFT", "FT" or "off" | Types of indoor lighting: Incandescent, halogen, light emitting diodes, compact fluorescent lighting, uncovered fluorescent tubes, covered fluorescent tubes and fluorescent tubes. |
| Light_on_times | [light on time(h), light off time(h)] | A light of times when indoor lights are turned on and off. |
| glass | "glass_C", "low_emissivity", "low_emissivity_film" | Types of window glass used for the attenuation of outdoor light by wavelength range. |
| HMIX | 0.02 | Surface to volume ratio. |
| Initials_from_run | True or False | Option to include initial gas concentrations |
| Initial_conditions_gas | "initial.txt" | Text file containing initial species concentrations in molecules $cm^{-3}$ |
| Timed_concentrations | True or False | Changes in forced density at specific time points during a simulation. |
| Timed_inputs | {"species":[start time(s), end time(s), rate (mol $cm^{-3}$ $s^{-1}$)]} | List the species, their times and rates of the forced concentration changes. |
| dt | 120 | Time between outputs in seconds. |

| | | |
|---|---|---|
| t0 | 0 | Time of day, in seconds from midnight, to start the integration. |
| Seconds_to_integrate | 86400 | How long the model will run for (s). |
| Custom_name | "plastics_indoors" | Name given folder to store model run data. |
| Output_graph | True or False | Produces a graph of selected species concentrations. Will also save this data in a csv. |
| Output_species | ['species 1', 'species 2'] | A list of species names plotted on output_graph if set to *True*. |

### 3.8.3. Inputting VOC emission rates into model

To implement the previously calculated VOC emission rates within the INCHEM-Py model, they must be converted to molecule cm$^{-3}$ s$^{-1}$ using the following equation:

$$Molecule\ cm^{-3}\ s^{-1}\ =\ \frac{(\frac{ER \times 10^{-9}}{MW}) \times N_A}{3600} \qquad [3.8]$$

where $10^{-9}$ converts from ng to g, NA is $6.022 \times 10^{23}$ which is Avogadro's constant (molecule mol$^{-1}$), and 3600 converts to seconds giving final units of molecule cm$^{-3}$ s$^{-1}$. The emission rate is multiplied by the total surface area of product found within the indoor environment, to give units of molecule s$^{-1}$. This value is then divided by the volume of the modelled room to give a final emission rate in molecule cm$^{-3}$ s$^{-1}$. Naphthalene could not be implemented into the model as the MCM does not have a degradation scheme for this particular compound.

### 3.9 Conclusion

In summary, the selected plastic types underwent polymer identification to confirm their base polymer type aligned with the product labelling assigned to them, using ATR-FTIR. VOC emission rates from the plastics were obtained through a series of experiments, where plastic sample pieces are encapsulated in glass chambers connected to the PTR-TOF-MS instrument after calibration. These area specific emission rates are then converted into readable model inputs, to initialise the INCHEM-Py model to investigate the secondary pollutant concentrations occurring in simulated indoor environments.

# 4. Temperature driven variations in VOC emissions from plastics and impact on indoor air chemistry.

## 4.1. Introduction

Populations in developed nations spend almost 90 % of their time indoors (Klepeis et al. 2001). Therefore, good indoor air quality (IAQ) is essential for an individual's health and well-being. With energy saving measures and enhanced insulation techniques increasingly being implemented in many UK homes (Ministry of Housing 2019), ventilation with outdoor air can decrease (Vardoulakis et al. 2015). This reduction in airflow through a building can result in increased exposure to accumulated volatile organic compounds (VOCs) from a variety of sources indoors, such as building materials and human activities such as cooking and cleaning (Arata et al. 2021).

VOCs, such as benzene, phenol and naphthalene, as well as very volatile organic compounds (VVOCs) like formaldehyde, have been under scrutiny (Wallace 2001) because of their association with adverse health effects (Even et al. 2019). These health effects include pulmonary effects and irritation of both the eyes and respiratory tract (Jones 2002). Consequently, building materials, including some types of flooring (Cox et al. 2002; Afshari et al. 2004), particleboard and fiberboard (Jiang et al. 2017; Zhou et al. 2019), soft furnishings (Oz et al. 2019) and wooden furniture (Xiong et al. 2019), have been extensively evaluated for their chemical emissions and influence on IAQ (Kruza et al. 2017).

However, there is insufficient research on smaller, common household plastics for the purpose of realistic risk or exposure assessments. Polymeric materials are commonly present within the home setting and are used for a variety of purposes such as food storage, household products, personal-care products, decorative ornaments and construction materials (Haug et al. 2022). These plastic polymers, which have long been assumed to be chemically inert, can release VOCs into their surroundings (Yu and Crump 1998). These VOCs include aromatic BTEX compounds (benzene, toluene, ethylbenzene and xylene) (Hazrati et al. 2016) as well as other smaller hydrocarbon chained compounds such as formaldehyde and acetaldehyde (Xiong et al. 2015). The accumulation of plastic surfaces in the home increases the overall surface area (SA) of polymer materials indoors. To what extent these VOC emissions from plastic surfaces contribute to indoor air quality is not fully understood.

Material emissions can be influenced by environmental parameters within a room, such as temperature. Thermal comfort has been rated as one of the most important components of IAQ for occupant satisfaction within the indoor environment, with air temperature being the main factor (Frontczak and Wargocki 2011; Taleghani et al. 2013). Indoor air temperature is influenced by outdoor climate, season, as well as type of building. Teare et al. (2020) conducted an investigation into the correlation between

indoor and outdoor temperatures in different locations across Eastern Cape Province in South Africa. Indoor temperatures were, on average, 4°C higher compared to outdoor temperatures all year round, especially in the warmest months when the recorded outdoor temperatures were over 35°C. Recent trends in climate change suggest there will be more extreme weather events in the future including heatwaves (Petrou et al. 2019), such as in the UK in July 2022 when temperatures reached 40°C (Met Office 2022). We are also likely to observe higher indoor temperatures in the future. Indoor overheating caused by heatwave events can cause a sharp spike in recorded heat-related deaths among vulnerable groups in the population (Petrou et al. 2019; Gasparrini et al. 2022). Thus, it is vital to consider the effects that these temperatures have on IAQ.

Characterisation of emissions from materials in real rooms can be difficult. Isolation of materials in chambers is a common way of determining emission concentrations (Han et al. 2010), and amplifying these chamber conditions to room size can help give a more accurate representation of materials emissions in more realistic scenarios. Emissions from materials are usually detected using headspace techniques such as solid phase micro-extraction (SPME) and dynamic headspace (DHS) gas chromatography mass spectrometry (GC-MS) (Abe et al. 2013; Even et al. 2019; Singh et al. 2020), despite these being highly time-consuming and also requiring significant sample preparation. In contrast, Proton Transfer Reaction Time-of-flight Mass spectrometry (PTR-ToF-MS) presents an innovative analytical technique for the detection of VOCs. This highly sensitive, easy to use instrument provides emission data in real-time, without the need of sample preparation.

The ISO (International Organisation for Standardisation) 16000 series provides guidelines for measuring emissions of VOCs within indoor air. The focus of the standard is on emissions from building materials, but also leaves interpretation open by including "furnishings" within its scope. However, consumer products, including household plastic consumer products, are not specified within the scope of this ISO standard (ISO 2006). The recommendation for chamber size of up to 1000 L, is not suitable for investigations into small household consumer products, as the emissions would be too diluted in the air space and concentrations would be too low to detect. Some studies have investigated small polymer products such as children's toys and have used large volume chambers (Even et al. 2020). These large chambers can be thought of as a proxy for a child's room, though the emissions typically lead to low concentrations within such volumes and are challenging to measure. For these reasons, others have used smaller chamber sizes where the concentrations can be easier to measure, even if the conditions are less realistic (Masuck et al. 2011). Therefore, the ISO standard guidance may not be applicable to investigations of VOC emissions from household polymers, implying that smaller environmental test chambers are better suited for investigations into VOC emissions from plastics (Even et al. 2020).

This study aims to quantify VOC emissions from different household plastics over a realistic indoor temperature range. Firstly, the polymer type of each plastic sample was confirmed using Attenuated

Total Reflection Fourier Transform Infrared (ATR-FTIR) spectroscopy, the method for which is described in section 3.3. Sub-samples of the plastics were obtained and then subjected to a range of typical indoor temperatures (18-28 °C), with their VOC emissions monitored by PTR-ToF-MS and fit using the Arrhenius equation to calculate temperature dependent emission rates. The determined VOC emissions at two temperatures, 18 and 28 °C, were then used to initialise a detailed indoor chemistry model, INCHEM-Py, for realistic indoor settings. This allowed us to determine the influence of indoor temperature on primary emissions from household plastics and, consequently, the production of potentially more harmful secondary species in a typical home.

## 4.2. Methodology

4.2.1 Plastic Polymers

The plastics used in this study are summarised in Table 4.1. They were all purchased from UK retailers between 2019 and 2020. The age of each plastic from their date of manufacturing, was expected to be over one year at the time of investigation. Six shampoo bottle plastics were selected, because they occur within the top 20 leading shampoo brands used in the UK. All were made with the same polymer type but are different in colour, indicating different polymer additives. The colours included black, white, red, green, orange and blue. The other plastics were a selection of two common food storage containers (one clear and the other white), one clear drinking bottle, a stripped piece of black electrical cable that is typically used to provide power to electronic items (with the internal metal wiring removed), a black bin bag liner (or a garbage bag) and a small white tubing piece used for plumbing fixtures around a kitchen sink.

The product content, if any, was discarded and the plastics were each rinsed once with acetone for a few seconds to remove any product residue and then rinsed three times with deionised water to prevent any degradation from the acetone. All plastics were stored separately in a zip-lock bags, so as not to cross-contaminate, within a cold room at 4 °C in the dark prior to any testing so as to prevent exposure to any thermal- or photo-degradation. A small plastic piece was cut from each product with an approximate length and width of 10 cm by 3 cm (with varying degrees of thickness), to allow it to fit into small environmental chambers. Exact dimensions were determined prior to sampling to enable accurate calculation of the sample surface area (SA). Exact dimensions of the whole plastic products were also measured, providing the total product SA. Plastics samples were handled whilst wearing nitrile gloves, to limit contamination with skin oils.

*Table 4.1: The plastics used in the study, a brief description of their intended use, colour along with the sample surface area (SA) and the total product SA.*

| Abbreviation | Material | Intended Use | Colour | SA-sample (cm²) | SA-total product (cm²) |
|---|---|---|---|---|---|
| HDPE-storage-container-white | High density Polyethylene (HDPE) | food container | white | 32.3 | 1458 |
| PET-bottle | Polyethylene Terephthalate (PET) | water bottle | clear | 23.9 | 415 |
| Rubber-wire | Polyester rubber | electrical wiring cover | black | 46.6 | 1887 |
| PP-storage-container-clear | Polypropylene (PP) | food container | clear | 36.3 | 697 |
| HDPE-binbag | (HDPE) | bin bag | black | 65.2 | 6650 |
| PS-tubing | Polystyrene (PS) | tubing | white | 21.0 | 156 |
| HDPE-black | (HDPE) | shampoo bottle | black | 31 | 392 |
| HDPE-white | (HDPE) | shampoo bottle | white | 52.8 | 392 |
| HDPE-red | (HDPE) | shampoo bottle | red | 29.8 | 550 |
| HDPE-blue | (HDPE) | shampoo bottle | blue | 29.8 | 550 |
| HDPE-green | (HDPE) | shampoo bottle | green | 29.8 | 550 |
| HDPE-orange | (HDPE) | shampoo bottle | orange | 29.8 | 550 |

4.2.2 Instrumentation

A PTR-ToF-MS (Ionicon Analytik GmbH, Austria) was used to measure the VOC concentrations within the chambers, as described in section 3.6 in Chapter 3. In brief, this method is based on ionising trace VOC gases in continuously sampled air in proton-transfer reactions and measuring the concentrations of product ions, using hydronium ions ($H_3O^+$) as a chemical reagent. This soft ionisation prevents significant fragmentation of product ions (so the mass of each resulting ion equals the VOC mass plus one) (Han et al. 2010; Taiti et al. 2017). The instrument monitors the ion count per second (cps), which is proportional to the number of ions detected, allowing the volume mixing ratios of the target compounds to be calculated, see section 3.5.3. PTR-ToF-MS can only determine the nominal mass-to-charge ratio of the protonated product ions, therefore not always allowing for the identification of specific isomers of VOCs (Taiti et al. 2017). However, PTR-ToF-MS technology is ideal for fingerprinting and monitoring VOC emissions from plastic polymers. The operating conditions of the PTR-ToF-MS instrument used in this study are shown in Table 3.4 in section 3.5.2.

4.2.3 Experimental

A schematic for the experimental set up can be found in section 3.6.1, Figure 3.7 and described in section 3.6. In brief, four 0.1 L borosilicate glass lab flasks (the sampling chambers) (Schott-Duran, Cole-Palmer, UK) were used for measurements of VOC emissions from the plastic samples. Before initial use and experimental replicates, these flasks were rinsed three times with deionised water and then baked at 100 °C for 30 minutes, in order to volatilise any residues. These flasks had polyether ether ketone (PEEK) lids containing integrated 1/8" I.D. inlet and outlet ports, allowing them to be connected to a stainless steel multivalve coated with sulfinert, located within the PTR-ToF-MS instrument via PEEK tubing. PEEK tubing is chemically inert and routinely used for VOC sampling. To minimise the adsorption of VOCs, all sample lines were heated to 60 °C using heating tape and insulated with foam pipe lagging. The flasks were housed within a temperature-controlled water bath (TX150, Grant, Cambridge) and covered with an opaque Perspex lid which served to maintain water temperature, block out all light and allow the suspension of the flasks within the water bath.

A zero-air generator (ZA, FID, AIR C, Swissgas), connected via a mass flow controller (EL Flow, Bronkhurst, NL) provided VOC-free air, at a rate of 0.8 L min⁻¹, divided equally across each of four flasks (0.2 L min⁻¹), as previously explained in section 3.6.1. Both the temperature and humidity of the air exiting the chambers was monitored by an EI1050 digital temperature/humidity probe (Labjack, USA). The humidity remained consistent throughout all experiments at 50 % (± 5 %). One of the flasks acted as a blank, containing no plastic samples throughout all experimental runs, whilst the others allowed for three replicates of each sample material. An automation sequence, generated using the PTR software, was programmed to sample from each chamber with a 1-minute sample resolution for a total

of 90 minutes at each set temperature, with an average concentration (in ppbv) calculated using the last 30 minutes. This ensured the internal environment of the flasks reached the set temperature and the VOCs achieved a steady state concentration before measurements commenced. The raw data were acquired using TofDaq software 2016 (Tofwerk AG, Switzerland) and were post processed using Tofware (version 3.2.2.1).

All calculations regarding conversions to emission rates are described in section 3.6.3. Any VOC analytes detected in the empty background chamber were accounted for when calculating the emissions from the plastic samples, as the average background concentrations were subtracted from sample averages.

### 4.2.4 Modelling

To model VOC degradation pathways, the INdoor CHEMical model in Python (INCHEM-Py v.1.1.1) was used (Shaw and Carslaw 2021), as described in section 3.8. For this study, INCHEM-Py was initialised to represent a room with a volume of 20 m³, with a low but realistic air exchange rate with outdoor air of 0.2 hr$^{-1}$, to minimise the influence of VOCs infiltrating from outdoors. It was assumed that there were no indoor lights, but attenuated outdoor light, with outdoor photolysis values obtained from Wang et al. (2022). A constant relative humidity of 50 % was assumed. The model simulations were run for two days to ensure steady-state conditions and results are reported for day two. The plastics investigated within this study act as the only indoor emission sources of the selected VOCs. Although there are clearly other sources, this paper focuses on the impact of the emissions from the plastics. The VOC emissions rates of the twelve individual plastic types, at the highest and lowest experimental temperatures (18 °C and 28 °C), were introduced into the modelled room, and scaled up to a surface area of 8.6 m$^2$ (explained further in section 4.3.3). All other model assumptions are listed in Table 4.2. Particle formation was not considered in these simulations. A total of 26 model variations were simulated with the twelve plastics modelled at the highest and lowest experimental temperatures. Additionally, two background simulations, containing no plastic emissions, were also run to provide comparative baseline concentrations. Secondary pollutant concentrations were averaged between 08:00 and 18:00 hours for all simulations and the relative percentage difference to background compared. The difference, either positive or negative, of pollutants caused by the introduction of the individual plastic-specific emissions provides an insight into which plastic types have the largest influence on indoor air chemistry.

*Table 4.2: Model settings and assumptions.*

| Model settings | Value |
|---|---|
| Relative humidity | 50 % |
| Number density of air molecules | 2.5e+19 molecules cm$^{-3}$ |
| Air change rate with outdoors per hour | 0.2 |
| Chosen city location | "London_suburban" |
| Diurnal outdoor concentrations | True |
| Latitude of simulation | 51.5 |
| Date of simulation | 21-06-2022 |
| Indoor lighting type | None |
| Glass type | "low_emissivity" |
| Surface area to volume ratio | 0.023039954 (cm$^{-1}$) |
| Initial outdoor concentrations for key species (ppb): | CO: 0.13<br>HONO: 0.65<br>OH: 4e-05 |
| Specific outdoor concentrations for London_suburban setting (ppb): | O$_3$: 24.88<br>NO$_2$: 3.40<br>NO: 2.78 |

## 4.3. Results and discussion

4.3.1 Material characterisation

Average reflectance spectra were acquired for each of the plastic polymer materials investigated and were matched to similar spectra contained in a built-in library within the Agilent software. Only those with a Hit Quality (HQ) of 0.8 or higher were considered a good enough fit for identification of the polymer. Things that can potentially contribute to a lower HQ score include intentionally and non-intentionally added additives within the polymer structure. Such additives result in slight spectral differences in the sample spectra compared with the library spectra. However, good quality spectra were obtained, with a few cases where a slight band shift was observed (±10 counts) in comparison with literature values (Saviello et al. 2016). Among the twelve samples, eight were identified as high-density polyethylene (HDPE), one as polystyrene (PS) with acrylonitrile copolymer, one as polypropylene (PP),

one as polyethylene terephthalate (PET) and one as polyester rubber, which was consistent with the original product labelling. The highest match fit to a library spectrum was the absorbance spectra for the polyester rubber wire, with a quality match fit of 0.91. Only the base polymer of the plastics was identified using this method, the polymer additives contained within the material were unfortunately not. Table 3.2 contains the spectral matches for the other plastic polymers the average HQ values.

4.3.2 Plastic VOC emissions

Emission signatures were obtained at each set temperature (18, 21, 24, 28 °C) for the 12 plastic products tested. The PTR-ToF-MS dataset of the sampling time (minutes), normalised ion counts (ncps) which is then converted to concentration (ppb), and the ion masses (m/z). Over 400 different species of VOCs were detected as emissions from the plastic materials. The nine selected VOCs of interest, which are the focus for this study, accounted for 7–8 % of the Total VOC emissions from all plastic types. As an illustration, Figure 4.1 shows the average concentrations of benzene emitted from the HDPE-white plastic sample, at each of the set temperatures, for one of the replicate experiments. There is an increase in the concentration of the detected ion with temperature, from 0.06 ppb at 18 °C to 0.13 ppb at 28 °C, more than a 2-fold increase. Also, Figure 4.1 demonstrates how the VOC concentrations do not deplete during the time of the sampling experiments.
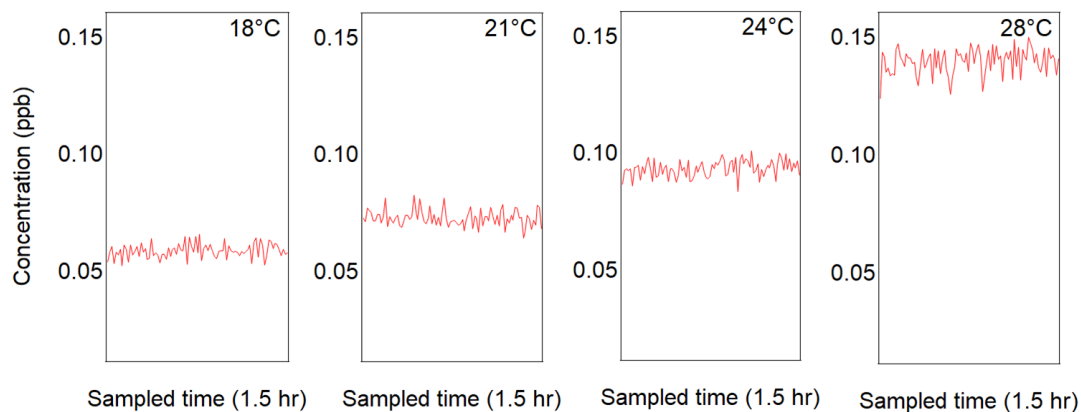


*Figure 4.1: Concentrations of benzene ($C_6H_6H^+$) at each set temperature for the HDPE-white plastic sample.*

Table 4.3 demonstrates the calculated emissions rates from a selection of the plastic types, averaged across the three replicate experiments at the set temperatures.

*Table 4.3: Raw data of calculated emissions rates from the VOCs of interest, averaged over three replicate experiments for temperatures 18, 21, 24 and 28 C, for plastic types Rubber-wire, HDPE-orange and HDPE-binbag.*

| Plastic Type | Temp (°C) | Compounds of interest (VOCs) emission rates (ng cm$^2$ hr$^{-1}$) | | | | | | | | |
|---|---|---|---|---|---|---|---|---|---|---|
| | | Form-aldehyde | Propene | Acet-aldehyde | Acrolein | Benzene | Toluene | Phenol | Styrene | Nap-thalene |
| Rubber wire | 18 | 0.012 | 0.013 | 0.018 | 0.0042 | 0.0078 | 0.0052 | 0.0061 | 0.0089 | 0.0078 |
| Rubber wire | 21 | 0.013 | 0.019 | 0.019 | 0.0054 | 0.0103 | 0.00706 | 0.0090 | 0.013 | 0.0107 |
| Rubber wire | 24 | 0.014 | 0.025 | 0.021 | 0.0060 | 0.013 | 0.0091 | 0.011 | 0.017 | 0.014 |
| Rubber wire | 28 | 0.016 | 0.035 | 0.025 | 0.0076 | 0.017 | 0.012 | 0.016 | 0.023 | 0.019 |
| HDPE-orange | 18 | 0.0028 | 0.013 | 0.0045 | 0.00078 | 0.0043 | 0.0019 | 0.0017 | 0.00304 | 0.017 |
| HDPE-orange | 21 | 0.00069 | 0.018 | 0.0032 | 0.00083 | 0.0065 | 0.0027 | 0.0023 | 0.0045 | 0.0206 |
| HDPE-orange | 24 | 0.0025 | 0.024 | 0.0079 | 0.0014 | 0.0081 | 0.0034 | 0.00401 | 0.0065 | 0.023 |
| HDPE-orange | 28 | 0.0032 | 0.035 | 0.014 | 0.0018 | 0.012 | 0.0051 | 0.0058 | 0.0093 | 0.033 |
| HDPE-binbag | 18 | 0.0012 | 0.0074 | 0 | 0.00016 | 0.0014 | 0.00099 | 0.00073 | 0.0019 | 0.0055 |
| HDPE-binbag | 21 | 0.00011 | 0.0081 | 0 | 7.8E-05 | 0.0016 | 0.00091 | 0.00069 | 0.0019 | 0.0058 |
| HDPE-binbag | 24 | 0.0012 | 0.0095 | 0.0018 | 0.00031 | 0.0019 | 0.00101 | 0.0021 | 0.0023 | 0.0068 |
| HDPE-binbag | 28 | 0.00078 | 0.012 | 0.0013 | 0.00038 | 0.0024 | 0.0011 | 0.0016 | 0.0026 | 0.0088 |

Figure 4.2a shows the VOC emission rates in ng cm$^{-2}$ hr$^{-1}$ from each plastic sample at 21 °C, whilst Figure 4.2b shows the calculated total product surface area VOC emission rates per hour at the same temperature. The calculated emission rates per cm$^2$ have been scaled up to the total SA of the plastic product, found in Table 4.1.
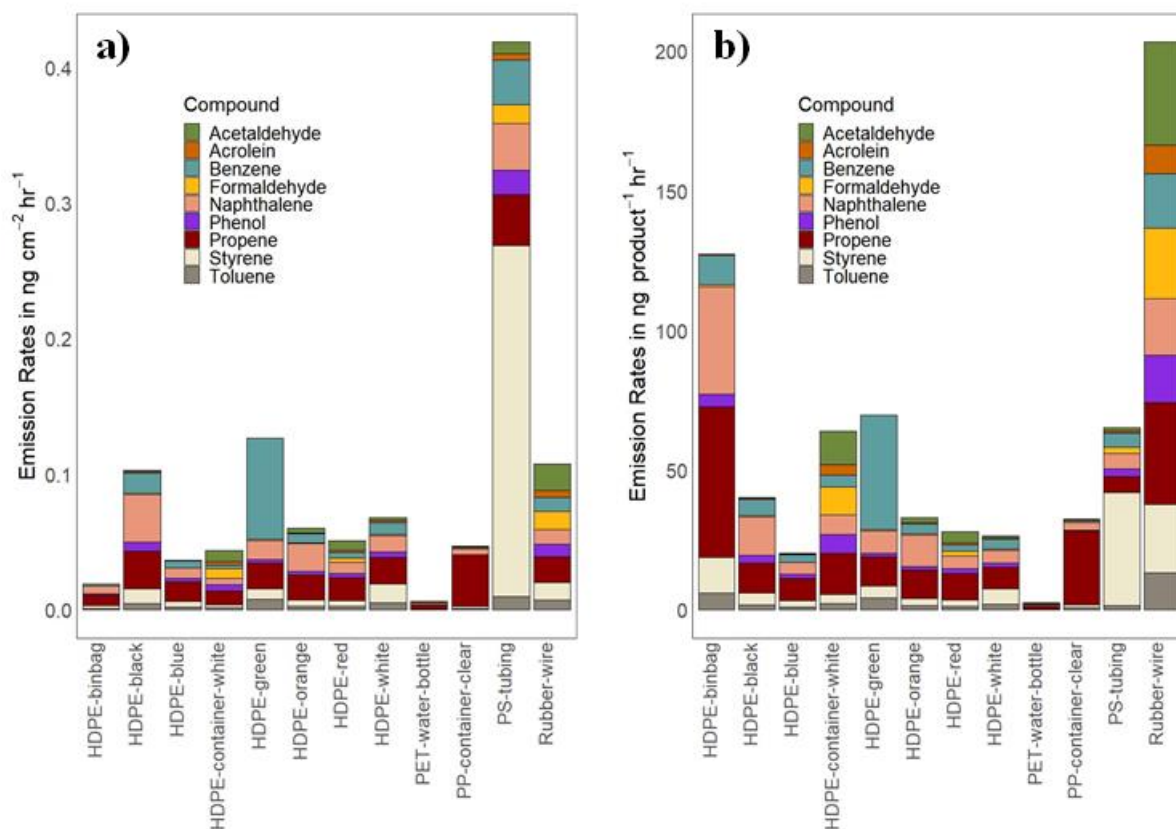
*Figure 4.2: Collective emission rates of all nine VOCs per (a) cm2 and (b) total product SA.*

The PS-tubing plastic proved to be the highest overall emitter of the selected VOCs when compared to the same area of the other plastic types, with styrene accounting for 60 % of the selected VOC emissions. However, when taking into account the total SA of the plastic products, the rubber-wire polymer has the highest emissions of VOCs, as shown in Figure 2b. It has the highest emissions of phenol, acetaldehyde and formaldehyde. HDPE-binbag releases the highest amount of propene and naphthalene. The clear PP-storage-container is the third highest emitter of propene, which makes up nearly 81 % of its total emissions. The PET water bottle plastic shows the overall lowest VOC emissions and did not emit any phenol or styrene.

For emissions from the total surface area of the products (Figure 2b), it might be expected that emissions would be highest from the HDPE-binbag plastic, given it has the largest surface area (6650 cm$^2$). However, the HDPE-green plastic, with a SA of 550 cm$^2$, emits a larger amount of benzene overall than the HDPE-binbag, despite having a much smaller SA. A similar comparison can be made when comparing the PET water bottle plastic (414.29 cm$^2$) to the PS-tubing plastic (115.5 cm$^2$) and the white PE-storage-container plastic (392.25 cm$^2$). Despite the PET plastic having a larger surface area

compared to the PS-tubing and the white PE-storage-container, higher concentrations of nearly all selected VOCs were found to be emitted from the PS-tubing and the white PE-storage-container.

When observing the VOC emissions from the two storage containers, slightly higher overall emissions can be found from the clear PP-storage-container than the white PE-storage-container per cm$^2$, but when considering the larger SA of the white PE-storage-container (over double the size), higher VOC emissions are found from this plastic product in a typical home. Consumers should be wary of the VOC emissions from storage containers, especially when they are involved in storing foods, as many studies have found evidence of volatile compounds migrating from plastic materials upon contact with food substances (Alamri et al. 2021), in particular when they are microwaved (Nerín et al. 2002).

The emission rates determined in this study are found to be lower than many other polymer materials examined throughout the literature. For example, Petry et al. (2013) identified emission rates of formaldehyde and benzene from scented candles to be between 17-109 and 0.4-3.6 µg hr$^{-1}$, respectively under various experimental chamber conditions. Palmisani et al. (2020) identified emissions of aromatic compounds, such as benzene, toluene and styrene, from polyester and PVC heating bags of up to 18, 485 and 70 ng hr$^{-1}$, respectively. These are over a thousand times higher than the values reported here. This may be due to the age of the plastic in the current study being older, >1 year than most of the previous studies. Emissions of VOCs from plastic polymers, and other materials, can change during their lifetime, due to how they are used and what they may be exposed to. Many studies have shown that emissions from polymers are highest, following initial production, and decrease rapidly with time (Lin et al. 2009; Even et al. 2019) to reach a constant emission rate. Even et al. (2020) observed a quick decrease of aromatic VOC emissions through chamber measurements kept at a constant temperature, including o-xylene, phenol and cyclohexanone, in the first few hours or days after unpacking toy samples made from PVC and PE. Phenol emissions from one of the PVC toys dropped from 594 ng hr$^{-1}$ to 48.5 ng hr$^{-1}$ per sample piece in 5 days and then slowly decreased further, below the detection limits, after 10 days. Noguchi and Yamasaki (2020) investigated VOC emissions from polymer sheets under thermal degradation over different time lengths. They found that after 1 day of storing samples at 25, 50 and 75 °C, VOC emissions increased relative to the start of the experiment, but that emissions decreased despite being stored at these three temperatures after 30 days.

4.3.2.1 Temperature-dependency

The temperature dependency of the emission rates (k), in most cases, can be described using the Arrhenius equation, shown in equation 4.1.

$$k = Ae^{\frac{-Ea}{RT}}$$                    [4.1]

In equation 4.1, $A$ is the pre-exponential constant (independent of the temperature), $E_a$ is the activation energy for emission, $R$ is the universal gas constant, and $T$ is the absolute temperature. The natural log (Ln) of emission rates for the nine selected VOCs for the Rubber wire polymer are plotted against the reciprocal temperature in Figure 4.3. The Arrhenius plots for the other plastic types can be found in Figures S4.1–4.11. Where a linear relationship was found the components of the Arrhenius equation could be derived. Temperature response coefficients, generated using the Arrhenius equation, for calculating the predicted emission rates at the selected model temperatures, including the slope, intercept, $R^2$ value and calculated activation energies, are displayed in Table S4.1.

Where there was a non-linear fit the VOC emission rate cannot be fully temperature dependent and the Arrhenius equation does not apply. This was found for VOC emissions from the PET water bottle plastic. This particular plastic was clear in colour indicating it contained fewer additives, therefore its emissions were considerably lower when compared to the other plastic types investigated.
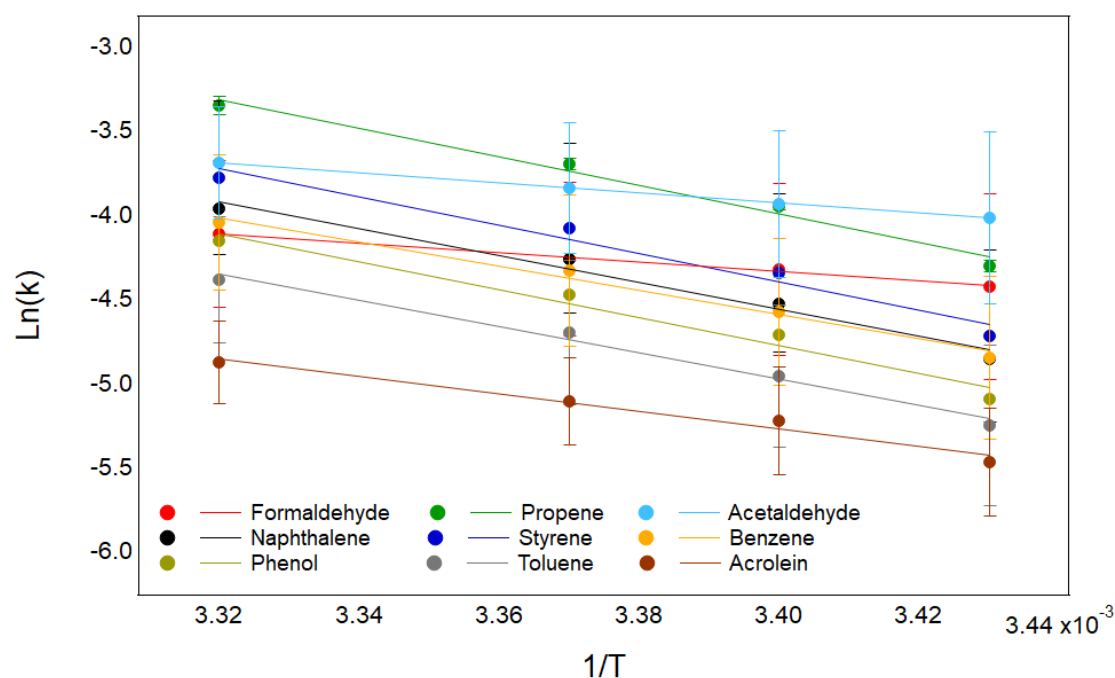


*Figure 4.3: Arrhenius plots for the emission rates of nine VOCs from the rubber wire plastic.*

The increase in emission rates with temperature has been observed by many researchers (Xiong et al. 2013) for other materials commonly found indoors. Myers (1985) reported that the emission rate of formaldehyde from particleboard increased by a factor of 5.2 between 23 and 40 °C. Lin et al. (2009) showed that the initial emission rates and concentrations of toluene and xylene from flooring materials increased between factors of 7.2–17.8 and 1.3–4.0 respectively, when temperatures increased from 15 to 30 °C. Crawford and Lungu (2011) found that styrene emissions from vinyl composite materials used

as building materials increased from 0.127 mg m$^{-3}$ to 0.166 mg m$^{-3}$ from temperatures of 23 to 40 °C within the sampling chambers, an increase of 1.3 times. In the current study, all calculated VOC emission rates increased by at least a factor between 1.1 and 2 between 18 and 28 °C. In some instances, for example acrolein emissions from the HDPE-green and blue plastic sample, emission rates increased by factors of 8.8 and 13.1 respectively, potentially owing to the additives within the polymer structure.

### 4.3.3 Modelling

VOC emission rates, obtained from the experiments, were converted to model inputs for simulations in INCHEM-Py, see section 3.8.3 of the methodology chapter. Initial concentrations of VOCs within the INCHEM-Py simulations were set to zero to match observed gradients from the experiment. A low, but realistic, air change rate with outdoor air was set to 0.2 hr$^{-1}$, with outdoor concentrations of the selected VOCs also set to zero. This was to ensure that the only VOC emissions into the indoor environment were from the plastics.

The World Health Organisation (WHO) determines a safe indoor air temperature to be in the range of 18–24 °C. However, maximum acceptable indoor temperatures vary across the globe, from 25 °C in the UK and the US to 32 °C for countries such as Thailand (Teare et al. 2020). The temperatures used for the modelled scenarios, 18 and 28 °C, were chosen as they cover a range of climates.

A study conducted by Manuja et al. (2019), characterised the surfaces within numerous locations and measured the total areas of different surface types, to a resolution of ~1 cm. From ten bedrooms, nine kitchens and three bathrooms, the average surface area of plastics found in these rooms came to 8.6 m$^2$. The highest surface area of plastic was found to be 43 m$^2$ in one of the office locations, accounting for almost 30 % of all surfaces measured in the room. The average value of 8.6 m$^2$ was selected as the total surface area of each individual plastic for the modelled simulations for this study. It is recognised by the authors that in more realistic scenarios, one would experience the collective VOC emissions from a variety of plastic types. However, the aim of this study is to determine the influence of the individual plastic VOC emission effects on the indoor air chemistry, hence why they have been used to initiate the model simulations individually.

Figure 4.4 shows how the concentrations of radical species fluctuate throughout a 24-hour period, with and without the presence of a plastic surface, e.g. PS-tubing plastic. Throughout the simulated day, the diurnal variation of attenuated sunlight impacts the OH and HO$_2$ radical production. In the presence of PS-tubing plastic, there are lower concentrations of OH, yet higher concentrations of HO$_2$ compared to the case with no plastic. These differences are greater when the temperature is increased from 18 to 28 °C.
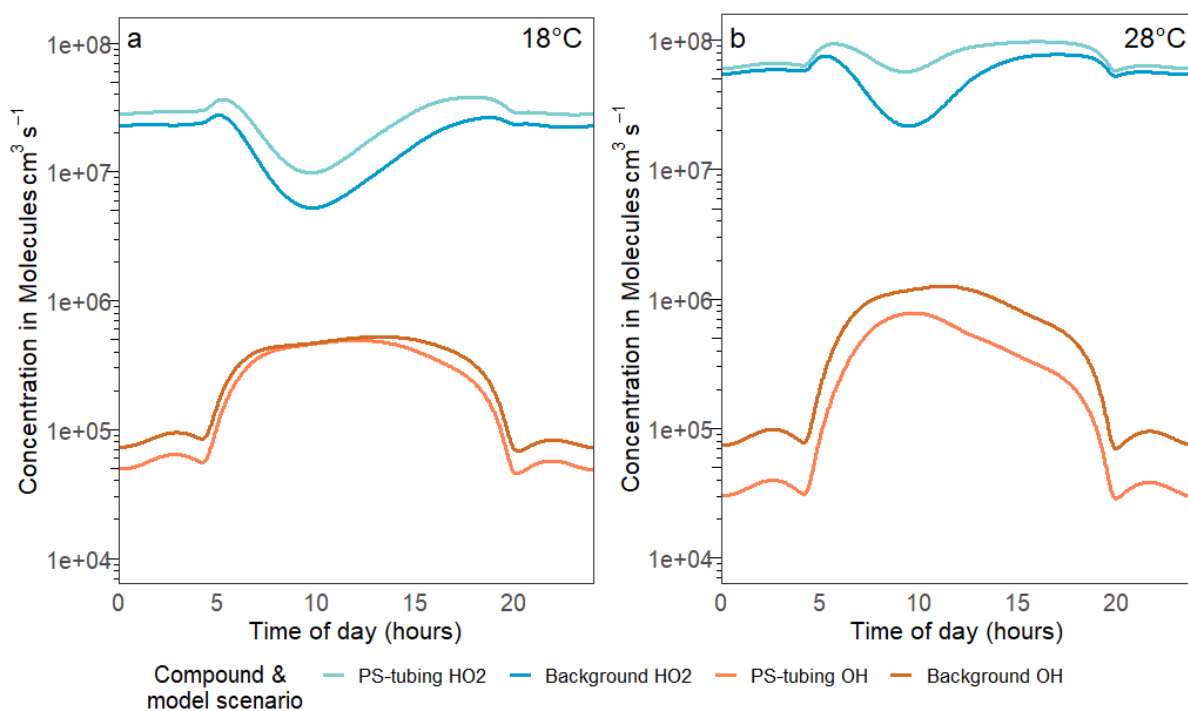
*Figure 4.4: Time series of radical species concentrations in the background modelled scenarios (no plastic content) compared to PS-tubing plastic modelled scenarios at both 18°C (a) and 28°C (b), including OH and HO2 radicals.*

Figure 4.5 shows the percentage difference in concentrations for the modelled species with and without plastic present and for all plastic types investigated. The percentage differences highlighted in green (blue) show an increase (decrease) in concentration in the presence of plastic compared to the absence of that same plastic at the same temperature. As observed in Figure 4.5, as the temperature increases from 18 to 28 °C, there is a greater percentage difference, be it either positive or negative. The introduction of plastics into the modelled simulations provides more VOCs for the OH radicals to react with, in turn, lowering the OH concentrations (Figure 4.4, Figure 4.5). The effect is greater for those plastics with a higher overall VOC rate, such as the PS-tubing.

Concentrations of indoor $O_3$ are primarily driven by exchange with outdoor ozone, which itself is controlled by outdoor nitrogen oxide concentrations. Because of the low air exchange rate of 0.2 air changes per hour, the indoor $O_3$ concentrations only vary slightly with temperature and plastic emissions. The concentrations of NO and HONO decrease in the presence of plastics. HONO is formed through the reaction between OH and NO in our simulations. Given that OH and NO both decrease with the addition of plastics, so does HONO. As plastics are introduced into the system and VOC concentrations increase, there are more peroxy radicals formed (Figure 4.4, Figure 4.5). These effectively titrate NO from the system, decreasing its concentration as plastics are added.

| Plastic Modelled Scenario | O3 | OH | GLYOX | HO2 | HONO | NO | NO2 | HCHO |
|---|---|---|---|---|---|---|---|---|
| HDPE-blue 28C | 0.94 | -4.87 | -1.03 | 6.87 | -0.76 | -4.76 | 0.5 | 15.14 |
| HDPE-blue 18C | 0.43 | -0.54 | 0.64 | 4.53 | -0.09 | -1.27 | 0.17 | 11.69 |
| HDPE-red 28C | 1.13 | -5.88 | -1.73 | 8.16 | -0.91 | -5.66 | 0.6 | 19.61 |
| HDPE-red 18C | 0.5 | -0.66 | 0.59 | 5.28 | -0.11 | -1.48 | 0.2 | 15.61 |
| PET-bottle 28C | 0.14 | -0.65 | -0.21 | 0.96 | -0.11 | -0.68 | 0.07 | 2.27 |
| PET-bottle 18C | 0.16 | -0.2 | 0.12 | 1.67 | -0.03 | -0.47 | 0.06 | 7.48 |
| PE-container-white 28C | 1.09 | -5.73 | -0.7 | 7.9 | -0.89 | -5.48 | 0.56 | 23.75 |
| PE-container-white 18C | 0.37 | -0.55 | 0.87 | 3.92 | -0.09 | -1.11 | 0.15 | 22.5 |
| HDPE-binbag 28C | 0.48 | -2.46 | -0.89 | 3.47 | -0.39 | -2.45 | 0.26 | 7.07 |
| HDPE-binbag 18C | 0.38 | -0.47 | 0.4 | 4.04 | -0.08 | -1.13 | 0.15 | 9.55 |
| PP-container-clear 28C | 2.97 | -15.43 | -10.38 | 22.64 | -2.11 | -14.33 | 1.7 | 41.84 |
| PP-container-clear 18C | 1.11 | -1.48 | -0.64 | 11.85 | -0.23 | -3.23 | 0.45 | 20.27 |
| HDPE-orange 28C | 1.44 | -7.44 | -1.21 | 10.55 | -1.15 | -7.21 | 0.76 | 21.99 |
| HDPE-orange 18C | 0.67 | -0.83 | 1.1 | 7.06 | -0.14 | -1.97 | 0.26 | 18.38 |
| HDPE-white 28C | 1.49 | -7.99 | 0.26 | 10.97 | -1.25 | -7.56 | 0.77 | 23.18 |
| HDPE-white 18C | 0.79 | -0.96 | 1.68 | 8.38 | -0.17 | -2.35 | 0.3 | 18.61 |
| HDPE-black 28C | 1.62 | -8.55 | 0.35 | 12.04 | -1.32 | -8.15 | 0.84 | 22.98 |
| HDPE-black 18C | 0.84 | -1.01 | 1.9 | 8.98 | -0.18 | -2.49 | 0.32 | 15.57 |
| Rubber-wire 28C | 1.71 | -9.29 | 2.28 | 12.78 | -1.45 | -8.7 | 0.87 | 41.95 |
| Rubber-wire 18C | 0.94 | -1.21 | 3.33 | 9.91 | -0.21 | -2.79 | 0.35 | 47.63 |
| HDPE-green 28C | 1.36 | -5.71 | 18.7 | 10.75 | -1.07 | -7.11 | 0.56 | 14.79 |
| HDPE-green 18C | 0.6 | -0.32 | 6.52 | 6.53 | -0.1 | -1.81 | 0.2 | 10.06 |
| PS-tubing 28C | 7.29 | -47.66 | -30.91 | 61.59 | -4.58 | -32.78 | 5.04 | <100 |
| PS-tubing 18C | 6.41 | -10.76 | -0.1 | 76.14 | -1.62 | -18.76 | 2.33 | <100 |

*Figure 4.5: Summary of percentage differences of secondary pollutant species within each plastic-specific modelled scenario from their respective temperature background simulations.*

In the majority of the model simulations displayed in Figure 4.5, the plastic content affects the concentrations of secondary species, such as $O_3$, $NO_2$ and HONO by <5 %. HCHO is both emitted from the plastics and also created through secondary chemistry, which is why there is a larger deviation from the background compared to the other secondary species.

In more realistic settings, a large contribution to indoor air VOC concentrations is outdoor sources of air pollution, which infiltrate through air exchange (Carslaw and Shaw 2019), i.e., through windows and doors. Outdoor concentrations of aromatic compounds, such as benzene, toluene, phenol and styrene, can typically be a few ppb. Depending on the outdoor concentrations of these species, ventilation may provide larger contributions to the indoor concentrations of the VOCs than emissions from plastics. Indoor activities such as cooking and cleaning will also have a larger impact than

emissions from the plastics. Therefore, the impact of VOC emissions from plastics will depend on the specific conditions and activities within the building.

Note that the rubber wire product is associated with electronic items, which can become warm during use, causing elevated air temperatures in their immediate vicinity, which in turn can lead to increased VOC emissions. Additionally, the white PE container product and the clear PP container product are both examples of food storage containers that can be used when heating foods in the microwave. This is another example of where elevated temperatures surrounding the plastic products would cause VOC emissions to be increased (Nerín et al. 2002). The same could also be the case for any of the plastic products left on a windowsill in direct sunlight (perhaps in a bathroom), where elevated temperatures could increase VOC emissions, potentially causing hotspots of VOC concentrations.

This work has shown experimentally that VOC emissions from plastics increase with temperature, owing to the migration of chemical compounds from the bulk polymer to the surface which then diffuse into the surrounding air. This in turn impacts the secondary pollutant concentrations present in indoor air as shown through our model simulations. When comparing these experimental and modelled concentrations of VOCs to values outlined in the UK Public Health England (PHE) guidelines for indoor air quality (Public Health England 2019), the determined concentrations did not surpass the limit values for acetaldehyde, benzene, formaldehyde, styrene and toluene. However, the guidelines are limited by the number of VOCs listed and also acknowledge the lack of consideration of the combined effect of the presence of VOCs in indoor air. As demonstrated in this work, products emit mixtures of substances, some of which currently have unknown health effects. Moreover, it should be acknowledged that consumer products only represent an additional source to other material emissions and human activities that contribute to poor IAQ.

### 4.3.4. Limitations

From the emission rates obtained in this study, it is challenging to identify the origin of the compounds being emitted, without knowing the composition and quantities of the additives within the plastic polymer itself. This information, as well as the manufacturing process for these selected plastic types, is not available, an issue for many other studies (e.g. Wiesinger et al. (2021)). The variability in VOC emission rates observed in this study could therefore be due to the additives present in the plastic polymer matrix, non-intentionally added substances (ending up in the polymer mixture during the manufacturing process) or simply variability with the batch production of the individual items.

The authors recognise that the nine VOCs of interest only make up a small percentage of the overall total of compounds emitted from the plastic types, and that ~90 % of emitents are not accounted for in the model simulations. It may be possible that compounds in the remaining 90 % have an influence on

the atmospheric chemistry indoors. However, their chemical degradation cannot be determined within the INCHEM-Py model, as they do not have a degradation scheme associated with them. This makes it challenging to account for the entirety of VOC emissions from plastics. A sensitivity test was carried out to attempt to account for the 90 % of VOCs that were not input into the model. Alkene and aromatic species were determined as the highest contributors to the total VOCs emitted that were unaccounted for in the model, at 25 % and 30 % of the total respectively. Therefore, propene was used as a proxy for this additional alkene emission, and the 4 aromatic species in the model (benzene, toluene, phenol and styrene) as a proxy for the additional aromatic species. Increasing the VOC emission rates had a larger impact on the secondary chemistry as would be expected, with the major impacts on the hydroxyl radical concentration (71 % decrease compared to the case with no plastic emissions), and formaldehyde (188 % increase compared to the case with no plastic emissions). Clearly, a deeper understanding of both the identification of chemical species emitted and their subsequent degradation pathways is needed .

The authors also recognise that the scaling of VOC emission rates into modelled rooms has its limits. The aim of the model runs was to simulate the conditions of a typical room, rather than reproduce conditions in the chamber. The results from the chamber experiments were used to calculate emission rates per $cm^2$ of plastic, correcting for the chamber conditions. Also, as previously mentioned, in more realistic scenarios, one would experience the cumulative effects of a variety of plastic VOC emissions indoors, however this study focuses on the individual plastic VOC effects on the indoor chemistry.

## 4.4. Conclusion

This work demonstrates a method for determining emission rates of VOCs from plastic products using a proton transfer time-of-flight mass spectrometer (PTR-ToF-MS) and flow through chambers (glass flasks). The individual emission signatures from the twelve selected plastic types showed a wide degree of variation, owing to differences in polymer type and the presence of additives in the polymer structures. Almost all selected VOC emission rates in this study increased with temperature, with the aromatic compounds (e.g., benzene and styrene) showing the strongest response. Differences in emission rates were observed between the plastic types, even between those with the same base polymer.

The modelled scenarios, using INCHEM-Py, provided an insight into the detailed indoor air chemistry as a result of introducing a variety of plastics into a room. The production of secondary pollutants such as $NO_2$, $HO_2$, $O_3$, HCHO and to some degree glyoxal, increased with temperature at varying rates across the different model simulations. However, for OH, NO and HONO, the opposite was found, as these species are removed from the system through oxidation reactions. Future research will focus on

investigating other abiotic factors influencing VOC emissions from common household plastics, such as exposure to sunlight and indoor lighting, as well as how the age of the plastic influences VOC emissions.

# 5. How does visible and UV light influence the VOC emissions from selected plastic products and the subsequent chemistry within the indoor environment?

## 5.1. Introduction

The interaction between solar radiation (e.g. ultraviolet and visible light) and plastic materials in an indoor setting is a relatively unexplored research area in the indoor air quality field. Plastics are ubiquitous in the home and workplace, and exposure to light, especially ultraviolet (UV) light, can cause photo-oxidative degradation, which results in the breakdown of the hydrocarbon chains in the polymer backbone (Yousif and Haddad 2013). This decomposition leads to the formation of airborne free radical species, reduces molecular weight and causes deterioration of the mechanical properties of the material itself. Photo-degradation of plastics in the outdoor environment, presents a threat for humans, as well as ecology, in various environments including terrestrial and aquatic systems (Ward et al. 2019; Uheida et al. 2021). However, no study to date has investigated the influence of solar radiation on plastic emissions indoors and the subsequent photolysis of these compounds in the indoor environment, where humans typically spend 90 % of their lives (Klepeis et al. 2001).

The role of photolysis indoors has not always been considered or recognised in the same way as photolysis outdoors in ambient air (Zhou et al. 2021). Nazaroff and Cass (1986) were the first to recognize the importance of indoor photolysis. The authors used a simple mathematical model to show that increased photolysis rates enhanced the rate of chemical reactions, producing higher concentrations of reactive species. Carslaw (2007) used a detailed chemical box model to investigate the indoor air chemistry of a typical urban residence in the UK and showed that the levels of light indoors were a determining factor for model uncertainty when simulating OH concentrations. Whilst assuming that UV and visible light were transmitted indoors at 3 % and 10 %, respectively, the simulated indoor OH concentration was ~$4 \times 10^5$ molecule cm$^{-3}$. However, this concentration increased by 281 % when UV and visible transmission increased to 27.5 % and 75 %, respectively. These higher simulated OH concentrations were confirmed by the measurements of Alvarez et al. (2013), who measured up to 1.8 $\times 10^6$ molecule cm$^{-3}$ of OH in a school classroom in Marseille, when light shone directly through a window and photolysed nitrous acid (HONO) to produce OH.

The propagation of solar radiation (e.g., sunlight) indoors is predominantly controlled by season, latitude on the Earth's surface, and level of cloudiness Crawford et al. (2003). The Earth's orbit around

the sun and the declination angle (the angle between the equator and the plane of the Earth's orbit around the sun) determine the variations in seasons (Blocquet et al. 2018). The summer solstice in the northern hemisphere corresponds to the maximum declination angle of +23.45°, and the summer solstice in the southern hemisphere corresponds to the minimum declination angle of -23.45°. Thus, an identical building, with the same indoor activities, could have completely different concentrations of species depending on its location on the Earth and the time of year (Wang et al. 2022).

Photons of light that infiltrate indoors can be absorbed and/or scattered by indoor materials. Almost all solid materials will scatter light and absorb energy from photons. This absorbed energy, at certain wavelengths, can disturb the molecular structure or additives within the material (Yousif and Haddad 2013). Types of radiation can have different wavelengths: Infrared (700-1000 nm) and visible light (380-750 nm) have longer wavelengths, whilst UV (400-100 nm) light has shorter wavelengths. This shorter wavelength light has higher energy that can interact with the electrons in chemical bonds of materials, such as plastics. Such interactions can transfer enough energy into an electron to remove it from that chemical bond, causing bond breakage through a process called chain scission (Zou 2014). Results of chain scission include embrittlement, discoloration and can even affect the physical properties of polymers (Zou 2014).

When chain scission occurs in a plastic polymer, it can lead to the release of a variety of volatile organic compounds (VOCs), including aromatic BTEX (benzene, toluene, ethylbenzene and xylene) compounds, as well as other smaller hydrocarbons such as acrolein and acetaldehyde (Even et al. 2019; Kang et al. 2020). These VOCs can react with and can be broken down by radical species, such as hydroxyl (OH) radicals, and through photolysis, lead to the formation of smaller secondary compounds, such as formaldehyde (Atkinson and Arey 2007). The diurnal oscillation of light entering an indoor environment can cause fluctuations in photolysis and therefore the concentrations of secondary species can also vary.

In the outdoor environment, photodegradation reactions result in the production of not only OH radicals, but also hydroperoxyl ($HO_2$) and other organic peroxy ($RO_2$) radicals. These radical species can react to form a wide range of compounds in the atmosphere (Wang et al. 2020). Figure 5.1 demonstrates the reactions that take place to form these radicals. Within the indoor environment, the absence of strong sunlight and washout means these oxidation species have a much longer lifetime (Carslaw et al. 2017). Artificial light sources indoors include xenon arc lamps, fluorescent lighting, and sun lamps (Shah 2007). Light indoors, either artificial or filtered sunlight through a window, does not typically contain photons at the short wavelengths (290-330 nm), which are responsible for a large proportion of photolysis outdoors. In fact, indoor photolysis was not even considered an important source of oxidants until recent studies demonstrated that indoor sources of light can emit wavelengths as short as 300 nm (Blocquet et al. 2018). Compounds such as nitrous acid (HONO) and formaldehyde (HCHO) can be

photolyzed under irradiation from indoor lights to generate radical species (Wang et al. 2020), thereby increasing the oxidising capacity of air indoors (Figure 5.1).



*Figure 5.1: A schematic for the formation of radicals and different secondary species (highlighted in different colours). hv denotes the photolysis reactions (taken from Wang et al. (2020)).*

In Chapter 4, VOC emission rates were determined from a selection of common household plastics when exposed to different temperatures in the dark. The focus of this chapter is to determine how VOC emissions from different plastic types change in response to increasing levels of light, both within the visible and UV range. These light-driven VOC emission rates will then be simulated within INCHEM-Py to evaluate their effect on the indoor air chemistry.

## 5.2. Methodology

### 5.2.1 Plastics used.

Five of the original plastic types used throughout this thesis were selected for the light experiments described below. These included the polyester rubber wiring, the two storage container plastics (one white polyethylene (PE) and one clear polypropylene (PP)), the high-density polyethylene (HDPE) black bin liner (bin-bag) and the green coloured HDPE shampoo bottle. These were selected from the original twelve plastics as some of the highest emitting plastic types from the temperature-only experiments described in the previous chapter. The same plastic samples from the previous temperature

experiments were used in this investigation. The size and surface area of these plastic samples are reported in Table 4.1 in the previous chapter.

### 5.2.2 LED lamp experimental set up

To observe how light influences the VOC emissions from plastics, a PAR (photosynthetically active radiation) light sensor (Skye Instruments, UK) and a UVA sensor (Skye Instruments, UK) provided measurements of light intensity integrated over a fixed wavelength range. The PAR sensor measures within the visible range of 400 to 750 nm (nanometres) whilst the UVA sensor measures within the range of 315 to 400 nm. The sensors provide an irradiance, proportional to the total actinic flux within their detectable range, provided in W m$^{-2}$. These sensors were used within the two experimental set ups (using an LED lamp and sunlight) described subsequently.

Individual plastic samples were contained within 100 ml borosilicate glass chambers (Schott-Duran, Cole-Palmer, UK). The use of glass flasks is ideal for identifying the light effect on plastics as it represents what happens in indoor spaces as the solar radiation has to pass through a layer of glass before reaching the plastic sample. Each chamber had a polyether ether ketone (PEEK) lid with integrated 1/8" I.D. inlet and outlet ports. They were connected to a stainless steel multivalve coated with sulfinert, located within the PTR-ToF-MS instrument via PEEK capillary tubing. This is the same set up as seen in Chapter 4. Measurements of VOCs were performed using a PTR-TOF-MS (Ionicon Anlytik GmbH, Innsbruck, Austria), operating in the H$_3$O$^+$ reagent ion mode. The PTR-ToF-MS sampled from the exhaust of each chamber at a rate of 100 ml min$^{-1}$. The flow rate through each chamber was measured at the start of each experimental run using a flowmeter (4100 series, TSI, UK). To minimise the adsorption, all sample lines were heated to 60 °C using heating tape and insulated with foam pipe lagging.

To monitor the VOC emission rates in a controlled environment, Figure 5.2 depicts the laboratory set up, where plastic samples were exposed to different intensities of light within the visible range only (400-750 nm). Three chambers containing plastic samples (along with a fourth blank chamber) were positioned on a lab bench inside a temperature-control room with a PAR sensor aligned adjacent. An LED lamp (GENOA-SUPBIO-WIDE-CASED, RS Components, UK) was placed on the lab bench opposite the chambers facing them, whilst lined up against a measuring tape. The lamp was then moved away from the chambers at regular intervals; at distances 15 cm (position 1), 35 cm (position 2), 55 cm (position 3) and 75 cm (position 4). At these set distances, the lamp was switched on for 12 hours, allowing the PTR-ToF-MS to sample from each chamber for 3 hours each. This was repeated for each position. PAR sensor readings, temperatures and relative humidity readings were also recorded, with each experiment replicated two times.
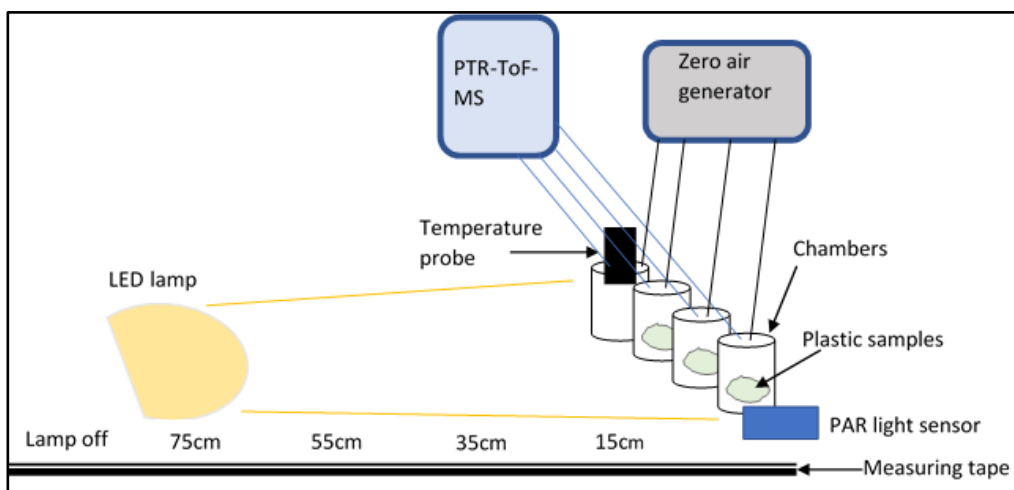
*Figure 5.2: Schematic of experimental laboratory set up of investigating the influence of visible light from an LED lamp on plastic types, encapsulated within glass chambers along with a blank chamber, a temperature & humidity probe and a PAR light sensor.*

### 5.2.3 Sunlight experimental set-up

Depicted in Figure 5.3 is the experimental set up for measuring the VOC emissions from plastic samples during exposure to solar radiation (sunlight). Five chambers containing the plastic sample, a UVA sensor (Skye Instruments, UK), PAR/visible light sensor, a temperature and an EI1050 digital temperature/ humidity probe (Labjack, USA), as well as a blank chamber, were positioned outside the laboratory window facing north.

The PTR-TOF-MS was programmed with a 1-minute sample resolution and was scheduled to sample from the blank chamber from 22:00 (in the absence of sunlight) for 3 hours, to allow the concentrations in the chamber to reach a steady-state, before sampling from the plastic-containing chamber until 12:00 (midday) the following day. This was so the PTR-TOF-MS would capture the VOC emission profile from the plastic as the sun rose in the morning. The PAR/visible light sensor, UVA sensor and temp/humidity probe were also programmed with a 1-minute sample resolution.
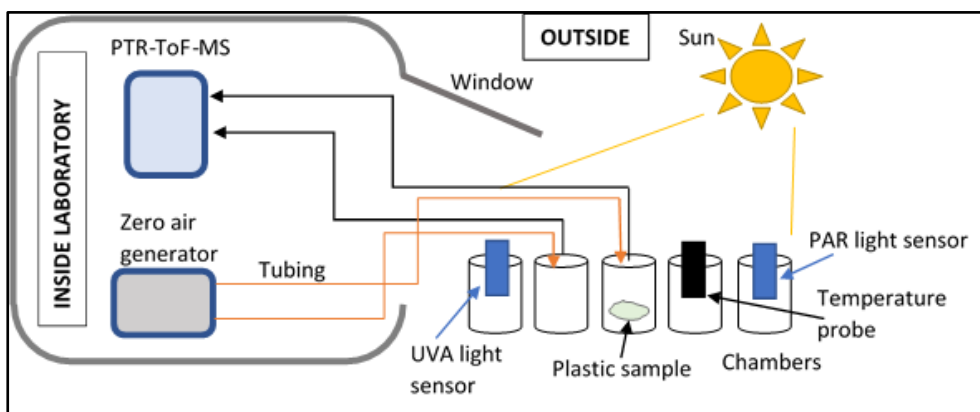
*Figure 5.3: Schematic of experimental laboratory set up of investigating the influence of sunlight on plastic types, encapsulated within glass chambers along with a UVA sensor, a blank chamber, a temperature & humidity probe and a PAR light sensor.*

### 5.2.4 Modelling

To model how the light-initiated emissions of VOCs from the plastic types influence the indoor air chemistry, INCHEM-Py was used to simulate the emissions from each individual plastic within an indoor setting. For the simulations of VOC emissions due to sunlight (from the sunlight experiments) the model development required to carry out these simulations will be further explained in the section below (5.2.4.1).

Descriptions of the calculations of emission rates in ng cm$^2$ hr$^{-1}$, and conversions to model inputs in molecule cm$^3$ s$^{-1}$, can be found in the methodology chapter, section 3.6.2 and 3.9.3.

### 5.2.4.1 Development of model for UVA dependent plastic emissions

INCHEM-Py includes terms that represent both indoor lighting and attenuated outdoor lighting. This study focuses on the attenuated outdoor light, obtained with the UV light sensor data from the sunlight experiments, being implemented into the model. Sunlight is simulated within INCHEM-Py as described in Wang et al. (2022). In brief, sunlight is modelled using the latitude of the simulated location and the calculation of the solar zenith angle for the specific day of the year. Light is transmitted through three different glass types selected from Blocquet et al. (2018). The absorption cross-section and quantum yield for each of the photolysing species were used to calculate a weighted transmission factor. A full description of the implementation of this indoor photolysis is given in Shaw et al. (2023).

To increase the accuracy of simulating the plastic VOC emissions obtained from the sunlight experiments, the cosine of the solar zenith angle calculated within INCHEM-Py was scaled to fit the solar noon value of UV light readings obtained during these experiments. This was done for the experimental location (Edinburgh, UK, at latitude 55.9°) at the date on which the experiments took place and to ensure that the intensity of sunlight received by the plastic sample in the experiments was

simulated as closely as possible by the model. Figure 5.4 shows the simulated UV irradiance values for the five plastics in red, along with the measured UVA values in black. The measured UVA irradiance does not start at dawn due to local shade from buildings at the experimental site. The model assumes clear-sky values, whereas the measured values are affected by local cloud cover.
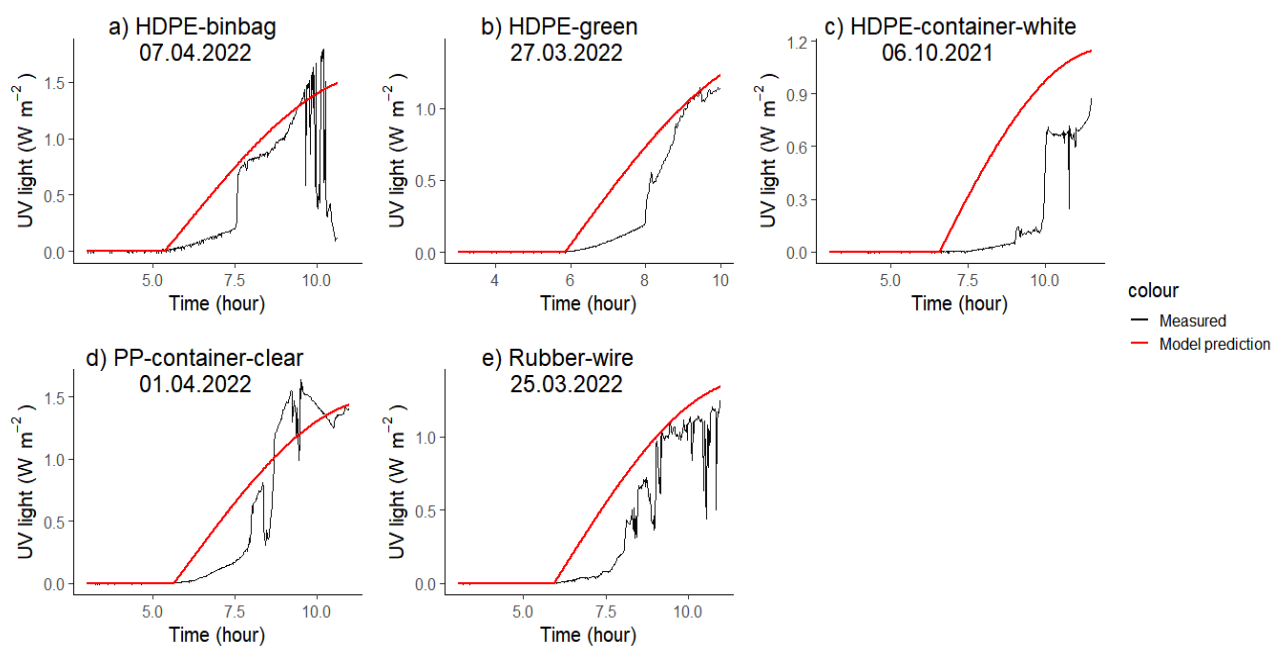


*Figure 5.4: A comparison of the measured UV light readings from the sunlight experiments with (a) the HDPE-binbag, (b) HDPE-green shampoo bottle, (c) white HDPE storage container, (d) the clear PP storage container and (e) the rubber wire, and the simulated UV light profiles (red) for each date the experiments were carried out.*

## 5.3. Results and discussion

### 5.3.1 Controlled laboratory experiments

The VOC emission rates from each plastic type were calculated and averaged at each of the light positions for the 3-hour exposure time, after background concentrations were subtracted (obtained from the blank chamber). Figure 5.5a shows the positive relationship between benzene emissions from the five plastic types and the recorded light intensity. The same positive relationship can be seen between these VOC emissions and the temperature recorded at each light position, in Figure 5.5b. This positive relationship with both temperature and light intensity values was seen across all VOCs measured and all plastic types investigated.
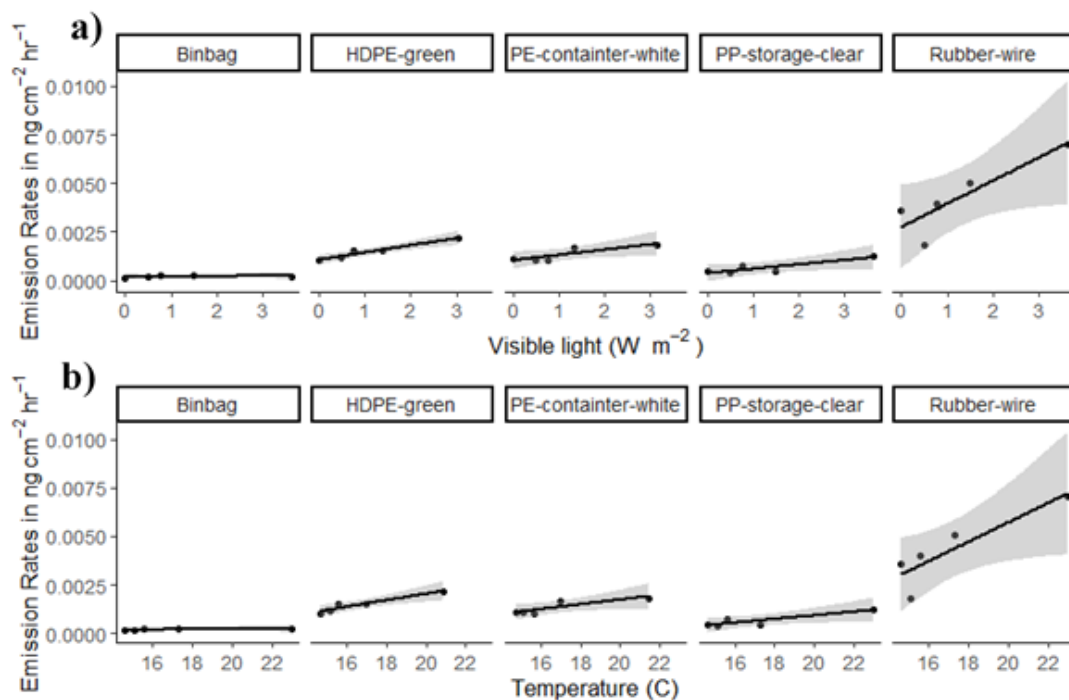
*Figure 5.5: Emission rates of benzene from all plastic types investigated vs (a) the PAR recorded light values and (b) the recorded temperature values, with a 95 % confidence interval highlighted in grey.*

The recorded temperature and PAR sensor readings also correlated well, indicating that the closer the light source was to the chambers, the higher the recorded temperature was. T-tests were carried out to determine whether or not there was a significant difference between the slopes of the VOC emission rates vs the recorded temperature and the VOC emission rates vs the recorded PAR values. Over 80 % of the p-values were above the significance value of 0.05, so the slopes were not statistically significantly different from each other.

Chapter 4 determined the emission rates at different temperatures. The Arrhenius coefficients from Chapter 4 were used to estimate the temperature-only emissions. Subtracting these emission rates from those observed here, allowed the light-dependent fraction to be estimated. For example, to calculate the temperature-only emission rate ($k$) of benzene from the white PE storage container plastic type, the Arrhenius equation generated from Chapter 4 can be used as:

$$Ln(k) = -7228.7(x) + 19.9$$  [5.1]

where $x$ is the inverse of the selected temperature ($T$) in Kelvin and

$$x = \frac{1}{(T + 273.15)}.$$  [5.2]

Figure 5.6 shows how the combined light and temperature emission rates of the VOCs (at just one of the sampling positions during the controlled lamp experiment) compared to the temperature-only predicted emission rates for the same compounds, for the polyester rubber wire plastic.
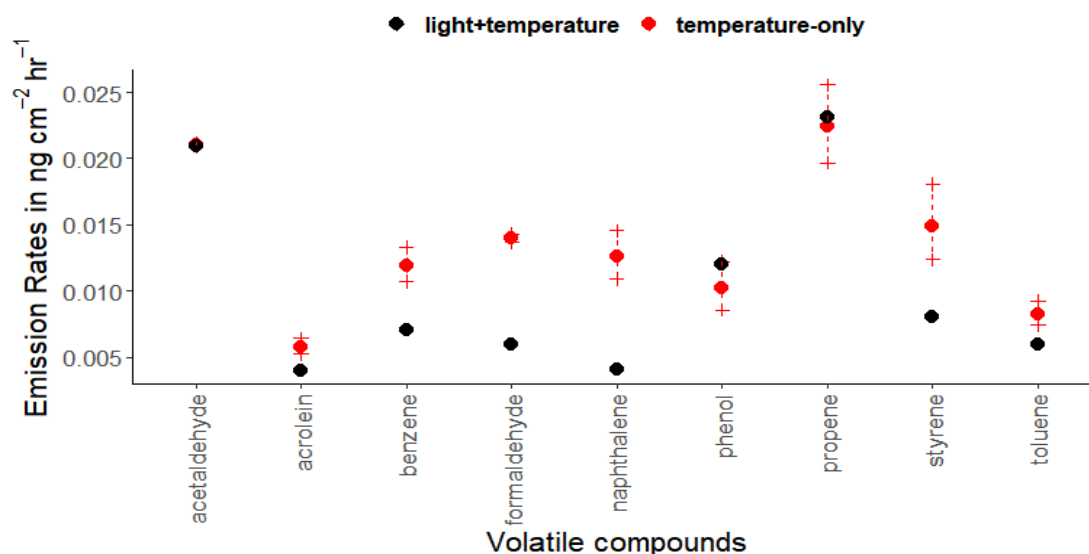


*Figure 5.6: VOC emissions from the polyester rubber wire plastic type at one temperature. Red points represent the temperature-only emissions compared to the emission rates obtained from the controlled lamp experiments in darkness. The red error bars represent ± one standard deviation.*

As observed in Figure 5.6, the predicted temperature-only emission rates (red points) are typically higher than those obtained from the light experiments (black points). Higher temperature-only emission rate values were found for over 80 % of the data, across all plastic types and all VOCs. By normalising for temperature, the light-only emission rates for this set of experiments would be negative. The consistently observed lower emission rates during these light experiments may be a result of the age of the plastic, as the light experiments were conducted after the temperature analysis on the same plastic samples (approximately 6 months after). Those that fall outside of the error bar range (95 % confidence intervals) may indicate that there is a much larger variability in emission rates from the plastics than was captured within the original temperature-only replicates, in Chapter 4.

From this, it can be concluded that visible light does not cause substantial degradation (and hence VOC emissions) of plastic polymers over short periods of time. Visible light has a lower energy level compared to other forms of electromagnetic radiation, such as UV (Yousif and Haddad 2013). The energy level of light within the visible range is not high enough to excite bonds within the polymer chain to cause scission, therefore, there was no observed an increase in VOC emissions from the plastic types. Previous studies have investigated ways to utilise visible light to aid in the breakdown of plastic debris by using a photocatalyst, such as zinc oxide (ZnO), to enhance the visible light absorption Uheida et al. (2021). However, as there was no photocatalyst used within the experiments of the current study,

no photodegradation of the plastic samples under visible light was observed. The increase in VOC emissions from the plastics in relation to the position of the LED lamp is believed to be temperature driven only. Therefore, the change in temperature explains the change in emission rate, with visible light not significantly affecting the VOC emission rates.

5.3.2 Sunlight experiments

With the LED lamp experiments showing no relationship between VOC emissions from plastics and visible light, next was the assessment of how exposure to the UVA portion (e.g. 315-400 nm) of solar radiation influenced the VOC emissions from the plastics.

The plots in Figure 5.7 show the UVA light profile (in black) and temperature profile (in blue) recorded during measurements from a chamber containing the white HDPE storage container plastic type, on October 6th 2021, between 05:00 and 12:30 hrs. During the night hours (04:00 to ~ 07:00 hrs), both light and temperature values are low, before gradually increasing from 08:00 hrs, shortly after the official sunrise, which was 07:30 hrs. The sharp spike in the light levels detected, around 10:35, is the time when the sun reached high enough in the sky that it appeared over the top of the adjacent building to the laboratory window and shone directly onto the experimental set up in position. The variations in the UVA readings between 11:15 and 11:45, where the levels decrease and increase rapidly, reflect the changes in local cloud cover.
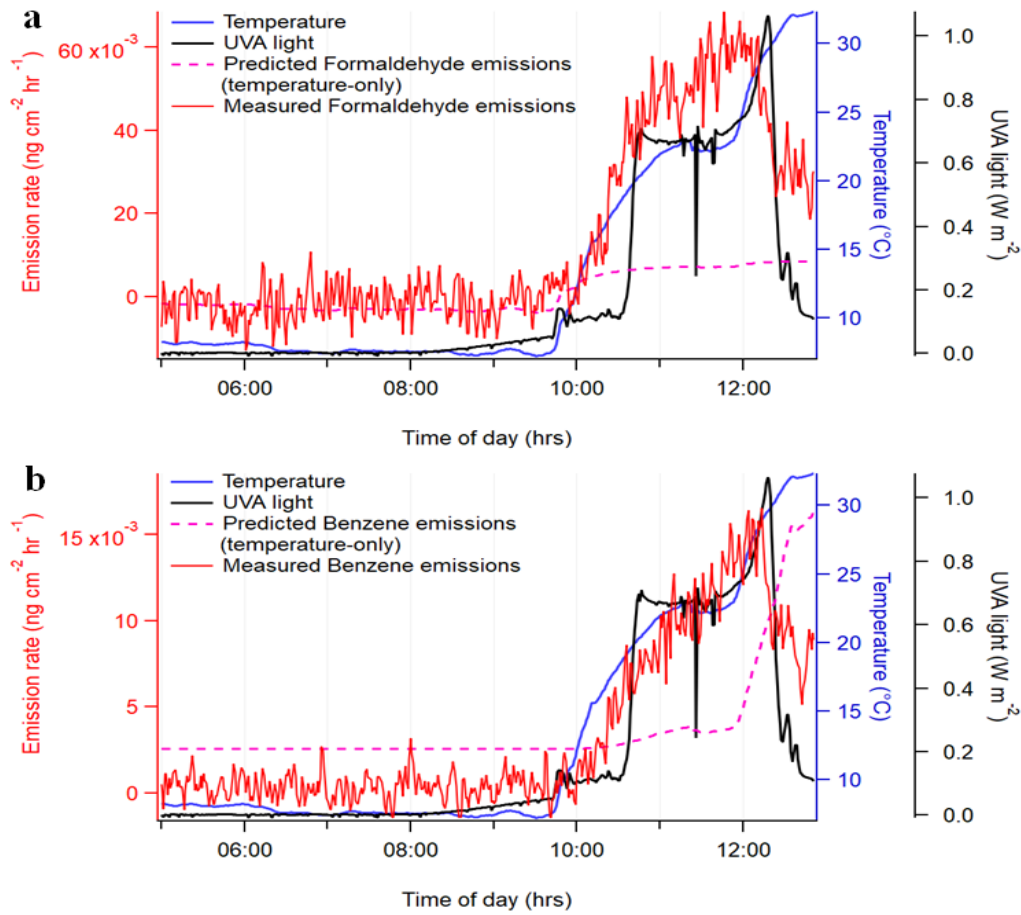
*Figure 5.7: UVA (black) and temperature (blue) profiles obtained during the overnight sunlight experiment for the white HDPE storage container plastic type, also displaying the measured (a) formaldehyde and (b) benzene emissions in red and their subsequent temperature-only predicted emissions in relation to the temperature profile in pink.*

Temperature-only emission rates for the compounds (in pink) displayed in Figure 5.7a and b were predicted using Equations 5.1 and 5.2 and in combination with the Arrhenius coefficients derived in Chapter 4. As shown in Figure 5.7a, the predicted temperature-only formaldehyde emissions were much lower than those measured, indicating that the presence of UV light causes comparatively more formaldehyde to be emitted from the plastic. The same can be said for benzene (Figure 5.7b), despite it having a stronger relationship with temperature than formaldehyde (see Chapter 4). UVA light readings decrease sharply after 12:00 hours, indicating an increase in clouds present in the sky at this time. Despite the temperature remaining high within the chambers, the VOC emissions drop with the decreasing UVA levels, further demonstrating the control UVA radiation has on the emission rate from the plastic samples. Interestingly, the VOC emissions appear to drop first, just slightly before the UVA readings from the sensor. This can be attributed to the horizontal positioning of the chambers and the order in which they were aligned. Shading from cloud cover may have partially occurred over the chamber containing the plastic sample and not the UVA light sensor, at this particular time of day. As

this was the first conducted sunlight experiment, in October 2021, the chambers in the following experiments, which were conducted in March and April of the following year, were realigned vertically so as to avoid this occurring again.

Table 5.1 provides information on the relative magnitude of emissions during sunlight exposure, in comparison to the temperature-only emissions, from all of the plastics investigated. This comparison is expressed as a factor, using the average value for each experimental run from 08:00 to 12:00 h, when the Sun was positioned high enough in the sky that it was shining directly onto the experimental set up. Where the factor is less than 1, it signifies the temperature-only emissions were greater than the measured emissions during the sunlight experiment. Those factors highlighted in red indicate that the sunlight+temperature measurements do not fall outside of the 95% confidence intervals and therefore can be described as not statistically significantly higher or lower than the temperature-only emissions. Missing information indicates that there wasn't a strong enough correlation between temperature and VOC emissions in the previous chapter, so a factor could not be calculated.

*Table 5.1: Table showing the ratio of sunlight+temperature: Temperature-only emission rates from all plastic types.*

| plastic | formaldehyde | propene | acetaldehyde | acrolein | benzene | toluene | phenol | styrene | naphthalene |
|---------|--------------|---------|--------------|----------|---------|---------|--------|---------|-------------|
| PE-storage-white | 3.8 | 1.2 | 4.2 | 1.8 | 1.7 | 1.2 | 0.9 | 0.3 | 2.5 |
| Rubber-wire | 1.0 | 1.2 | 0.9 | 1.2 | 1.3 | 1.1 | 1.3 | 1.2 | 1.2 |
| HDPE-green | 79.5 | 3.0 | - | 21.0 | 0.3 | 0.9 | 3.1 | 1.0 | 1.7 |
| PP-storage-clear | 27.5 | 0.6 | 191.5 | 39.9 | 8.2 | 2.7 | 13.9 | 1.4 | 1.3 |
| HDPE-binbag | 43.2 | 6.7 | - | 62.8 | 13.3 | 3.5 | 9.1 | 2.9 | 0.3 |

Many of the smaller VOCs, such as formaldehyde, propene, acetaldehyde and acrolein, have considerably higher factors than the larger aromatic compounds, indicating that the measured emissions were higher than the temperature-only predictions. For example, the highest factor for the clear PP storage container plastic type was acetaldehyde (191.5), followed by acrolein (40) and then formaldehyde (27.5). For the HDPE-green plastic type, formaldehyde had the highest factor (79.5), followed by acrolein (21) and then propene and phenol followed close together at 3.0 and 3.1 respectively. However, it should be noted that the determined temperature responses for both formaldehyde and acetaldehyde emissions were low in the previous chapter.

Occasionally, the aromatic compounds had lower emissions when exposed to sunlight in comparison to the temperature-related emissions, indicated by a factor value less than 1. For example, phenol and styrene had factors of 0.9 and 0.3 respectively for the white PE storage container. Benzene and toluene had factors of 0.3 and 0.9 respectively for the green HDPE plastic. The much higher factors for the smaller VOCs, could potentially suggest that larger VOC species, emitted from the plastics, are undergoing photolytic degradation within the chamber as they are released, and forming these smaller VOCs. This could be happening from other compounds than the ones being considered in this study. For instance, cyclohexanone can be photolysed to form both ethene and propene.

With the experiments providing evidence of sunlight-driven (particularly UV) emissions occurring from the plastic types, the calculated temperature-only emission rates were subtracted from their corresponding temperature+light emission rates to obtain light-only VOC emission rates. Figure 5.8 shows the measured fluxes normalised by temperature response to give the UV dependent emission response for the white HDPE storage container plastic type. Where the predicted temperature flux exceeded the measured flux, values were set to zero.
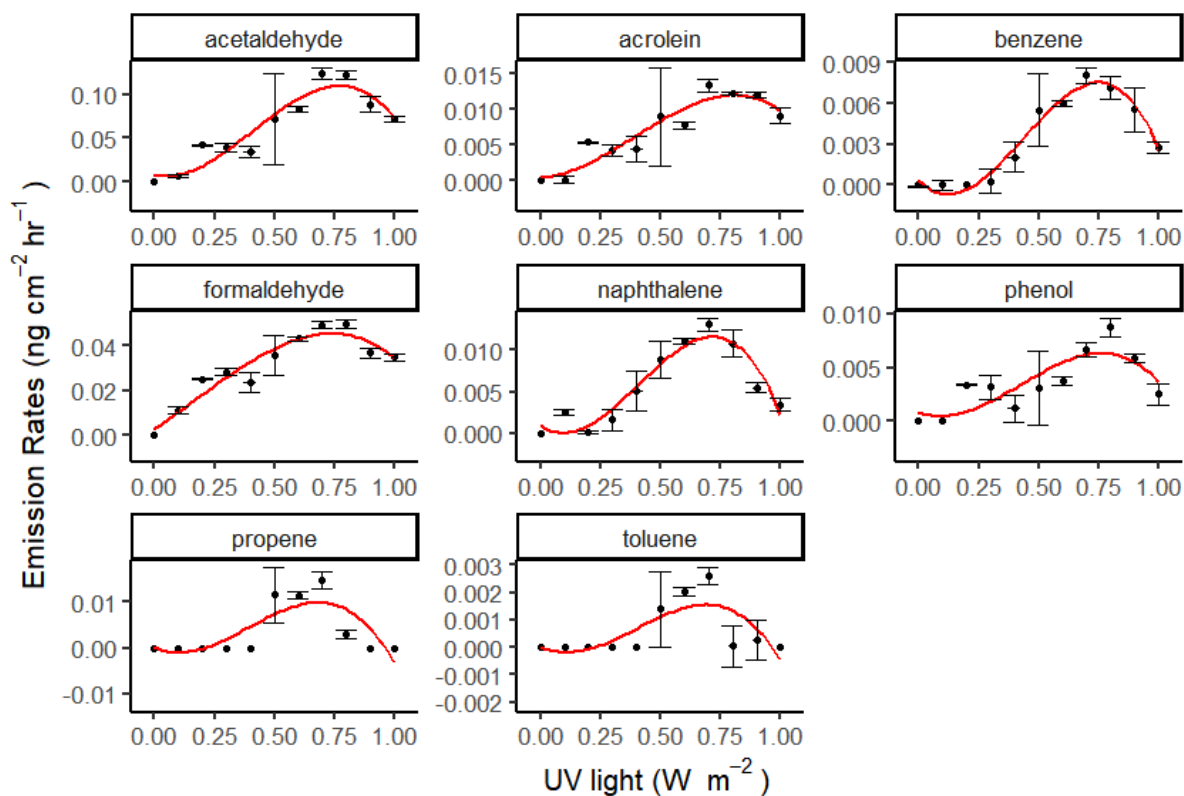


*Figure 5.8: Relationship between light-only emission rates and the UVA light for all compounds for the white HDPE storage container plastic type. The error bars are ± one standard deviation.*

Figure 5.8, and Figures S5.2 - S5.5 in Appendix B, present the relationships between the normalised emission rates (e.g. UV only) and measured UVA light. These plots were generated by averaging the measured fluxes into grouped bins of UVA measurements (e.g. 0.1, 0.2, 0.3, etc.) with error bars of one standard deviation. The pattern for most of the VOCs displays an S-shape, indicated by the polynomial fit with a degree of 4 terms which was determined as the overall best fit for all compounds and all plastic types. The cause of the decline in emission rate at light intensities > 0.75 Wm$^{-2}$ is not clear. One explanation is that the emissions are driven from a surface film on the plastic and once this pool of VOC is depleted, emission rates fall to reflect those solely from the photo degradation of the plastic polymer. A second possibility is that UVA is not the main driver of the emissions, but rather UVB plays a more important role. The wavelength cut off of the Schott Duran glass flasks is 310 nm, which just infringes on the UVB band (280 - 315 nm). The ratio between UVA and UVB is driven by the angle of the Sun above the horizon, or the solar zenith angle. Kollias et al. (2011) calculated the ratio of UVA/UVB from measurements taken through the day over an 8-month period and determined that the ratio is lower during the time of day when the Sun is highest in the sky, indicating a higher measurement of UVB. This potentially indicates that, even when observed UVA values are high, there may be lower values of UVB and this may explain why there is a drop in VOC emissions as UVA increases above 0.75 W m$^{-2}$.

To directly compare the sunlight+temperature VOC emissions from each of the plastic types obtained throughout the sunlight experiments, Figure 5.9 displays the average emission rates of the VOCs, per cm$^{-2}$ of plastic during each experimental run from 08:00 to 12:00 h. Figure 5.9 demonstrates that the Rubber-wire plastic and the HDPE-green bottle show higher VOC emissions in comparison to the other plastic types, which was similarly found in Chapter 4.
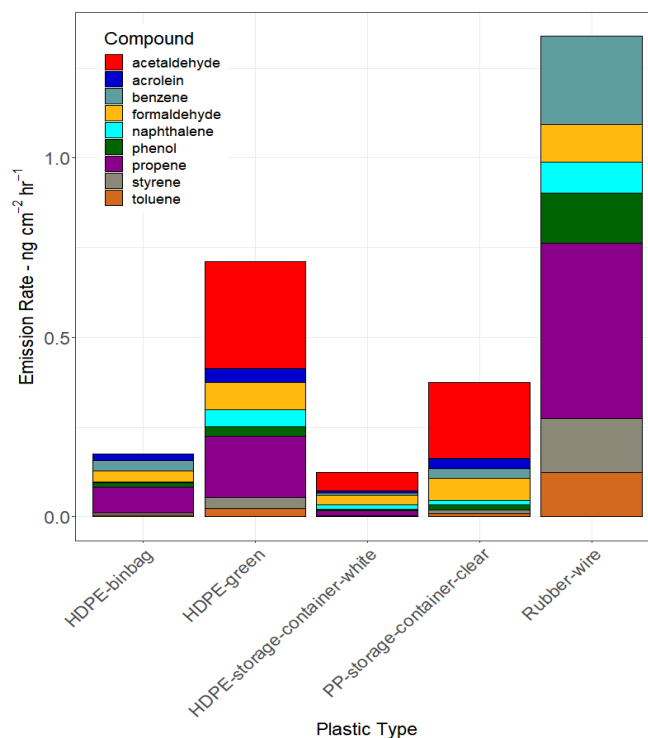
*Figure 5.9: Average emission rates (between the hours of 08:00 – 12:00) of all nine VOCs per cm-2 for the plastic types investigated, during each individual sunlight experiment.*

### 5.3.3. Model simulations

As the increase in VOC emissions from the plastics in relation to the position of the LED lamp is believed to be temperature driven only, Section 1 in Appendix B demonstrates how these emissions would affect secondary species concentrations within INCHEM-Py simulations.

The polynomial fit coefficients, determined through the sunlight experiments, were implemented within INCHEM-Py to model the emissions from the individual plastics in response to changing irradiance throughout the simulated day, after the emission rates were converted to model inputs, (molecule $cm^{-3}$ $s^{-1}$), with a surface area of 8.6 $m^2$. A custom input file containing the light-only coefficients was included for each of the model simulations. When implementing the polynomial fits indoor lighting was assumed to be off, so that photolysis rate coefficients were based only on the transmission of outdoor sunlight.

Each of the five plastic types were simulated individually with the three glass types; "glass_C", "low_emissivity" and "low_emissivity_film", with the corresponding date set to that on which each individual experiment was carried out (Wang et al. 2021). Each model run had an associated background run, so that a percentage difference from background could be calculated, a total of 30 model runs. All other model parameters were kept consistent between simulations, including the air exchange rate (0.2

hr$^{-1}$), latitude (55.9°) and a temperature of 25°C (298.15 K). Figure 5.10 displays the diurnal profiles of secondary species and their concentrations for one plastic type (the HDPE-binbag).

The wavelength range varies between each of the glass types; 315-800 nm, 330-800 nm and 380-800 nm for "glass_C", "low_emissivity" (LE) and "low_emissivity_film" (LEWF), respectively. More light comes through glass_C and LE than LEWF, which leads to more photolysis of HONO and $NO_2$, hence the lower HONO and $NO_2$ concentrations for LE and glass_C compared to LEWF. Photolysis of HONO produces OH radicals, so the highest OH concentration is found for glass_C. Furthermore, O atoms can be produced by the photolysis of $NO_2$ where the O atoms react with $O_2$ to form $O_3$. This process leads to greater concentrations of $O_3$ for glass C and LE compared to LEWF.
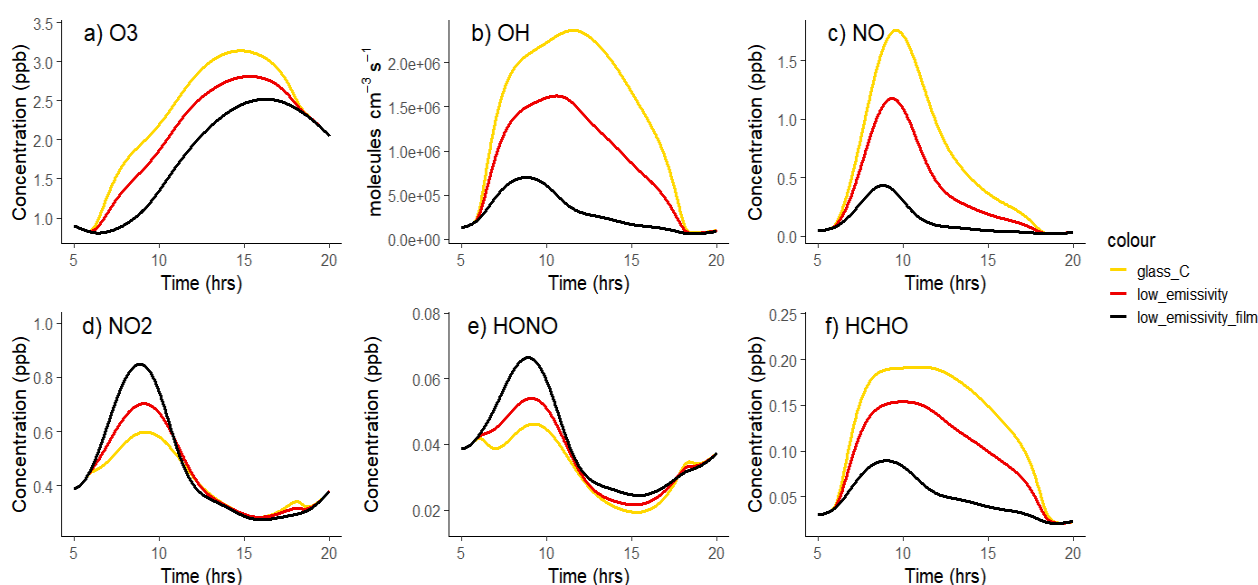


*Figure 5.10: Comparison of diurnal concentrations of key species (O3 and OH) and secondary species, formed through photolysis reactions within INCHEM-Py simulations, with the three different glass types; glass_C (yellow), low_emissivity (red) and low_emissivity_film (black).*

The plots in Figure 5.11 highlight the variations in the concentrations of secondary species when different plastic types are added to the model. The overall profile is clearly driven by the sunlight infiltrating through the selected glass type, in this case Figure 5.11 presents glass type "glass_C". The white PE storage container plastic (blue line) experiment was conducted in the month of October, whilst the other plastic types were tested in the months of March and April. This explains why there is a slight shift in the initial increase of compounds at the start of the simulated day, as the months of March and April experience longer daylight hours compared to October. Photolysis of $O_3$ produces OH, and photolysis of $NO_2$ forms NO and O, with the latter reacting with $O_2$ to form $O_3$. Therefore, with the longer days in springtime, more photolysis can occur and result in higher concentrations of $O_3$ and OH.
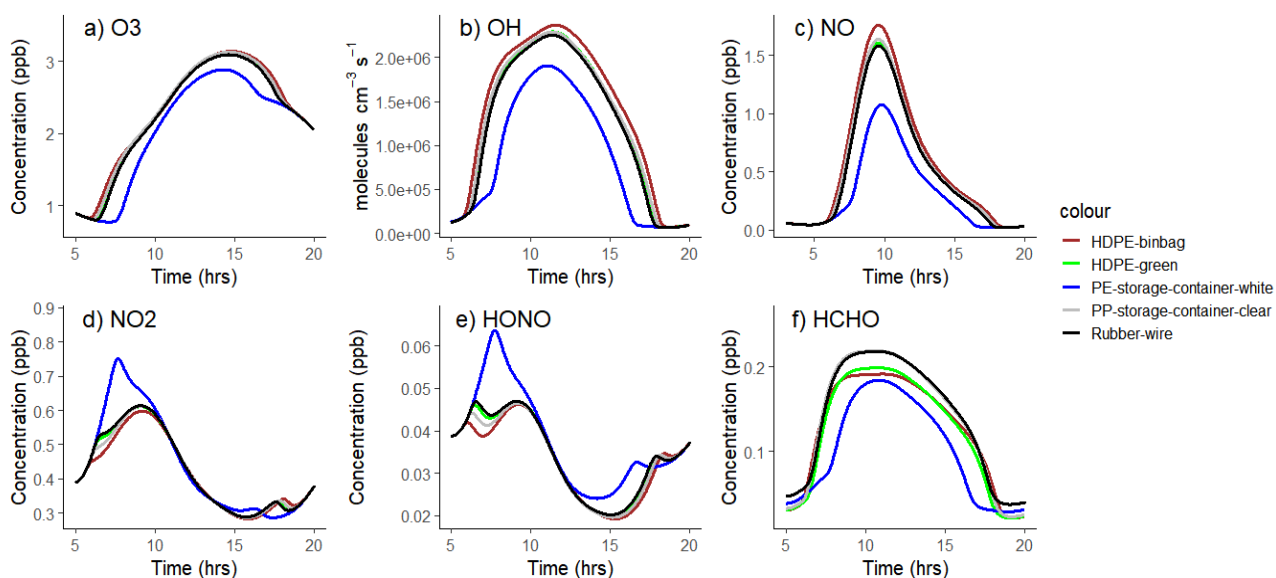
*Figure 5.11: Comparison of diurnal concentrations of key species (O3 and OH) and secondary species, formed through photolysis reactions within INCHEM-Py simulations, for the five plastic types; HDPE-binbag (brown), HDPE-green (green), HDPE-storage-container-white (blue), PP-storage-container-clear (grey) and the Rubber wire (black).*

Some of the VOC species implemented in the model simulations are shown in Figure 5.12, for the HDPE bin-bag as an example as similar trends were seen for all plastic types. The initial concentrations of the species are driven upwards but then begin to fall as the polynomial coefficients reduce the VOC concentrations (emitted from the simulated plastic), such as propene, benzene, toluene, styrene and phenol. This reduction is more exaggerated with glass types with a larger wavelength range (glass_C) as the VOC concentrations are also being driven down by photolysis. The opposite is seen for acetaldehyde and acrolein as these compounds are additionally produced through reactions in the degradation mechanisms of other species, like aromatic hydrocarbons, as well as the plastic emissions.
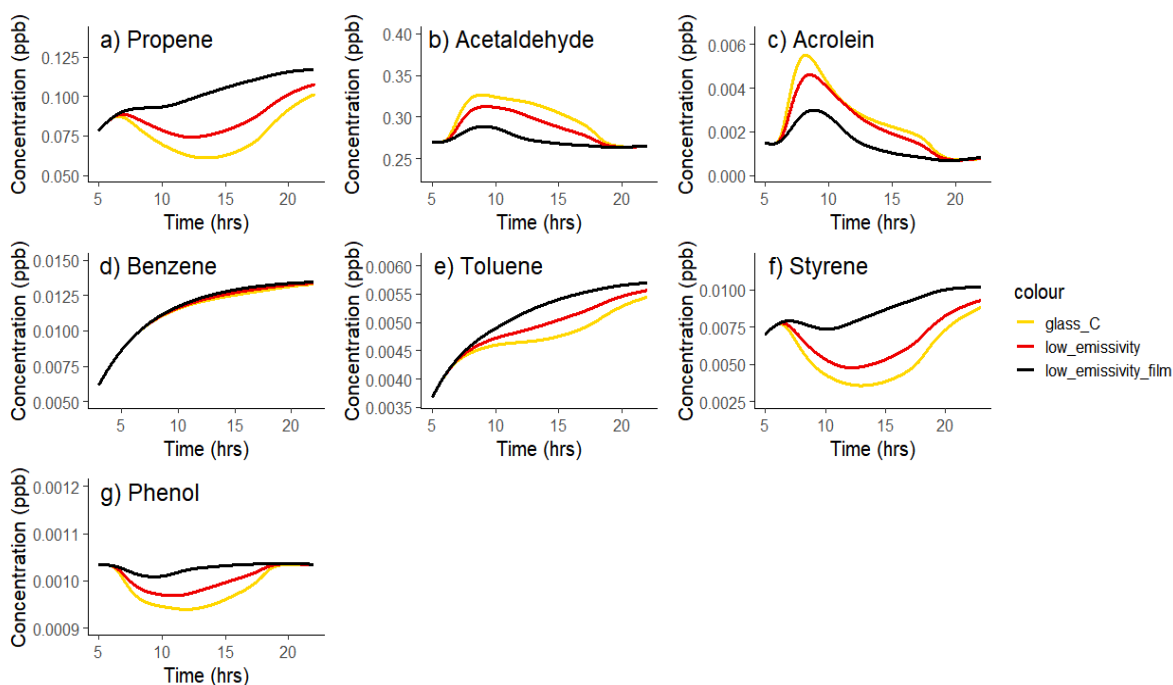
*Figure 5.12: Concentration profiles of plastic VOC emissions in a 24-hour simulation for each glass type: glass_C (yellow), low_emissitivty (red) and low_emissivity_film (black).*

Figure 5.13 shows the percentage difference in concentrations for the modelled species with plastic present, compared to background simulations with no plastic emissions. The percentage differences highlighted in green (blue) show an increase (decrease) in concentration. The introduction of plastics into the modelled simulations provides more VOCs for the OH radicals to react with, in turn, results in a negative percentage difference from background simulations for the OH concentrations. The concentrations of NO and HONO also decrease with the presence of plastics. HONO is formed through the reaction between OH and NO in our simulations. Given that OH and NO both decrease with the addition of plastics, so does HONO. As plastics are introduced into the system and VOC concentrations increase, there are more peroxy radicals ($HO_2$) formed, hence the positive percentage difference. This happens through the oxidation of the VOCs and through photolysis of intermediate compounds (originating from aromatics such as benzene). These effectively titrate NO from the system, decreasing its concentration when plastics are added. Overall, the average concentrations of $O_3$, OH, $HO_2$, GLYOX and $NO_2$ are higher for Glass C and LE compared to LEWF, and the concentrations are slightly lower for HONO, and NO.

Interestingly, the direction of percentage change for HCHO varies depending on the plastic type. For the HDPE-binbag, the white HDPE storage container and the Rubber wire plastics, the percentage difference decreases with increasing sunlight exposure (LEWF < LE < glass_C). For the green HDPE

bottle and clear PP storage container the opposite can be observed. This can be attributed to the differences in emissions from the plastic types themselves, see Figure 5.9.



| Plastic type | O3 | OH | GLYOX | HO2 | HONO | NO | NO2 | HCHO |
|---|---|---|---|---|---|---|---|---|
| HDPE-green_LEWF | 0.07 | -3.52 | 4.42 | 1.52 | 0 | -1.69 | 0.06 | 6.41 |
| HDPE-green_LE | 0.38 | -2.38 | 6.99 | 2.73 | -0.22 | -2.27 | 0.19 | 7.25 |
| HDPE-green_glassC | 0.69 | -1.5 | 8.87 | 3.66 | -0.52 | -2.44 | 0.27 | 7.55 |
| HDPE-binbag_LEWF | 0.03 | -1.23 | -0.78 | 0.54 | 0 | -0.62 | 0.02 | 3.27 |
| HDPE-binbag_LE | 0.14 | -0.84 | -0.28 | 0.86 | -0.09 | -0.75 | 0.07 | 3.19 |
| HDPE-binbag_glassC | 0.22 | -0.6 | 0.01 | 1.02 | -0.2 | -0.71 | 0.11 | 3.16 |
| PP-storage-clear_LEWF | 0.14 | -6.51 | -5.73 | 3.02 | 0 | -3.35 | 0.11 | 13.4 |
| PP-storage-clear_LE | 0.73 | -4.63 | -3.43 | 4.84 | -0.41 | -4.11 | 0.42 | 15.91 |
| PP-storage-clear_glassC | 1.24 | -3.3 | -2 | 5.83 | -0.96 | -3.99 | 0.64 | 16.7 |
| HDPE-storage-white_LEWF | 0.04 | -2.52 | -1.11 | 0.87 | -0.01 | -1.02 | 0.03 | 20.86 |
| HDPE-storage-white_LE | 0.19 | -1.98 | -0.36 | 1.44 | -0.11 | -1.34 | 0.12 | 13.27 |
| HDPE-storage-white_glassC | 0.27 | -1.74 | -0.04 | 1.65 | -0.19 | -1.36 | 0.16 | 12.22 |
| Rubber-wire_LEWF | 0.08 | -4.69 | -0.98 | 1.61 | -0.01 | -1.96 | 0.06 | 38.98 |
| Rubber-wire_LE | 0.41 | -3.47 | 0.86 | 2.75 | -0.3 | -2.53 | 0.23 | 23.88 |
| Rubber-wire_glassC | 0.72 | -2.62 | 2.09 | 3.41 | -0.7 | -2.54 | 0.33 | 20.24 |

Secondary Compounds

Difference (%): 40 / 0 / -40

*Figure 5.13: Percentage differences from background model runs of secondary species with each plastic-specific modelled scenario.*

### 5.3.4. Limitations of the work

The experimental set-up of the sunlight experiments was devised to explore the VOC emission profiles from different plastic types using an internal windowsill in direct sunlight. Kowal et al. ((2017) determined that the percentage of light 1 metre away from a light source would decrease to only 2-15% compared to measurements made adjacent to the source. This potentially indicates a limitation of the experimental set-up used in this study, as the emission profiles obtained in the sunlight experiments may not reflect situations where plastics in a room are located further away from a window. The LED

lamp experimental design made it difficult to completely separate and account for the temperature and light dependent emissions. Future experiments could involve containing the light source, e.g. the LED lamp, in a glass container or using a see-through barrier to reduce the influence of temperature.

Some of the VOC measurements were difficult to explain when only UVA light and temperature parameters were obtained with no other factors considered. With repeated measurements taken in future experiments, it would be good to consider including an additional chamber flask covered up, with no light exposure, as a comparison to help fully understand the influence of the solar radiation with the same temperature profile.

## 5.4. Conclusion

This work demonstrates a method for determining and calculating light-driven emission rates of VOCs from plastic products using a PTR-ToF-MS and glass chambers. It showed that visible light has a negligible impact on VOC emission rates for the plastic types investigated, in agreement with most of the reported literature. The emission profiles generated through the sunlight experiments showed an S-shape relationship with increasing sunlight, particularly UVA, when accounting for the influence of temperature. This could have been a result of the influence of cloud cover or even the influence of UVB light infiltrating into the chambers.

This study also shows, through modelling with INCHEM-Py, that photolysis plays an important role in determining species concentrations in indoor environments. The polynomial fits of plastic VOC emissions, determined through the experimental work, showed how the concentrations vary with increasing sunlight within the indoor environment, with some compounds showing a decrease with increasing light levels. The subsequent air chemistry affects the concentrations of secondary species, such as HCHO which showed a percentage decrease with increasing light levels for the HDPE bin-bag, white HDPE storage container and the rubber wire, but increased with light levels for the green HDPE shampoo bottle and the clear PP storage container.

Future experimental work should focus on capturing the effect of other wavelengths of light, such as UVB, whilst simultaneously measuring the VOC emissions within a covered chamber to compare the plastic emissions exposed to the same temperature profile but in darkness.

# 6. Natural ageing of plastic products in a home and their VOC emissions

## 6.1. Introduction

As explored in previous chapters, plastic polymers are used abundantly throughout our daily lives within indoor environments and can release chemical compounds into the surrounding air. Emissions from materials can be defined as either primary, from the physical release of compounds from a new product, or secondary, which are compounds produced by a chemical reaction in the product or within the surrounding environment (Brown et al. 2013). Levels of primary emissions from materials are typically found to be highest following their manufacture but can then decay over a long period of time (Kruza et al. 2017), e.g., over a number of months or years. Various substances, such as antioxidants and stabilisers, are added to the polymer mixture during manufacturing to give the polymers their desired properties, determining their strength, permeability, porosity and colour (Marturano et al. 2017). Many of these additives are used to prolong the working life of plastics, slowing environmental degradation processes. Environmental degradation rates of plastics in the peer-reviewed literature vary widely, as explored in the literature review in Chapter 2, section 2.3.2. However, we currently understand very little about how plastics within our indoor environment degrade through degradation or ageing processes.

Different processes of oxidative degradation of plastics have been previously discussed in section 2.1. Multiple degradation mechanisms such as thermal-, photo- and mechanical degradation can act upon plastic materials at the same time as they are being used. These processes can cause significant changes in not only the chemical structure within the material and on its surface, but also the physical properties of the material as well (Almond et al. 2020). UV-induced oxidation is considered to be the most effective degradation mechanism for many plastic materials found in the natural environment (Chamas et al. 2020). A stronger response in emissions from plastics exposed to UV from sunlight compared to light just in the visible range was observed in the previous chapter, in agreement with the literature. However, few studies have quantified the emissions of VOCs from common household plastic products over periods of time any longer than a month, such as the course of a year. Plastic polymers are subject to degradation through their entire lifecycle (Tocháček and Vrátníčková 2014), from production, throughout their use and after they are discarded. The longer a plastic persists in the indoor environment, the more they are subject to typical daily routine activities involving their use and exposure to heat, air and sunlight which can cause them to weather and degrade.

In order to assess the stability of polymer materials, and how they stand over time, one can expose these materials to various environmental and loading conditions that simulate an extended period of natural ageing conditions. In such procedures, the long-term durability of polymer materials can be predicted by subjecting them to cycles of radiations, temperatures, moisture and other external agents at levels well above those found in true conditions in order to accelerate the degradation process (Frigione and Rodríguez-Prieto 2021). Experiments are typically carried out in designed climatic chambers, where polymer specimens are exposed to high levels of humidity, variations in temperature, UV radiations and possibly even heavy mechanical stress. Almost all accelerated ageing procedures employ radiation produced by different lamps as an intense source of light, either a mercury arc lamp, a fluorescent tube or xenon lamps, as it is well recognised that photo-chemical processes are the principal responsible for degradation of polymers (Tocháček and Vrátníčková 2014).

Although numerous studies have been carried out to reproduce the effects of polymer degradation using accelerating procedures, to reduce analysis times, discrepancies were generally observed between in-situ field tests and accelerated ex-situ tests due to the ineffectiveness of the latter to accurately reproduce the effects of complex weathering conditions. To reproduce the effects of natural exposure in short observation times, the acceleration factors are frequently excessively amplified, making the results unrealistic. Therefore, natural ageing of polymer materials is the only approach able to provide reliable results (Frigione and Rodríguez-Prieto 2021).

The oxidative degradation of polymers can be monitored via a series of different methods, with one of the most common analytical techniques being Fourier transform infrared (FTIR) spectroscopy. FTIR analysis is capable of monitoring chemical changes that take place throughout the lifetime of a material, by detecting the functional groups present at distinct bands in the generated spectra (Almond et al. 2020). Observing changes in the carbonyl band (C=O), has led to the rise of a method called the carbonyl index (CI). The CI is a measure of the presence of carbonyl groups, a product of thermal or photo-oxidation processes (Ángeles-López et al. 2017), by measuring a ratio of the carbonyl peak relative to a reference peak. The carbonyl band will be located at different points in the spectra depending on the plastic type being investigated, therefore the calculation of the CI will differ for each plastic type.

In this chapter, a 12-month study was conducted during the year of 2021, with ten selected plastic types placed in locations in a typical family home and exposed to natural indoor ageing conditions. A sample piece of each plastic polymer was removed from its indoor environment each month and placed into air-tight chambers connected to a Proton Transfer Reaction Time-of-Flight Mass Spectrometer (PTR-TOF-MS). This procedure enabled the measurement of the volatile organic compound (VOC) emissions, and how they changed over the course of the year. Calculated emission rates were obtained per surface area of each plastic sample, as per calculations in previous chapters. Plastic samples collected during months 1, 3, 5, 7, 9 and 11 were then further analysed through Attenuated Total

Reflection Fourier Transform Infrared (ATR-FTIR) spectroscopy, to observe chemical changes happening to the polymers, by detecting the carbonyl peak present at distinct bands.

## 6.2. Methodology

### 6.2.1 Plastic types

Ten of the original twelve plastic types were used for this natural ageing experiment in the home. These included the six high density polyethylene (HDPE) coloured shampoo bottles, both food storage containers (made from polyethylene (PE) and polypropylene (PP)), a plastic water bottle made from polyethylene terephthalate (PET) and a polyester rubber wire (typically used for electrical appliances). Please refer to Table 3.1 for more details on the plastics used. The whole plastic products were pre-cut into twelve pieces with an approximate length and width of 10 cm by 3 cm (with varying degrees of thickness), to allow them to fit into the small environmental chambers for analysis after a period of ageing. Exact dimensions were determined prior to sampling to enable accurate calculation of the sample surface area (SA). Each of the twelve pieces of each plastic type were placed in their intended location. One piece of each plastic type was extracted from its location every month for one year for analysis.

### 6.2.2. Location

These ten plastic products were spread across two locations: a kitchen and a bathroom. These rooms are located in a typical family home in Buckinghamshire, England, UK, with an approximate latitude of 51.8° N. The six shampoo bottles were positioned within a 3-piece family bathroom along a windowsill and the other four plastic types were placed in a similar position (on a windowsill) in the kitchen. Care was taken to ensure there was equal spacing between each plastic sample and that there was no overlap between the adjacent plastic pieces, see Figure 6.1.
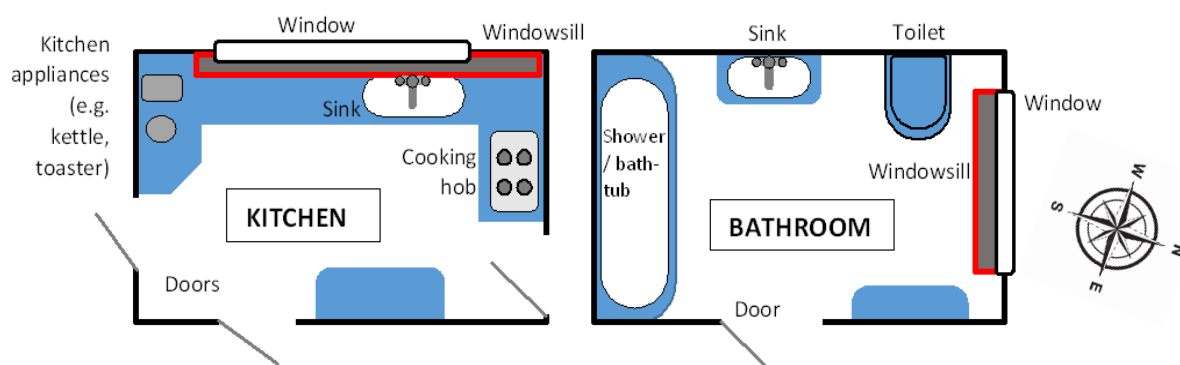
*Figure 6.1: Layout of the two room locations. The windowsill area, highlighted in red, is where the plastic pieces were positioned in each room.*

6.2.3. Degradation exposure

The plastic types were exposed to a range of indoor temperatures, indoor lighting conditions and human activities, such as cooking, cleaning and showering, within the rooms in this typical family home. These factors are further described in Table 6.1. Temperature, humidity and light readings were taken occasionally throughout the year to monitor any changes in these factors. All plastics were positioned on a windowsill in each of the rooms, where they would be exposed to thermal ageing and photo-ageing processes under "natural conditions", so no accelerated ageing processes. At the end of every month in 2021, one plastic sample piece of each plastic type was extracted from its location and individually sealed in zip-lock bags, so as to prevent any cross-contamination. These bags were then packaged and sent to the lab for analysis, further described in section 6.2.4.

*Table 6.1: Summary of conditions in each of the locations.*

| Factor | Kitchen | Bathroom |
|---|---|---|
| Temperature range throughout the year | 19-24°C | 22-26°C |
| Light range throughout the year | 0.001-0.32 µmol s$^{-1}$ m$^2$ | 3.8 – 5.01 µmol s$^{-1}$ m$^2$ |
| Humidity range throughout the | 40% (±20%) The highest humidity values were observed when cooking food (~60%) | 40% (±20%) The highest humidity values were observed when showering (~90%) |
| Activities that took place | Cooking and cleaning | Showering and cleaning |

| Dimensions | Length: 2.67m<br>Width: 2.11m<br>Height: 2.45m | Length: 2.46m<br>Width: 1.38m<br>Height: 2.42m |
|---|---|---|

### 6.2.4. PTR-TOF-MS analysis of VOC emissions

Over the course of 12 months of a year, a sample piece from each plastic type was removed from its location and sent to the lab for analysis to measure its VOC emissions. The laboratory set up for analysing VOC emissions has been previously explained in section 3.6 of the methodology, with a similar experimental set up described in Chapter 4. A zero-air generator (ZA FID AIR C, Swissgas) was used to provide a source of VOC free air which was circulated through four glass chambers. The flow of air was divided equally across the four chambers, with one chamber acting as a blank (containing no plastics throughout all of the experiments) and the other three chambers containing the individual plastic samples. These chambers were housed in the temperature-controlled water bath, as described in Chapter 4. This was to maintain the temperature of the chambers whilst sampling the plastic piece samples. The sampling lines, made from PEEK tubing, were heated to 60 °C using heating tape and insulated with foam pipe lagging to minimise adsorption of the VOCs. The plastics were encapsulated within the glass chambers, with the air sampled from them for four hours each. The VOC concentrations (in ppbv) and emission rates (in ng cm$^{-2}$ hr$^{-1}$) were calculated as described in sections 3.5.3 and 3.6.2.

### 6.2.5. ATR-FTIR analysis

Plastic samples collected during months 1, 3, 5, 7, 9 and 11 were analysed through Attenuated Total Reflection Fourier Transform Infrared (ATR-FTIR) spectroscopy, to observe chemical changes happening to the plastics as they degraded over time, by detecting functional groups present at distinct bands. This technique is described in section 3.3 of the methodology. Infrared spectra were obtained using an ATR-FTIR instrument (Agilent Cary 630 FTIR, USA), with a type IIa diamond crystal. The plastic sample pieces were analysed in triplicate by absorbance spectra in the region between 375–4000 cm$^{-1}$, with a spectral resolution of 4 cm$^{-1}$ and 50 scans per sample.

### 6.2.5.1 Calculations of the carbonyl index

After reviewing the literature for the best method of calculation the CI for PE and PP plastic types, the standardised calculation determined by Almond et al. (2020) for both PE and PP, is as follows:

$$= \frac{Area\ under\ the\ band\ 1850 - 1650\ cm^{-1}}{Area\ under\ the\ band\ 1500 - 1420\ cm^{-1}}$$ [6.1]

This is a calculation of the ratio between the integrated absorbance band of the carbonyl (C=O) peak from 1,850 to 1,650 cm$^{-1}$ and that of the methylene (CH$_2$) scissoring peak from 1,500 to 1,420 cm$^{-1}$.

For determining the CI for PET plastics, the CI calculation used by Chelliah et al. (2017) was employed. The ranges in equation 6.2 have been selected to capture the full peak of the stretched C=O bond of all replicates, to include the shifts over time.

$$= \frac{Area\ under\ the\ band\ 1750 - 1650\ cm^{-1}}{Area\ under\ the\ band\ 1420 - 1380\ cm^{-1}}$$ [6.2]

Calculation of the CI for types of rubber, investigated by Muthukumar et al. (2011) used the following equation:

$$= \frac{Area\ under\ the\ band\ 1760 - 1640\ cm^{-1}}{Area\ under\ the\ band\ 1300 - 1190\ cm^{-1}}$$ [6.3]

The carbonyl (C=O) degradation product is typically detected between 1735–1745 cm$^{-1}$, but again this range has been expanded to account for the shift in peak over time as the rubber degrades. The methyl group (CH$_3$) typically found at 1260 cm$^{-1}$, is used as a reference peak for this calculation (Liu et al. 2005).

## 6.3. Results and discussion

6.3.1 Plastic VOC emission plots

Figures 6.2 and 6.3 show how each individual VOC emission rate changes over the course of the year from each plastic type. For many plastics, VOC emission rates are generally higher in the earlier months (1 to 4) of testing than the months that followed. Some VOC species do, however, show a rise in emission rates towards the end of the experimental testing period.

For the plastics located in the kitchen, Figure 6.2, the rubber-wire plastic type had the highest overall emissions of VOCs per surface area (cm$^2$) across the experimental time period. The PET plastic type shows the lowest overall VOC emissions, which has been observed in previous work (see previous experiments in Chapter 4). There does not appear to be a consistent trend in many of the VOC emission profiles over the months of 2021. Many of the aromatic VOCs, such as benzene, toluene and styrene, typically showed higher emissions in the earlier months, from 1 to 4, which then decreased in months

5, 6 and 7, to then show an increase in emissions from month 9 onwards. Naphthalene also shows a similar trend to this. The smaller VOCs, such as acetaldehyde, formaldehyde, propene and acrolein appear to vary considerably for the rubber wire plastic over the 12 months, however, they show little variation in emissions (or no emissions at all) for the PET water bottle or two storage container plastics. Figure S6.1 in Appendix C reports the VOC emission trends seen in Figure 6.2 without the Rubber-wire, so as to view the emission trends for the other plastic types on a different scale. The emissions from the PET water bottle, white HDPE storage container and clear PP storage container plastic types show similarly to what is described here, with no overall trends seen for many of the compounds, however phenol appears to show a gradual increase over the whole 12-month period, and benzene, styrene and naphthalene all show an increase from month 9 onwards.
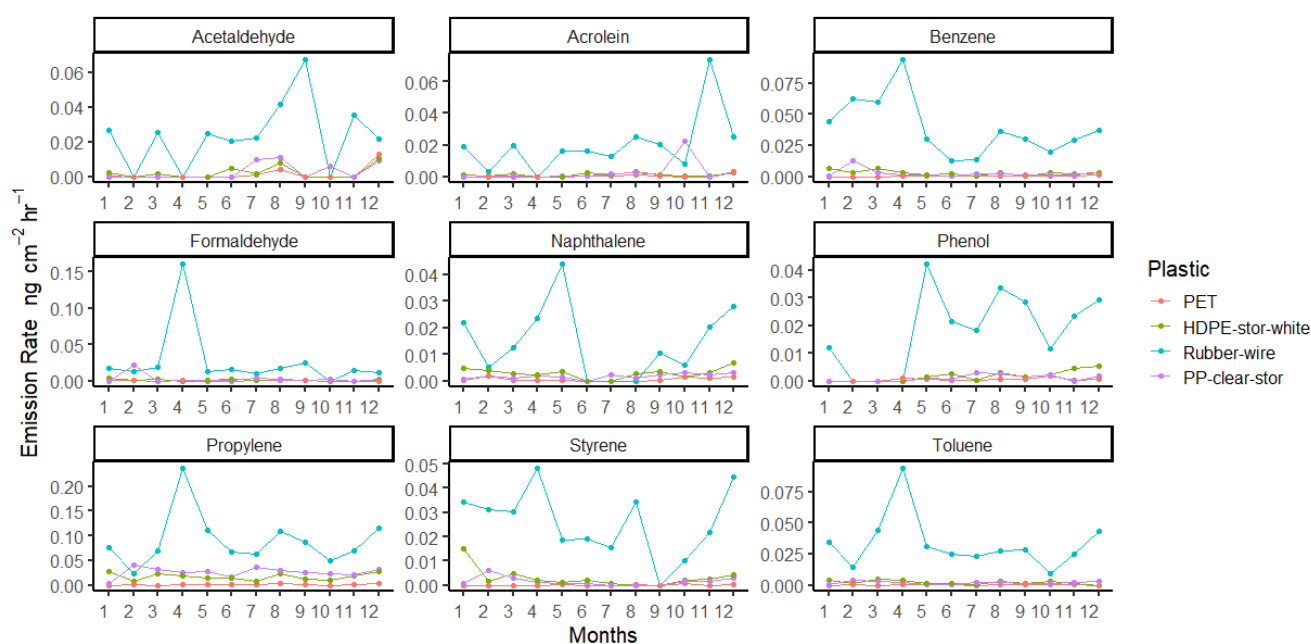


*Figure 6.2: VOC emissions for each of the kitchen plastics over the 12-month testing period, with month 1 = January 2021.*
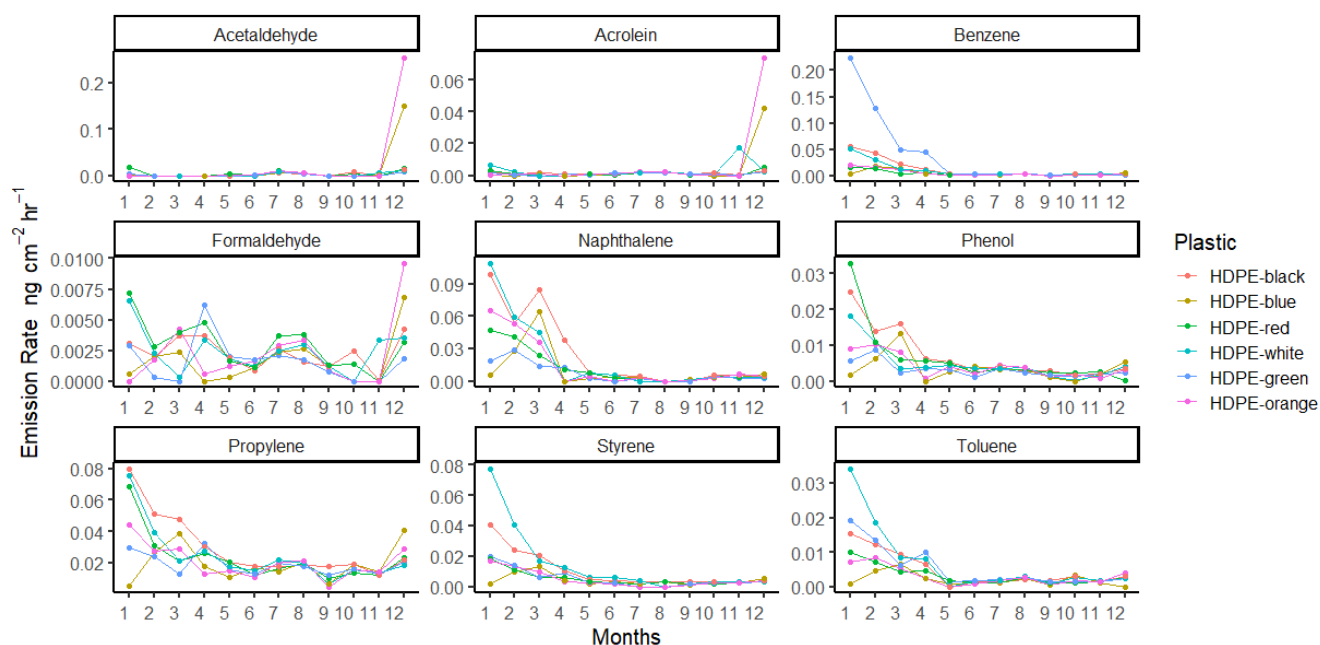
*Figure 6.3: VOC emissions for each of the bathroom plastics over the 12-month testing period, with month 1 = January 2021.*

The plastic types in the bathroom location, Figure 6.3, show very similar trends in VOC emissions over the 12-month experimental period, potentially owing to the fact that they are made of the same base polymer. It is clear to see trends in emissions decreasing with time. The aromatic compounds, benzene, toluene, phenol and styrene, along with propene and naphthalene, all show highest emissions from the plastics in the earlier months, with a gradual decrease over the year. Both acetaldehyde and acrolein show consistently low emissions throughout the year, with a small increase in the middle, during months 7 and 8, as well as a rise in emissions in the final month, Month 12, for HDPE-blue and HDPE-orange. The slight increase seen for months 7 and 8 may correspond to the warmer months observed during the summer season, as there were higher levels of temperature and light occurring indoors at this time. The plastic samples would also have been exposed to sunlight infiltrating through the windows for a longer period of time during the day in these summer months. Formaldehyde emissions for all of the plastic types are shown to vary across the months of the year, with an increase in emissions also shown for month 12.

Table 6.2 below contains the percentage difference between months 1 and 12, indicating how large the decrease (or increase) in VOC emissions were for each compound for each plastic type. Where there is a value of zero in the table, this was where the calculated emission rate at the start of the experimental period, month 1, was zero, therefore a percentage difference could not be calculated. However, this indicates that this particular VOC showed an increase in emissions from months 1 to 12.

*Table 6.2: Calculated percentage difference between emission rates at months 1 and 12 of the experimental testing period. Those compounds with a decrease in emissions from month 1 to 12 are highlighted in green, those that showed an increase in emissions are highlighted in red.*

| | HDPE-black | HDPE-blue | HDPE-green | HDPE-orange | HDPE-red | HDPE-white | HDPE-storage-white | PET | PP-storage-clear | Rubber-wire |
|---|---|---|---|---|---|---|---|---|---|---|
| **Formaldehyde** | 35.06 | 1021.3 | -35.81 | 0 | -55.93 | -46.16 | -60.91 | -100 | 9515.68 | -31.52 |
| **Propene** | -72.79 | 670.95 | -29.73 | -34.68 | -66.10 | -75.54 | -5.95 | 2455.11 | 644.97 | 53.063 |
| **Acetaldehyde** | 0 | 13445 | 170.99 | 0 | -19.48 | 171.52 | 358.27 | 1845.20 | 0 | -18.48 |
| **Acrolein** | 11.45 | 13083 | 33.20 | 10982.3 | 62.21 | -67.87 | 101.68 | 15385.9 | 17396.7 | 30.73 |
| **Benzene** | -93.71 | 57.47 | -99.02 | -79.34 | -82.20 | -92.60 | -50.84 | 19249.4 | 1124.26 | -16.64 |
| **Toluene** | -81.29 | -100 | -87.77 | -44.66 | -71.83 | -93.32 | -100 | -100 | 852.13 | 25.30 |
| **Phenol** | -85.22 | 186.77 | -57.38 | -65.15 | -99.02 | -77.66 | 0 | 0 | 0 | 142.38 |
| **Styrene** | -90.39 | 166.09 | -84.98 | -76.52 | -79.57 | -95.43 | -72.51 | 0 | 240.39 | 30.29 |
| **Naphthalene** | -95.23 | 10.42 | -85.05 | -92.20 | -92.33 | -96.46 | 38.77 | 3938.52 | 434.27 | 28.47 |

Compounds that showed the largest drop in emissions, e.g. 100 %, were toluene for the HDPE-blue, the white HDPE storage container and the PET water bottle plastics, as well as formaldehyde for PET. The aromatics generally showed the most consistent decrease in the bathroom. The plastic types found in the bathroom location, on average, saw the greatest drop in VOC emissions overall during the experimental period. This could be due to a number of environmental factors. The bathroom location typically experiences higher temperatures throughout the year, as it was positioned on the first floor of the house, and also experienced higher levels of light infiltrating through the external window. Despite the kitchen window being larger in size, this is in fact an internal window which looks onto another room in the house, therefore the kitchen location has no external windows, hence why the light levels measured were lower compared to the bathroom in Table 6.1. Additionally, activities that take place in the bathroom, such as showering, increase the humidity of the room to ~90 % humidity. This can cause hydrolytic degradation to occur within these plastic types, as the materials absorb moisture in the air which creates hydrolytic cleavages in the polymer chain (Krzan et al. 2006).

With the kitchen location being larger in size and having three entry points, it experiences lower temperatures (with increased circulation/changing of air) and lower levels of light compared to the bathroom. This may explain why the VOC emission rates were so varied and showed no overall trend over time. Although the activities that took place in this location, such as cooking, still caused the

humidity to temporarily increase, it was not to the same extent as showering in the bathroom, with much smaller dimensions.

The presence of water and water films on the surface of plastics can potentially enhance or inhibit surface emissions. For example, water-soluble VOCs (such as formaldehyde and acrolein), can easily partition into water films (Duncan et al. 2018), and other organic species, such as phthalates, have been found to transfer into aqueous films on indoor surfaces (Jaeger and Rubin 1970). High relative humidity has also been shown to drive other organic compounds from surfaces indoors, showing that these processes are currently poorly quantified (Ault et al. 2020).

6.3.2 FTIR Spectra analysis

Figures 6.4, 6.5 and 6.6 show the evolution of the carbonyl regions over time. FTIR spectroscopy was used to identify and track the changes in the carbonyl region in the molecular structure of the investigated plastics. The carbonyl peak intensity, in the region of 1700- 1790 cm$^{-1}$, increases from month 1 to 3 for both the white HDPE plastic in Figure 6.4 and the rubber wire in Figure 6.6. However, these peaks then reduce slightly and fluctuate across the following months, showing minimal changes as the natural ageing exposure time increases. This variability was observed in the spectra comparisons for all plastic types.

Degradation of plastic polymers through all types of processes, including thermal- and photo-degradation, lead to the generation of carbonyl groups on the material surface (Roy et al. 2007). Carbonyl groups intrinsic to polymeric chain oxidation reactions are located within the absorption band of 1690 - 1785 cm$^{-1}$. In Figure 6.5, it is clear to see that the peak intensity in this region assigned to the C=O stretching of carbonyl groups experiences a slight band broadening over time due to overlapping of stretching bands of carboxylic acid groups (1700 cm$^{-1}$) and aldehydes and/ or esters (1710-1725 cm$^{-1}$) (Roy et al. 2007), as the exposure to natural ageing is prolonged.
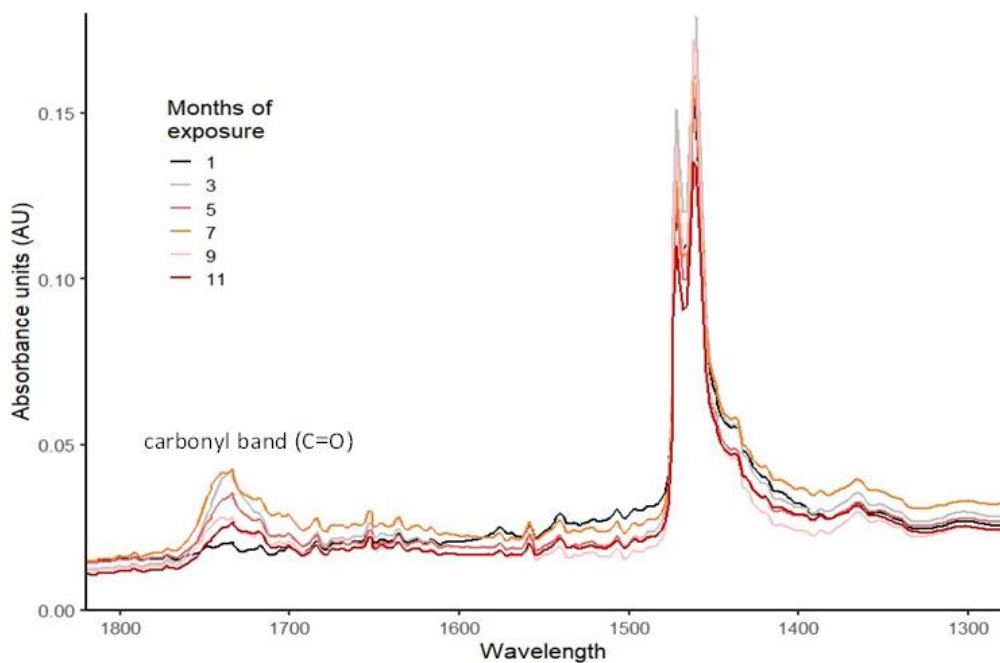
*Figure 6.4: FTIR spectra of the HDPE-white shampoo bottle after 1, 3, 5, 7, 9 and 11 months of exposure to natural ageing in the bathroom.*
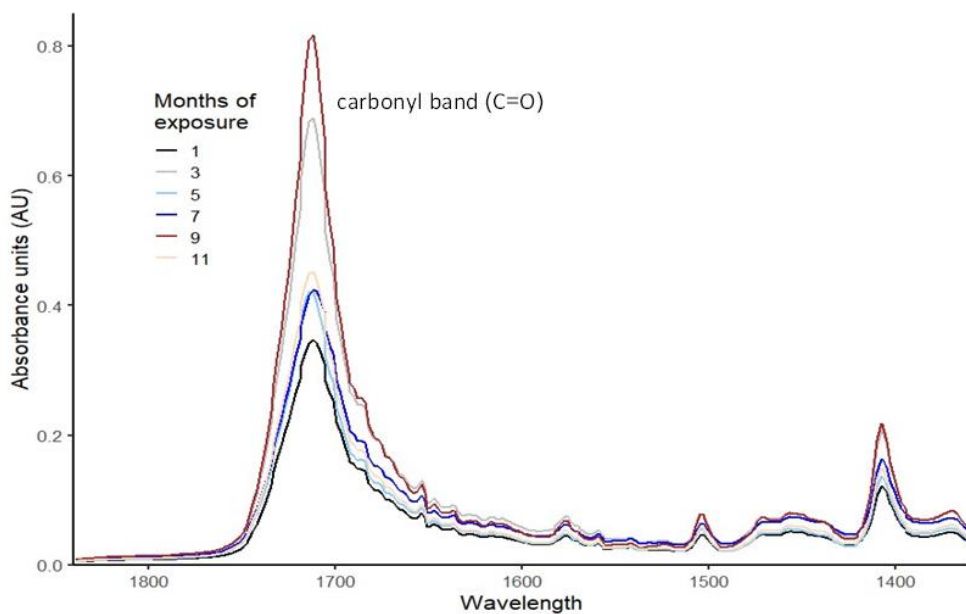


*Figure 6.5: FTIR spectra of the PET water bottle after 1, 3, 5, 7, 9 and 11 months of exposure to natural ageing in the kitchen.*
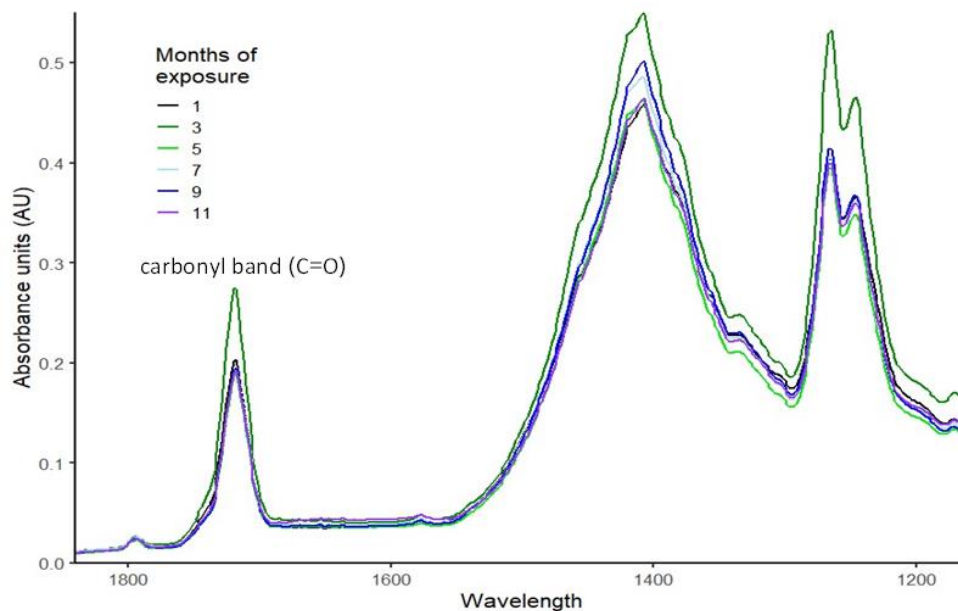
*Figure 6.6: FTIR spectra of the rubber wire after 1, 3, 5, 7, 9 and 11 months of exposure to natural ageing in the kitchen.*

6.3.3 Carbonyl index values

Figures 6.7 and 6.8 depict the CI measurements of the plastics at 1, 3, 5, 7, 9 and 11 months of exposure to natural ageing processes in each of the specified locations. The CI values for the plastic types located in the bathroom, in Figure 6.7, show fluctuating values, with the all plastic types showing a decrease in CI values over the time period investigated. However, the white HDPE plastic showed an overall increase in the CI value from months 3 to 11, from 0.37 to 0.58, respectively, indicating an increase in carbonyl-containing product formation during the plastics degradation. The CI values for the plastic types placed in the kitchen location, in Figure 6.8, also show fluctuating values with no overall trend with time. This potentially shows that the additives, incorporated within the plastic polymers, slow the degradation which is why we only observe small changes in CI values.
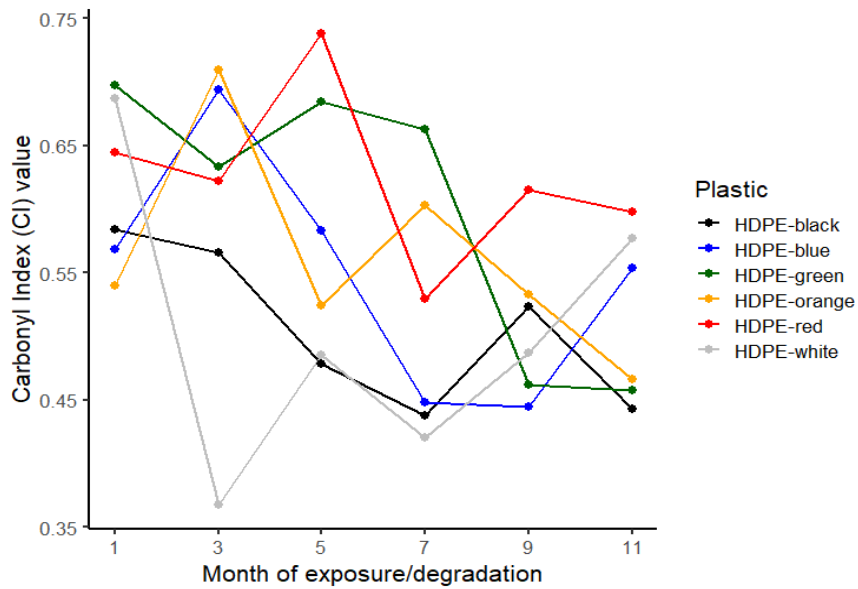
*Figure 6.7: Carbonyl Indices for the six coloured shampoo bottle plastics located in the bathroom.*
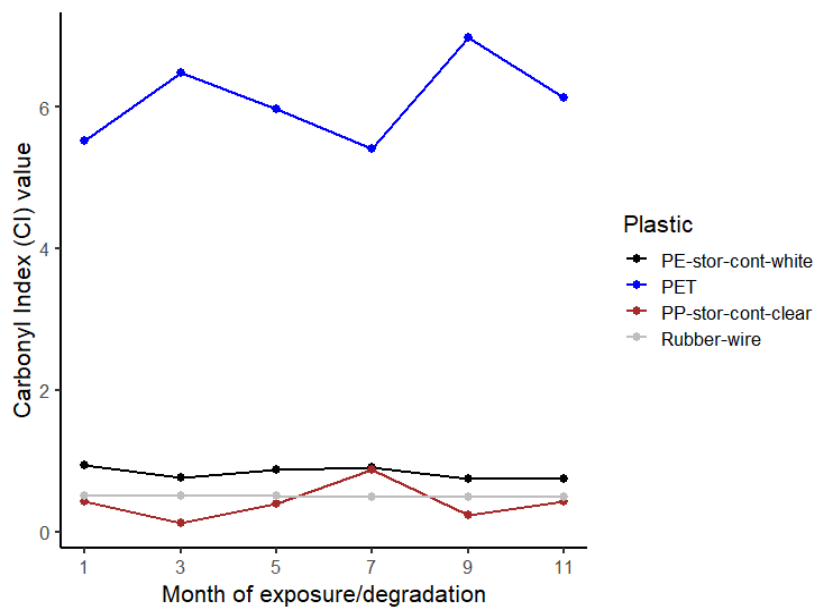


*Figure 6.8: Carbonyl Indices for the four plastic types located in the kitchen.*

6.3.3.1 Analysis of Variance (ANOVA)

A one-way ANOVA was employed to determine whether there was a statistically significant difference between the CI values across months 1 to 11. During the analysis, the null hypothesis was that all CI mean values, belonging to the same plastic type, across months 1 to 11 were equal. Only one plastic type had a *p*-value of less than 0.05: the white HDPE shampoo bottle. Therefore, it can be concluded

that this was the only plastic type where the CI was significantly affected by the natural ageing processes it underwent, whilst all other plastic types were not.

6.3.3.2 Rationale behind choosing peak area measurements

The rationale behind the choice of peak area measurement rather than intensity at one specific wavenumber is based on the fact that the breakdown of plastics during ageing processes produces dozens of different carbonyl products (Hakkarainen & Albertsson 2004). Some of these carbonyl species can be identified individually, for example, γ-lactones can be identified at ~1,780 cm$^{-1}$, esters and/or aldehydes at ~1,733 cm$^{-1}$, ketones at ~1,714 cm$^{-1}$ and carboxylic acids at ~1700 cm$^{-1}$. However, these species do not have specific static peak assignments (Almond et al. 2020). It is also known that the peak position between ATR-FTIR and other FTIR methods, such as transmission FTIR spectroscopy, often shifts slightly due to the change in refractive index, so comparing results between other literature values can prove to be challenging. Therefore, using the area under the band technique reduces any potential error due to shifting peak positions, or broadening of peaks as observed in the spectra in Figures 6.4-6.6, as the area under the band will still account for this and be less influenced than any individual peaks within the specified region. The peak area can simply be considered as a series of overlapping height bands. Assigning the complex series of peaks can often be beyond the capabilities of the operator and can be open to different interpretations (Almond et al. 2020). This is crucial due to the complexity of species produced during degradation of the plastic types.

Focusing on singular peak heights introduces another issue: if a single wavenumber is chosen to represent CI, then it raises the question as to whether this is always the same C=O species being measured (Antunes et al. 2017). At a 4 cm$^{-1}$ resolution (used in this investigation), this band will be a composite of multiple carbonyl species. Running at a higher resolution of 1–2 cm$^{-1}$ (which some spectrometers may struggle to replicate) can create greater noise interference in the C=O band rather than providing clarity (Almond et al. 2020). When looking at the CI values calculated using the area under the band, it gives a more balanced representation of the relative total concentration of carbonyl containing species and is thus reflected in a higher CI.

6.3.4. Hit Quality of spectra

The Hit Quality (HQ) of FTIR spectra can be described as how well the sample spectra were matched to a Library spectra within the Agilent Polymer ATR Library database. A HQ score of over 0.8 (with the highest possible HQ value being 1) was considered a good fit, as previously mentioned in section 3.3. Figure 6.9 shows the HQ scores for the sample spectra for each of the plastic types after 1, 3, 5, 7, 9 and 11 months of natural ageing. Where there are points missing, a HQ score could not be obtained,

as the sample spectra could not be identified using the Agilent Polymer ATR Library. The four lower plots in Figure 6.9 are the four plastic types located within the kitchen. These plastic types show a consistent HQ score throughout the test period. The other six plots in Figure 6.9 are the six shampoo bottle plastics that were located in the bathroom. These plastics show a downward trend in HQ values, although there are several missing values in the later parts of the test period. The spectra obtained in these months became less recognisable to the FTIR instrument and its built-in spectral Library, caused by the subsequent degradation these samples were subjected to.
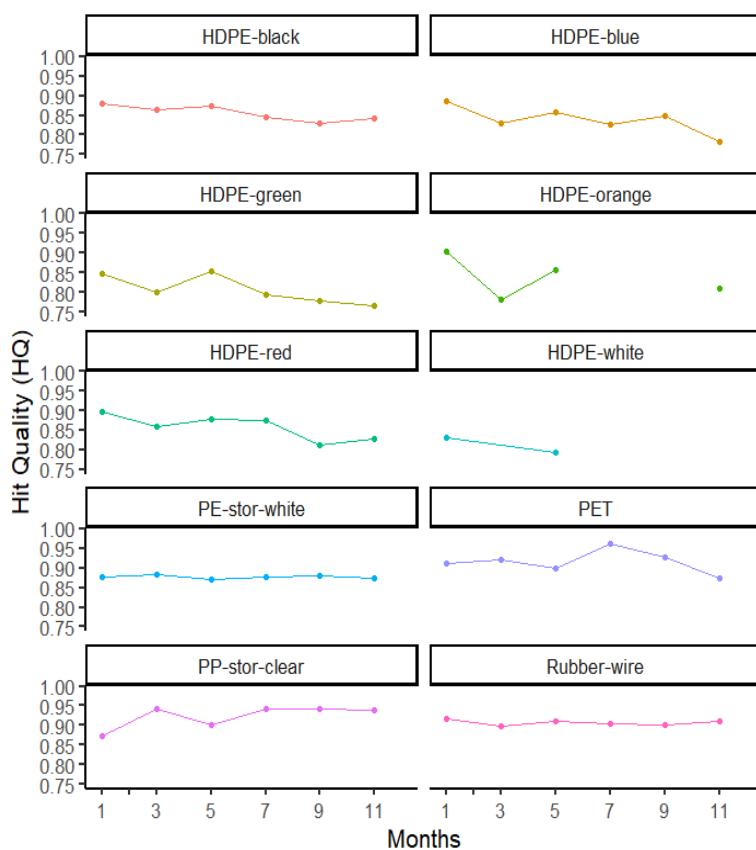


*Figure 6.9: Hit Quality (HQ) values obtained from comparing the sample spectra of each plastic type, during 1, 3, 5, 7, 9 and 11 months of natural ageing processes, to Library spectra within the Agilent Polymer ATR Library database.*

## 6.4. Conclusion

The current study investigated the effects of natural ageing over the course of a year for ten plastic types and their VOC emissions, when positioned across two locations in a family house; a kitchen and a bathroom. Higher temperatures, humidity values and light readings were observed in the bathroom location compared to the kitchen. However, the CI values, calculated from the ATR-FTIR spectrums

showed no trend over the testing time period. A broadening of the carbonyl peaks within the sample spectrums, however, does indicate that some degradation had occurred within the plastic samples.

The VOC emissions from the plastic types placed in the kitchen varied over the course of the year. However, the plastic types in the bathroom showed a clearer trend of decreasing emissions as the exposure duration to natural ageing increased, with aromatic compounds (such as toluene) generally showing a more consistent decrease with time. It is possible that the natural ageing processes that these plastic types were exposed to were not enough to see significant changes in the testing time period and, potentially, the additives in plastics slowed the degradation of plastics.

# 7. Conclusions

## 7.1 Research gap overview

The key findings from Klepeis et al. (2001), that many individuals spend over 90% of their lives within indoor environments, sparked an interest among atmospheric scientists and has drawn more attention to the impacts of indoor air quality (IAQ) over the last two decades. Identifying and quantifying particular compounds emitted from material surfaces indoors is a large field within the indoor air quality research area. For example, building materials, including types of flooring (Cox et al. 2002; Afshari et al. 2004), particleboard and fiberboard (Jiang et al. 2017; Zhou et al. 2019), soft furnishings (Oz et al. 2019) and wooden furniture (Xiong et al. 2019), have been extensively evaluated for their chemical emissions and influence on IAQ (Kruza et al. 2017). However, smaller plastic products, such as decorative articles, tools, utensils, textiles and children's toys, have not yet been fully explored (Haug et al. 2022). With the ever-growing production and consumption of plastic products, we may continually see plastics present in our lives and within our indoor environments, especially our homes.

The work conducted for this thesis has explored this knowledge gap, with the objective of determining how VOC emissions from different plastic consumer products, commonly found in the home, are influenced by abiotic factors, such as temperature, light and natural ageing. The emission rates obtained through controlled experiments were implemented within an indoor atmospheric model, INCHEM-Py, to further explore how these VOCs influence indoor air chemistry and secondary product creation.

## 7.2 Summary of findings

Chapters 4-6 investigated the degradation of selected common household plastic products under a range of environmental conditions, typical of indoor environments. The experimental design for determining the influence of abiotic factors on plastics was chosen to control the exposure of samples to indoor temperatures (Chapter 4) and both the diurnal variation of sunlight (containing UV) and varying intensities of light from an LED lamp (with no UV) (Chapter 5). Both of these studies contained a modelling element, whereby the emission rates obtained for target VOCs were extrapolated to replicate an $8.6 \text{ m}^2$ surface area of plastic within a simulated space, and then compared to background simulations (where there was no plastic). The VOC emissions showed a positive relationship with temperature and with light in the UV range (315-400 nm). The production of secondary pollutants, simulated through modelling, such as $NO_2$, $HO_2$, $O_3$, HCHO and to some degree glyoxal, increased with temperature at varying rates across the simulations. However, for OH, NO and HONO, the opposite was found, as these species are removed from the system through oxidation reactions.

Chapter 6 explored the natural ageing of these plastic types under typical indoor conditions, where the plastic types were exposed to degradation processes, such as thermal-, photo- and mechanical degradation, all happening simultaneously. These processes can cause significant changes within the material and on its surface, which was monitored over time using ATR-FTIR spectroscopy. Samples from the plastic types, contained within the two household locations, were extracted and tested for their VOC emissions, many of which showed a gradual decrease over the course of the year. The results show that all abiotic factors play an important role on the emissions from plastics and hence the indoor air chemistry.

7.2.1 Suggestions to further the experimental work

To move the field of plastic emissions indoors forward, the experiments in this work could be further improved by incorporating another analytical technique, such as GC-MS, to aid with the identification of more compounds emitted from the plastic types. Additionally, more plastic replicates could be tested to determine the full variability in VOC emission rates within a batch of produced items.

With regards to the light experiments conducted in Chapter 5, repeat measurements could be taken in a similar fashion on multiple days. The use of additional light sensors, including a UVB sensor, could be considered to determine how this portion of light infiltrates through the glass chambers and interacts with surface emissions. As previously mentioned, it would also be good to consider including an additional covered chamber containing a plastic sample, to help understand the influence of the solar radiation separately from the temperature.

With regards to the natural ageing experiments conducted in Chapter 6, all of the plastics could have been placed in both locations, to quantify the natural ageing processes in both rooms. This would allow the researcher to determine whether the changes in emissions were due to the plastic type or the different environmental exposures. The build-up of surface films on the plastic samples during this time period could have also been determined, whilst swab samples from the plastic surfaces could have determined the presence of microbial colonies.

## 7.3 Characterisation of further products and emitted chemicals

7.3.1 Other product materials

The plastic types investigated for this work were selected as they were considered common plastics that are typically found in a home. These plastics provided a good range of different base polymer types, as they fell into four of the seven UK recycling code categories (PET, HDPE, PP and PS) as well as the

additional polyester rubber. However, future research should consider other consumer articles, and their VOC emissions, to better understand the influence of consumer products on our indoor environments. A fairly new polymer type that was not included in the present work is recycled plastic. Recent studies have focused on the characterisation and quantification of VOCs in recycled products (Cabanes et al. 2020). Several compounds, including acetophenone and diethyl phthalate, were detected in recycled polyethylenes (Horodytska et al. 2020). Consumer products made of recycled polymers are controlled like non-recycled products with respect to chemical safety aspects (Cabanes et al. 2020). However, they are more likely to be contaminated with non-intentionally added substances due to their manufacturing procedures involving previously used polymers from multiple origins. It has also been found that recycled plastics contain higher concentrations of substances such as antimony and Bisphenol A, as they become more concentrated within the polymer mixture (Gerassimidou et al. 2022).

Another plastic type that was not considered for investigation in this thesis was bioplastics. Bioplastics are currently and increasingly used as substitutes of conventional plastics, principally as food packaging containers and films and more recently, in electronics and in the manufacture of synthetic fibres (Karamanlioglu et al. 2017). These have been utilised in order to cope with problems related to plastic-based pollution. Bioplastics are applied in building products because they are based on natural resources and can be disposed of easily (Friedrich 2022). Certified international standards identify the criteria a bioplastic must comply with in order to be labelled as compostable and/or biodegradable. A study conducted by (Folino et al. 2023) established many issues within this area, one of which is that some biopolymers are labelled as biodegradable but may not degrade fully in industrial waste treatment plants due to adequate processing conditions not being in place. This is still an ongoing area of development of bioplastics, and potential future studies should consider exploring VOC emissions from bioplastics in the home, and how they may contribute to indoor air chemistry.

### 7.3.2 Comparison of results to other products

As previously mentioned, there are many other sources of VOCs within the indoor environment. Some emissions reported in the literature are greater for consumer products other than the plastic types investigated throughout this work. For example, Petry et al. (2013) identified emission rates of formaldehyde and benzene from scented candles to be between 17-109 and 0.4-3.6 $\mu$g hr$^{-1}$, respectively under various experimental chamber conditions. Palmisani et al. (2020) identified emissions of aromatic compounds, such as benzene, toluene and styrene, from polyester and PVC heating bags of up to 18, 485 and 70 ng hr$^{-1}$, respectively. These are over a thousand times higher than the values reported here.

The emission rates determined through this work, alone, would not contribute to concentrations indoors that would surpass air quality guidelines outlined within UK standards. However, the cumulative effect, of both multiple sources and multiple VOCs in indoor air, is not yet fully understood. Despite plastic

emissions only contributing a small amount to the overall concentrations of air pollutants observed indoors, it is still important to consider these emissions in future modelling scenarios as this will help determine more accurately the full extent of human exposure to VOCs in indoor air.

### 7.3.3 Uncertainties and limits associated with PTR-TOF-MS measurements and experiments

It is important to recognise that, whilst this work focused on polymer-based consumer products and a selection of VOC emissions, a range of other chemicals are emitted from plastic polymers that could be relevant to human health exposure. The decision to focus on nine specific VOCs predominately stems from the precision and accuracy of the instrument used to identify and quantify the emissions: the PTR-TOF-MS. Chemical ionisation using proton-transfer-reactions with hydronium ions ($H_3O^+$) is widely used for trace gas detection in air (Pagonis et al. 2019). However, a limitation of this method is that it cannot distinguish isomers with the same ion mass. Therefore, compounds such as meta-, ortho- and para-xylene and ethylbenzene, with a protonated mass of 107, and two propyl-benzene, two ethyl-toluene, and three trimethylbenzene, with a protonated mass of 121 (de Gouw & Warneke 2007), have been excluded from analysis. As previously addressed, in section 3.7, other fragments of products can contribute to the ion mass signal detected using PTR-TOF-MS, therefore it is highlighted that the emission rates determined throughout this thesis are upper limits for the plastic polymers measured under these conditions.

However, there is an extensive body of literature on the detection of different trace gases by PTR-MS using proton-transfer reactions with $H_3O^+$ ions. Work conducted by Pagonis et al. (2019) summarises existing information in an online, publicly available library that allows users to look up which m/z trace gas of interest is detected, and which trace gases may be responsible for a detected product ion. By cross-checking the compounds of interest reported in this thesis, we report with confidence that the ions detected at those specified masses are the associated identified compounds.

Another area of limitation and uncertainty is the measurements made of the plastic samples surface area determined throughout this work. An important note to highlight is that these were carried out by hand, using a calibrated Sigma Aldrich ruler. Emission rates determined using these surface area measurements may have been over or underestimated, limited by the precision of this measurement technique to the nearest 0.01cm.

### 7.3.4 Knowledge limitations on additives

As previously discussed, the source of VOC emissions from the plastic types investigated throughout this work can be attributed to the additives contained within the polymer matrix. These additives are incorporated into plastics during their manufacturing process, and help maintain, enhance and give the

plastics their specific characteristics (Lambert 2013), many of which are discussed in section 2.2. Other chemicals are involved in the production of plastics which are used to ease the process, such as polymerisation catalysts or lubricants (Fink 2009). As well as these intentionally used chemicals, other non-intentionally added substances (NIAS) can be present in plastics, including breakdown products and contaminants (Geueke 2013). Because these compounds are not chemically bound to the polymer matrix, they can migrate to the surface of the plastic and be released into the environment through exposure to degradation. A systematic review conducted by Wiesinger et al. (2021), reported that over 2,400 substances (out of 10,000 identified substances) incorporated in plastics as cited in the literature, are not adequately regulated or even approved for use in food-contact plastics in some jurisdictions. Wiesinger et al. (2021), highlights that there is a substantial information gap in the public domain due to a lack of transparency regarding substances present in plastic materials and a lack of easy information access to manufacturing procedures and regulations in many parts of the world (Nerin et al. 2013). This lack of transparency has made gathering information on the plastics used in this thesis a major challenge.

## 7.4 Modelling scenarios

Beyond understanding the influence of a single plastic type with a specified area of 8.6 $m^2$ in INCHEM-Py, other scenarios may be considered. Scenarios could have included the plastics being used during an activity conducted within the home, such as showering in the bathroom or cooking or cleaning in a kitchen. Previous work has investigated the air chemistry following cleaning events indoors, with a particular focus on photolysis (Wang et al. 2020). This study found that the use of cleaning agents leads to an increase in concentrations of radical species of orders of magnitude higher than background levels, but how the presence of plastic surfaces may have influenced the outcome was not explored.

In addition to exploring emissions from plastic products typically found in the home setting, high concentrations of VOCs emitted from polymer-based consumer products can also reach workers in manufacturing or retail environments. Workers in these particular indoor environments can be constantly exposed to freshly manufactured goods. Different studies have examined the exposure of workers in shopping and storage areas. A recent study investigated 10 retail stores in France (Robert et al. 2020). However, VOCs similar to the ones explored in this thesis, were only detected at low concentrations in the French study; formaldehyde and toluene concentrations reached 53 µg $m^{-3}$ and 252 µg $m^{-3}$, respectively, which were below occupational guideline values.

Certain model parameters were kept consistent in each of the model simulations, so as not to add any further complexity. A low air exchange rate with outdoor air of 0.2 $hr^{-1}$, was used. However, real indoor environments are often better ventilated (Bornehag et al. 2005), but this allows the consideration of a

worst-case scenario. Other surfaces were not included within the model simulations, such as soft furnishings, as these are known to influence the $O_3$ and hydrogen peroxide concentrations indoors (Carter et al. 2023). The types of scenarios described in this section were not explored in the work presented in this thesis, as it focuses on exposure to plastic-emitted VOCs within the home. However, these emission rates can be used by future researchers to determine human exposures in other scenario settings that include plastics, as well as other surface interactions and occupant activities.

## 7.5 Regulatory standards

Regulation of VOC emissions from polymer-based consumer products is still missing. Experimental protocols and data interpretation strategies need to be clearly defined and standardised. As previously discussed in Chapter 4, the ISO 16000 series does provide guidance for measuring emissions of VOCs from building materials, and defines parameters for chamber measurements, such as a stable temperature of 23°C and a relative humidity of 50 % (ISO 2006). However, it leaves interpretation open by including "furnishings" within its scope. Consumer products are not specified within the scope of this ISO standard. The recommendation for chamber size of up to 1000 L, is not suitable for investigations into small household consumer products, as the emissions would be too diluted in the air space and concentrations would be too low to detect.

There has also been a variety of editions of the WHO quality guidelines on acceptable concentrations of gaseous compounds within indoor environments. The WHO Air Quality guidelines published in 2010 recognised that the work assessing the health effects of indoor air pollution lagged behind that on outdoor pollution. Although the WHO guideline values have been set upon reviewing globally accumulated scientific evidence, they only present a selection of individual gaseous compounds that are thought to be safe for the human population. However, the WHO recognises that exposure to combinations of air pollutants is inevitable. Information detailing the effects of co-exposure to air pollutants is very limited and therefore it is not possible to recommend guidelines for such combinations (WHO 2010).

Even (2021) found very similar struggles in her PhD work and agrees that regulations should be harmonised with other VOC-emitting consumer products such as fragranced products. As mentioned in an article by Goldsmith et al. (2014), a consumer product database would allow laboratories to rely on each other's data to efficiently perform their own risk assessments and may raise awareness and public information.

## 7.6 Future perspectives

To further this work, more plastic types could be investigated, to build on our understanding of plastic emissions in the indoor environment, as the plastic types selected for this work only account for a small selection of the available plastics on the market. Investigation of the impact of biodegradable and recycled plastics would also be beneficial as discussed earlier. Incorporation of another analytical technique, such as GC-MS, more regularly through the series of experiments could also aid with identification of more compounds within the emitted mixture.

Future trends in housing developments show a focus on reducing carbon emissions and improving the energy efficiency of buildings. Many countries have adopted low-carbon development schemes as a means to achieve global emission reduction targets for 2050 (Huang et al. 2022). An advancement in this area is the construction of large glass spans or windows, which have become an increasingly popular building feature over the last ten to fifteen years (Ganobjak et al. 2023). These structures allow for increased natural lighting indoors and also prove to be strong insulating materials. However, as explored in Chapter 5, increased lighting indoors can result in more photolysis of compounds and also increase material emissions, including those from plastics.

High airtightness of buildings also has a significant role on indoor air quality and energy efficiency (Ji et al. 2022) and may lead to a greater concentration of VOCs indoors. Coupling this with more glass in newly constructed buildings, the impacts of weather events, such as heat waves, may be amplified. As previously mentioned in Chapter 4, recent trends in climate change suggest there will be more extreme weather events in the future including heatwaves (Petrou et al. 2019). Indoor overheating caused by heatwave events can cause a sharp spike in recorded heat-related deaths among vulnerable groups in the population (Petrou et al. 2019; Gasparrini et al. 2022). However, they could also lead to increased emissions from plastics.

Like many environmentally conscious consumers, some production companies acknowledge the plastic pollution problem. They direct their efforts to reduce their environmental impact by either utilising plastic waste to produce goods or give a certain percentage of their profits to organisations dedicated to environmental conservation (Williams and Rangel-Buitrago 2022). Although this helps in reducing plastic waste globally, it does not resolve the issue of increasing plastic production. The amount of plastic in circulation continues to grow. Consumerism continually drives the amount of plastic in our homes, and in the environment, upwards. The growth of online platforms, due to the impact of the COVID-19 pandemic, has increased the accessibility to consumer goods and makes it the preferred choice when purchasing items for our home. A systematic change would provide a starting point for resolving the plastic issue but would involve changes in both policy and business.

# 8. References

Abe, Yutaka, Miku Yamaguchi, Motoh Mutsuga, Hiroshi Akiyama, and Yoko Kawamura. 2013. "Volatile Substances in Polymer Toys Made from Butadiene and Styrene." *American Journal of Analytical Chemistry* 04 (05): 229–37. https://doi.org/10.4236/ajac.2013.45029.

Afshari, A., L. Gunnarsen, P. A. Clausen, and V. Hansen. 2004. "Emission of Phthalates from PVC and Other Materials." *Indoor Air* 14 (2): 120–28. https://doi.org/10.1046/j.1600-0668.2003.00220.x.

Afshari, A., B. Lundgren, and L. E. Ekberg. 2003. "Comparison of Three Small Chamber Test Methods for the Measurement of VOC Emission Rates from Paint." *Indoor Air* 13 (2): 156–65. https://doi.org/10.1034/J.1600-0668.2003.00146.X.

Ahmed, Fahad, Sahadat Hossain, Shakhaoat Hossain, Abu Naieum Muhammad Fakhruddin, Abu Tareq Mohammad Abdullah, Muhammed Alamgir Zaman Chowdhury, and Siew Hua Gan. 2019. "Impact of Household Air Pollution on Human Health: Source Identification and Systematic Management Approach." *SN Applied Sciences* 1 (5). https://doi.org/10.1007/s42452-019-0405-8.

Alamri, M. S., Akram A.A. Qasem, Abdellatif A. Mohamed, Shahzad Hussain, Mohamed A. Ibraheem, Ghalia Shamlan, Hesham A. Alqah, and Ali S. Qasha. 2021. "Food Packaging's Materials: A Food Safety Perspective." *Saudi Journal of Biological Sciences* 28 (8): 4490–99. https://doi.org/10.1016/j.sjbs.2021.04.047.

Almond, Jasmine, Piriya Sugumaar, Margot N. Wenzel, Gavin Hill, and Christopher Wallis. 2020. "Determination of the Carbonyl Index of Polyethylene and Polypropylene Using Specified Area under Band Methodology with ATR-FTIR Spectroscopy." *E-Polymers* 20 (1): 369–81. https://doi.org/10.1515/epoly-2020-0041.

Alvarez, Elena Gómez, Damien Amedro, Charbel Afif, Sasho Gligorovski, Coralie Schoemacker, Christa Fittschen, Jean Francois Doussin, and Henri Wortham. 2013. "Unexpectedly High Indoor Hydroxyl Radical Concentrations Associated with Nitrous Acid." *Proceedings of the National Academy of Sciences of the United States of America* 110 (33): 13294–99. https://doi.org/10.1073/PNAS.1308310110/SUPPL_FILE/PNAS.201308310SI.PDF.

Ambrogi, V., P. Cerruti, C. Carfagna, M. Malinconico, V. Marturano, M. Perrotti, and P. Persico. 2011. "Natural Antioxidants for Polypropylene Stabilization." *Polymer Degradation and Stability* 96 (12): 2152–58. https://doi.org/10.1016/J.POLYMDEGRADSTAB.2011.09.015.

Ángeles-López, Y G, Gutiérrez-Mayen, A M, Velasco-Pérez*, M, Beltrán-Villavicencio, M, Vázquez-Morillas, A, Cano-Blanco, M. 2017. "Abiotic Degradation of Plastic Films." *Journal of Physics; Conf. Series* 792. https://doi.org/10.1088/1742-6596/792/1/012027.

Antunes, Marcela C., José A.M. Agnelli, Alex S. Babetto, Baltus C. Bonse, and Sílvia H.P. Bettini. 2017. "Abiotic Thermo-Oxidative Degradation of High Density Polyethylene: Effect of Manganese Stearate Concentration." *Polymer Degradation and Stability* 143 (September): 95–103. https://doi.org/10.1016/J.POLYMDEGRADSTAB.2017.06.012.

Arata, Caleb, Pawel K. Misztal, Yilin Tian, David M. Lunderberg, Kasper Kristensen, Atila Novoselac, Marina E. Vance, Delphine K. Farmer, William W. Nazaroff, and Allen H. Goldstein. 2021. "Volatile Organic Compound Emissions during HOMEChem." *Indoor Air* 31 (6): 2099–2117. https://doi.org/10.1111/INA.12906.

Arkatkar, Ambika, J. Arutchelvi, Sumit Bhaduri, Parasu Veera Uppara, and Mukesh Doble. 2009. "Degradation of Unpretreated and Thermally Pretreated Polypropylene by Soil Consortia." *International Biodeterioration & Biodegradation* 63 (1): 106–11. https://doi.org/10.1016/J.IBIOD.2008.06.005.

Armenta, Sergio, Manel Alcala, and Marcelo Blanco. 2011. "A Review of Recent, Unconventional Applications of Ion Mobility Spectrometry (IMS)." *Analytica Chimica Acta* 703 (2): 114–23. https://doi.org/10.1016/j.aca.2011.07.021.

Atkinson, Roger, and Janet Arey. 2007. "Mechanisms of the Gas-Phase Reactions of Aromatic Hydrocarbons and Pahs with Oh and NO3 Radicals." *Polycyclic Aromatic Compounds* 27 (1): 15–40. https://doi.org/10.1080/10406630601134243.

Ault, Andrew P., Vicki H. Grassian, Nicola Carslaw, Douglas B. Collins, Hugo Destaillats, D. James Donaldson, Delphine K. Farmer, et al. 2020. "Indoor Surface Chemistry: Developing a Molecular Picture of Reactions on Indoor Interfaces." *Chem* 6 (12): 3203–18. https://doi.org/10.1016/j.chempr.2020.08.023.

Bari, Md Aynul, Warren B. Kindzierski, Amanda J. Wheeler, Marie Ève Héroux, and Lance A. Wallace. 2015. "Source Apportionment of Indoor and Outdoor Volatile Organic Compounds at Homes in Edmonton, Canada." *Building and Environment* 90: 114–24. https://doi.org/10.1016/j.buildenv.2015.03.023.

Bartkow, Michael E., Kees Booij, Karen E. Kennedy, Jochen F. Müller, and Darryl W. Hawker. 2005. "Passive Air Sampling Theory for Semivolatile Organic Compounds." *Chemosphere* 60 (2): 170–76. https://doi.org/10.1016/J.CHEMOSPHERE.2004.12.033.

Bartsch, Jennifer, Erik Uhde, and Tunga Salthammer. 2016. "Analysis of Odour Compounds from Scented Consumer Products Using Gas Chromatography-Mass Spectrometry and Gas Chromatography-Olfactometry." *Analytica Chimica Acta* 904: 98–106. https://doi.org/https://doi.org/10.1016/j.aca.2015.11.031.

Bartzis, John G., Costas Michael, Stella Michaelidou, Dafni A. Missia, Dikaia E. Saraga, Evangelos I. Tolis, S. Psoma, Christine Petaloti, Dimitrios Kotzias, and Josefa M. Barero-Moreno. 2008. "Concentrations of VOCs and Ozone in Indoor Environments: A Case Study in Two Mediteranean Cities during Winter Period." *Fresenius Environmental Bulletin* 17 (9 B): 1480–84.

Beauchamp, Jonathan, and Erika Zardin. 2017. "Odorant Detection by On-Line Chemical Ionization Mass Spectrometry." In , 49–50. https://doi.org/10.1007/978-3-319-26932-0_18.

Bekö, Gabriel, Charles J. Weschler, Aneta Wierzbicka, Dorina Gabriela Karottki, Jørn Toftum, Steffen Loft, and Geo Clausen. 2013. "Ultrafine Particles: Exposure and Source Apportionment in 56 Danish Homes." *Environmental Science and Technology* 47 (18): 10240–48. https://doi.org/10.1021/es402429h.

Bernstein, Jonathan A., Neil Alexis, Hyacinth Bacchus, I. Leonard Bernstein, Pat Fritz, Elliot Horner, Ning Li, et al. 2008. "The Health Effects of Nonindustrial Indoor Air Pollution." *Journal of Allergy and Clinical Immunology* 121 (3): 585–91. https://doi.org/10.1016/j.jaci.2007.10.045.

Bicchi, C., C. Cordero, E. Liberto, P. Rubiolo, B. Sgorbini, and P. Sandra. 2007. "Sorptive Tape Extraction in the Analysis of the Volatile Fraction Emitted from Biological Solid Matrices." *Journal of Chromatography A* 1148 (2): 137–44. https://doi.org/10.1016/J.CHROMA.2007.03.007.

Blocquet, M, F Guo, M Mendez, M Ward, S Coudert, S Batut, C Hecquet, N Blond, C Fittschen, and C Schoemaecker. 2018. "Impact of the Spectral and Spatial Properties of Natural Light on Indoor Gas-Phase Chemistry: Experimental and Modeling Study." *Indoor Air.* 28: 426–40. https://doi.org/10.1111/ina.12450.

BOENIG, HERMAN V. 1965. *Unsaturated Polyesters: Structure and Properties. American Elsevier, New York*. John Wiley & Sons, Ltd. https://doi.org/10.1002/POL.1965.100030141.

Bortoluzzi, Janaina H., Eduardo A. Pinheiro, Eduardo Carasek, and Valdir Soldi. 2005. "Solid Phase Microextraction to Concentrate Volatile Products from Thermal Degradation of Polymers." *Polymer Degradation and Stability* 89 (1): 33–37. https://doi.org/10.1016/J.POLYMDEGRADSTAB.2004.12.021.

Bottino, Francesco A., Anna Rosa Cinquegrani, Giovanna Di Pasquale, Lucrezia Leonardi, Alice Orestano, and Antonino Pollicino. 2004. "A Study on Chemical Modifications, Mechanical Properties and Surface Photo-Oxidation of Films of Polystyrene (PS) Stabilised by Hindered Amines (HAS)." *Polymer Testing* 23 (7): 779–89. https://doi.org/10.1016/J.POLYMERTESTING.2004.04.003.

Brown, Veronica M., Derrick R. Crump, and Paul T.C. Harrison. 2013. "Assessing and Controlling Risks from the Emission of Organic Chemicals from Construction Products into Indoor Environments." *Environmental Sciences: Processes and Impacts* 15 (12): 2164–71. https://doi.org/10.1039/c3em00413a.

Byun, Youngjae, Young Teck Kim, and Scott Whiteside. 2010. "Characterization of an Antioxidant Polylactic Acid (PLA) Film Prepared with α-Tocopherol, BHT and Polyethylene Glycol Using Film Cast Extruder." *Journal of Food Engineering* 100 (2): 239–44. https://doi.org/10.1016/J.JFOODENG.2010.04.005.

Cabanes, A., F. J. Valdés, and A. Fullana. 2020. "A Review on VOCs from Recycled Plastics." *Sustainable Materials and Technologies* 25 (September): e00179. https://doi.org/10.1016/J.SUSMAT.2020.E00179.

Calzonetti, Jo Ann, and Christopher J. Laursen. 2010. "PATENTS OF CHARLES GOODYEAR: HIS INTERNATIONAL CONTRIBUTIONS TO THE RUBBER INDUSTRY." *Rubber Chemistry and Technology* 83 (3): 303–21. https://doi.org/10.5254/1.3525687.

Carslaw, N., L. Fletcher, D. Heard, T. Ingham, and H. Walker. 2017. "Significant OH Production under Surface Cleaning and Air Cleaning Conditions: Impact on Indoor Air Quality." *Indoor Air* 27 (6): 1091–1100. https://doi.org/10.1111/ina.12394.

Carslaw, Nicola. 2007. "A New Detailed Chemical Model for Indoor Air Pollution." *Atmospheric Environment* 41 (6): 1164–79. https://doi.org/10.1016/j.atmosenv.2006.09.038.

Carslaw, Nicola. 2013. "A Mechanistic Study of Limonene Oxidation Products and Pathways Following Cleaning Activities." *Atmospheric Environment* 80: 507–13. https://doi.org/10.1016/j.atmosenv.2013.08.034.

Carslaw, Nicola, Mike Ashmore, Andrew C Terry, and David C Carslaw. 2015. "Crucial Role for Outdoor Chemistry in Ultrafine Particle Formation in Modern Office Buildings." https://doi.org/10.1021/acs.est.5b02241.

Carslaw, Nicola, Tiago Mota, Michael E Jenkin, Mark H Barley, and Gordon Mcfiggans. 2012. "A Significant Role for Nitrate and Peroxide Groups on Indoor Secondary Organic Aerosol." https://doi.org/10.1021/es301350x.

Carslaw, Nicola, and David Shaw. 2019. "Secondary Product Creation Potential (SPCP): A Metric for Assessing the Potential Impact of Indoor Air Pollution on Human Health." *Environmental Science: Processes and Impacts* 21 (8): 1313–22. https://doi.org/10.1039/c9em00140a.

Carter, Toby J, Dustin G Poppendieck, David Shaw, and Nicola Carslaw. 2023. "A Modelling Study of Indoor Air Chemistry : The Surface Interactions of Ozone and Hydrogen Peroxide." *Atmospheric Environment* 297 (January): 119598. https://doi.org/10.1016/j.atmosenv.2023.119598.

Carvalho, Lilian R.F., Pérola C. Vasconcellos, Waldir Mantovani, Cristina S. Pool, and Silvana O. Pisani. 2005. "Measurements of Biogenic Hydrocarbons and Carbonyl Compounds Emitted by Trees from Temperate Warm Atlantic Rainforest, Brazil." *Journal of Environmental Monitoring* 7 (5): 493–99. https://doi.org/10.1039/b414881a.

Chamas, Ali, Hyunjin Moon, Jiajia Zheng, Yang Qiu, Tarnuma Tabassum, Jun Hee Jang, Mahdi Abu-Omar, Susannah L Scott, and Sangwon Suh. 2020. "Degradation Rates of Plastics in the Environment." *Cite This: ACS Sustainable Chem. Eng* 8: 3511. https://doi.org/10.1021/acssuschemeng.9b06635.

Chanda, Manas, and Salil K. Roy. 2006. "Plastics Technology Handbook." *Plastics Technology Handbook*, December. https://doi.org/10.1201/9781420006360.

Chelliah, Ashwinder, Malini Subramaniam, Ritu Gupta, and Arun Gupta. 2017. "Evaluation on the Thermo-Oxidative Degradation of PET Using Prodegradant Additives." *Indian Journal of Science and Technology* 10 (6): 1–5. https://doi.org/10.17485/IJST/2017/V10I6/111212.

Choi, Hyunok, Norbert Schmidbauer, Jan Sundell, Mikael Hasselgren, John Spengler, and Carl-Gustaf Bornehag. 2010. "Common Household Chemicals and the Allergy Risks in Pre-School Age Children." Edited by Dominik Hartl. *PLoS ONE* 5 (10): e13423. https://doi.org/10.1371/journal.pone.0013423.

Ciliz, Nilgun Kiran, Ekrem Ekinci, and Colin E. Snape. 2004. "Pyrolysis of Virgin and Waste Polypropylene and Its Mixtures with Waste Polyethylene and Polystyrene." *Waste Management* 24 (2): 173–81. https://doi.org/10.1016/J.WASMAN.2003.06.002.

Clausen, Per, Zhe Liu, Ying Xu, Vivi Kofoed-Sørensen, and John Little. 2010. "Influence of Air Flow Rate on Emission of DEHP from Vinyl Flooring in the Emission Cell FLEC: Measurements and CFD Simulation." *Atmospheric Environment* 44: 2760–66. https://doi.org/10.1016/j.atmosenv.2010.04.020.

Commission, European. 2020. "Sustainable Products Initiative." 2020. https://ec.europa.eu/info/law/better-regulation/have-your-say/initiatives/12567-Sustainable-products-initiative_en.

Cox, Steven S., John C. Little, and Alfred T. Hodgson. 2002a. "Predicting the Emission Rate of Volatile Organic Compounds from Vinyl Flooring." *Environmental Science and Technology* 36 (4): 709–14. https://doi.org/10.1021/es010802+.

Cox, Steven S., John C. Little, and Alfred T. Hodgson. 2002b. "Predicting the Emission Rate of Volatile Organic Compounds from Vinyl Flooring." *Environmental Science & Technology* 36: 709–14. https://doi.org/10.1021/es010802.

Crawford, J., R. E. Shetter, B. Lefer, C. Cantrell, W. Junkermann, S. Madronich, and J. Calvert. 2003. "Cloud Impacts on UV Spectral Actinic Flux Observed during the International Photolysis Frequency Measurement and Model Intercomparison (IPMMI)." *Journal of Geophysical Research: Atmospheres* 108 (16): 1–11. https://doi.org/10.1029/2002jd002731.

Crawford, Shaun, and Claudiu T. Lungu. 2011. "Influence of Temperature on Styrene Emission from a Vinyl Ester Resin Thermoset Composite Material." *Science of the Total Environment* 409 (18): 3403–8. https://doi.org/10.1016/j.scitotenv.2011.05.042.

Curran, Katherine, Mark Underhill, Lorraine T. Gibson, and Matija Strlic. 2016. "The Development of a SPME-GC/MS Method for the Analysis of VOC Emissions from Historic Plastic and Rubber Materials." *Microchemical Journal* 124 (January): 909–18. https://doi.org/10.1016/J.MICROC.2015.08.027.

D'amico, Alessandro, Agnese Pini, Simone Zazzini, Daniela D'alessandro, Giovanni Leuzzi, and Edoardo Currà. 2021. "Modelling VOC Emissions from Building Materials for Healthy Building Design." *Sustainability (Switzerland)* 13 (1): 1–26. https://doi.org/10.3390/su13010184.

Deming, Benjamin L., Demetrios Pagonis, Xiaoxi Liu, Douglas A. Day, Ranajit Talukdar, Jordan E. Krechmer, Joost A. De Gouw, Jose L. Jimenez, and Paul J. Ziemann. 2019. "Measurements of Delays of Gas-Phase Compounds in a Wide Variety of Tubing Materials Due to Gas-Wall Interactions." *Atmospheric Measurement Techniques* 12 (6): 3453–61. https://doi.org/10.5194/amt-12-3453-2019.

Dodds, James N, and Erin S Baker. 2019. "Ion Mobility Spectrometry: Fundamental Concepts, Instrumentation, Applications, and the Road Ahead." *Journal of the American Society for Mass Spectrometry* 30 (11): 2185–95. https://doi.org/10.1007/s13361-019-02288-2.

Dodson, Robin E., Vincent Bessonneau, Julia O. Udesky, Marcia Nishioka, Martha McCauley, and Ruthann A. Rudel. 2018. "Passive Indoor Air Sampling for Consumer Product Chemicals: A Field Evaluation Study." *Journal of Exposure Science & Environmental Epidemiology 2018 29:1* 29 (1): 95–108. https://doi.org/10.1038/s41370-018-0070-9.

Duncan, S M, K G Sexton, and B J Turpin. 2018. "Oxygenated VOCs, Aqueous Chemistry, and Potential Impacts on Residential Indoor Air Composition." *Indoor Air* 28 (1): 198–212. https://doi.org/https://doi.org/10.1111/ina.12422.

Effah, Evans, Jarmo K. Holopainen, and Andrea Clavijo McCormick. 2019. "Potential Roles of Volatile Organic Compounds in Plant Competition." *Perspectives in Plant Ecology, Evolution and Systematics* 38 (March): 58–63. https://doi.org/10.1016/j.ppees.2019.04.003.

Even, Morgane. 2021. "Characterization of the Emissions of Volatile Organic Compounds from Polymer-Based Consumer Products : Towards a Realistic Exposure Assessment."

Even, Morgane, Mathilde Girard, Anna Rich, Christoph Hutzler, and Andreas Luch. 2019. "Emissions of VOCs From Polymer-Based Consumer Products: From Emission Data of Real Samples to the Assessment of Inhalation Exposure." *Frontiers in Public Health* 7 (August): 1–10. https://doi.org/10.3389/fpubh.2019.00202.

Even, Morgane, Christoph Hutzler, Olaf Wilke, and Andreas Luch. 2020. "Emissions of Volatile Organic Compounds from Polymer-Based Consumer Products: Comparison of Three Emission Chamber Sizes." *Indoor Air* 30 (1): 40–48. https://doi.org/10.1111/ina.12605.

Fahey, Leona M. 2017. "Predicting the Cell-Wall Compositions of Pinus Radiata (Radiata Pine) Wood Using ATR and Transmission FTIR Spectroscopies." *University of Aukland*.

Farmer, D K, M E Vance, J P D Abbatt, A Abeleira, M R Alves, C Arata, E Boedicker, et al. 2019. "Overview of HOMEChem: House Observations of Microbial and Environmental Chemistry †." *This Journal Is Open Access Article. Published On* 21: 1280–1300. https://doi.org/10.1039/c9em00228f.

Fischer, Lukas, Martin Breitenlechner, Eva Canaval, Wiebke Scholz, Marcus Striednig, Martin Graus, Thomas G. Karl, Tuukka Petäjä, Markku Kulmala, and Armin Hansel. 2021. "First Eddy Covariance Flux Measurements of Semi-Volatile Organic Compounds with the PTR3-TOF-MS." *Atmospheric Measurement Techniques* 14 (12): 8019–39. https://doi.org/10.5194/amt-14-8019-2021.

Folino, Adele, Domenica Pangallo, and Paolo Salvatore Calabrò. 2023. "Assessing Bioplastics Biodegradability by Standard and Research Methods: Current Trends and Open Issues." *Journal of

*Environmental Chemical Engineering* 11 (2): 109424. https://doi.org/https://doi.org/10.1016/j.jece.2023.109424.

Friedrich, Daniel. 2022. "How Building Experts Evaluate the Sustainability and Performance of Novel Bioplastic-Based Textile Façades: An Analysis of Decision Making." *Building and Environment* 207 (PB): 108485. https://doi.org/10.1016/j.buildenv.2021.108485.

Frigione, Mariaenrica, and Alvaro Rodríguez-Prieto. 2021. "Can Accelerated Aging Procedures Predict the Long Term Behavior of Polymers Exposed to Different Environments?" *Polymers 2021, Vol. 13, Page 2688* 13 (16): 2688. https://doi.org/10.3390/POLYM13162688.

Frontczak, Monika, and Pawel Wargocki. 2011. "Literature Survey on How Different Factors Influence Human Comfort in Indoor Environments." *Building and Environment* 46 (4): 922–37. https://doi.org/10.1016/j.buildenv.2010.10.021.

Ganobjak, Michal, Wim J. Malfait, Janis Just, Marcel Käppeli, Francisco Mancebo, Samuel Brunner, and Jannis Wernery. 2023. "Get the Light & Keep the Warmth - A Highly Insulating, Translucent Aerogel Glass Brick for Building Envelopes." *Journal of Building Engineering* 64 (September 2022): 105600. https://doi.org/10.1016/j.jobe.2022.105600.

Gasparrini, Antonio, Pierre Masselot, Matteo Scortichini, Rochelle Schneider, Malcolm N Mistry, Francesco Sera, Helen L Macintyre, Revati Phalkey, and Ana Maria Vicedo-Cabrera. 2022. "Small-Area Assessment of Temperature-Related Mortality Risks in England and Wales: A Case Time Series Analysis." *The Lancet. Planetary Health* 6 (7): e557–64. https://doi.org/10.1016/S2542-5196(22)00138-3.

George, G. A. 1974. "The Mechanism of Photoprotection of Polystyrene Film by Some Ultraviolet Absorbers." *Journal of Applied Polymer Science* 18 (1): 117–24. https://doi.org/10.1002/APP.1974.070180110.

Gerassimidou, Spyridoula, Paulina Lanska, John N. Hahladakis, Elena Lovat, Silvia Vanzetto, Birgit Geueke, Ksenia J. Groh, et al. 2022. "Unpacking the Complexity of the PET Drink Bottles Value Chain: A Chemicals Perspective." *Journal of Hazardous Materials* 430 (March): 128410. https://doi.org/10.1016/j.jhazmat.2022.128410.

Geueke, Birgit. 2013. "Non-Intentionally Added Substances (NIAS)," no. April. https://doi.org/10.5281/zenodo.33514.

Geyer, Roland, Jenna R. Jambeck, and Kara Lavender Law. 2017. "Production, Use, and Fate of All Plastics Ever Made." *Science Advances* 3 (7). https://doi.org/10.1126/SCIADV.1700782/SUPPL_FILE/1700782_SM.PDF.

Gijsman, Pieter, Jan Hennekens, and Daan Tummers. 1993. "The Mechanism of Action of Hindered Amine Light Stabilizers." *Polymer Degradation and Stability* 39 (2): 225–33. https://doi.org/10.1016/0141-3910(93)90099-5.

Gouw, J. A. de, P. D. Goldan, C. Warneke, W. C. Kuster, J. M. Roberts, M. Marchewka, S. B. Bertman, A. A. P. Pszenny, and W. C. Keene. 2003. "Validation of Proton Transfer Reaction-Mass Spectrometry (PTR-MS) Measurements of Gas-Phase Organic Compounds in the Atmosphere during the New England Air Quality Study (NEAQS) in 2002." *Journal of Geophysical Research: Atmospheres* 108 (D21): 4682. https://doi.org/10.1029/2003JD003863.

Gouw, Joost De, and Carsten Warneke. 2007. "Measurements of Volatile Organic Compounds in the Earth's Atmosphere Using Proton-Transfer-Reaction Mass Spectrometry." *Mass Spectrometry Reviews*. Mass Spectrom Rev. https://doi.org/10.1002/mas.20119.

Groh, Ksenia J., Thomas Backhaus, Bethanie Carney-Almroth, Birgit Geueke, Pedro A. Inostroza, Anna Lennquist, Heather A. Leslie, et al. 2019. "Overview of Known Plastic Packaging-Associated Chemicals and Their Hazards." *Science of the Total Environment* 651: 3253–68. https://doi.org/10.1016/j.scitotenv.2018.10.015.

Guo, Ying, and Kurunthachalam Kannan. 2012. "Challenges Encountered in the Analysis of Phthalate Esters in Foodstuffs and Other Biological Matrices." *Analytical and Bioanalytical Chemistry* 404 (9): 2539–54. https://doi.org/10.1007/S00216-012-5999-2/METRICS.

Hakkarainen, Minna, and Ann-Christine Albertsson. 2004. "Environmental Degradation of Polyethylene BT  - Long Term Properties of Polyolefins." In , edited by Ann-Christine Albertsson, 177–200. Berlin, Heidelberg: Springer Berlin Heidelberg. https://doi.org/10.1007/b13523.

Halios, Christos H, Charlotte Landeg-Cox, Scott D Lowther, Alice Middleton, Tim Marczylo, and Sani Dimitroulopoulou. 2022. "Chemicals in European Residences – Part I: A Review of Emissions, Concentrations and Health Effects of Volatile Organic Compounds (VOCs)." *Science of The Total Environment* 839: 156201. https://doi.org/https://doi.org/10.1016/j.scitotenv.2022.156201.

Han, K. H., J. S. Zhang, P. Wargocki, H. N. Knudsen, and B. Guo. 2010. "Determination of Material Emission Signatures by PTR-MS and Their Correlations with Odor Assessments by Human Subjects." *Indoor Air* 20 (4): 341–54. https://doi.org/10.1111/j.1600-0668.2010.00662.x.

Hansel, A., A. Jordan, R. Holzinger, P. Prazeller, W. Vogel, and W. Lindinger. 1995. "Proton Transfer Reaction Mass Spectrometry: On-Line Trace Gas Analysis at the Ppb Level." *International Journal of Mass Spectrometry and Ion Processes* 149–150 (C): 609–19. https://doi.org/10.1016/0168-1176(95)04294-U.

Haug, Helen, Luise Klein, Tilman Sauerwald, Birte Poelke, Jonathan Beauchamp, and Alexander Roloff. 2022. "Sampling Volatile Organic Compound Emissions from Consumer Products: A Review." *Https://Doi.Org/10.1080/10408347.2022.2136484*. https://doi.org/10.1080/10408347.2022.2136484.

Hazrati, Sadegh, Roohollah Rostami, Manoochehr Farjaminezhad, and Mehdi Fazlzadeh. 2016. "Preliminary Assessment of BTEX Concentrations in Indoor Air of Residential Buildings and Atmospheric Ambient Air in Ardabil, Iran." *Atmospheric Environment* 132: 91–97. https://doi.org/10.1016/j.atmosenv.2016.02.042.

Henry, Beverley, Kirsi Laitala, and Ingun Grimstad Klepp. 2019. "Microfibres from Apparel and Home Textiles: Prospects for Including Microplastics in Environmental Sustainability Assessment." *Science of the Total Environment* 652: 483–94. https://doi.org/10.1016/j.scitotenv.2018.10.166.

Hernández-Mesa, Maykel, David Ropartz, Ana M García-Campaña, Hélène Rogniaux, Gaud Dervilly-Pinel, and Bruno Le Bizec. 2019. "Ion Mobility Spectrometry in Food Analysis: Principles, Current Applications and Future Trends." *Molecules (Basel, Switzerland)* 24 (15). https://doi.org/10.3390/molecules24152706.

Hodgson, Alfred T., John D. Wooley, and Joan M. Daisey. 1993. "Emissions of Volatile Organic Compounds from New Carpets Measured in a Large-Scale Environmental Chamber." *Air and Waste* 43 (3): 316–24. https://doi.org/10.1080/1073161X.1993.10467136.

Hodgson, Jennifer L., and Michelle L. Coote. 2010. "Clarifying the Mechanism of the Denisov Cycle: How Do Hindered Amine Light Stabilizers Protect Polymer Coatings from Photo-Oxidative Degradation?" *Macromolecules* 43 (10): 4573–83. https://doi.org/10.1021/MA100453D/SUPPL_FILE/MA100453D_SI_001.PDF.

Holøs, Sverre B., Aileen Yang, Merethe Lind, Kari Thunshelle, Peter Schild, and Mads Mysen. 2019. "VOC Emission Rates in Newly Built and Renovated Buildings, and the Influence of Ventilation – a Review and Meta-Analysis." *International Journal of Ventilation* 18 (3): 153–66. https://doi.org/10.1080/14733315.2018.1435026.

Horodytska, O., A. Cabanes, and A. Fullana. 2020. "Non-Intentionally Added Substances (NIAS) in Recycled Plastics." *Chemosphere* 251 (July): 126373. https://doi.org/10.1016/J.CHEMOSPHERE.2020.126373.

Huang, He, Honglei Wang, Yu Jie Hu, Chengjiang Li, and Xiaolin Wang. 2022. "The Development Trends of Existing Building Energy Conservation and Emission Reduction—A Comprehensive Review." *Energy Reports* 8: 13170–88. https://doi.org/10.1016/j.egyr.2022.10.023.

IPCC. 2018. "Global Warming of 1.5°C." https://doi.org/10.1017/9781009157940.

Jaeger, Rudolph J, and Robert J Rubin. 1970. "Plasticizers from Plastic Devices: Extraction, Metabolism, and Accumulation by Biological Systems." *Science* 170 (3956): 460–62. https://doi.org/10.1126/science.170.3956.460.

Jenkin, M E, S M Saunders, V Wagner, and M J Pilling. 2003. "Atmospheric Chemistry and Physics Protocol for the Development of the Master Chemical Mechanism, MCM v3 (Part B): Tropospheric Degradation of Aromatic Volatile Organic Compounds." *Atmos. Chem. Phys* 3: 181–93. www.atmos-chem-phys.org/acp/3/181/.

Jenkin, Michael E., Sandra M. Saunders, and Michael J. Pilling. 1997. "The Tropospheric Degradation of Volatile Organic Compounds: A Protocol for Mechanism Development." *Atmospheric Environment* 31 (1): 81–104. https://doi.org/10.1016/S1352-2310(96)00105-7.

Ji, Yongming, Lin Duanmu, and Songtao Hu. 2022. "Measurement and Analysis of Airtightness Safeguard Measures for Typical Ultra-Low Energy Buildings." *Energy and Built Environment*, no. September. https://doi.org/10.1016/j.enbenv.2022.11.003.

Jia, Chunrong, and Stuart Batterman. 2010. "A Critical Review of Naphthalene Sources and Exposures Relevant to Indoor and Outdoor Air," 2903–39. https://doi.org/10.3390/ijerph7072903.

Jiang, Chuanjia, Dandan Li, Pengyi Zhang, Jinge Li, Juan Wang, and Jiaguo Yu. 2017. "Formaldehyde and Volatile Organic Compound (VOC) Emissions from Particleboard: Identification of Odorous Compounds and Effects of Heat Treatment." *Building and Environment* 117: 118–26. https://doi.org/10.1016/j.buildenv.2017.03.004.

Jochmann, Maik A, Jens Laaks, and Torsten C Schmidt. 2014. "Solvent-Free Extraction and Injection Techniques." In *Practical Gas Chromatography: A Comprehensive Reference*, edited by Katja Dettmer-Wilde and Werner Engewald, 371–412. Berlin, Heidelberg: Springer Berlin Heidelberg. https://doi.org/10.1007/978-3-642-54640-2_11.

Jones, A. P. 2002. "Chapter 3 Indoor Air Quality and Health." *Developments in Environmental Science* 1 (C): 57–115. https://doi.org/10.1016/S1474-8177(02)80006-7.

Kamal-Eldin, Afaf, and Lars Åke Appelqvist. 1996. "The Chemistry and Antioxidant Properties of Tocopherols and Tocotrienols." *Lipids* 31 (7): 671–701. https://doi.org/10.1007/BF02522884.

Kang, Peng, Peng Wu, Yan Jin, Shengpeng Shi, Dali Gao, and Guangxin Chen. 2020. "Formation and Emissions of Volatile Organic Compounds from Homo-PP and Co-PP Resins during Manufacturing Process and Accelerated Photoaging Degradation." *Molecules* 25. https://doi.org/https://www.mdpi.com/1420-3049/25/12/2761.

Karamanlioglu, Mehlika, Richard Preziosi, and Geoffrey D. Robson. 2017. "Abiotic and Biotic Environmental Degradation of the Bioplastic Polymer Poly(Lactic Acid): A Review." *Polymer Degradation and Stability* 137: 122–30. https://doi.org/10.1016/j.polymdegradstab.2017.01.009.

Klepeis, Neil E., William C. Nelson, Wayne R. Ott, John P. Robinson, Andy M. Tsang, Paul Switzer, Joseph V. Behar, Stephen C. Hern, and William H. Engelmann. 2001. "The National Human Activity Pattern Survey (NHAPS): A Resource for Assessing Exposure to Environmental Pollutants." *Journal of Exposure Analysis and Environmental Epidemiology* 11 (3): 231–52. https://doi.org/10.1038/sj.jea.7500165.

Kockott, Dieter. 1989. "Natural and Artificial Weathering of Polymers." *Polymer Degradation and Stability* 25 (2–4): 181–208. https://doi.org/10.1016/S0141-3910(89)81007-9.

Kolb, B., C. Welter, and C. Bichler. 1992. "Determination of Partition Coefficients by Automatic Equilibrium Headspace Gas Chromatography by Vapor Phase Calibration." *Chromatographia* 34 (5–8): 235–40. https://doi.org/10.1007/BF02268351/METRICS.

Kremser, Andreas, Maik A. Jochmann, and Torsten C. Schmidt. 2016. "Systematic Comparison of Static and Dynamic Headspace Sampling Techniques for Gas Chromatography." *Analytical and Bioanalytical Chemistry* 408 (24): 6567–79. https://doi.org/10.1007/S00216-016-9843-Y/METRICS.

Kruza, M., A. C. Lewis, G. C. Morrison, and N. Carslaw. 2017. "Impact of Surface Ozone Interactions on Indoor Air Chemistry: A Modeling Study." *Indoor Air* 27 (5): 1001–11. https://doi.org/10.1111/INA.12381.

Krzan, Andrej, Sarunya Hemjinda, Stanislav Miertus, Andrea Corti, and Emo Chiellini. 2006. "Standardization and Certification in the Area of Environmentally Degradable Plastics." *Polymer Degradation and Stability* 91 (12): 2819–33. https://doi.org/10.1016/j.polymdegradstab.2006.04.034.

Lambert, Scott. 2013. "Environmental Risk of Polymer and Their Degradation Products," no. May: 1–198. http://etheses.whiterose.ac.uk/4194/.

Levasseur, Jessica L, Stephanie C Hammel, Kate Hoffman, Allison L Phillips, Sharon Zhang, Xiaoyun Ye, Antonia M Calafat, Thomas F Webster, and M Stapleton. 2021. "Young Children's Exposure to Phenols in the Home : Associations between House Dust , Hand Wipes , Silicone Wristbands , and Urinary Biomarkers." *Environment International* 147: 106317. https://doi.org/10.1016/j.envint.2020.106317.

Lin, Chi Chi, Kuo Pin Yu, Ping Zhao, and Grace Whei-May Lee. 2009. "Evaluation of Impact Factors on VOC Emissions and Concentrations from Wooden Flooring Based on Chamber Tests." *Building and Environment* 44 (3): 525–33. https://doi.org/10.1016/j.buildenv.2008.04.015.

Lindinger, W., A. Hansel, and A. Jordan. 1998. "On-Line Monitoring of Volatile Organic Compounds at Pptv Levels by Means of Proton-Transfer-Reaction Mass Spectrometry (PTR-MS) Medical Applications, Food Control and Environmental Research." *International Journal of Mass Spectrometry and Ion Processes* 173 (3): 191–241. https://doi.org/10.1016/s0168-1176(97)00281-4.

Liu, Heping, Greg Cash, David Birtwhistle, and Graeme George. 2005. "Characterization of a Severely Degraded Silicone Elastomer HV Insulator - An Aid to Development of Lifetime Assessment Techniques." *IEEE Transactions on Dielectrics and Electrical Insulation* 12 (3): 478–86. https://doi.org/10.1109/TDEI.2005.1453452.

Lomonaco, Tommaso, Enrico Manco, Andrea Corti, Jacopo La Nasa, Silvia Ghimenti, Denise Biagini, Fabio Di Francesco, et al. 2020. "Release of Harmful Volatile Organic Compounds (VOCs) from Photo-Degraded Plastic Debris: A Neglected Source of Environmental Pollution." *Journal of Hazardous Materials* 394 (February): 122596. https://doi.org/10.1016/j.jhazmat.2020.122596.

Lucas, Nathalie, Christophe Bienaime, Christian Belloy, Michèle Queneudec, Françoise Silvestre, and José Edmundo Nava-Saucedo. 2008. "Polymer Biodegradation: Mechanisms and Estimation Techniques - A Review." *Chemosphere* 73 (4): 429–42. https://doi.org/10.1016/j.chemosphere.2008.06.064.

Lugasi, A. 1997. "Natural Antioxidants Chemistry, Health Effects, and Applications. Edited by F. Shahidi. VIII and 432 Pages, Numerous Figures and Tables. AOCS Press, Champaign, Illinois, 1997. Price: 105.00 U$." *Food / Nahrung* 41 (5): 321–321. https://doi.org/10.1002/FOOD.19970410536.

Lunderberg, David M., Pawel K. Misztal, Yingjun Liu, Caleb Arata, Yilin Tian, Kasper Kristensen, Robert J. Weber, William W. Nazaroff, and Allen H. Goldstein. 2021. "High-Resolution Exposure Assessment for Volatile Organic Compounds in Two California Residences." *Environmental Science and Technology*. https://doi.org/10.1021/acs.est.0c08304.

Mametov, Radik, Ileana-Andreea Ratiu, Fernanda Monedeiro, Tomasz Ligor, and Bogusław Buszewski. 2021. "Evolution and Evaluation of GC Columns." *Critical Reviews in Analytical Chemistry* 51 (2): 150–73. https://doi.org/10.1080/10408347.2019.1699013.

Manuja, Archit, Jenna Ritchie, Khantil Buch, Yaoxing Wu, Clara M.A. Eichler, John C. Little, and Linsey C. Marr. 2019. "Total Surface Area in Indoor Environments." *Environmental Science: Processes and Impacts* 21 (8): 1384–92. https://doi.org/10.1039/c9em00157c.

Marć, Mariusz, Krzysztof Formela, Marek Klein, Jacek Namieśnik, and Bożena Zabiegała. 2015. "The Emissions of Monoaromatic Hydrocarbons from Small Polymeric Toys Placed in Chocolate Food Products." *The Science of the Total Environment* 530–531 (October): 290–96. https://doi.org/10.1016/j.scitotenv.2015.05.105.

Marć, Mariusz, Jacek Namieśnik, and Bożena Zabiegała. 2017. "The Miniaturised Emission Chamber System and Home-Made Passive Flux Sampler Studies of Monoaromatic Hydrocarbons Emissions from Selected Commercially-Available Floor Coverings." *Building and Environment* 123 (October): 1–13. https://doi.org/10.1016/J.BUILDENV.2017.06.035.

Marć, Mariusz, Bozena Zabiegała, and Jacek Namieśnik. 2012. "Testing and Sampling Devices for Monitoring Volatile and Semi-Volatile Organic Compounds in Indoor Air." *TrAC - Trends in Analytical Chemistry* 32: 76–86. https://doi.org/10.1016/j.trac.2011.09.006.

Mark, H. F., N. M. Bikales Bikales, C. G. Menges, and G. Overberger. 1985. *Encyclopedia of Polymer Science and Engineering, 2nd Edition. Wiley-Interscience, New York*. Vol. 2. John Wiley & Sons, Ltd. https://doi.org/10.1002/PI.4980170412.

Marturano, Valentina, Pierfrancesco Cerruti, and Veronica Ambrogi. 2017. "Polymer Additives." *Physical Sciences Reviews* 2 (6): 1–20. https://doi.org/10.1515/psr-2016-0130.

Masuck, I., C. Hutzler, O. Jann, and A. Luch. 2011. "Inhalation Exposure of Children to Fragrances Present in Scented Toys." *Indoor Air* 21 (6): 501–11. https://doi.org/10.1111/j.1600-0668.2011.00727.x.

Matysik, Silke, Abou Bakr Ramadan, and Uwe Schlink. 2010. "Spatial and Temporal Variation of Outdoor and Indoor Exposure of Volatile Organic Compounds in Greater Cairo." *Atmospheric Pollution Research* 1 (2): 94–101. https://doi.org/10.5094/APR.2010.012.

Meng, Xin, Weijie Chen, Zhong Xin, and Chushi Wu. 2018. "Effect of Benzofuranone on Degradation and Mechanical Properties of Polypropylene in Processing." *Journal of Vinyl and Additive Technology* 24 (2): 124–29. https://doi.org/10.1002/VNL.21535.

Menghi, Roberto, Silvia Ceccacci, Alessandra Papetti, Marco Marconi, and Michele Germani. 2018. "A Method to Estimate the Total VOC Emission of Furniture Products." *Procedia Manufacturing* 21: 486–93. https://doi.org/10.1016/j.promfg.2018.02.148.

Miller, Sylvia C. 2014. "Application of Proton Transfer Reaction Mass Spectrometry To," no. July. https://doi.org/10.21954/ou.ro.0000f066.

Minaeian, Jamie. 2016. "Development and Deployment of an Airborne Gas Chromatography / Mass Spectrometer to Measure Tropospheric Volatile Organic Compounds," no. September.

Ministry of Housing. 2019. "Ventilation and Indoor Air Quality in New Homes." *Ministry of Housing, Communities & Local Government*, no. SPECIAL ISSUE: 1–84.

Modern Plastics Global. n.d. "Modern Plastics Global • Plastic Putting the 'P' in Packaging." Accessed March 3, 2021. https://www.modernplasticsglobal.com/2020/12/03/plastic-putting-the-p-in-packaging/.

Morgan, Alexander B., and Jeffrey W. Gilman. 2013. "An Overview of Flame Retardancy of Polymeric Materials: Application, Technology, and Future Directions." *Fire and Materials* 37 (4): 259–79. https://doi.org/10.1002/FAM.2128.

Mull, Birte, Tilman Sauerwald, Caroline Schultealbert, Wolfgang Horn, Doris Brödner, and Matthias Richter. 2017. "Reproducibly Emitting Reference Materials for Volatile and Semi-Volatile Organic Compounds—Using Finite Element Modeling for Emission Predictions." *Air Quality, Atmosphere and Health* 10 (10): 1237–46. https://doi.org/10.1007/S11869-017-0508-6/FIGURES/8.

Muthukumar, Thangavelu, Adithan Aravinthan, Karunamoorthy Lakshmi, Ramasamy Venkatesan, Loganathan Vedaprakash, and Mukesh Doble. 2011. "Fouling and Stability of Polymers and Composites in Marine Environment." *International Biodeterioration and Biodegradation* 65 (2): 276–84. https://doi.org/10.1016/j.ibiod.2010.11.012.

Nagai, Y., T. Ogawa, Y. Nishimoto, and F. Ohishi. 1999. "Analysis of Weathering of a Thermoplastic Polyester Elastomer. II. Factors Affecting Weathering of a Polyether-Polyester Elastomer." *Polymer Degradation and Stability* 65 (2): 217–24. https://doi.org/10.1016/S0141-3910(99)00007-5.

Nandasena, Sumal. 2013. "Indoor Air Pollution and Respiratory Health of Children in the Developing World." *World Journal of Clinical Pediatrics* 2 (2): 6. https://doi.org/10.5409/wjcp.v2.i2.6.

Nazaroff, William W. 2021. "Residential Air-Change Rates: A Critical Review." *Indoor Air* 31 (2): 282–313. https://doi.org/https://doi.org/10.1111/ina.12785.

Nazaroff, William W., and Charles J. Weschler. 2004. "Cleaning Products and Air Fresheners: Exposure to Primary and Secondary Air Pollutants." *Atmospheric Environment* 38 (18): 2841–65. https://doi.org/10.1016/j.atmosenv.2004.02.040.

Nazaroff, William W, and Glen R Cass. 1986. "Mathematical Modeling of Chemically Reactive Pollutants in Indoor Air." *Environ. Sci. Technol* 20: 924–34. https://pubs.acs.org/sharingguidelines.

Nerín, C., D. Acosta, and C. Rubio. 2002. "Potential Migration Release of Volatile Compounds from Plastic Containers Destined for Food Use in Microwave Ovens." *Food Additives and Contaminants* 19 (6): 594–601. https://doi.org/10.1080/02652030210123887.

Noguchi, Miyuki, and Akihiro Yamasaki. 2020. "Volatile and Semivolatile Organic Compound Emissions from Polymers Used in Commercial Products during Thermal Degradation." *Heliyon* 6 (3): e03314. https://doi.org/10.1016/J.HELIYON.2020.E03314.

Nohr, Michael, Wolfgang Horn, Katharina Wiegner, Matthias Richter, and Wilhelm Lorenz. 2014. "Development of a Material with Reproducible Emission of Selected Volatile Organic Compounds – µ-Chamber Study." *Chemosphere* 107 (July): 224–29. https://doi.org/10.1016/J.CHEMOSPHERE.2013.12.047.

Norbäck, Dan. 2009. "An Update on Sick Building Syndrome." *Current Opinion in Allergy and Clinical Immunology*. Curr Opin Allergy Clin Immunol. https://doi.org/10.1097/ACI.0b013e32831f8f08.

Office, Met. 2022. "A Milestone in UK Climate History." 2022. https://doi.org/https://www.metoffice.gov.uk/about-us/press-office/news/weather-and-climate/2022/july-heat-review.

Oz, Kira, Bareket Merav, Sabach Sara, and Dubowski Yael. 2019. "Volatile Organic Compound Emissions from Polyurethane Mattresses under Variable Environmental Conditions." https://doi.org/10.1021/acs.est.9b01557.

Pagonis, Demetrios, Kanako Sekimoto, and Joost De Gouw. 2019. "A Library of Proton-Transfer Reactions of H 3 O + Ions Used for Trace Gas Detection." *American Society for Mass Spectrometry* 30: 1330–35. https://doi.org/10.1007/s13361-019-02209-3.

Palmisani, Jolanda, Alessia Di Gilio, Ezia Cisternino, Maria Tutino, and Gianluigi de Gennaro. 2020. "Volatile Organic Compound (VOC) Emissions from a Personal Care Polymer-Based Item: Simulation of the Inhalation Exposure Scenario Indoors under Actual Conditions of Use." *Sustainability (Switzerland)* 12 (7). https://doi.org/10.3390/su12072577.

Palmisano, Anna C, and Charles A Pettigrew. 1992. "Biodegradability of Plastics." *BioScience* 42 (9): 680–85. https://doi.org/10.2307/1312174.

Panagiotaras, D, D Nikolopoulos, D Koulougliotis, E Petraki, I Zisos, A Yiannopoulos, A Bakalis, and A Zisos. 2013. "Indoor Air Quality Assessment: Review on the Topic of VOCs," no. September: 91–101.

Panagiotaras, Dionisios. 2014. "Comprehensive Experience for Indoor Air Quality Assessment: A Review on the Determination of Volatile Organic Compounds (VOCs)." *Journal of Physical Chemistry & Biophysics* 4 (5). https://doi.org/10.4172/2161-0398.1000159.

Partyka, Monika, Bozena Zabiegała, Jacek Namieśnik, and Andrzej Przyjazny. 2007. "Application of Passive Samplers in Monitoring of Organic Constituents of Air." *Http://Dx.Doi.Org/10.1080/10408340600976523* 37 (1): 51–78. https://doi.org/10.1080/10408340600976523.

Pathak, A. K., and C. Viphavakit. 2022. "A Review on All-Optical Fiber-Based VOC Sensors: Heading towards the Development of Promising Technology." *Sensors and Actuators A: Physical* 338 (January): 113455. https://doi.org/10.1016/j.sna.2022.113455.

Petrou, Giorgos, Phil Symonds, Anna Mavrogianni, Anastasia Mylona, and Mike Davies. 2019. "The Summer Indoor Temperatures of the English Housing Stock: Exploring the Influence of Dwelling and Household Characteristics." *Building Services Engineering Research and Technology* 40 (4): 492–511. https://doi.org/10.1177/0143624419847621.

Petry, Thomas, Elodie Cazelle, Paul Lloyd, Reuben Mascarenhas, and Gerard Stijntjes. 2013. "A Standard Method for Measuring Benzene and Formaldehyde Emissions from Candles in Emission Test Chambers for Human Health Risk Assessment Purposes." *Environmental Sciences: Processes and Impacts* 15 (7): 1369–82. https://doi.org/10.1039/c3em00011g.

Plaisance, H., A. Blondel, V. Desauziers, and P. Mocho. 2014. "Characteristics of Formaldehyde Emissions from Indoor Materials Assessed by a Method Using Passive Flux Sampler Measurements." *Building and Environment* 73 (March): 249–55. https://doi.org/10.1016/J.BUILDENV.2013.12.011.

Posner, S. 2009. "Developments in Flame Retardants for Interior Materials and Textiles." *Interior Textiles: Design and Developments*, January, 211–28. https://doi.org/10.1533/9781845696870.2.211.

Public Health England. 2019. "Indoor Air Quality Guidelines for Selected Volatile Organic Compounds (VOCs) in the UK About Public Health England."

https://assets.publishing.service.gov.uk/government/uploads/system/uploads/attachment_data/file/831 319/VO__statement_Final_12092019_CS__1_.pdf.

Rabek, J F. 1990. *Photostabilization of Polymers: Principles and Applications*. *TA - TT  -*. London SE -: Elsevier Applied Science. https://doi.org/LK - https://worldcat.org/title/20088331.

Rajmohan, Kunju Vaikarar Soundararajan, Chandrasekaran Ramya, Manakkal Raja Viswanathan, and Sunita Varjani. 2019. "Plastic Pollutants: Effective Waste Management for Pollution Control and Abatement." *Current Opinion in Environmental Science and Health* 12: 72–84. https://doi.org/10.1016/j.coesh.2019.08.006.

Robert, Laurence, Romain Guichard, Jennifer Klingler, Valérie Cochet, and Corinne Mandin. 2021. "Indoor Air Quality in Shopping and Storage Areas." *Indoor Air* 31 (4): 1238–51. https://doi.org/10.1111/INA.12783.

Roberts, S Craig, Pawel K Misztal, and Ben Langford. 2020. "Decoding the Social Volatilome by Tracking Rapid Context-Dependent Odour Change." https://doi.org/10.1098/rstb.2019.0259.

Roy, P. K., P. Surekha, C. Rajagopal, S. N. Chatterjee, and V. Choudhary. 2007. "Studies on the Photo-Oxidative Degradation of LDPE Films in the Presence of Oxidised Polyethylene." *Polymer Degradation and Stability* 92 (6): 1151–60. https://doi.org/10.1016/J.POLYMDEGRADSTAB.2007.01.010.

Royer, SJ., S. Ferron, S. T. Wilson, and D. M. Karl. 2018. "Production of Methane and Ethylene from Plastic in the Environment." *PLoS ONE* 13 (8): e0200574. https://doi.org/10.1371/journal.pone.0200574.

Ruiz-jimenez, Jose, Ilmari Heiskanen, Ville Tanskanen, Kari Hartonen, and Marja-liisa Riekkola. 2022. "Analysis of Indoor Air Emissions: From Building Materials to Biogenic and Anthropogenic Activities." *Journal of Chromatography Open* 2 (January): 100041. https://doi.org/10.1016/j.jcoa.2022.100041.

Sajid, Muhammad, Mazen Khaled Nazal, Małgorzata Rutkowska, Natalia Szczepańska, Jacek Namieśnik, and Justyna Płotka-Wasylka. 2018. "Solid Phase Microextraction: Apparatus, Sorbent Materials, and Application." *Https://Doi.Org/10.1080/10408347.2018.1517035* 49 (3): 271–88. https://doi.org/10.1080/10408347.2018.1517035.

Salthammer, Tunga. 2009. "Environmental Test Chambers and Cells." *Organic Indoor Air Pollutants: Occurrence, Measurement, Evaluation: Second Edition*, October, 101–15. https://doi.org/10.1002/9783527628889.CH5.

Sarwar, Golam, Richard Corsi, Yosuke Kimura, David Allen, and Charles J. Weschler. 2002. "Hydroxyl Radicals in Indoor Environments." *Atmospheric Environment* 36 (24): 3973–88. https://doi.org/10.1016/S1352-2310(02)00278-9.

Saunders, Ra, Nicola Carslaw, Stephen Pascoe, Michael Pilling, Michael Jenkin, and Richard Derwent. 1999. "Development of the Master Chemical Mechanism (MCMv2.0) Web Site and Recent Applications of Its Use in Tropospheric Chemistry Models." http://chem.leeds.ac.uk/Atmospheric/MCM/mcmproj.html.

Saviello, Daniela, Lucia Toniolo, Sara Goidanich, and Francesca Casadio. 2016. "Non-Invasive Identification of Plastic Materials in Museum Collections with Portable FTIR Reflectance Spectroscopy: Reference Database and Practical Applications." *Microchemical Journal* 124: 868–77. https://doi.org/10.1016/j.microc.2015.07.016.

Schaller, K H, G Triebig, and B Beyer. 1989. "[Formaldehyde determination in tobacco smoke--studies under experimental and  actual conditions]." *Zentralblatt fur Hygiene und Umweltmedizin = International journal of hygiene and  environmental medicine* 189 (2): 103–10.

Scharte, Bernhard. 2010. "Phosphorus-Based Flame Retardancy Mechanisms—Old Hat or a Starting Point for Future Development?" *Materials 2010, Vol. 3, Pages 4710-4745* 3 (10): 4710–45. https://doi.org/10.3390/MA3104710.

Schripp, T, B Nachtwey, J Toelke, T Salthammer, E Uhde, M Wensing, and M Bahadir. 2007. "A Microscale Device for Measuring Emissions from Materials for Indoor Use." *Analytical and Bioanalytical Chemistry* 387 (5): 1907–19. https://doi.org/10.1007/s00216-006-1057-2.

Shah, Aamer Ali, Fariha Hasan, Abdul Hameed, and Safia Ahmed. 2008. "Biological Degradation of Plastics: A Comprehensive Review." *Biotechnology Advances* 26 (3): 246–65. https://doi.org/10.1016/J.BIOTECHADV.2007.12.005.

Shah, Vishu. 2007. "Handbook of Plastics Testing and Failure Analysis," 509. https://www.wiley.com/en-us/Handbook+of+Plastics+Testing+and+Failure+Analysis%2C+4th+Edition-p-9781118943632.

Shalaby, S. W. 1979. "Radiative Degradation of Synthetic Polymers: Chemical Physical, Environmental, and Technological Considerations." *Journal of Polymer Science: Macromolecular Reviews* 14 (1): 419–58. https://doi.org/10.1002/POL.1979.230140105.

Shanmugam, Vigneshwaran, Oisik Das, Rasoul Esmaeely Neisiany, Karthik Babu, Sunpreet Singh, Mikael S. Hedenqvist, Filippo Berto, and Seeram Ramakrishna. 2020. "Polymer Recycling in Additive

Manufacturing: An Opportunity for the Circular Economy." *Materials Circular Economy* 2 (1). https://doi.org/10.1007/S42824-020-00012-0.

Sharma, Rakesh. 2012. "Enzyme Inhibition: Mechanisms and Scope." In , edited by Rakesh R Sharma, Ch. 1. Rijeka: IntechOpen. https://doi.org/10.5772/39273.

Shaw, David, and Nicola Carslaw. 2021. "INCHEM-Py: An Open Source Python Box Model for Indoor Air Chemistry." *Journal of Open Source Software* 6: 1–4. https://doi.org/10.21105/joss.03224.

Shinohara, Naohide, Minoru Fujii, Akihiro Yamasaki, and Yukio Yanagisawa. 2007. "Passive Flux Sampler for Measurement of Formaldehyde Emission Rates." *Atmospheric Environment* 41 (19): 4018–28. https://doi.org/10.1016/J.ATMOSENV.2007.01.028.

Singh, Baljit, and Nisha Sharma. 2008. "Mechanistic Implications of Plastic Degradation." *Polymer Degradation and Stability* 93 (3): 561–84. https://doi.org/10.1016/J.POLYMDEGRADSTAB.2007.11.008.

Singh, Rohit Kumar, Biswajit Ruj, Anup Kumar Sadhukhan, and Parthapratim Gupta. 2020. "Thermal Degradation of Waste Plastics under Non-Sweeping Atmosphere: Part 2: Effect of Process Temperature on Product Characteristics and Their Future Applications." *Journal of Environmental Management* 261 (January): 110112. https://doi.org/10.1016/j.jenvman.2020.110112.

Sundell, J. 2004. "On the History of Indoor Air Quality and Health." *Indoor Air* 14 (SUPPL. 7): 51–58. https://doi.org/10.1111/J.1600-0668.2004.00273.X.

Sycor. 2019. "The Different Types of Wire & Cable Insulations!" 2019. https://www.sycor.com/blog/post/wiring-insulation-types/.

Taiti, C., C. Costa, W. Guidi Nissim, S. Bibbiani, E. Azzarello, E. Masi, C. Pandolfi, F. Pallottino, P. Menesatti, and S. Mancuso. 2017. "Assessing VOC Emission by Different Wood Cores Using the PTR-ToF-MS Technology." *Wood Science and Technology* 51 (2): 273–95. https://doi.org/10.1007/s00226-016-0866-5.

Taleghani, Mohammad, Martin Tenpierik, Stanley Kurvers, and Andy Van Den Dobbelsteen. 2013. "A Review into Thermal Comfort in Buildings." *Renewable and Sustainable Energy Reviews* 26: 201–15. https://doi.org/10.1016/j.rser.2013.05.050.

Tátraaljai, Dóra, Luca Major, Eniko Földes, and Béla Pukánszky. 2014. "Study of the Effect of Natural Antioxidants in Polyethylene: Performance of β-Carotene." *Polymer Degradation and Stability* 102 (1): 33–40. https://doi.org/10.1016/J.POLYMDEGRADSTAB.2014.02.012.

Teare, June, Angela Mathee, Nisha Naicker, Cheryl Swanepoel, Thandi Kapwata, Yusentha Balakrishna, David Jean du Preez, Danielle A. Millar, and Caradee Y. Wright. 2020. "Dwelling Characteristics Influence Indoor Temperature and May Pose Health Threats in LMICs." *Annals of Global Health* 86 (1): 1–13. https://doi.org/10.5334/aogh.2938.

Tocháček, Jiří, and Zlata Vrátníčková. 2014. "Polymer Life-Time Prediction: The Role of Temperature in UV Accelerated Ageing of Polypropylene and Its Copolymers." *Polymer Testing* 36: 82–87. https://doi.org/10.1016/j.polymertesting.2014.03.019.

Trantallidi, M, C Dimitroulopoulou, P Wolkoff, S Kephalopoulos, and P Carrer. 2015. "EPHECT III: Health Risk Assessment of Exposure to Household Consumer Products." https://doi.org/10.1016/j.scitotenv.2015.05.123.

Uhde, E., A. Borgschulte, and T. Salthammer. 1998. "Characterization of the Field and Laboratory Emission Cell—FLEC: Flow Field and Air Velocities." *Atmospheric Environment* 32 (4): 773–81. https://doi.org/10.1016/S1352-2310(97)00345-2.

Uheida, Abdusalam, Hugo Giraldo Mejía, Mohamed Abdel-Rehim, Wael Hamd, and Joydeep Dutta. 2021. "Visible Light Photocatalytic Degradation of Polypropylene Microplastics in a Continuous Water Flow System." *Journal of Hazardous Materials* 406 (March): 124299. https://doi.org/10.1016/J.JHAZMAT.2020.124299.

Vardoulakis, Sotiris, Chrysanthi Dimitroulopoulou, John Thornes, Ka Man Lai, Jonathon Taylor, Isabella Myers, Clare Heaviside, et al. 2015. "Impact of Climate Change on the Domestic Indoor Environment and Associated Health Risks in the UK." *Environment International* 85 (December): 299–313. https://doi.org/10.1016/J.ENVINT.2015.09.010.

Wallace, Lance A. 2001. "HUMAN EXPOSURE TO VOLATILE ORGANIC POLLUTANTS: Implications for Indoor Air Studies *." www.annualreviews.org.

Wan Kuen, Wan Kuen, Jong Hyo LEE, Ho Jin LIM, and Woo Sik JEONG. 2008. "Naphthalene Emissions from Moth Repellents or Toilet Deodorant Blocks Determined Using Head-Space and Small-Chamber Tests." *Journal of Environmental Sciences* 20 (8): 1012–17. https://doi.org/10.1016/S1001-0742(08)62201-9.

Wang, Zhenshuang, Wanchen Xie, and Chengyi Zhang. 2023. "Towards COP26 Targets: Characteristics and Influencing Factors of Spatial Correlation Network Structure on U.S. Carbon Emission." *Resources Policy* 81 (March): 103285. https://doi.org/10.1016/J.RESOURPOL.2022.103285.

Wang, Zixu, David Shaw, Tara Kahan, Coralie Schoemaecker, and Nicola Carslaw. 2022. "A Modeling Study of the Impact of Photolysis on Indoor Air Quality." *Indoor Air* 32 (6): 1–10. https://doi.org/10.1111/INA.13054.

Ward, Collin P., Cassia J. Armstrong, Anna N. Walsh, Julia H. Jackson, and Christopher M. Reddy. 2019. "Sunlight Converts Polystyrene to Carbon Dioxide and Dissolved Organic Carbon." Rapid-communication. *Environmental Science and Technology Letters* 6 (11): 669–74. https://doi.org/10.1021/acs.estlett.9b00532.

Weschler, C. J. 2004. "Chemical Reactions among Indoor Pollutants: What We've Learned in the New Millennium." *Indoor Air, Supplement* 14 (SUPPL. 7): 184–94. https://doi.org/10.1111/j.1600-0668.2004.00287.x.

Weschler, Charles J. 2009. "Changes in Indoor Pollutants since the 1950s." *Atmospheric Environment* 43 (1): 153–69. https://doi.org/10.1016/j.atmosenv.2008.09.044.

Weschler, Charles J., and William W. Nazaroff. 2008. "Semivolatile Organic Compounds in Indoor Environments." *Atmospheric Environment* 42 (40): 9018–40. https://doi.org/10.1016/j.atmosenv.2008.09.052.

Weschler, Charles J., and Helen C. Shields. 1996. "Production of the Hydroxyl Radical in Indoor Air." *Environmental Science and Technology* 30 (11): 3250–58. https://doi.org/10.1021/es960032f.

Weschler, Charles J, and Nicola Carslaw. 2018. "Indoor Chemistry." https://doi.org/10.1021/acs.est.7b06387.

West, Sheila K., Michael N. Bates, Jennifer S. Lee, Debra A. Schaumberg, David J. Lee, Heather Adair-Rohani, Dong Feng Chen, and Houmam Araj. 2013. "Is Household Air Pollution a Risk Factor for Eye Disease?" *International Journal of Environmental Research and Public Health*. Int J Environ Res Public Health. https://doi.org/10.3390/ijerph10115378.

Westhoff, M, P Litterst, L Freitag, W Urfer, S Bader, and J-I Baumbach. 2009. "Ion Mobility Spectrometry for the Detection of Volatile Organic Compounds in Exhaled Breath of Patients with Lung Cancer: Results of a Pilot Study." *Thorax* 64 (9): 744–48. https://doi.org/10.1136/thx.2008.099465.

Wheeler, Amanda J., Suzy Wong, Cheryl Khouri, and Jiping Zhu. 2013. "Predictors of Indoor BTEX Concentrations in Canadian Residences." *Health Reports / Statistics Canada, Canadian Centre for Health Information* 24: 11–17.

WHO. 2010. "WHO Guidelines for Air Quality." *World Health Organisation; Regional Office for Europe* 35 (8): 812–15.

WHO. 2022. "Household Air Pollution." 2022. https://www.who.int/news-room/fact-sheets/detail/household-air-pollution-and-health.

Wiesinger, Helene, Zhanyun Wang, and Stefanie Hellweg. 2021. "Deep Dive into Plastic Monomers, Additives, and Processing Aids." *Environmental Science and Technology* 55 (13): 9339–51. https://doi.org/10.1021/ACS.EST.1C00976/ASSET/IMAGES/MEDIUM/ES1C00976_0005.GIF.

Williams, Allan T., and Nelson Rangel-Buitrago. 2022. "The Past, Present, and Future of Plastic Pollution." *Marine Pollution Bulletin* 176 (February): 113429. https://doi.org/10.1016/j.marpolbul.2022.113429.

Wit, Cynthia A. De. 2002. "An Overview of Brominated Flame Retardants in the Environment." *Chemosphere* 46 (5): 583–624. https://doi.org/10.1016/S0045-6535(01)00225-9.

Wojnowski, Wojciech, Tomasz Majchrzak, Tomasz Dymerski, Jacek Gębicki, and Jacek Namieśnik. 2017. "Dynamic Headspace Sampling as an Initial Step for Sample Preparation in Chromatographic Analysis." *Journal of AOAC INTERNATIONAL* 100 (6): 1599–1606. https://doi.org/10.5740/JAOACINT.17-0206.

Wolkoff, Peder. 1998. "Impact of Air Velocity, Temperature, Humidity, and Air on Long-Term Voc Emissions from Building Products." *Atmospheric Environment* 32 (14–15): 2659–68. https://doi.org/10.1016/S1352-2310(97)00402-0.

Wolkoff, Peder. 2013. "Indoor Air Pollutants in Office Environments: Assessment of Comfort, Health, and Performance." *International Journal of Hygiene and Environmental Health* 216 (4): 371–94. https://doi.org/10.1016/j.ijheh.2012.08.001.

Wolkoff, Peder, Per Clausen, P A Nielsen, H Gustafsson, B Johnson, and E Rasmusen. 1991. "Field and Laboratory Emission Cell: FLEC." In , 160–65.

Wolkoff, Peder, and Gunnar D. Nielsen. 2001. "Organic Compounds in Indoor Air-Their Relevance for Perceived Indoor Air Quality?" *Atmospheric Environment* 35 (26): 4407–17. https://doi.org/10.1016/S1352-2310(01)00244-8.

World Health Organization, for Europe. 1987. "Air Quality Guidelines for Europe." WHO Regional Publications. European Series No.23. Copenhagen : WHO Regional Office for Europe.

Wright, Stephanie L., and Frank J. Kelly. 2017. "Plastic and Human Health: A Micro Issue?" *Environmental Science and Technology* 51 (12): 6634–47. https://doi.org/10.1021/acs.est.7b00423.

Wright, Truman. 2016. "Calibration Methodolgy for a Proton Transfer Reaction Mass," 1–47.

Xiong, Jianyin, Fangquan Chen, L. Sun, Xuefei Yu, Jing Zhao, Yanjun Hu, and Yuanzheng Wang. 2019. "Characterization of VOC Emissions from Composite Wood Furniture: Parameter Determination and Simplified Model." *Building and Environment* 161 (July): 106237. https://doi.org/10.1016/j.buildenv.2019.106237.

Xu, Mingjun, Zhentao Tang, Yixiang Duan, and Yong Liu. 2016. "GC-Based Techniques for Breath Analysis: Current Status, Challenges, and Prospects." *Critical Reviews in Analytical Chemistry* 46 (4): 291–304. https://doi.org/10.1080/10408347.2015.1055550.

Yousif, Emad, and Raghad Haddad. 2013. "Photodegradation and Photostabilization of Polymers, Especially Polystyrene: Review." *SpringerPlus* 2 (1): 1–32. https://doi.org/10.1186/2193-1801-2-398.

Yu, Kuo Pin, Grace Whei May Lee, Ching Pei Hsieh, and Chi Chi Lin. 2011. "Evaluation of Ozone Generation and Indoor Organic Compounds Removal by Air Cleaners Based on Chamber Tests." *Atmospheric Environment* 45 (1): 35–42. https://doi.org/10.1016/J.ATMOSENV.2010.09.051.

Zhang, Junfeng (Jim), and Kirk R Smith. 2003. "Indoor Air Pollution: A Global Health Concern." *British Medical Bulletin* 68 (1): 209–25. https://doi.org/10.1093/bmb/ldg029.

Zhang, Junfeng, and Kirk R. Smith. 2007. "Household Air Pollution from Coal and Biomass Fuels in China: Measurements, Health Impacts, and Interventions." *Environmental Health Perspectives*. National Institute of Environmental Health Sciences. https://doi.org/10.1289/ehp.9479.

Zhao, Dongye, John C. Little, and Steven S. Cox. 2004. "Characterizing Polyurethane Foam as a Sink for or Source of Volatile Organic Compounds in Indoor Air." *Journal of Environmental Engineering* 130 (9): 983–89. https://doi.org/10.1061/(ASCE)0733-9372(2004)130:9(983).

Zhao, Jun, and Renyi Zhang. 2004. "Proton Transfer Reaction Rate Constants between Hydronium Ion (H3O+) and Volatile Organic Compounds." *Atmospheric Environment* 38 (14): 2177–85. https://doi.org/10.1016/J.ATMOSENV.2004.01.019.

Zhou, Shan, Shawn F. Kowal, Alyssa R. Cregan, and Tara F. Kahan. 2021. "Factors Affecting Wavelength-Resolved Ultraviolet Irradiance Indoors and Their Impacts on Indoor Photochemistry." *Indoor Air* 31 (4): 1187–98. https://doi.org/10.1111/INA.12784.

Zhou, Xiaojun, Yanfeng Liu, Cong Song, Xinke Wang, Fenghao Wang, and Jiaping Liu. 2019. "A Novel Method to Determine the Formaldehyde Emission Characteristic Parameters of Building Materials at Multiple Temperatures." *Building and Environment* 149 (December 2018): 436–45. https://doi.org/10.1016/j.buildenv.2018.12.041.

Zou, Tan. 2014. "Effects of Heat, Moisture, and UV-Irradiation on the Properties of Polyurethane Membranes." https://escholarship.org/uc/item/1541g9rg.

# 9. Appendix A - Supplementary information for Chapter 4

This section contains the supplementary information for Chapter 4: Temperature driven variations in VOC emissions from plastics and impact on indoor air chemistry.

Partial supplementary of Beel, Georgia, Ben Langford, Nicola Carslaw, David Shaw, and Nicholas Cowan. 2023. "Temperature Driven Variations in VOC Emissions from Plastic Products and Their Fate Indoors: A Chamber Experiment and Modelling Study." Science of the Total Environment 881 (January): 163497. https://doi.org/10.1016/j.scitotenv.2023.163497.



*Figure S4.1: Arrhenius plots for the VOCs from PS-tubing plastic only at the four experimental*

*temperatures.*

*Figure S4.2: Arrhenius plots for the VOCs from HDPE-black plastic only at the four experimental temperatures.*
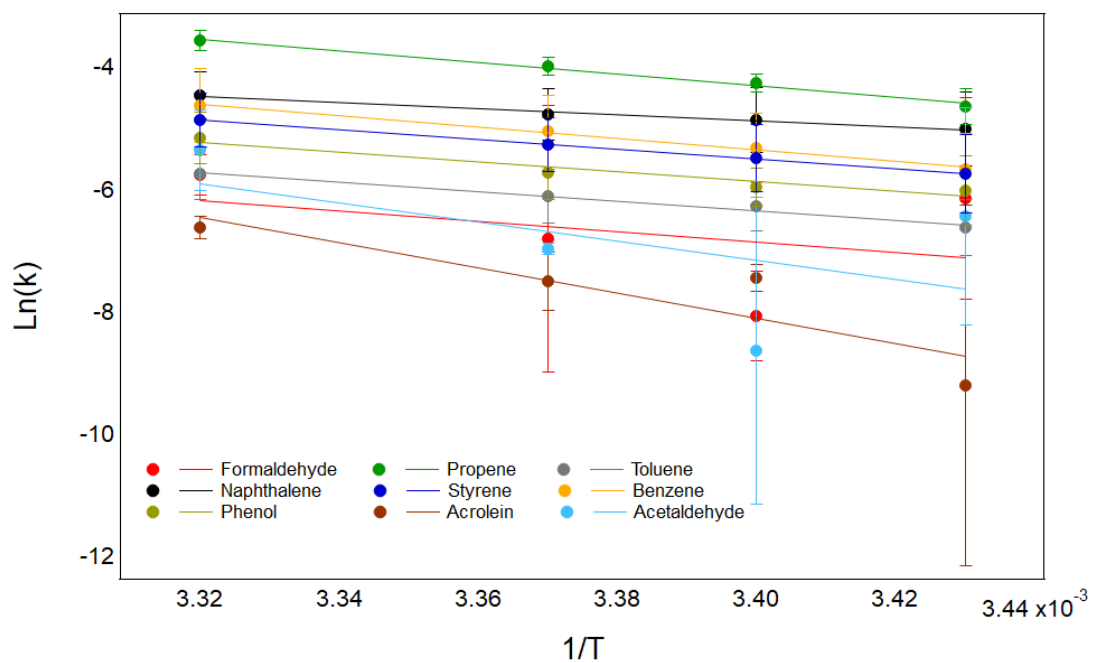


*Figure S4.3: Arrhenius plots for the VOCs from HDPE-blue plastic only at the four experimental temperatures.*
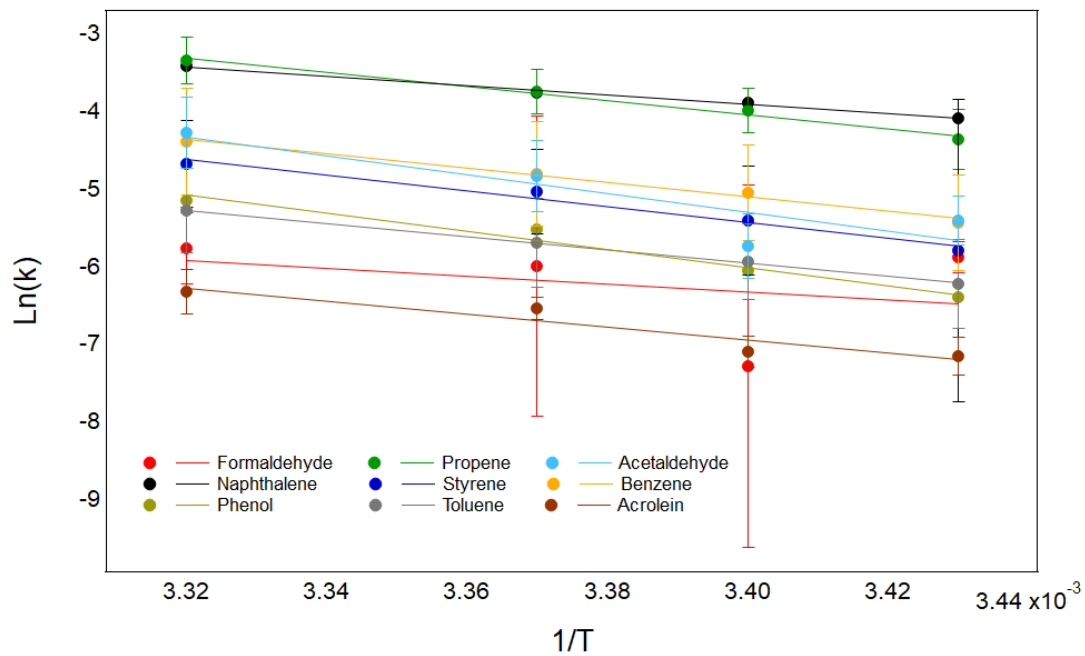
*Figure S4.4: Arrhenius plots for the VOCs from HDPE-orange plastic only at the four experimental temperatures.*
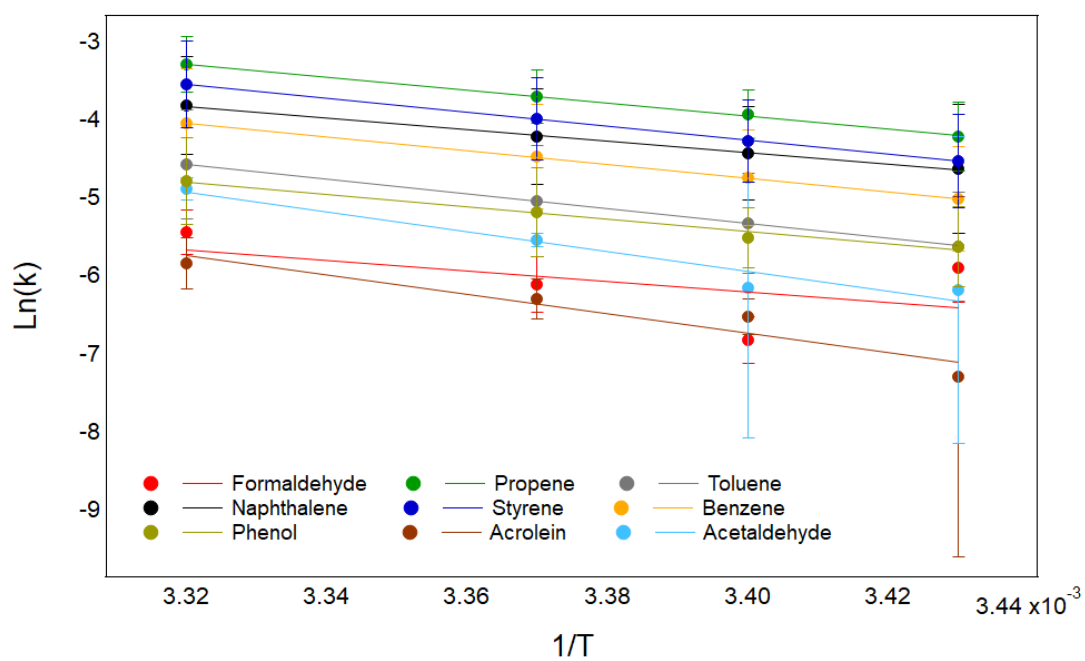


*Figure S4.5: Arrhenius plots for the VOCs from HDPE-white plastic only at the four experimental temperatures.*
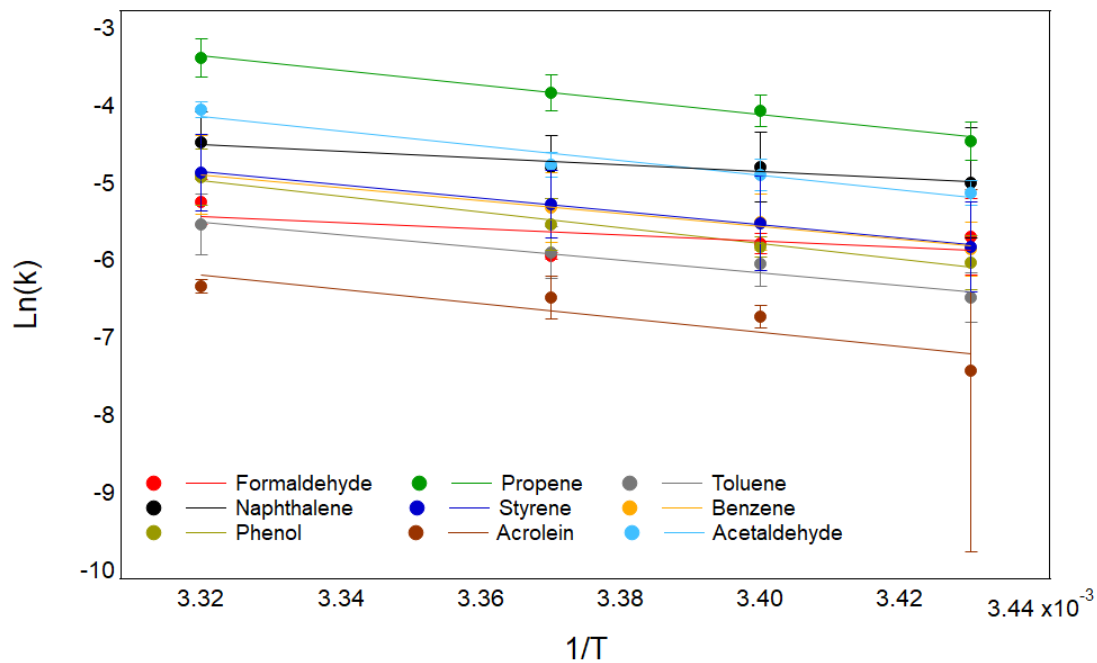
*Figure S4.6: Arrhenius plots for the VOCs from HDPE-red plastic only at the four experimental temperatures.*
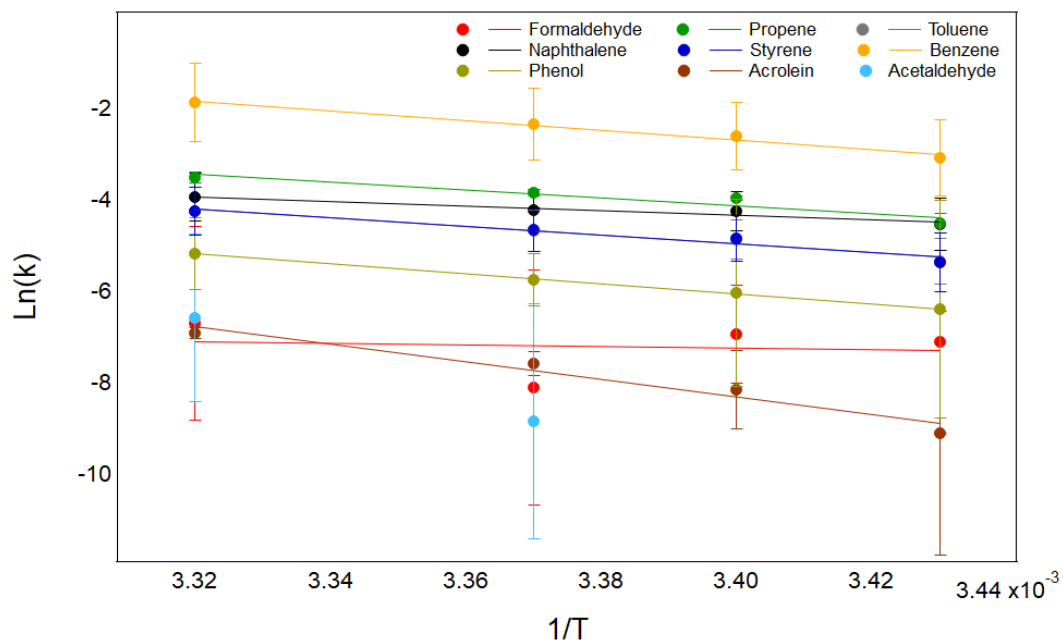


*Figure S4.7: Arrhenius plots for the VOCs from HDPE-green plastic only at the four experimental temperatures.*
*The line of fit for acetaldehyde was excluded as no linear relationship was found.*
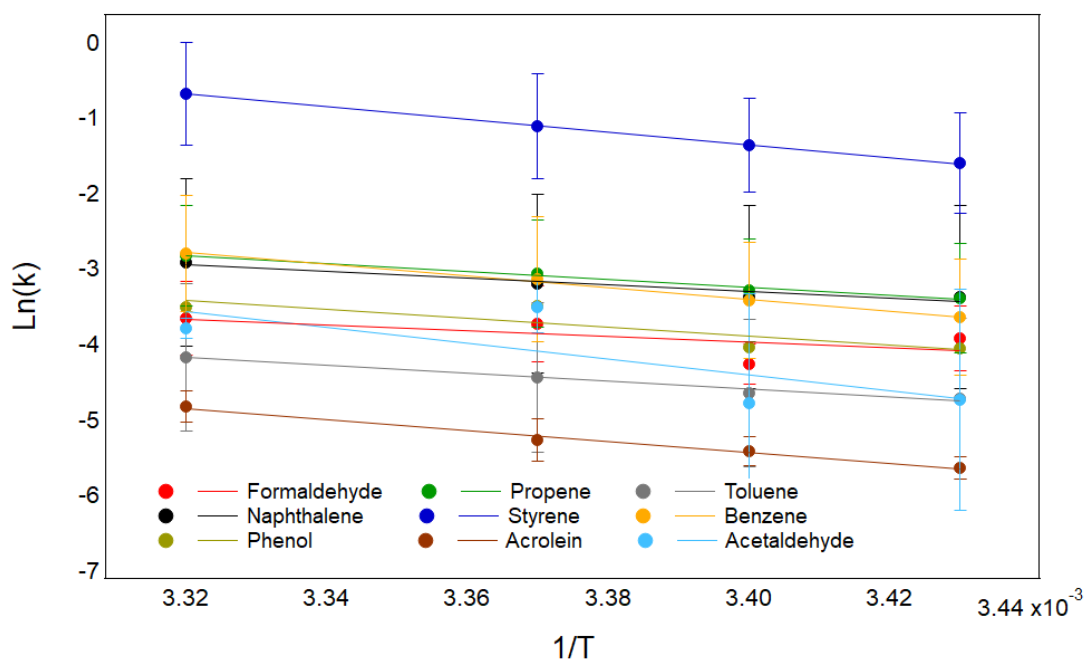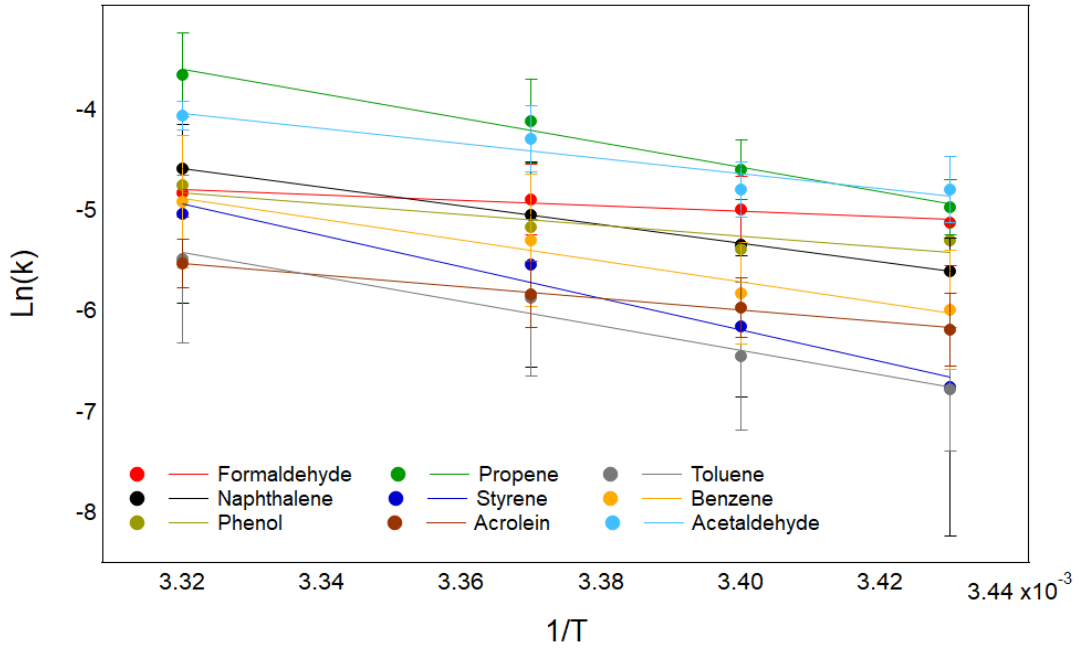
*Figure S4.8: Arrhenius plots for the VOCs from PE-container-white plastic only at the four experimental temperatures.*
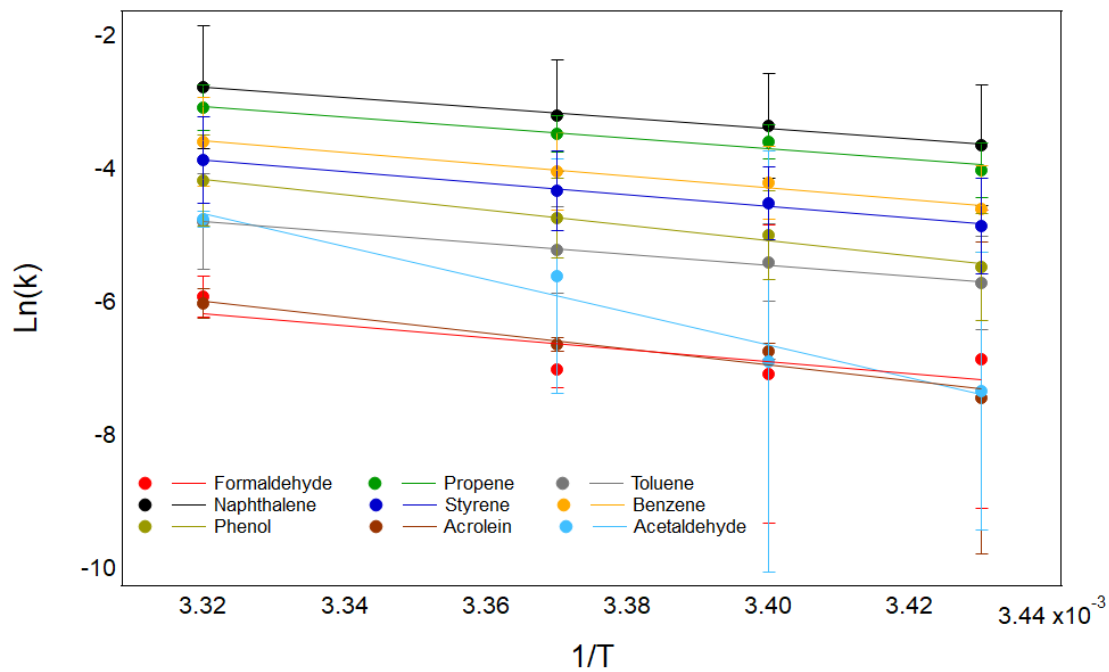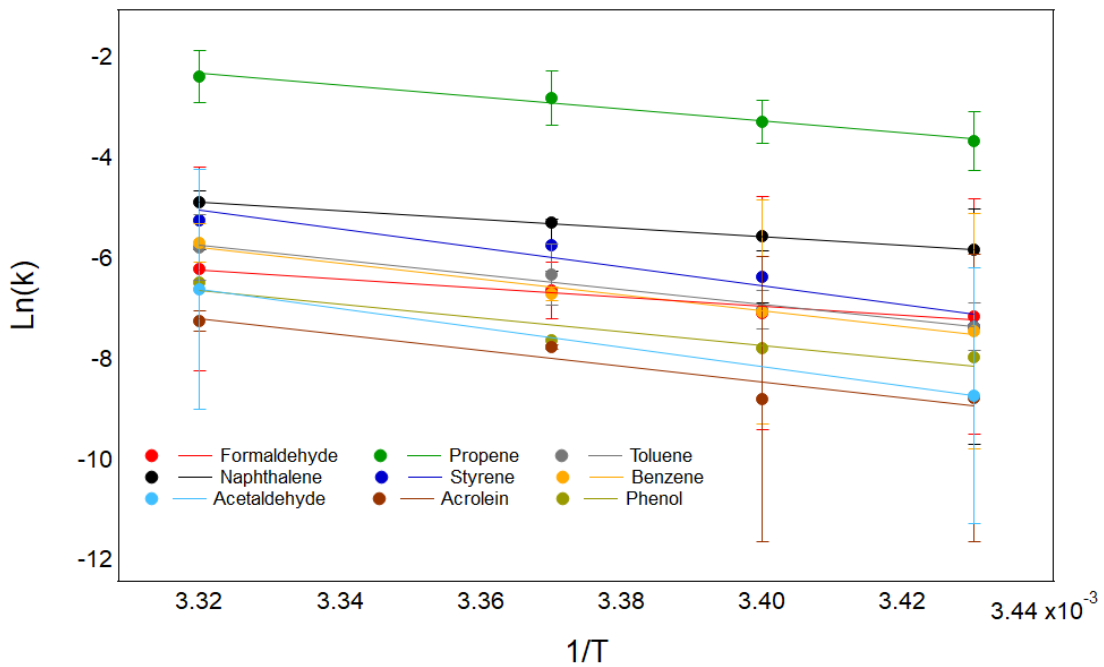


*Figure S4.9: Arrhenius plots for the VOCs from PP-container-clear plastic only at the four experimental temperatures.*
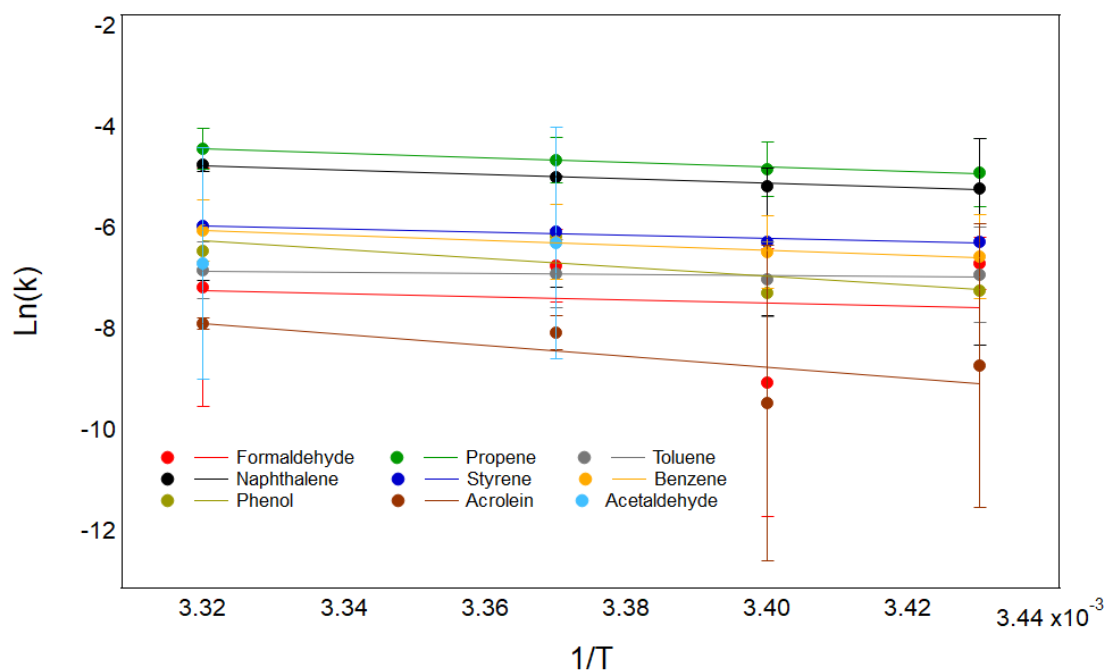
*Figure S4.10: Arrhenius plots for the VOCs from HDPE-binbag plastic only at the four experimental temperatures. The line of fit for acetaldehyde was excluded as no linear relationship was found.*
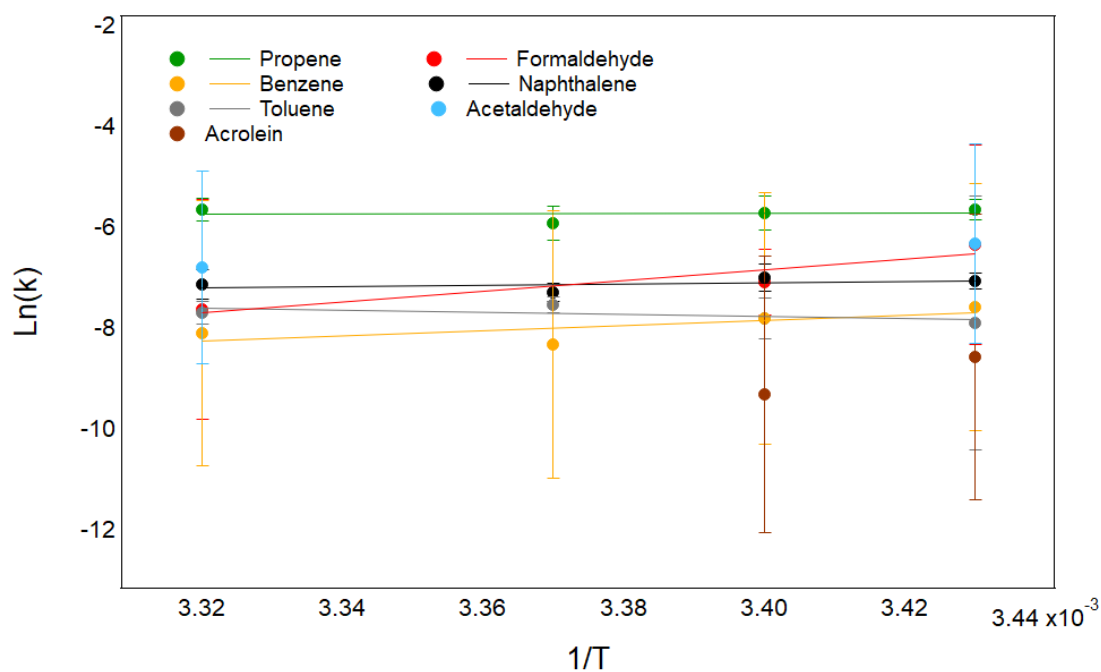


*Figure S4.11: Arrhenius plots for the VOCs from PET water bottle plastic only at the four experimental temperatures. The lines of fit for acrolein and acetaldehyde were excluded as no linear relationship was found.*

*Table S4.1: Arrhenius coefficient values for each compound for each plastic type.*

| Plastic | Compound | Gradient | SD | Intercept | SD | R2 | $E_a$ |
|---|---|---|---|---|---|---|---|
| Rubber-wire | Formaldehyde | -2774.7 | 130 | 5.1 | 0.438 | 0.995 | 23.058 |
| Rubber-wire | Propylene | -8507.8 | 748 | 24.9 | 2.53 | 0.984 | 70.699 |
| Rubber-wire | Acetaldehyde | -2967.9 | 35.3 | 6.1 | 0.119 | 0.999 | 24.663 |
| Rubber-wire | Acrolein | -5222.4 | 588 | 12.4 | 1.99 | 0.975 | 43.398 |
| Rubber-wire | Benzene | -7228.7 | 610 | 19.9 | 2.06 | 0.985 | 60.071 |
| Rubber-wire | Toluene | -7804 | 620 | 21.5 | 2.1 | 0.987 | 64.851 |
| Rubber-wire | Phenol | -8322.9 | 1.0E+03 | 23.5 | 3.4 | 0.971 | 69.163 |
| Rubber-wire | Styrene | -8383.6 | 1.0E+03 | 24.1 | 3.64 | 0.968 | 69.667 |
| Rubber-wire | Naphthalene | -8018.9 | 835 | 22.7 | 2.82 | 0.978 | 66.637 |
| HDPE-orange | Formaldehyde | -5087.3 | 1.0E+04 | 10.9 | 33.9 | 0.114 | 42.275 |
| HDPE-orange | Propylene | -9078.1 | 684 | 26.8 | 2.31 | 0.988 | 75.439 |

| | | | | | | |
|---|---|---|---|---|---|---|
| HDPE-orange | Acetaldehyde | -12157 | 4.4E+03 | 36.034 | 15.1 | 0.787 | 101.02 |
| HDPE-orange | Acrolein | -8323.9 | 2.0E+03 | 21.356 | 6.77 | 0.896 | 69.171 |
| HDPE-orange | Benzene | -9286.3 | 753 | 26.473 | 2.55 | 0.987 | 77.169 |
| HDPE-orange | Toluene | -8539.3 | 226 | 23.081 | 0.763 | 0.998 | 70.961 |
| HDPE-orange | Phenol | -11714 | 1.4E+03 | 33.819 | 4.8 | 0.971 | 97.343 |
| HDPE-orange | Styrene | -10130 | 1.1E+03 | 29.015 | 3.91 | 0.974 | 84.180 |
| HDPE-orange | Naphthalene | -6004 | 324 | 16.511 | 1.09 | 0.994 | 49.893 |
| PP-container-clear | Formaldehyde | -9131 | 1.4E+03 | 24.096 | 4.83 | 0.953 | 75.878 |
| PP-container-clear | Propylene | -11821 | 1.1E+03 | 36.924 | 3.97 | 0.980 | 98.232 |
| PP-container-clear | Acetaldehyde* | -19267 | | 57.351 | | 1 | 50.131 |
| PP-container-clear | Acrolein* | -15652 | 3.8E+03 | 44.761 | 13 | 0.892 | 160.10 |
| PP-container-clear | Benzene | -15815 | 1.4E+03 | 46.728 | 5.01 | 0.982 | 130.06 |
| PP-container-clear | Toluene | -14821 | 1.7E+03 | 43.476 | 5.78 | 0.974 | 131.42 |

| | | | | | | | |
|---|---|---|---|---|---|---|---|
| PP-container-clear | Phenol | -13557 | 3.3E+03 | 38.366 | 11.4 | 0.889 | 123.16 |
| PP-container-clear | Styrene | -18763 | 3.9E+03 | 57.247 | 13.2 | 0.920 | 112.65 |
| PP-container-clear | Naphthalene | -8483.8 | 134 | 23.285 | 0.454 | 0.999 | 155.92 |
| HDPE-binbag | Formaldehyde | -2909.7 | 1.6E+04 | 2.4236 | 56.5 | 0.014 | 70.500 |
| HDPE-binbag | Propylene | -4469.7 | 334 | 10.411 | 1.13 | 0.988 | 24.179 |
| HDPE-binbag | Acetaldehyde | 70260 | 2.6E+04 | -240.72 | 90.9 | 0.773 | 37.143 |
| HDPE-binbag | Acrolein* | -10805 | 7.6E+03 | 27.994 | 25.8 | 0.501 | -583.86 |
| HDPE-binbag | Benzene | -4858.4 | 359 | 10.093 | 1.21 | 0.989 | 89.789 |
| HDPE-binbag | Toluene | -1096.2 | 795 | -3.2068 | 2.69 | 0.487 | 40.373 |
| HDPE-binbag | Phenol* | -8846.1 | 5.7E+03 | 23.126 | 19.3 | 0.547 | 9.109 |
| HDPE-binbag | Styrene | -3142.5 | 696 | 4.4906 | 2.35 | 0.910 | 73.511 |
| HDPE-binbag | Naphthalene | -4442.4 | 557 | 9.9992 | 1.88 | 0.969 | 26.114 |

| | | | | | | | |
|---|---|---|---|---|---|---|---|
| PE-container-white | Formaldehyde | -2656.1 | 528 | 4.0254 | 1.78 | 0.926 | 36.916 |
| PE-container-white | Propylene | -12104 | 999 | 36.583 | 3.38 | 0.986 | 22.072 |
| PE-container-white | Acetaldehyde | -7482.8 | 1.8E+03 | 20.808 | 6.29 | 0.890 | 100.58 |
| PE-container-white | Acrolein | -5825.5 | 315 | 13.816 | 1.07 | 0.994 | 62.182 |
| PE-container-white | Benzene | -10322 | 1.4E+03 | 29.387 | 4.74 | 0.964 | 48.409 |
| PE-container-white | Toluene | -12089 | 1.5E+03 | 34.721 | 5.21 | 0.968 | 85.775 |
| PE-container-white | Phenol | -5371.3 | 1.7E+03 | 13.01 | 5.99 | 0.821 | 100.45 |
| PE-container-white | Styrene | -15635 | 2.0E+03 | 46.981 | 6.78 | 0.968 | 44.635 |
| PE-container-white | Naphthalene | -9210.1 | 91.9 | 25.989 | 0.311 | 0.999 | 129.92 |
| PS-tubing | Formaldehyde | -3744.2 | 3.1E+03 | 8.7719 | 10.7 | 0.411 | 76.535 |
| PS-tubing | Propylene | -5282.1 | 468 | 14.723 | 1.58 | 0.984 | 31.114 |
| PS-tubing | Acetaldehyde | -10546 | 6.2E+03 | 31.457 | 21.2 | 0.586 | 43.894 |
| PS-tubing | Acrolein | -7255.3 | 536 | 19.247 | 1.81 | 0.989 | 87.637 |

| | | | | | | | |
|---|---|---|---|---|---|---|---|
| PS-tubing | Benzene | -7778.1 | 320 | 23.051 | 1.08 | 0.996 | 60.291 |
| PS-tubing | Toluene | -5220.2 | 558 | 13.162 | 1.89 | 0.977 | 64.636 |
| PS-tubing | Phenol | -5865.5 | 2.4E+03 | 16.067 | 8.31 | 0.740 | 43.379 |
| PS-tubing | Styrene | -8455.6 | 97.9 | 27.406 | 0.331 | 0.999 | 48.742 |
| PS-tubing | Naphthalene | -4460.4 | 939 | 11.874 | 3.17 | 0.918 | 70.266 |
| PET-water-bottle | Formaldehyde | -180.38 | 5.3E+04 | -4.6483 | 181 | 0.884 | 37.065 |
| PET-water-bottle | Propylene* | 105.93 | 1.8E+03 | -6.0852 | 6.25 | 0.002 | 1.498 |
| PET-water-bottle | Acetaldehyde* | 13980 | 5.6E+04 | -50.531 | 190 | 0.029 | -0.880 |
| PET-water-bottle | Acrolein | -93143 | 4.1E+04 | 310.35 | 141 | 0.714 | -116.17 |
| PET-water-bottle | Benzene* | 5102.7 | 3.3E+03 | -25.198 | 11.3 | 0.538 | 774.01 |
| PET-water-bottle | Toluene* | -1974.9 | 1.8E+03 | -1.0492 | 6.13 | 0.372 | -42.403 |
| PET-water-bottle | Phenol* | 0 | 0 | 0 | 0 | 0 | 16.411 |

151

| | | | | | | | |
|---|---|---|---|---|---|---|---|
| PET-water-bottle | Styrene* | 0 | 0 | 0 | 0 | 0 | 0 |
| PET-water-bottle | Naphthalene* | 1205 | 1.7E+03 | -11.195 | 5.8 | 0.197 | 0 |
| HDPE-green | Formaldehyde | -1843 | 9.1E+03 | -0.98007 | 31.1 | 0.019 | -10.013 |
| HDPE-green | Propylene | -8502.9 | 1.7E+03 | 24.783 | 6 | 0.919 | 15.315 |
| HDPE-green | Acetaldehyde* | 73253 | 4.4E+04 | -251.45 | 151 | 0.572 | 70.659 |
| HDPE-green | Acrolein | -19217 | 3.0E+03 | 57.02 | 10.2 | 0.953 | -608.73 |
| HDPE-green | Benzene | -10623 | 1.1E+03 | 33.426 | 3.76 | 0.978 | 159.69 |
| HDPE-green | Toluene | -9546.1 | 1.2E+03 | 27.485 | 4.25 | 0.966 | 88.277 |
| HDPE-green | Phenol | -10960 | 247 | 31.208 | 0.836 | 0.998 | 79.328 |
| HDPE-green | Styrene | -9636 | 1.4E+03 | 27.795 | 5 | 0.955 | 91.077 |
| HDPE-green | Naphthalene | -4902 | 907 | 12.33 | 3.07 | 0.935 | 80.075 |
| HDPE-black | Formaldehyde | -8975.8 | 5.0E+03 | 23.621 | 17.1 | 0.612 | 40.735 |

| | | | | | | |
|---|---|---|---|---|---|---|
| HDPE-black | Propylene | -7992.3 | 1.1E+03 | 23.473 | 3.72 | 0.963 | 74.588 |
| HDPE-black | Acetaldehyde | -24700 | 3.4E+03 | 77.34 | 11.8 | 0.961 | 66.416 |
| HDPE-black | Acrolein | -11959 | 2.1E+03 | 33.717 | 7.23 | 0.939 | 205.25 |
| HDPE-black | Benzene | -8884.7 | 764 | 25.925 | 2.58 | 0.985 | 99.379 |
| HDPE-black | Toluene | -8192.9 | 396 | 22.416 | 1.34 | 0.995 | 73.831 |
| HDPE-black | Phenol | -11418 | 889 | 33.752 | 3.01 | 0.988 | 68.083 |
| HDPE-black | Styrene | -8728.9 | 618 | 25.116 | 2.09 | 0.990 | 94.883 |
| HDPE-black | Naphthalene | -7730.9 | 569 | 22.891 | 1.92 | 0.989 | 72.537 |
| HDPE-red | Formaldehyde | -3990.1 | 3.5E+03 | 7.8259 | 11.9 | 0.392 | 64.243 |
| HDPE-red | Propylene | -9536 | 697 | 28.307 | 2.36 | 0.989 | 33.157 |
| HDPE-red | Acetaldehyde | -9570.6 | 1.6E+03 | 27.643 | 5.5 | 0.945 | 79.244 |
| HDPE-red | Acrolein | -9215.1 | 3.2E+03 | 24.411 | 11.1 | 0.797 | 79.531 |
| HDPE-red | Benzene | -8402.3 | 581 | 23.012 | 1.96 | 0.990 | 76.577 |

| | | | | | | | |
|---|---|---|---|---|---|---|---|
| HDPE-red | Toluene | -8188.9 | 1.2E+03 | 21.693 | 4.08 | 0.958 | 69.823 |
| HDPE-red | Phenol | -10165 | 913 | 28.791 | 3.09 | 0.984 | 68.049 |
| HDPE-red | Styrene | -8611.5 | 291 | 23.743 | 0.983 | 0.997 | 84.471 |
| HDPE-red | Naphthalene | -4352.5 | 837 | 9.9539 | 2.83 | 0.931 | 71.561 |
| HDPE-blue | Formaldehyde | -8381.9 | 1.4E+04 | 21.645 | 47.7 | 0.149 | 36.169 |
| HDPE-blue | Propylene | -9513.5 | 704 | 28.05 | 2.38 | 0.989 | 69.653 |
| HDPE-blue | Acetaldehyde | -15650 | 1.7E+04 | 46.052 | 58.6 | 0.289 | 79.057 |
| HDPE-blue | Acrolein | -20644 | 7.2E+03 | 62.09 | 24.5 | 0.802 | 130.05 |
| HDPE-blue | Benzene | -9356.2 | 406 | 26.464 | 1.37 | 0.996 | 171.55 |
| HDPE-blue | Toluene | -7772.6 | 760 | 20.09 | 2.57 | 0.981 | 77.750 |
| HDPE-blue | Phenol | -8067.8 | 1.5E+03 | 21.566 | 5.33 | 0.929 | 64.590 |
| HDPE-blue | Styrene | -8052.9 | 108 | 21.884 | 0.366 | 0.999 | 67.043 |
| HDPE-blue | Naphthalene | -4882.4 | 417 | 11.734 | 1.41 | 0.985 | 66.919 |

| | | | | | | | |
|---|---|---|---|---|---|---|---|
| HDPE-white | Formaldehyde | -6687.2 | 7.3E+03 | 16.535 | 24.9 | 0.292 | 40.572 |
| HDPE-white | Propylene | -8261.1 | 248 | 24.137 | 0.837 | 0.998 | 55.570 |
| HDPE-white | Acetaldehyde | -12752 | 2.2E+03 | 37.411 | 7.53 | 0.942 | 68.649 |
| HDPE-white | Acrolein | -12368 | 2.7E+03 | 35.319 | 9.14 | 0.912 | 105.96 |
| HDPE-white | Benzene | -8778.9 | 138 | 25.105 | 0.467 | 0.999 | 102.77 |
| HDPE-white | Toluene | -9480.4 | 61.6 | 26.902 | 0.208 | 0.999 | 72.952 |
| HDPE-white | Phenol | -7918.8 | 840 | 21.489 | 2.84 | 0.977 | 78.782 |
| HDPE-white | Styrene | -8961 | 94 | 26.204 | 0.318 | 0.999 | 65.805 |
| HDPE-white | Naphthalene | -7318.9 | 273 | 20.464 | 0.924 | 0.997 | 74.465 |

*A non-linear relationship between emission rates and temperature was determined for this compound.

# 10. Appendix B - Supplementary information for Chapter 5

This section contains the supplementary information for Chapter 5: How does visible and UV light influence the VOC emissions from selected plastic products and the subsequent photo-chemistry within the indoor environment?

Section 1: LED lamp simulations

The attenuation of outdoor light through a window was turned off for the model runs that purely explored the influence of VOC emissions driven by the LED lamp experiments, and the indoor lighting setting was set to "LED". The VOC emission rates, at each of the set distances from the LED lamp, were implemented into INCHEM-Py. Figure S5.1 shows how the concentration profile of secondary species varies.
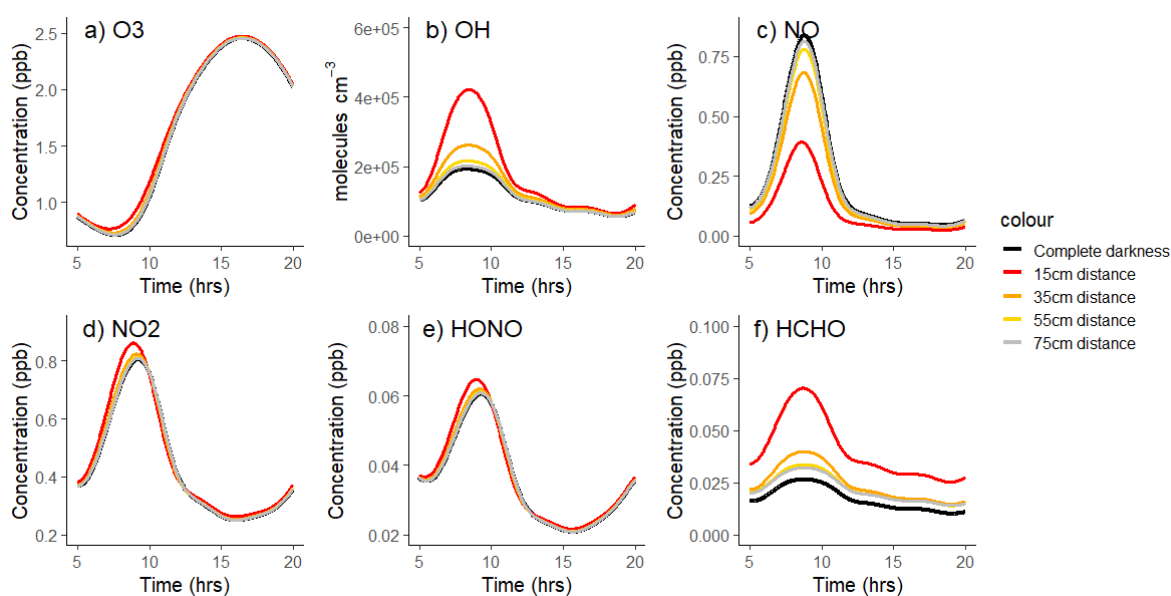


*Figure S5.1: Comparison of diurnal concentrations of key species (O3 and OH) and secondary species, formed through photolysis reactions within INCHEM-Py simulations, in complete darkness (black) and with the LED light setting on with the plastic type (rubber-wire) at different distances from the light source; 15cm (red), 35cm (orange), 55cm (yellow) and 75cm (grey).*

As previously shown in the experimental data, the shorter the distance from the light source, generally the higher the initial VOC emissions are compared to when the LED light source is further away. This

is also reflected in the secondary species concentrations and also with the key indicator species, such as $O_3$ and OH. However, this is believed to be primarily driven by the temperature.

The development of indoor artificial lighting for INCHEM-Py is described in Wang *et al.*, (2022), where the authors compared the influence of different indoor lights on the concentrations of secondary species. Their work showed that there was little variation in the predicted concentrations of indoor species when the indoor artificial light type changes, but the highest OH and $O_3$ values were seen for a different light type: uncovered fluorescent tube lighting (UFT). Although $O_3$ is photolysed indoors, its production via NO photolysis outweighs the photolytic loss, so that overall, more indoor lighting increases ozone concentrations (and reduces NO concentrations), which is also shown in Figure 5.9.
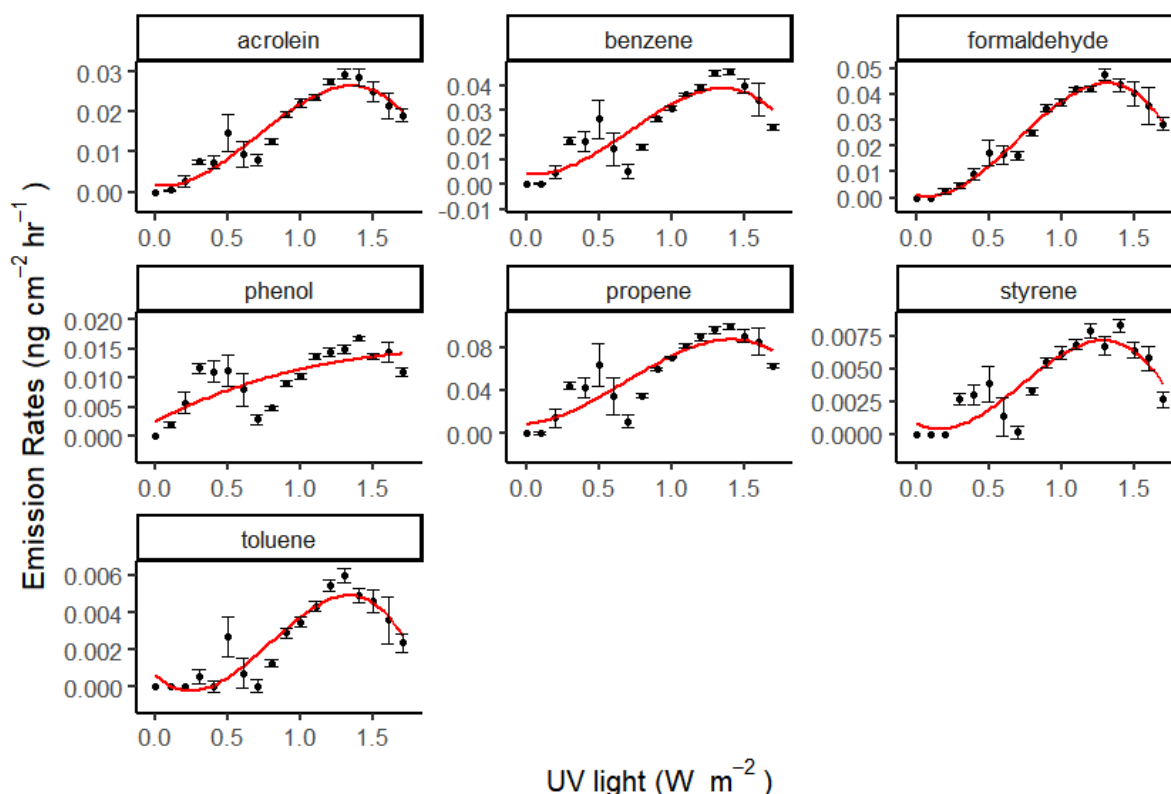


*Figure S5.2: Relationship between light-only emission rates and the UVA light for all compounds for the HDPE-binbag plastic type. The error bars are ± one standard deviation.*
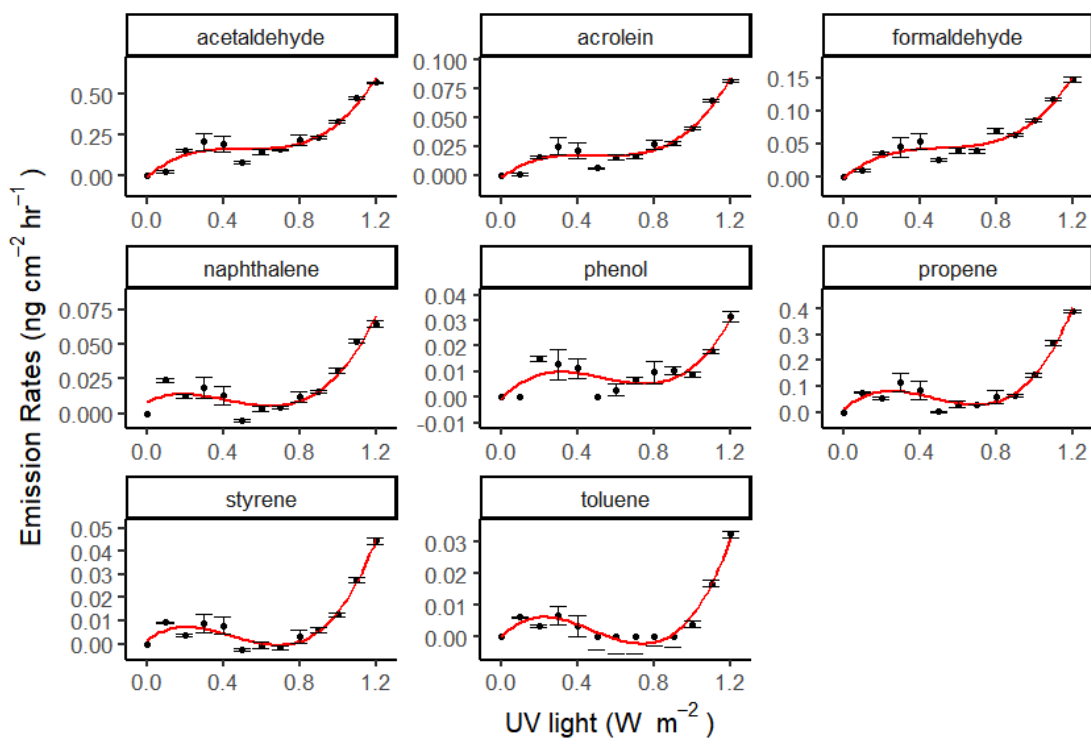
*Figure S5.3: Relationship between light-only emission rates and the UVA light for all compounds for the HDPE-green plastic type. The error bars are ± one standard deviation.*
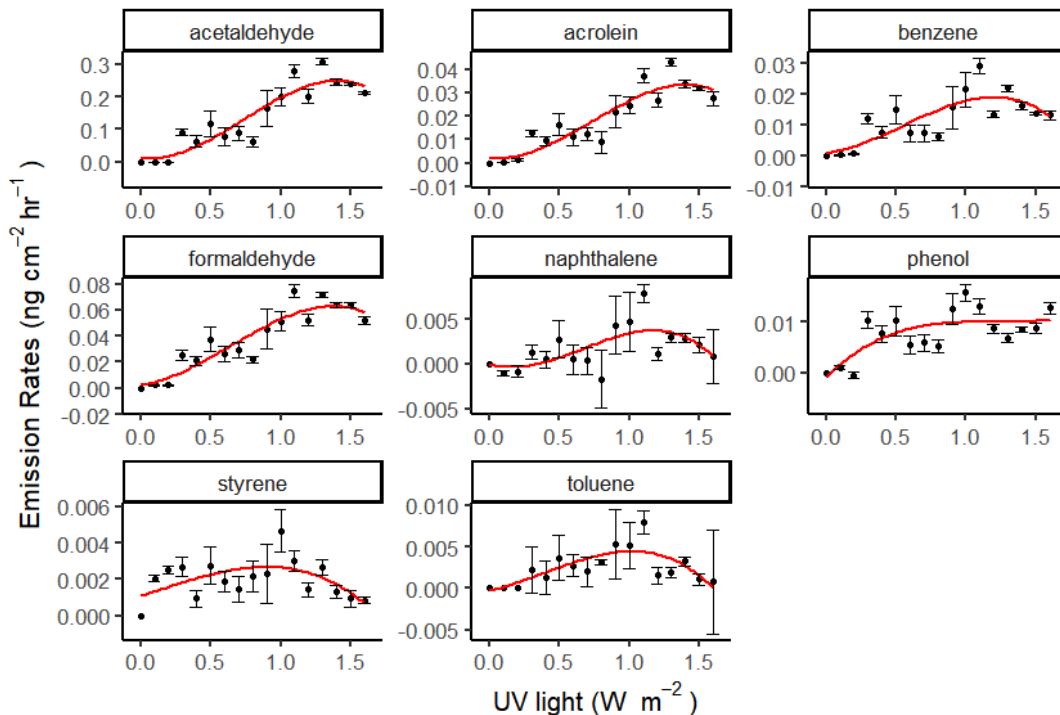


*Figure S5.3: Relationship between light-only emission rates and the UVA light for all compounds for the clear PP storage container plastic type. The error bars are ± one standard deviation.*
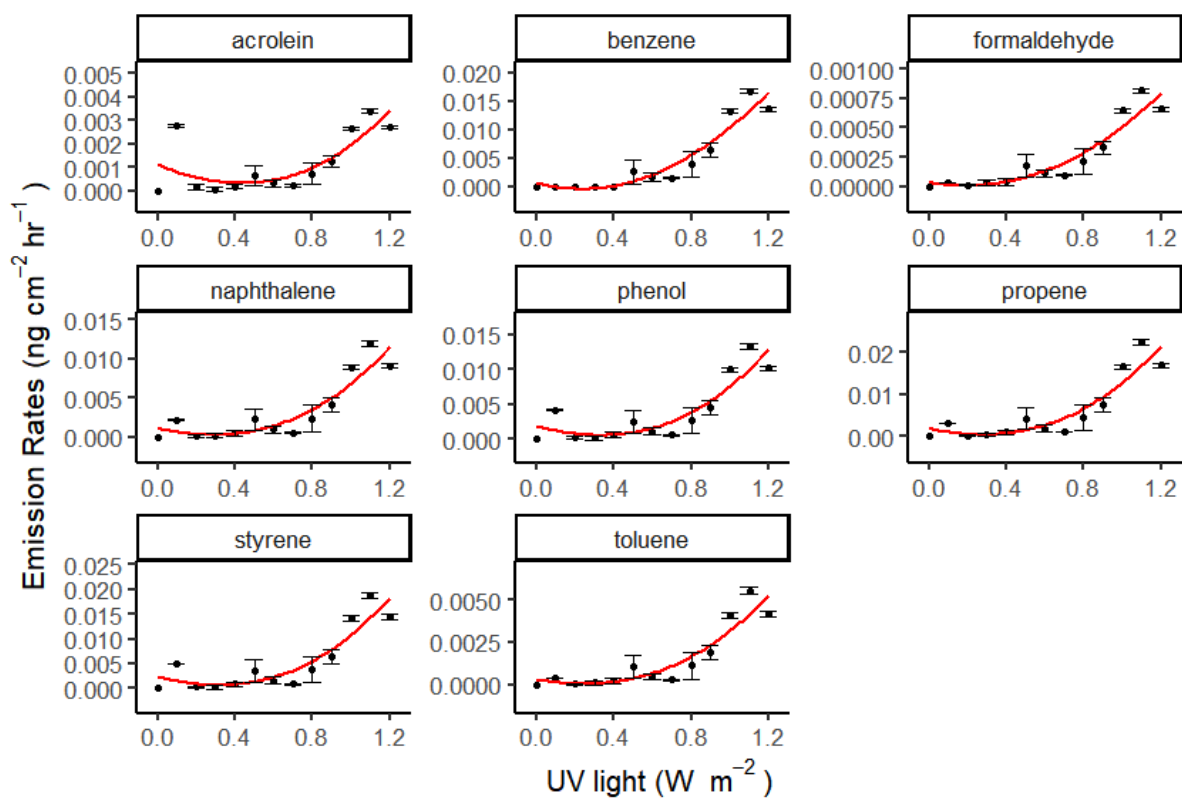
158

*Figure S5.5: Relationship between light-only emission rates and the UVA light for all compounds for the Rubber wire plastic type. The error bars are ± one standard deviation.*

*Table S5.1: The polynomial fit coefficients implemented within the INCHEM-Py simulations to determine the VOC concentrations.*

| Plastic | Compound | Polynomial coefficient (term 1) | Polynomial coefficient (term 2) | Polynomial coefficient (term 3) | Polynomial coefficient (term 4) |
|---|---|---|---|---|---|
| HDPE-storage-container-white | Formaldehyde | 0 | 2.21E+06 | 28263 | -1.40E+06 |
| | Propene | 0 | -3.84E+05 | 2.22E+06 | -1.89E+06 |
| | Acetaldehyde | 0 | -28725 | 9.06E+06 | -7.83E+06 |
| | Acrolein | 0 | 61657 | 5.54E+05 | -4.90E+05 |
| | Benzene | 0 | -1.44E+05 | 7.57E+05 | -5.88E+05 |
| | Toluene | 0 | -51041 | 2.49E+05 | -2.13E+05 |
| | Phenol | 0 | -15382 | 2.90E+05 | -2.46E+05 |
| | Styrene | 0 | - | - | - |
| Rubber-wire | Formaldehyde | 0 | -1961.5 | 9679.1 | 4479.2 |

| | | | | | |
|---|---|---|---|---|---|
| | Propene | 0 | 14277 | -24367 | 2.27E+05 |
| | Acetaldehyde | 0 | - | - | - |
| | Acrolein | 0 | 39870 | -91164 | 74954 |
| | Benzene | 0 | -69110 | 1.69E+05 | -3936.3 |
| | Toluene | 0 | -1804.6 | 6450.3 | 19939 |
| | Phenol | 0 | 26458 | -60090 | 90304 |
| | Styrene | 0 | 25355 | -56115 | 1.04E+05 |
| HDPE-green | Formaldehyde | 0 | 5.56E+06 | -1.05E+07 | 6.98E+06 |
| | Propene | 0 | 1.20E+07 | -3.16E+07 | 2.20E+07 |
| | Acetaldehyde | 0 | 1.60E+07 | -3.20E+07 | 2.12E+07 |
| | Acrolein | 0 | 1.48E+06 | -3.26E+06 | 2.32E+06 |
| | Benzene | 0 | - | - | - |

| | | | | | |
|---|---|---|---|---|---|
| | Toluene | 0 | 4.87E+05 | -1.42E+06 | 9.88E+05 |
| | Phenol | 0 | 5.74E+05 | -1.33E+06 | 8.44E+05 |
| | Styrene | 0 | 5.00E+05 | -1.43E+06 | 1.02E+06 |
| PP-storage-container-clear | Formaldehyde | 0 | 6.48E+05 | 1.41E+06 | -7.93E+05 |
| | Propene | 0 | - | - | - |
| | Acetaldehyde | 0 | 51826 | 6.05E+06 | -2.87E+06 |
| | Acrolein | 0 | 51729 | 5.64E+05 | -2.74E+05 |
| | Benzene | 0 | 1.04E+05 | 1.94E+05 | -1.32E+05 |
| | Toluene | 0 | 21081 | 57810 | -44303 |
| | Phenol | 0 | 1.80E+05 | -1.41E+05 | 36904 |
| | Styrene | 0 | 50912 | -38150 | 5366 |
| HDPE-binbag | Formaldehyde | 0 | -2.39E+05 | 2.21E+06 | -1.08E+06 |

| | | | | | |
|---|---|---|---|---|---|
| | Propene | 0 | 8.51E+05 | 9.95E+05 | -6.07E+05 |
| | Acetaldehyde | 0 | - | - | - |
| | Acrolein | 0 | 33085 | 5.11E+05 | -2.59E+05 |
| | Benzene | 0 | 1.02E+05 | 4.32E+05 | -2.32E+05 |
| | Toluene | 0 | -38582 | 1.23E+05 | -54286 |
| | Phenol | 0 | 1.84E+05 | -1.31E+05 | 36469 |
| | Styrene | 0 | -15446 | 1.13E+05 | -55744 |

# 11. Appendix C - Supplementary Information for Chapter 6

This section contains the supplementary information for Chapter 6: Natural ageing of plastic products in a home and their VOC emissions.
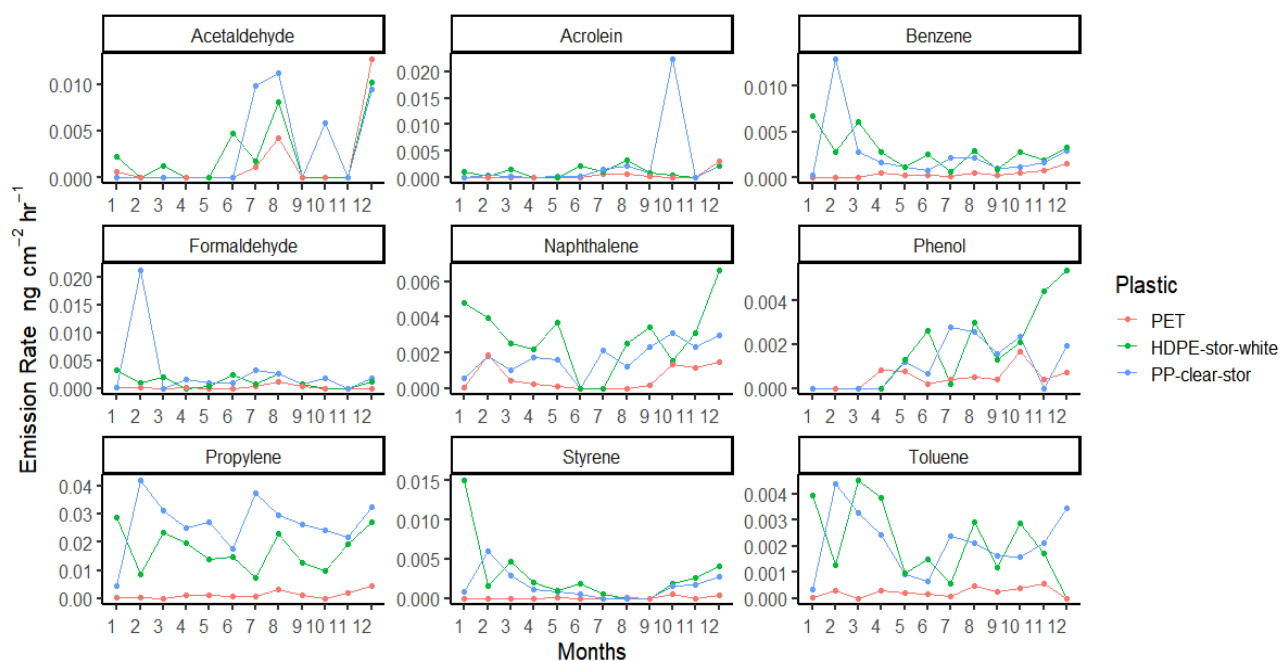


*Figure S6.1: VOC emissions for each of the kitchen plastics (apart from the Rubber-wire) over the 12-month testing period.*